J Pharmacokinet Pharmacodyn (2016) 43:S11–S122
DOI 10.1007/s10928-016-9485-x

ABSTRACTS

Abstracts accepted for American Conference on Pharmacometrics 2016 (ACoP7)

M-01

Population Pharmacokinetics of AZD-5847 in Adults with Tuberculosis

Abdullah Alsultan[1,2], Jennifer J. Furin[3], Jeannine Du Bois[4], Elana van Brakel[4], Phalkun Chheng[3], Amour Venter[5], Bonnie Thiel[3], Sara A. Debanne[6], W. Henry Boom[3], Andreas H. Diacon[4,5], and John L. Johnson[3], Charles A. Peloquin[2]

[1]King Saud University College of Pharmacy, [2]University of Florida College of Pharmacy, [3]Tuberculosis Research Unit, Case Western Reserve University, [4]TASK Applied Science, [5] MRC Centre for Tuberculosis Research, [6]Department of Epidemiology and Biostatistics, Case Western Reserve University

Objective: AZD-5847 is an oxazolidinone derivative being developed for the treatment of tuberculosis (TB). A phase II trial to evaluate its pharmacokinetics and early bactericidal activity in adults with pulmonary TB was recently completed. We developed a population pharmacokinetic (PK) model for AZD-5847 using data from patients in this phase 2 study.
Methods: The study included 60 adults with newly-diagnosed, drug-susceptible TB. Patients were randomized to four treatment arms - 500 mg once daily, 500 mg twice daily, 800 mg twice daily or 1200 mg once daily. PK sampling occurred on day 1 and 14. Blood samples were collected at 0, 1, 2, 3, 4, 5, 6, 8, 12, 13, 15, 16, 17, 18, 20 and 24 hours.
Results: A total of 1723 samples were used for the analysis. A two compartment model with linear elimination and Tlag for absorption adequately described the data. AZD-5847 showed non-linear absorption likely due to saturable absorption. Bioavailability started to decrease at the 800 mg daily dose and was 67% at the 1200 mg dose. Typical values (relative standard error %) for Tlag, Ka, Cl, V1, Q and V2 were 0.27 hours (18%), 0.38 hour^{-1} (9%), 7.96 L/hour (3%), 43.3 L (7%), 8.9 L/hour (13%) and 31.9 L (9%). The coefficient of variation (relative standard error %) for Tlag, Ka, Cl, V1, Q and V2 were 68.6% (22%), 21.6% (19%), 22% (10%), 14.9% (36%), 47.1% (28%), 55.6% (13%). The figure below shows the typical PK profile for AZD-5847 at steady state.
Conclusion: AZD-5847 shows biphasic elimination. Absorption of AZD-5847 is nonlinear and administering doses above 800 mg might not be beneficial.

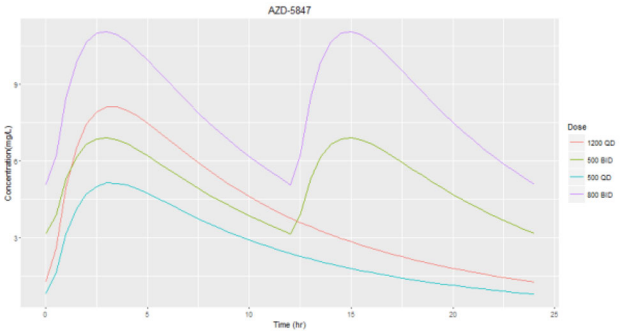

M-02

Population Pharmacokinetic Analysis of ABT-493 Exposures in HCV-Infected Subjects

Aksana K. Jones[1,*], Chih-Wei Lin[1], Wei Liu[1], Sandeep Dutta[1]

[1]Clinical Pharmacology and Pharmacometrics, AbbVie

Objectives: To characterize population pharmacokinetics of ABT-493, a nonstructural protein 3/4 A protease inhibitor discovered by AbbVie and Enanta, in HCV genotypes 1 to 6 subjects when co-administered with ABT-530, a nonstructural protein 5A inhibitor. Identify demographics, pathophysiologic, and treatment factors that impact the exposure.
Methods: Plasma concentration samples from 641 subjects enrolled in 4 Phase 2 studies were analyzed using non-linear mixed-effects modeling using NONMEM 7.3. One, two and three compartment models were explored for structural model development. To characterize the greater than dose-proportional increase in ABT-493 exposure, a dose-dependent relative bioavailability was incorporated into the structural model. Both, categorical and continous measures for demographics, pathophysiologic and treatment factors were tested for their effects on ABT-493 pharmacokinetics. Model evaluation and validation techniques were used to assess adequacy and robustness of the pharmacokinetic models.
Results: A two-compartment PK model with first-order absorption and elimination optimally described the ABT-493 concentration-time

profile. The ABT-493 model-predicted concentration-time profile was comparable to the median (IPRED) profile of the observed data (Figure, left). A polynomial function fitted to the log-transformed AUC values was used to describe the non-linear dose-dependent increase in ABT-493 exposures (Figure, right). The identified sources of variability in the population pharmacokinetics were: body weight on volume of distribution (10% increase per 10 kg increase), and cirrhotic status on bioavailability (increased to 2.2 fold in cirrhotics). Genotype and ABT-530 dose were not significant factors. The population mean estimates (at the model's reference covariate value) of ABT-493 CL/F was 1090 L/day and V2/F was 134 L.

Conclusions: The population pharmacokinetic model described the concentration-time profiles, as well as the non-linearity and variability of ABT-493 across ABT-493 doses, in HCV infected subjects with or without cirrhosis well. Genotype and ABT-530 dose have no impact on ABT-493 exposures.

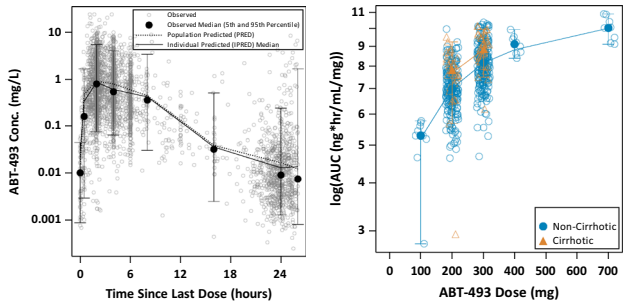

Figure 1 Observed and Model-Predicted ABT-493 Concentration Versus Time (Time After Last Dose) Profile for 300/120 mg ABT 493/ABT 530 (*Left*) and Log-Transformed AUC Versus ABT-493 Dose (*Right*). *Left Panel*: Gray circles: individual subject concentration; *Black Circles* and *Error Bars*: median of the observed binned concentrations and 5th and 95th percentile; *Black Line* (*solid*): model-predicted individual (IPRED) median concentration-time profile; *Black Line* (*dotted*): model-predicted population (PRED) median concentration-time profile. *Right Panel*: *Open blue circles* and *yellow triangles* represent individual observed AUC values for non-cirrhotic and cirrhotic subjects, respectively. *Filled blue circles* and *yellow triangles* with error bars respresent the median and 5th and 95th percentile of observed data for non-cirrhotic and cirrhotic subjects, respectively. *Solid blue and yellow line* represent the model fit for non-linearity for non-cirrhotic and cirrhotic subjects, respectively (Color figure online)

M-03

Population Pharmacokinetics of a Pangenotypic NS5A inhibitor, ABT-530, in HCV infected Patients with and without Cirrhosis : A Pooled Analysis from Phase 2 Studies

Aksana K. Jones[1,*], Chih-Wei Lin[1], Wei Liu[1], Sandeep Dutta[1]

[1]Clinical Pharmacology and Pharmacometrics, AbbVie

Objectives: ABT-530 in combination with ABT-493 is a novel 2 direct-acting antiviral agents (DAA) combination being developed for the treatment of HCV genotypes 1 to 6. The purpose of this analysis was to characterize the population pharmacokinetics of ABT-530 and explore demographics, pathophysiologic, and treatment factors that may impact ABT-530 exposure.

Methods: Population pharmacokinetic models were built using non-linear mixed-effects modeling approach in NONMEM 7.3. ABT-530 concentration data from 634 subjects from 4 Phase 2 studies were analyzed. Categorical and continous measures for demographics, pathophysiologic and treatment factors were tested for their effect on ABT-530 exposure. Model evaluation and validation techniques were used to assess adequacy and robustness of the pharmacokinetic models.

Results: Observed ABT-530 pharmacokinetic profile was well characterized by a two-compartment PK model with first-order absorption. An Emax function for relative bioavailability was used to characterize the dose-dependent non-linear increase in ABT-530 exposure (Figure, left) and the effect of ABT-493 on ABT-530 bioavailability. The identified sources of variability were sex on apparent clearance (21% higher in male) and body weight on apparent volume of distribution (9% increase per 10 kg increase). These effects on ABT-530 exposures were minimal and not clinically meaningful. Prediction corrected visual predictive checks indicated that the final model incorporating these covariates described the central tendency of the data well and the variability of the data adequately (Figure, right). The non-parametric bootstrap evaluation demonstrated good agreement with the estimated parameter values. The population mean estimates (at the model's reference covariate values) of ABT-530 CL/F was 6520 L/day and V2/F was 1270 L.

Conclusions: The ABT-530 population pharmacokinetic model provided robust characterization of the observed ABT-530 exposures in HCV infected patients. None of the tested covariates have clinically meaningful impacts on ABT-530 exposure and do not require dose adjustment.

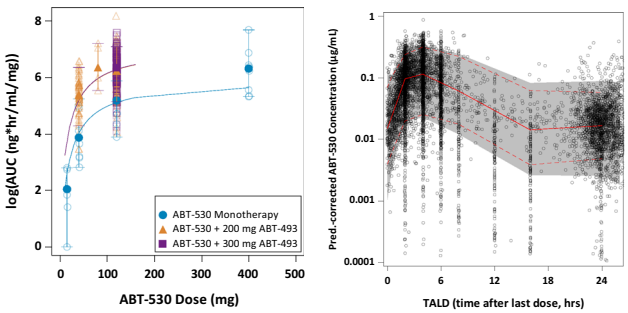

Figure 1 Log-transformed AUC Versus ABT-530 Dose (*Left*) and Prediction Corrected Visual Predictive Check (*Right*). *Left Panel*: *Open symbols* represent individual observed AUC values, filled symbols with error bars respresenting the median and 5th and 95th percentile. *Solid lines* represent the model fit for non-linearity. *Right Panel*: *Open circles* represent prediction corrected observed ABT-530 concentrations. The *shaded gray area* represents the 90% prediction interval of the prediction corrected simulated ABT-530 concentrations. The *solid red line* represents median, the *dashed red lines* represent the 5th and 95th percentile of the prediction corrected observed ABT-530 concentrations (Color figure online)

M-04

Understanding and Characterizing the Bystander Effect for Antibody Drug Conjugates

Aman P. Singh[1], Sharad Sharma[1], Dhaval K. Shah[1]

Kapoor Hall, Department of Pharmaceutical Sciences, School of Pharmacy and Pharmaceutical Sciences, University at Buffalo

Background: Once processed by the Antigen-positive (Ag+) cells, Antibody-drug conjugates (ADCs) can release cytotoxic drug molecules that can diffuse into the neighboring antigen-negative (Ag-) cells to induce their cytotoxicity. This additional efficacy of ADCs is known as the 'bystander effect'. Although widely acknowledged, the

rate and extent of the bystander killing is not quantitatively understood yet.

Objectives: The objectives of this research was to develop an *in vitro* PK-PD model linking the extracellular and intracellular concentrations of ADC to characterize the observed rate and extent of bystander effect in a coculture system of Ag+ and Ag- cells.

Methods: Trastuzumab-vc-MMAE, with an average DAR of 4 was synthesized and characterized. A coculture system was created with different HER2 expressing cell lines as Ag+ cells and GFP-transfected MCF7 cells as Ag- cells. Total cell count was assessed by MTT assay and GFP-MCF7 cell count was assessed by measuring the fluorescence. Analytical methods were developed to quantify total Trastuzumab, free MMAE and total MMAE concentrations in media and cell lysate. Cell viability experiments were performed in the presence of T-vc-MMAE in different cocultures and was mathematically characterized. Cellular disposition studies were performed in N87 and GFP-MCF7 cells, where a single cell disposition model was used to quantitatively characterize concentrations of different analytes of T-vc-MMAE.

Results: Cell viability experiments revealed that the extent of bystander effect increases with increasing fraction of Ag+ cells as well as increasing HER2 expression on Ag+ cells. A notable lag time was also observed prior to significant bystander killing. PD modeling analysis also suggested that the bystander effect of the ADC can dissipate over the period of time as the population of Ag+ cells decline. Cellular disposition studies revealed a significant binding of MMAE to tubulin resulting in retention inside the cell. Individual cellular PK models in two cell lines were then combined together to describe the disposition of T-vc-MMAE in a coculture system.

Conclusion: A novel single cell PK model for two cell lines was developed to characterize the bystander effect data. In future, the model will be integrated with a tumor disposition model (1) to characterize ADC exposures in a heterogeneous tumor.

Reference

1. Singh AP, Maass KF, Betts AM, Wittrup KD, Kulkarni C, King LE, et al. Evolution of Antibody-Drug Conjugate Tumor Disposition Model to Predict Preclinical Tumor Pharmacokinetics of Trastuzumab-Emtansine (T-DM1). The AAPS journal. 2016.

M-05

Physiologically Based Pharmacokinetic (PBPK) Modeling of Meropenem Pharmacokinetics in Healthy and Renally Impaired Adults

Andrew Castleman and Joel S Owen

Union University School of Pharmacy, Jackson, TN

Objectives: Develop a PBPK model for intravenous meropenem administered to healthy adults and adults with impaired renal function validated by reported data from literature. Further development is planned to incorporate dialysis as an additional route of elimination.

Methods: Meropenem's pharmacokinetics were simulated using the PBPKPlus™ Module of GastroPlus™ 9.0, and data were collected from published tables and graphs using GetData Graph Digitizer 2.24. The Population Estimates for Age-Related (PEAR) Physiology™ module was used to generate physiologies matching the average demographics (gender, weight and age) of the subjects from which data were obtained. Physiological and physiochemical parameters were predicted by GastroPlus™ or obtained from literature. No parameters were optimized. Total clearance consists of renal and non-renal mechanisms. Clearance values were estimated by equations derived from linear regression relating renal (CLr: mL/min) and total clearance (CL: mL/min) of meropenem to subjects' creatinine clearances (CrCl: mL/min). The difference of the renal and total clearance was assumed to be hepatic clearance.

Results: A single PBPK model was able to accurately predict the plasma concentrations of healthy adults (250-1000mg) and renally impaired adults (500mg) after intravenous meropenem administration. All predicted AUCs were within a 2-fold range of literature reported AUC values as shown in Table 1. Linear regression resulted in the equations used for clearance: CLr=1.877xCrCl-6.792 (R^2=0.95) and CL=2.255xCrCl+25.7 (R^2=0.89).

Table 1 Comparison of Literature and Simulated AUC Values

Dataset	Average Literature AUC (μg h/L)	Simulated AUC (μg h/L)	Simulated/ Literature
CrCl 6.1 mL/min	203	193.7	0.95
CrCl 12.1 mL/min	186.8	169.4	0.91
CrCl 17.1 mL/min	149.5	126.7	0.85
CrCl 34 mL/min	82.2	90.9	1.11
CrCl 61 mL/min	36.6	66.5	1.82
Healthy (250 mg)	14.4	14.1	0.98
Healthy (500 mg)	31.2	29.9	0.96
Healthy (500 mg)	58.3	38.6	0.66
Healthy (1000 mg)	66.9	75.7	1.13

Conclusions: Using linear equations to define the clearance terms of the PBPK model resulted in accurate predictions of meropenem pharmacokinetics in healthy and renally impaired adults. This model is suitable for further development to explore dialysis as an elimination pathway.

References

1. Bax RP, B. W. (1989). The Pharmacokinetics of Meropenem in Volunteers. *Journal of Antimicrobial Chemotherapy*, Suppl A 311-320.
2. Blumer. (1997). Meropenem: Evaluation of a New Generation Carbapenem. *International Journal of Antimicrobial Agents*, 73-92.
3. Craig. (1997). The Pharmacology of Meropenem, A New Carbapenem Antibiotic. *Clinical Infections Diseases*, S266-75.
4. Mouton JW, v. d. (1995). Meropenem Clinical Pharmacokinetics. *Clinical Pharmacokinetics*, 275-286.

M-06

Incorporation of Neuropsychiatric Inventory (NPI) Symptom Scores in an Alzheimer's Disease Simulation Model

Anuraag Kansal[1], Ali Tafazzoli[1], Divya Moorjaney[1], Peter Lockwood[2], Charles Petrie[3], Alexandra I. Barsdorf[3]

[1]Evidera, Bethesda, MD; [2] Pfizer, Groton, CT; [3]Pfizer, New York

Objectives: The behavioral and psychological symptoms (e.g., depression, anxiety, and irritability) of patients with dementia (BPSD) are a source of significant distress and poor quality of life to patients and their caregivers. BPSD are often measured with the Neuropsychiatric Inventory (NPI) which assess 12 symptoms based on caregiver information. The NPI outcome is usually expressed as the sum of the individual symptom scores. Evaluation of each symptom is useful when assessing the value of a therapeutic intervention on health economic outcomes, caregiver burden, or psychiatric medication use. Our objective was to update an established model of the NPI total score that was part of an Alzheimer's health economic model with one based on individual symptom scores.
Methods: NPI subscale correlation matrices were developed using baseline placebo NPI data on 954 patients extracted from several Alzheimer's clinical trials and a published confirmatory factor analysis (CFA) based on longitudinal data. A bounded distribution was assigned to each subscale based on the sample mean and standard deviation of a given NPI symptom score. Cholesky decomposition and multivariate sampling were used to simulate a dataset of subject level correlated NPI symptom scores. The NPI symptom scores, along with other disease markers (e.g., ADAS, MMSE) were then used to predict Alzheimer's disease progression.
Results: The correlation matrix derived from the clinical trial data agreed well with the matrix derived from the published CFA, and the simulation reproduced those correlations well (Figure 1). The strongest correlations were observed between the following subscales: agitation-irritability (0.50), anxiety-depression (0.40), delusion-hallucination (0.38), and irritability-depression (0.34). No negative correlations between subscales were identified.
Conclusions: Our method allows for characterization of individual neuropsychiatric symptom scores. Alzheimer's disease (AD) simulation models can incorporate this approach to explore the impact of treatments that may impact components of the NPI.

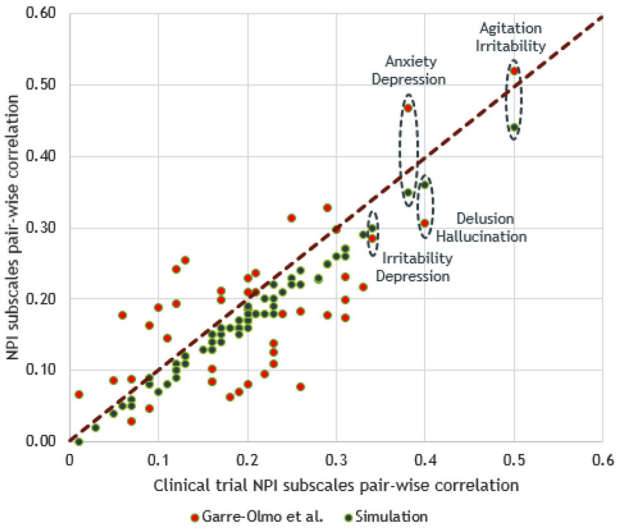

Figure 1 NPI subscales pair-wise correlations from the clinical trial are spread narrowly around the 45 degree diagonal line once compared against the simulated and the published Garre-Olmo et al. pair-wise correlations. This observation supports the generalizability of the proposed correction structure in this model and further highlights the accuracy of the simulation approach in generating correlated NPI subscales (Color figure online)

Reference

1. Garre-Olmo J et al. Journal of Alzheimer's Disease 22.4 (2010)

M-07

PK/PD modeling predicts robust target engagement and low probability of grade 4 hematological toxicity at recommended phase 2 starting dose of VX-970 in combination with carboplatin (AUC=5)

Brian Hare[1], Eric Haseltine[1], Marina Penney[1], Lakshmi Viswanathan[1], Jessica Brown[2], Mahesha Ganegoda[2], John Pollard[3], Tim Yap[2], Scott Z. Fields[1]

[1]Vertex Pharmaceuticals Incorporated, Boston, MA, USA; [2]Drug Development Unit, Royal Marsden Hospital and The Institute of Cancer Research, London, UK; [3]Vertex Pharmaceuticals Limited, Milton Park, UK.

Objectives: Perform model-based analyses of 1) preclinical pharmacokinetics (PK) and target engagement (TE) biomarker data and 2) PK and safety data from a phase 1 dose escalation trial of VX-970 in combination with carboplatin.
Methods: The exposure-response relationship between plasma PK and phosphorylated Chk1 (a TE biomarker for VX-970) in tumors was modeled using data from experiments in tumor-bearing mice dosed with VX-970 in combination with a DNA-damaging agent. The human phosphorylated Chk1 response was predicted using plasma PK of VX-970 in humans. PK/PD models for neutropenia and thrombocytopenia were developed using data from the phase 1 trial and a published model structure[1].
Results: Estimated plasma IC50 for VX-970 inhibition of Chk1 phosphorylation from preclinical experiments is 76 ng/ml (95% CI 42–108). Human VX-970 doses $\geq$90 mg/m^2 are predicted to achieve >75% inhibition of Chk1 phosphorylation. At 90 mg/m^2, preliminary clinical evidence of target modulation was reported[2]. Furthermore, exposures equivalent to the human dose of 90 mg/m^2 led to tumor regression in preclinical models. Models of hematological toxicity identified exposure response relationships and predicted a risk for grade 4 toxicity of <5% and <1% for neutropenia and thrombocytopenia, respectively, at 90 mg/m^2 VX-970 in combination with carboplatin (AUC=5). These rates of hematological toxicity are similar to predictions for carboplatin alone[2].
Conclusions: Modeling predicts robust target engagement and low probability of grade 4 hematological toxicity at the recommended starting phase 2 dose of 90 mg/m^2 VX-970 in combination with carboplatin (AUC=5).

References

1. Friberg et al., J. Clin. Oncology, 20:4713-4721, 2002
2. Yap TA, et al., Abstract PR14. AACR-NCI-EORTC, Boston, MA, November, 2015
3. Schmitt et al., J. Clin. Oncology, 28: 4568-4574, 2010

M-08

Mechanistic Modeling with DILIsym® Predicts Species Differences in CKA via Multiple Hepatotoxicity Mechanisms

Christina Battista[1], Kyunghee Yang[2], Jerome Mettetal[3], Simone Stahl[4], Paul Watkins[1], Brett Howell[2], Scott Siler[2]

[1]UNC-Chapel Hill, Chapel Hill, NC; [2]DILIsym Services, Inc., Research Triangle Park, NC; [3]AstraZeneca, Cambridge, MA; [4]AstraZeneca, Cambridge, UK

Objectives: To predict species differences in CKA-mediated hepatotoxicity using DILIsym®, a mechanistic model of drug-induced liver injury (DILI).
Methods: Inhibitory effects of CKA on bile acid (BA) and bilirubin transporters were assessed using transporter-overexpressing vesicles and cells. CKA-mediated oxidative stress and mitochondrial dysfunction were determined in HepG2 cells. These in vitro data were used to define hepatotoxicity parameters and combined with PBPK sub-model simulations of hepatic compound exposure to predict DILI in DILIsym®. Previously constructed human and rat simulated populations (SimPops™) that incorporate variablity in the aforementioned toxicity mechanisms were utilized to determine the impact of inter-individual variability upon administration of single CKA doses of 900mg and 500 mg/kg, respectively.
Results: CKA induces oxidative stress (oxidative stress production rate constant=7278mL/mol/hr human, 9705mL/mol/hr rat) and inhibits mitochondrial electron transport chain (ETC) flux (ETC inhibition coefficient=14.2mM human, 1.42mM rat). CKA inhibits human BSEP (IC_{50}=129.7μM), rat Bsep (IC_{50}=94μM), human MRP3 (IC_{50}=11.2μM), human NTCP (IC_{50}=19.5μM), rat Mrp2 (IC_{50}=68.5μM), and human OATP (IC_{50}=0.84μM)[1]. CKA was modeled as a noncompetitive inhibitor of BSEP/Bsep and MRP3/Mrp3 and a competitive inhibitor of NTCP/Ntcp. Due to lack of data, IC_{50} values for NTCP/Ntcp, MRP3/Mrp3, MRP2/Mrp2, and OATP/Oatp were assumed the same across species. Human SimPops™ predicted modest increases <1.5x upper limit of normal (ULN) in serum ALT, recapitulating the clinical data. Rat SimPops™ predicted ALT elevations >3xULN in 36.4% of the population, slightly underpredicting the 75% observed in preclinical trials (Figure 1). DILIsym® recapitulated preclinical observations in bilirubin increase due to both DILI and bilirubin transporter inhibition. Rat SimPops™ predicted increases in total bilirubin >2xULN for 100% of the population, mirroring preclinical data. Conversely, no significant increases in bilirubin were observed in human SimPops™, consistent with clinical observations.
Conclusions: Using in vitro data to determine toxicity parameters, DILIsym® accurately predicted CKA hepatotoxicity in rats and not in humans, consistent with observed preclinical and clinical data.

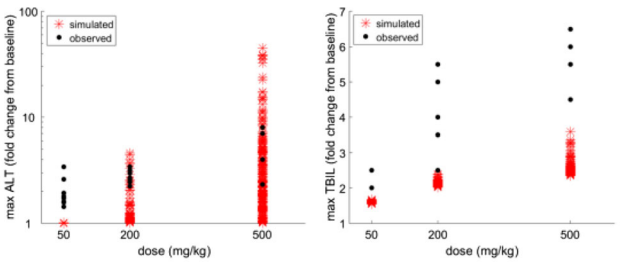

Figure 1 Simulated and observed peak serum ALT levels (*left*) and peak total bilirubin levels (*right*) in rats administered 50, 200, or 500 mg/kg CKA (Color figure online)

Reference

1. Ulloa et al. NMR Biomed. 26:1258—1270,2013.

M-09

A Quantitative Systems Pharmacology Platform of Brain and Serum Progranulin (PGRN) to Investigate Targets in Frontotemporal Dementia (FTD)

Christina M. Friedrich[1], James Soper[2], Colleen M. Witt[1], Meghan M. Pryor[1], Lauren Martens[2], Dooyoung Lee[2], Kelley Larson[2], Matthew Townsend[2], Cuyue Tang[2], Holger Patzke[2], Gerhard Koenig[2]

[1]Rosa & Co., LLC, 751 Laurel Street, Suite 127, San Carlos, CA 94070; [2]FORUM Pharmaceuticals Inc., 225 Second Ave., Waltham, MA 02451, USA

Objectives: Frontotemporal dementia (FTD), the second most common form of neurodegenerative dementia, is characterized by extensive neuronal loss, TDP-43 pathology, and gliosis. FTD can be caused by loss of function mutations in the *GRN* gene that results in a haploinsufficiency of the progranulin (PGRN) protein. Therapies are being developed to restore the expression and distribution of PGRN. Here, we describe the development of a PGRN PhysioPD™ Research Platform, a graphical and mathematical model of PGRN production, uptake, clearance, and transport in brain and periphery.
Methods: Platform development quantitatively integrated public and proprietary data sets into a mechanistic representation of PGRN dynamics. Key results were reproduced in simulated experiments.
Results: Platform development led to interesting insights, including:

1. Microglial PGRN production far exceeds neuronal PGRN production on a per cell basis, yet neuronal PGRN production *in vivo* contributes significantly to total brain PGRN concentration due to the higher numbers and longer PGRN intracellular half-life of neurons relative to microglial cells.
2. Modeling of two proprietary datasets revealed an apparent inconsistency in the intracellular half-life of PGRN in neurons. To reconcile the apparent conflict, the team formulated and tested hypotheses, revealing insights about neuronal PGRN production and uptake.
3. There are significant differences in PGRN dynamics in periphery vs. brain, suggesting that caution should be used in interpreting serum PGRN level as a biomarker for brain PGRN level. A recent study appears to support this modeling research insight (Wilke et al. Curr Alzheimer Res. 2016;13(6):654-62).

Conclusions: The PGRN PhysioPD Research Platform has proven useful to simulate the effects of modulating different targets and investigating drug effects on increasing PGRN for the treatment of FTD.

M-10

Synthesis of a Combined Neutropenia and Lymphopenia Model in Response to Chemotherapy

Christine Carcillo[1,*], Eugene J. Koay, MD, PhD[2], Robert S. Parker, PhD[1]

[1]University of Pittsburgh, Pittsburgh, PA; [2]The University of Texas MD Anderson Cancer Center, Houston, TX

Objectives: To build a biologically-motivated model of neutrophil and lymphocyte response to a standard dose of [DRUG] chemotherapy. The model structure is derived from the interactions in the hematopoiesis lineage tree, allowing the simultaneous assessment of mono- or combination chemotherapy that results in multiple hematological toxicities.
Methods: The model was built similarly to Friberg et al. [1] where a set of ordinary differential equations use a transit rate parameter to

mimick the lifespan of the cell type. Changes in circulating cell count signal a feedback response to the progenitor cells as cell count drops post chemotherapy. This model joins the neutrophils and lymphocytes under one common progenitor state, consistent with biology. Any pharmacokinetic model and dosing schedule can be used as an input to the model. The model was built in Pyomo and can be fit to data using IPOPT [2].

Results: Fifteen differential equations capture the dynamics behind chemotherapy-induced neutropenia and lymphopenia. The nadirs of both neutrophils and lymphocytes occur around 7 days post chemotherapy. The model can be fit to data by independently changing the transit rate parameters for neutrophils and lymphocytes. Independent chemotherapy kill effects can additionally act in N1 or L1 based on the neutropenic or lymphopenic potential of the drug(s), respectively (Figure 1).

Conclusions: The joint model of two hematological toxicities can be used to assess multiple drug combination effects with mixed or overlapping toxicity. The model is easily tailored to individual patient response fitting individual parameters (via IPOPT), and exogenous rescue agents (*e.g.*, G-CSF) that impact recovery and drug dosing can be incorporated into the parameterization or as additional blocks into the model diagram.

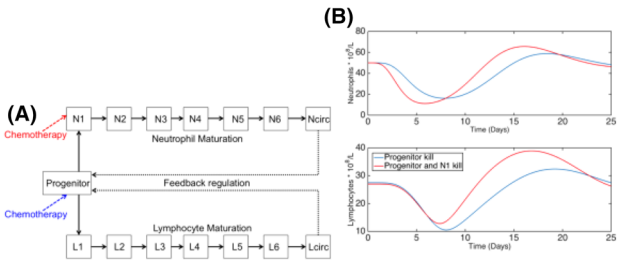

Figure 1 (A) Block diagram of model. Circulating neutrophils and lymphocytes provide feedback to common progenitor compartment. Chemotherapy kills progenitor states (*red*) impacting both cell types. (B) Neutrophils (*top*) and lymphocytes (*bottom*) over time after one dose of chemotherapy on day 0 (Color figure online)

References

1. Quartino, Angelica Linnea, Lena E. Friberg, and Mats O. Karlsson. *Investigational new drugs* 30.2 (2012): 833-845.
2. Wächter, Andreas, and Lorenz T. Biegler. *Mathematical programming* 106.1 (2006): 25-57.

M-11

Pharmacokinetics (PK) and exposure-response (E-R) analysis of Kadcyla (K) as a single agent or in combination with Perjeta (P) in patients with human epidermal growth factor receptor 2 positive (HER2+) metastatic breast cancer (MBC) who have not received prior chemotherapy for their metastatic disease

Dan Lu[1], Chunze Li[1], Daniel Polhamus[2], Jonathan French[2], Matthew Riggs[2], Priya Agarwal[1], Shang-Chiung Chen[1], Xin Wang[1], Melanie Smitt[1], Monika Patre[3], Alexander Strasak[3], Nataliya Chernyukhin[1], Angelica Quartino[1], Jin Yan Jin[1], Sandhya Girish[1]

[1]Genentech [2]Metrum Research Group [3] F.Hoffmann La Roche

Objectives: PK and E-R analysis for K and P was performed in a Phase III study to assess the efficacy and safety of K as a single agent or in combination with P as compared to Herceptin with taxane in first-line HER2+ MBC patients.

Methods: Post-hoc analysis using historical population PK models for K and P were performed to assess if there is any potential of drug interactions. Correlation of exposure with progression free survival (PFS), incidence of grade 3+ hepatotoxicity, thrombocytopenia and any adverse events were assessed by cox-regression, case matching or chi-square tests.

Results: Mean (± SD) trough concentrations of K conjugate at Cycle 1 day 21 was 1.36 ± 0.832 μg/mL (n=186) and 1.33 ± 0.772 μg/mL (n=189) for K alone and in combination with P. Mean (± SD) trough concentration at Cycle 1 day 21 for P was 64.89 ± 17.78 μg/mL (n=188). The PFS hazard ratio (HR) of patients in quartile 1, 2, 3 and 4 of K conjugate trough concentrations versus control is shown in Figure 1. There was no positive correlation between K exposure with safety endpoints, and no correlation between P exposure with efficacy and safety endpoints.

Conclusion: In conclusion, PK of K and P in first-line HER2+ MBC patients are similar to historical data. No impact of P on K PK and vice versa. Patients with K conjugate trough concentrations in Q1 have a trend of higher HR than others with overlapping confidence intervals.

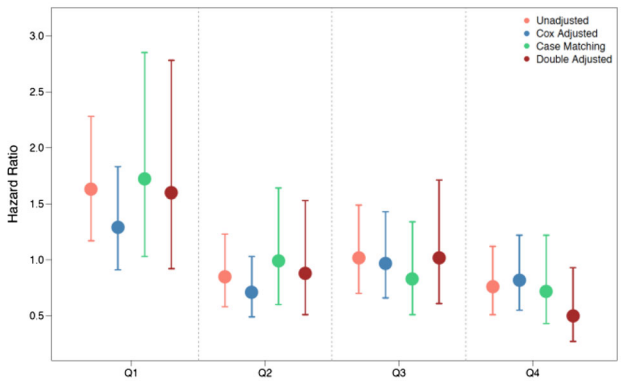

Figure 1 PFS HR of patients in quartile 1, 2, 3, 4 of K conjugate through concentrations versus control (Color figure online)

M-12

A Novel PK-Target Occupancy Link Model for a Covalent and Reversible Inhibitor of Bruton Tyrosine Kinase (BTK)

Dave RA[1], Smith P[2], and Karr D[3]

[1]University at Buffalo, NY, [2]D3 Medicine, NJ, [3]Principia Biopharma, CA

Objectives: Bruton's tyrosine kinase (BTK) is a key component of B cell receptor (BCR) signaling and functions as an important regulator of cell proliferation and cell survival in various B cell malignancies. Several small-molecule inhibitors of BTK have shown antitumor activity in animal models and, recently, in clinical studies [1, 2]. Ibrutinib, an irreversible covalent inhibitor, is currently the only FDA approved BTK inhibitor. PRN473 is a covalent and reversible inhibitor of BTK. The overall objective of this study was to develop a PK-BTK occupancy link modeling framework using the data for PRN473 in rats.

Methods: The model was developed using plasma concentration and splenocyte BTK occupancy data for 0.2-5 mg/kg IV and 10-30 mg/kg

PO doses of PRN473 in rats. The model was validated using the data for 2 mg/kg IV dose. Plasma concentrations were best captured by a two-compartment model with first order-absorption and linear disposition kinetics. The BTK occupancy was best captured by a model incorporating BTK expression and turnover as well as drug-BTK binding parameters. ID algorithm in ADAPT5 was implemented for model development.
Results: The model was able to reasonably capture both, plasma concentrations and BTK occupancy data, for PRN473. The estimated elimination rate was 10 hr^{-1}, which is consistent with the *in vitro* evidence of high hepatic metabolism. The estimated values of K_{ON} and K_{OFF} rates were 0.002 $((\mu g/L)^{-1} \times hr^{-1})$ and 0.00002 hr^{-1}, respectively. The residual variability in plasma concentrations and BTK occupancy was best described by a combined proportional and additive error model. The model was successfully validated as well.
Conclusion: We successfully developed a novel PK-BTK occupancy link modeling framework using the data for PRN473 in rats, which has application in evaluating PK-target occupancy relationships.

References

1. Hendriks, R.W., S. Yuvaraj, and L.P. Kil. Nat Rev Cancer, 2014. **14**(4)
2. Wang, Y., et al. Clin Pharmacol Ther, 2015. **97**(5)

M-13

A Mechanistic and Physiologically-Relevant PK/PD Model for the Drug of Abuse, γ-Hydroxybutyric Acid (GHB) in rats

Dave RA, Vijay N, Morse BL, and Morris ME

Department of Pharmaceutical Sciences, University at Buffalo, NY

Objectives: Overdose of gamma-hydroxybutyric acid (GHB) leads to coma, seizures, and death ^{due} to its direct binding to GABAB receptors in brain [1]. Atypical pharmacokinetics of GHB includes its saturable absorption, hepatic metabolism, and active renal reabsorption [1]. Monocarboxylate transporters (MCTs) [2], namely, MCT1, predominantly mediates active renal reabsorption [1] and uptake into the brain of GHB [3]. The pharmacodynamic endpoint of GHB intoxication is dose-dependent respiratory depression [4]. This study developed a mechanistic and physiologically-relevant PK/PD model for GHB in rats.
Methods: The model was developed using data for GHB plasma concentrations and cumulative amount excreted unchanged into urine as well as respiration frequency for IV bolus doses of 200, 600, and 1500 mg/kg in ADAPT 5. We extended our previously established PK model for GHB [5] to include GHB PD. The proposed PK/PD model for GHB consists of non-linear metabolism, MCT1-mediated renal reabsorption with physiologically-relevant concurrent fluid-reabsorption and uptake into the brain, and direct effects of binding of GHB to GABAB receptors on respiration frequency. The Michaelis-Menten affinity constant (KM) for metabolism, active renal reabsorption and uptake into brain were fixed to the observed *in vitro/in vivo* values. EC50 value of GHB binding to GABAB receptors was also fixed to the reported value of 82.8 μg/mL. The model was further validated using an independent data set for 600 mg/kg dose of GHB.
Results: The model reassembly captured the PK/PD of GHB and had a strong quantitative power. The estimated values (mean, %CV), 633 μg/min (4.2%), 2870 μg/min (9.7%), and 11.6 μg/min (7.3%) of Michaelis-Menten capacity parameters (VMAX) for metabolism, active renal reabsorption and uptake into brain, respectively, were, in agreement with the previously reported values. Model validation indicated the model was successfully validated.
Conclusion: We successfully developed and validated a mechanistic and physiologically- relevant PK/PD model for GHB in rats, which will be used to evaluate potential treatment strategies in GHB overdose in future.

References

1. Morris, M.E., K. Hu, and Q. Wang. J Pharmacol Exp Ther, 2005. **313**(3)
2. Morris, M.E. and M.A. Felmlee. AAPS J, 2008. **10**(2)
3. Roiko, S.A., M.A. Felmlee, and M.E. Morris. Drug Metab Dispos, 2012. **40**(1)
4. Morse, B.L., N. Vijay, and M.E. Morris. AAPS J, 2014. **16**(4)
5. Dave, R.A. and M.E. Morris. J Pharmacokinet Pharmacodyn, 2015. **42**(5)

M-14

Quantification of the modulation of Aβ oligomers following secretase inhibition - A systems pharmacology approach

Eline M.T. van Maanen[1,2], Tamara van Steeg[2], Juliya Kalinina [3], Julie Stone[3], Maria S. Michener[3], Mary J. Savage[3], Eric M. Parker[3], Meindert Danhof[1]

[1]LACDR, Leiden University, The Netherlands; [2]LAP&P, Leiden, The Netherlands; [3]Merck Research Laboratories, Whitehouse Station, NJ

Objectives: Previously, a systems pharmacology model of the amyloid precursor protein (APP) processing pathway was developed to characterize APP metabolite (sAPPβ, sAPPα, Aβ40, Aβ42) responses to BACE1 inhibition [1]. Using information from monomeric Aβ species, an Aβ42 oligomer pool was identified in the model. In the current study, Aβ oligomer (AβO) levels in CSF were quantified using an assay that had become available [2]. The objectives of the investigation were: (1) To elucidate the relationship between the oligo pool in the model and measurements of AβO; (2) To confirm that AβOs dissociate to restore the equilibrium between Aβ monomers and AβOs, following secretase inhibition.
Methods: Data on six biomarkers (sAPPβ, Aβ40, Aβ42, Aβ38, AβO, sAPPα) measured in CSF in cisterna-magna-ported rhesus monkeys receiving vehicle, BACE1 (MBi-5; 30, 125 mg/kg) or GS (L675; 240 mg/kg) inhibitors in a 4-way crossover design were available. Non-linear mixed effects modeling (NONMEM) was used to analyze the time course of the changes in the biomarkers on the basis of the underlying biological processes, using a comprehensive biomarker model (Figure 1).
Results: The APP systems model [1] was extended to describe Aβ38 and AβO response measurements to BACE1 inhibition in CSF. The comprehensive biomarker model quantified the response of all six biomarkers to BACE1 inhibition, using one drug effect term. This yielded pertinent information about the relationship between monomeric Aβ species and AβOs.
Conclusions: Decreases in monomeric Aβ responses resulting from BACE1 inhibition are partially compensated by dissociation of AβOs, suggesting that BACE1 inhibition reduces the putatively neurotoxic oligomer pool. Characterization of AβO modulation following GS inhibition is being further evaluated.

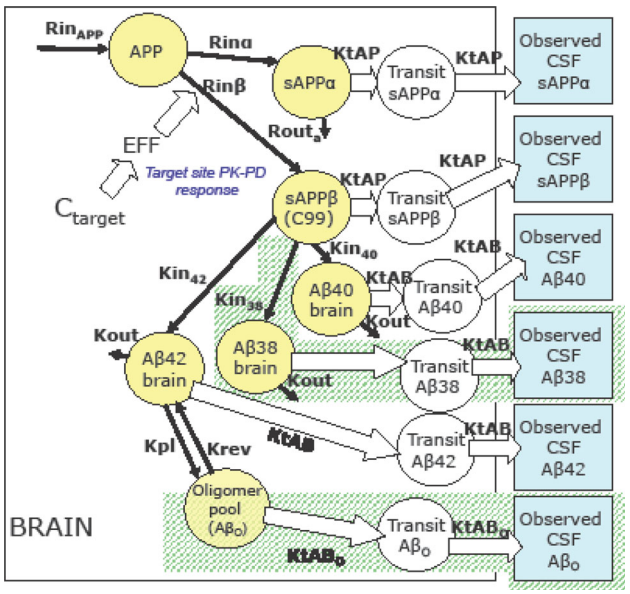

Figure 1 Schematic of systems model of APP processing. The model comprised thirteen compartments: Seven biomarker compartments in brain (*yellow circles*) and six transit compartments from brain to CSF (*white circles*). Six biomarkers were measured in CSF (sAPPα, sAPPβ, Aβ42, Aβ38 and $A\beta_O$), indicated by *blue boxes*. The drug effect (*EFF*) inhibited *Rinβ*. As driver of biomarker response C_{target} was used, which was derived from the PK model [1]. sAPPβ was used in the model structure as a surrogate substrate for C99 in the γ-secretase cleavage step. Additions to the model structure compared to the model previously presented [1] are indicated with the green shaded area. *APP*: Aβ-precursor protein; *Aβ*: amyloid-β-peptide; C_{target}: drug concentration target site; Kin_{38}: *Aβ*38 formation rate; Kin_{40}: *Aβ*40 formation rate; Kin_{42}: *Aβ*42 formation rate; Kin_x: *Aβx* formation rate; *Kout*: *Aβ*38, *Aβ*40 and *Aβ*42 degradation rate; *Koutx*: *Aβx* degradation rate; *Krev*: Oligomerization rate; *KtAB*: transit rate *Aβ* from brain to CSF; $KtAB_O$: transit rate $A\beta_O$ from brain to CSF; *RinAPP*: source of APP; *Rinβ*: sAPPβ formation rate; *Rin*: sAPPα formation rate; *Rout*: sAPPβ degradation rate; *Rout*: sAPPα degradation rate (Color figure online)

References

1. Van Maanen EMT, et al. (2016) J Pharmacol Exp Ther 1:205–16.
2. Savage MJ et al. (2014) J Neurosci 34:2884–97.

M-15

Performance Characteristics of NONMEM Parallelization

Evan Wang[1], Michael Heathman[1]

Eli Lilly and Company, Indianapolis, IN

Objectives: To understand the dependence of NONMEM runtime on the number of cores used and dataset size, for models of varying complexity. This can be used to determine the optimum number of cores for the fastest runtime or highest computational efficiency.
Methods: Benchmark runtimes and literature [1] were used to build a model for NONMEM runtime as a function of the number of cores used and dataset size. To evaluate the ability of the model to fit and ultimately predict NONMEM runtimes, benchmark NONMEM estimations were performed using a "simple" two-compartment pharmacokinetic model (FOCEI) and a "complex" one-target quasi-steady-state TMDD model [2] (FOCEI, IMPMAP, SAEM), representing the two extremes of runtime performance and efficiency. A series of dataset sizes and number of cores (up to 96 cores) was used. All data were simulated in order to ensure dataset homogeneity. All NONMEM models were run multiple times to average out the effects of network traffic.
Results: Predictions for the simple and complex models clearly demonstrate that the runtime model is flexible enough to capture the runtime dependence on cores and dataset size, including a non-monotonic runtime profile. An analytical solution for the number of cores corresponding to the minimum runtime was also derived using the model. With a few benchmark runs, users can apply this model to (1) map out the relationship between the number of cores and runtime, relative speedup, and computational efficiency and (2) find the number of cores that will result in the fastest runtime or highest efficiency.
Conclusions: For computationally expensive models, runtime profiling to determine the optimum number of cores is a worthwhile exercise, particularly in cases where a large number of models will need to be run.

References

1. Beal et al. NONMEM Users Guide. 2013.
2. Gibiansky et al. J. Pharmacokinet. Pharmacodyn. 2012, 39:17-35.

M-16

Predicting End-of-trial Fasting Glucose and HbA_{1c} via Mechanistic PK/PD Modeling based on Longitudinal Type 2 Diabetes Trial Data

Felipe K. Hurtado[1], Parag Garhyan[2], Jenny Y. Chien[2], Stephan Schmidt[1]

[1]Center for Pharmacometrics & Systems Pharmacology, University of Florida, Orlando, FL; [2]Global PK/PD & Pharmacometrics, Eli Lilly and Company, Indianapolis, IN

Objectives: The goal of this work was to develop and qualify a mechanism-based drug-disease modeling platform for type 2 diabetes mellitus (T2DM) that links drug-induced changes in fasting serum insulin (FSI) and fasting plasma glucose (FPG) to changes in the well accepted endpoint glycosylated hemoglobin A1C (HbA_{1c}).
Methods: Patient-level data from a combined database of clinical trials (4,249 patients, 37 arms) following placebo, mono, and combination therapy with metformin, sulfonylurea, thiazolidinedione was used to step-wise develop and qualify a drug-disease model for T2DM in NONMEM v7.3. First, the dynamic interplay between FSI, FPG, and HbA_{1c} was characterized by using cascading turnover models with negative feedback/feed forward mechanisms. Second, disease progression was modeled as a change from the patient's baseline beta-cell function loss. Finally, a log-linear relationship was used to characterize drug effect(s) following mono and combination therapy at different dose levels and placebo.
Results: This drug-disease model was able to characterize changes in FSI, FPG, and HbA_{1c} as the result of disease progression and/or therapeutic intervention in 4,249 patients receiving single or combination anti-hyperglycemic therapy for up to 104 weeks reasonably well. Body mass index, age, gender, and beta-cell function at baseline were identified as significant covariates for treatment response. In addition, treatment effects on disease progression were found to be additive for these 3 drugs. Longitudinal FSI, FPG and HbA_{1c} data

from short- and mid-term duration trials informed the magnitude of treatment effect, while long-term trials (≥52 weeks) informed the effects of underlying disease progression.

Conclusions: A drug-disease modeling platform for T2DM was developed that integrates information on clinically-relevant biomarkers, disease state and progression, treatment effects as well as covariates into a single, unified model. The mechanistic nature of this model allows for evaluation of drugs with novel mechanisms of action on disease progression.

M-17

Development of a PK/PD framework for Scopolamine-Induced Cognitive Impairment

Francesco Bellanti[1], Claire H Li[2], Han Witjes[1], Thomas Kerbusch[1], Jason M Uslaner[3], Arie Struyk[4], Mark S Forman[4], Marissa F Dockendorf[2], and Sreeraj Macha[2]

[1]Quantitative Solutions – A Certara Company, Oss, Netherlands; [2]Quantitative Pharmacology and Pharmacometrics, Merck & Co., Inc., Kenilworth, NJ, USA; [3]Pharmacology, Merck & Co., Inc., Kenilworth, NJ, USA; [4]Translational Pharmacology, Merck & Co., Inc., Kenilworth, NJ, USA

Objectives: To evaluate PKPD relationships of cognition endpoints assessed in scopolamine challenge studies using donepezil as a test drug to reverse scopolamine-induced impairment and to explore alternative trial designs.

Methods: Five Phase I, placebo controlled studies were pooled for the analysis of PK and PD data including Detection time (DET), Groton Maze Learning (GML) and Continuous Paired Associate Learning (CPAL) endpoints from 159 healthy volunteers receiving 0.5 or 0.8 mg scopolamine and 10 mg donepezil. Population PKPD models were developed for both scopolamine and donepezil and linked to the PD response. All endpoints shared a similar structural model: an indirect effect model with an effect compartment accounting for the dissociation between scopolamine PK and the PD measurements. Scopolamine effect was assumed to be proportional to baseline; similarly donepezil effect was assumed to be proportional to scopolamine. The population analyses along with the simulations for the optimization of scopolamine challenge studies were performed using the NLME modeling approach with the software package NONMEM, v7.2.

Results: Both scopolamine and donepezil PK were described by a two-compartmental model with first order absorption and lag time. Scopolamine exposure-response (ER) relationships were modeled in a linear fashion; whereas, given the flat PK profile of donepezil, its effects were assumed to be constant within the investigated time frame. The median [95% CI] donepezil effect in attenuating the scopolamine-induced cognition impairment was estimated to be 27.4% [26.1-28.8] for DET and 42.6% [34.5-50.6] for GML. Visual Predictive Checks show the adequacy of the PKPD models in describing both time-course and variability of DET and GML (Figure 1). Poor and inconsistent response in the case of CPAL did not allow an adequate characterization of the ER relationship for this endpoint. Furthermore, simulations show that 0.8 mg scopolamine, as compared to the commonly used 0.5 mg scopolamine, provides roughly a 2-fold increase in the population signal with a direct benefit on the relative effect size.

Conclusions: The PKPD relationships of DET and GML were succesfully characterized providing a framework that allows exploring alternative study designs for optimization of scopolamine challenge studies.

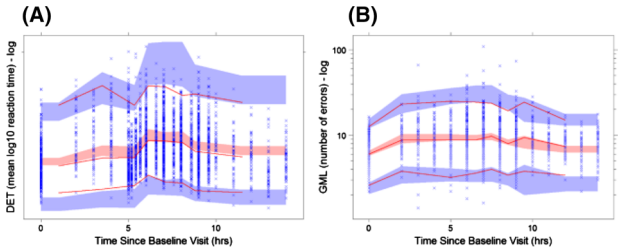

Figure 1 Visual predictive checks (VPC) of the PKPD models of detection time (A) and GML (B). *Blue symbols* represent the observed data; *red solid lines* represent median, 5th and 95th percentiles of the observed data; red shaded area represents the 95% CI of the stimulated median whereas the *blue shaded areas* represent the 95% CI of the simulated 5th and 95th percentiles (Color figure online)

M-18

Identification of Time-Varying CL in Population Pharmacokinetic Analysis: CWRES plot vs. Bayesian information criterion (BIC)

Haitao Yang[1*], Xu(Steven) Xu[2], Yan Feng[3],

University of Pittsburgh, PA; [2]Janssen Research & Development, NJ; [3]Bristol-Myers Squibb, NJ

Objectives: Graphic assessment has been widely used as diagnostics approach in population pharmacokinetic analysis (PPK) [1]. Diagnostic plot of weighted residual (CWRESI) vs. time is generally used to detect signal of time varying PK. We conducted model-based simulation analysis to evaluate whether CWRESI is sensitive for signal of time varying PK with clearance (CL) over time.

Methods: Concentration-time profiles in 500 virtual subjects were simulated by using a literature reported linear two-compartment PPK model with zero-order IV infusion and time-varying first-order elimination, for an IV administered monoclonal antibody. An E_{max} model was used to describe time varying CL. Simulation investigated CL change over time with different rate (slow to fast) and extent (mild to strong). The simulation scenarios in this analysis include: (1) Varying maximal CL decreased from 20% to 80% at a given rate of CL change (fix time of 50% of maximal effect (ET_{50}) to 60 days); (2) Varying rate of CL changes (ET_{50} = 10-600day) and fix the maximal decrease of CL to 80%; (3) Varying rate of CL changes (ET_{50} = 10-600day) and fix the maximal decrease of CL to 20%. BIC were calculated for model comparison.

Results: No time associated trend was observed in diagnostic plots (CWRESI vs. time) of PPK models with and without including time varying CL. BIC values in all simulations were lower in models with time varying CL than that in models without that, except the model with 20% maximal change of CL and ET_{50} =10 day. Difference of BIC values between models with and without accounting for time-varying CL increased when varying rate decrease.

Conclusions: Model evaluation using BIC or likelihood ratio test approach may be better choices for assessment of time-varying PK, as diagnostic assessment might not be sensitive to detect signal of CL change over time.

Reference

1. E. I. Ette and T. M. Ludden, Pharmaceutical Research, vol. 12, 1845–1855, 1995.

M-19

Challenges in Developing a Population Pharmacokinetic Model Describing the PK of Atazanavir and Supporting Dose Selection in HIV infected Pediatric Subjects

Heather Sevinsky,[1] Brenda Cirincione,[1] Joseph Raybon,[1] Vidya Perera,[1] Man Melody Luo,[1] Timothy Eley,[1] Donald E. Mager,[2] Scott VanWart,[2] Frank LaCreta,[1] Ihab Girgis[1]

[1]Clinical Pharmacology and Pharmacometrics, Bristol-Myers Squibb Company, Princeton, NJ 08540; [2]Enhanced Pharmacodynamics, LLC, Buffalo, NY 14203

Objectives: Atazanavir is a protease inhibitor used to treat HIV-1 infection. A previous 1-compartment population pharmacokinetic (PPK) model used to identify atazanavir doses for children was based on limited data in patients aged <6 months. The objective of this analysis was to revise the existing PPK model to better describe the time-course of atazanavir concentrations in a broader HIV-infected pediatric patient population.

Methods: Two pediatric clinical trials assessed the PK of ritonavir (RTV)-boosted atazanavir at doses that were identified in the original PPK model to provide exposures similar to adults [NCT0109957, NCT01335698]. The original PPK dataset was enriched with pediatric data from these 2 trials that included an additional 16 subjects aged <6 months. The original PPK model was re-evaluated and refined using the enriched dataset, including exploration of maturation functions (MAFs). Simulations were performed to support weight-based pediatric dosing recommendations.

Results: The original PPK model with the enriched dataset resulted in mis-specifications in the youngest subjects. The refined PPK model was a 2-compartment model with first-order absorption and linear elimination including MAFs to allow for an age-dependent non-linear decrease in ATV CL and bioavailability (F) due to RTV coadministration. The refined model was estimated well and adequately characterized atazanavir PK across all ages (Table 1). Simulations identified atazanavir doses that achieve similar exposures as adults.

Table 1 Parameter Estimates for Final 2-Compartment Model

Parameter	Estimate	Standard error (RSE%)	95% CIs
Fixed Effects			
Ka [1/hr]	2.14	0.273 (12.8)	(1.6, 2.68)
CL [L/hr]	36	3.53 (9.81)	(29.1, 42.9)
V2 [L]	287	31.9 (11.1)	(224, 350)
V3 [L]	21.1	5.89 (27.9)	(9.56, 32.6)
Q [L/hr]	3.17	0.596 (18.8)	(2, 4.34)
WT on CL	0.53	0.0639 (12.1)	(0.405, 0.655)
SEX on CL	−0.0946	0.0458 (48.4)	(−0.184, −0.00483)
WT on V2	0.811	0.0878 (10.8)	(0.639, 0.983)
Age_{50} [yr]	0.444	0.07 (15.8)	(0.307, 0.581)
HILL	2.07	0.388 (18.7)	(1.31, 2.83)
Eo	1.6	0.0359 (2.24)	(1.53, 1.67)
CHill	7.46	8.37 (112)	(−8.95, 23.9)
$CAge_{50}$ [yr]	0.71	0.225 (31.7)	(0.269, 1.15)
FEmax	2.27	0.241 (10.6)	(1.8, 2.74)
$Fage_{50}$ [yr]	0.437	0.131 (30)	(0.18, 0.694)
FAdult Comd	2.79	0.306 (11)	(2.19, 3.39)
Random Effects			
ZKA	1.62 (1.273)	0.255 (15.7)	(1.12, 2.12)
ZCL	0.411 (0.641)	0.047 (11.4)	(0.319, 0.503)
ZV2	0.551 (0.742)	0.105 (19.1)	(0.345, 0.757)
ZV3	0.307 (0.554)	0.198 (64.5)	(−0.0811, 0.695)

RTV MAF on $CL = E_0\text{-}(Age^{CHill}/(CAGE_{50}^{CHill} + Age^{CHill}))$; RTV MAF on $F = FEmax(Age/(Fage_{50} + Age))$

Conclusions: The refined PPK model incorporating maturation functions to account for the impact of physiological changes on atazanavir exposures adequately describe the time-course of atazanavir concentrations in all pediatric patients studied to date. This model informed dosing recommendations of RTV-boosted atazanavir in pediatric patients ≥3 months of age.

Reference

1. Hong Y, et al. AAC 2011;55(12):5746-52.

M-20

Extensive Simulation for Dosage Optimization of Factor Xa Inhibitors Considering the Difference in Pharmacokinetic and Pharmacodynamic Profiles: A Model-Based Meta-Analysis of Large Clinical Studies of Rivaroxaban, Apixaban, and Edoxaban

Hideki Yoshioka, Hisaka Akihiro

Department of Clinical Pharmacology and Pharmacometrics, Graduate School of Pharmaceutical Sciences, Chiba University

Objectives: The objective of this study is to estimate the optimal regimens of three factor Xa Inhibitors (FXaIs: rivaroxaban, apixaban, and edoxaban) by extensive simulation using model-based meta-analysis assuming that the therapeutic and adverse event responses relative to their blood anticoagulant activities are the same.

Methods: Based on the data from five randomized controlled trials which evaluate efficacy or safety of FXaIs in patients with atrial fibrillation, the mixed-effect logistic models were developed for the frequency of ischemic stroke or systemic embolism and major bleeding. Prothrombin time international normalized ratios (PT-INRs) at the steady state minimum, average and maximum drug concentrations were calculated from patient characteristics using the population pharmacokinetic/pharmacodynamic model and compared as variable in the developing models based on the goodness of fit of predictions to observations. The optimal fixed-dosages for each FXaI were calculated by minimization of model-predicting overall risk of event with testing of three different dosing-times; once, twice and three times a day (QD, BID and TID, respectively), and compared with the current regimens in simulated patient population. Modeling analysis in this study was performed using NONMEM 7.3.

Results: The frequencies of ischemic stroke or systemic embolism and major bleeding were modeled using estimated PT-INRs at the average and maximum plasma concentrations, respectively (Figure 1). The result of simulation showed that the overall event risks of rivaroxaban and edoxaban were reduced notably by modification of

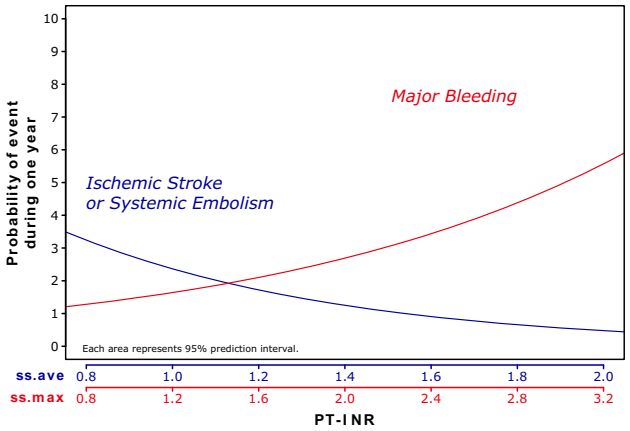

Figure 1 Model-predicting probability of event with change of PT-INR at steady state average (ss.ave) and maximum (ss.max) plasma concentrations (Color figure online)

dosage and increasing dosing times to BID from current QD, while that of apixaban, currently dosed BID, was consistently lower than them in any dosing time due to its stable profile of PT-INR.

Conclusions: Although the prediction accuracy of the present simulation would be restricted because the information of dose-response for individual drug is unavailable, this study suggested that the therapeutic dose of anticoagulants should be determined very carefully considering clinical problems such as medication adherence and may need to be reexamined.

M-21

Evaluation on efficacy of EGFR tyrosine kinase inhibitors in NSCLC patients: A meta-analysis of 68 randomized clinical trials

Hongmei Xu, Kaitlyn Minchella, Diansong Zhou, Nidal Al-Huniti

Quantitative Clinical Pharmacology, AstraZeneca, Waltham, MA

Objectives: Tyrosine kinase inhibitors (TKI) targeting epidermal growth factor receptor (EGFR) mutations have been the driving force for the treatment of Non-small cell lung cancer (NSCLC) in recent years. A challenge in oncology drug development is whether we can use early clinical endpoints from phase II or even phase I studies to predict phase III overall survival (OS) outcomes for new treatment. To investigate the correlations between progression free survival (PFS) and OS in EGFR TKIs in NSCLC patients.

Methods: The Pubmed database (March 2006 to February 2016) was searched for full publications of randomized clinical trials. Key search terms included NSCLC, gefitinib, erlotinib, afatinib, dacomitinib, and icotinib. Median progression free survival (PFS), median overall survival (OS) were analyzed using Spearman's rank order correlation and the quantile regression package (quantreg) in R.

Results: There were 68 studies and 102 arms that were treated with TKIs and reported both median PFS and OS values. The correlation between median PFS and median OS varied depending on the patient population. The strongest correlation was observed in 1st+ line treatment trials (R^2 = 0.591), followed by EGFR mutation positive populations (R^2 = 0.587), and clinically selected populations (R^2 = 0.474). Quantile regression of EGFR TKI monotherapy treatment demonstrated a nonlinear relationship between median OS and median PFS.

Conclusions: There appears to be a stronger correlation between median PFS and median OS in first+ line or EGFR positive populations. However the populations strongly overlap (14/22 or 14/18 studies respectively) in these two analyses; similar confounding factors may contribute to both correlations. There does not appear to be a strong correlation between median PFS and median OS based on other study characteristics. Quantile regression of EGFR TKI monotherapy studies showed a nonlinear relationship, which may explain the low correlation in most study categories.

M-22

Mechanistic modeling of drug-induced liver injury due to mtDNA depletion in DILIsym®

Jahid Ferdous[1], Kyunghee Yang[1], Jeffrey Woodhead[1], Brett Howell[1], Paul Watkins[1,2], Scott Siler[1,*]

[1]DILIsym Services, Inc., Durham, NC; [2]University of North Carolina, Chapel Hill, NC

Objective: To simulate drug-induced liver injury (DILI) due to mitochondrial DNA (mtDNA) depletion in DILIsym® using Fialuridine (FIAU) as an exampler compound.

Methods: FIAU-induced mtDNA depletion and the subsequent effects on mitochondria function, hepatocellular bioenergetics, and liver injury were modeled in DILIsym® by combining predictions of compound exposure with compound-induced reductions in mtDNA synthesis. A simplified physiologically-based pharmacokinetic (PBPK) model was employed to simulate FIAU exposure. All PBPK parameters were calculated based on physio-chemical properties of FIAU or optimized to clinical PK data [1]. FIAU effects on hepatocyte function within DILIsym® were based on reductions in mtDNA synthesis and subsequent disruptions in mitochondrial function. Parameters describing the rate of FIAU-imposed mtDNA reductions were calculated based on in vitro data [2] and subsequently optimized based on clinical DILI responses [3]. The FIAU dosing protocol described by McKenzie et al. [3] was simulated with a SimCohort™, a group of simulated patients with variability in certain system-level parameters.

Results: DILIsym® accurately captures the plasma FIAU PK in humans (Figure 1A). DILIsym® also recapitulates the hepatotoxicity reported for extended treatment with FIAU [3]. A comparable frequency of severe liver injury was predicted in the SimCohort™ (11 out of 15 patients) as was reported for clinical patients (7 out of 10 patients). Delayed presentation of severe liver injury (>9 weeks) was also predicted in the simulated patients. The proportion of simulated patients with maximum total plasma bilirubin concentrations

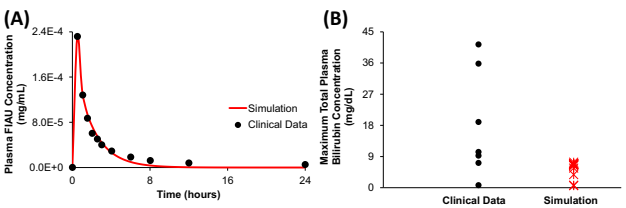

Figure 1 Plasma FIAU pharmacokinetics in human after a single 5 mg of oral dose (A). Maximum total plasma bilirubin concentration of the clinical patients before death and simulated human patients after 15 weeks of simulation where a total of 1030 mg of FIAU was administered to each simulated patient over almost 11 weeks (3 doses/day) (B) (Color figure online)

exceeding 3 mg/dL was comparable with the clinical patients (Figure 1B).
Conclusions: DILIsym® accurately simulates DILI due to FIAU administration and can be used to evaluate the DILI risk of compounds that have the potential to deplete mtDNA. Further investigation will be required to translate in vitro data into DILIsym® input parameters for drug-imposed mtDNA reductions.

References

1. Bowsher et al., Antimicrob Agents Chemother. 1994 Sep;38(9):2134-42.
2. Lewis et al., Proc Natl Acad Sci U S A. 1996 Apr 16; 93(8): 3592–3597.
3. McKenzie et al., N Engl J Med. 1995 Oct 26;333(17):1099-105.

M-23

Using Dose-Response Modeling to Improve Planning, Study Design, and Decision Making in Early Clinical Development

James Dunyak[1], Keith Tan[2], Joel Posener[3], Michael Perkinton[2], Nidal Al-Huniti[1]

[1]Quantitative Clinical Pharmacology, Astrazeneca; [2]Medimmune; [3]Astrazeneca Neuroscience

Objectives: To design an efficient and informative phase 1 study and clinical decision method, incorporating model based drug development (MBDD), for a monoclonal antibody preparing for first in man studies.
Methods: Based on a paired-comparison design, the project team originally proposed a Phase 1 program with a SAD/MAD design with standard size dose cohorts followed by one expanded dose cohort studied at one of the previous dose levels. The Phase1/2 transition go/no-go decision was originally based on a proof-of-mechanism (POM) of target suppression, with the extended cohort necessary to power the POM decision. The decision criteria used the method suggested in Lalonde[1], with specification of a target value (TV) representing best-expected performance and a lower reference value (LRV) representing minimal acceptable performance. The team then sought to develop a faster and less complex clinical plan through further integration of MBDD.
An updated decision analysis using dose-response modeling integrated with MBDD methods was developed to more fully capture available pre-clinical data and dose response. A modeling approach was applied to preclinical data and response. The SAD study design was then incorporated in a dose-response-model based analysis, which allows use of all measurements in the go/no-go analysis.
Results: The figure shows the performance characteristics of the original design (with extended cohort) and the model-based design (LRV=0.2, TV=0.5, response normalized with maximum of 1). The dose-response model based method showed superior performance at the LRV and TV.
Conclusions: As a consequence of the resulting decision criteria and program revisions, the Phase 2 POC study will begin 21 months earlier and cost >$1M USD less than in the original proposal. Incorporating pre-clinical data modeling and dose-response modeling into the formal Phase 1 decision process resulted in shorter time-lines, reduced cost, and improved decision performance.

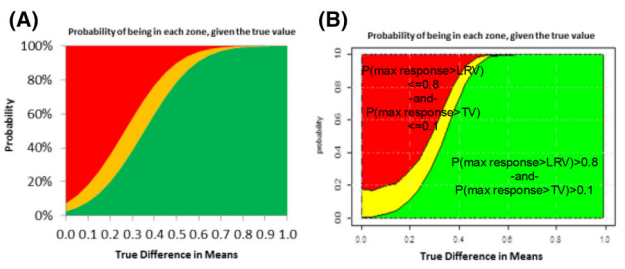

Figure 1 (A) Original analysis (N = 15/group in extended cohort) (B) Modeling based analysis (Color figure online)

Reference

1. LaLonde et al, CLINICAL PHARMACOLOGY & THERAPEUTICS, V 82 N1, July 2007

M-24

Integrating Dose Estimation into a Decision Making Framework for Model-Based Drug Development

James Dunyak[1], Nidal Al-Huniti[1]

[1]Quantitative Clinical Pharmacology, AstraZeneca, Waltham, MA

Objective: To describe a method for integrating dose-response modeling and clinical dose estimation into formal go/no-go decision criteria.
Methods: Lalonde et al. proposed a statistical-based decision criteria to formalize evidence-based decision criteria in drug development.[1] The approach uses *a priori* definitions of success or futility. Performance is characterized with a Target Value (TV) and a Lower Reference Value (LRV).
Sufficient efficacy is critical for eventual success, but the decision to advance development phase is also dependent on adequate knowledge of appropriate dose. To address this issue, we incorporate dose estimation through dose-response modeling into the go/no-go decision process. We apply the philosophy of MCPMod in Bretz[2] and incorporate a set of response models, followed by Buckland's method[3] to estimate a target clinical dose. Bootstrapping provides inferences, which are then compared to *a priori* reference values in the decision process.
Results: To demonstrate the methodology, we analyzed data *post hoc* from a phase 2 study (N=159) of naloxegol for opioid-induced constipation (OIC). Patients were classified as responders or non-responders, and logistic regression models were developed for the link-level dose-response models of linear, log-linear, emax, and quadratic. The Buckland[3] approach was applied to a dose providing 80% of maximum response over the studied range. The figure shows

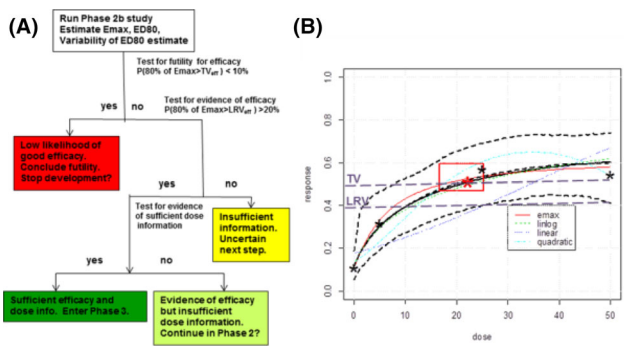

Figure 1 (A) Decision Tree (B) Estimated dose (*red* *) with study response rates (*black* *) and estimated dose response (Color figure online)

the results, with relevant confidence levels indicated by the rectangular box. In this case, the efficacy performance meets both TV and LRV, and the comparatively narrow width of the box indicates sufficient knowledge of dose for phase 3,which confirmed efficacy.[4]
Conclusions: Both efficacy and dose-knowledge may be included in model-based drug development and joint decision criteria, resulting in improved decision making.

References

1. Lalonde et al, CLINICAL PHARMACOLOGY & THERAPEUTICS, 82, 21-32, 2007
2. Bretz et al, BIOMETRICS 61, 738-748, 2005
3. Buckland et al, BIOMETRICS 53, 603-618, 1997
4. Chey et al, NEW ENGLAND JOURNAL OF MEDICINE 370, 2387-2396, 2014

M-25

Providing Insight into Novel Dosing Protocols Using a QSP Model of Drug-Induced Liver Injury

Jeffrey L. Woodhead, Scott Q. Siler, Brett A. Howell

DILIsym Services, Inc., RTP, NC, USA

Objective: Elevations in serum ALT were observed in phase I clinical studies for a novel inpatient anti-infective therapy (Compound X). Previously conducted in vitro and cellular assays identified oxidative stress and mitochondrial electron transport chain (ETC) inhibition as potential mechanisms for the ALT elevations. A novel dosing protocol for Compound X had been proposed; this work would use quantitative systems pharmacology (QSP) modeling to predict the safety of this protocol.
Methods: A model for Compound X was created within DILIsym®, a QSP platform for predicting drug-induced liver injury (DILI). DILIsym® was then used to predict the potential safety margin for the novel Compound X dosing protocol.
Results: DILIsym® recapitulated the clinical dose response with reasonable accuracy after optimization (Table 1). While the novel protocol had a narrow safety margin, DILIsym® results suggested that severe liver injury could be prevented if patients were monitored for ALT elevations daily and dosing halted when ALT was found to be above 3-fold higher than the upper limit of normal. Furthermore, the predicted safety margin of the drug improved when dosing was given on a weight-adjusted basis for each patient.
Conclusions: Modeling using DILIsym® suggested modifications to the dosing protocol that could potentially make the drug safer. These results suggest the utility of QSP methods in optimizing drug dosing protocols for maximum safety.

Table 1 Recapitulation of clinical trial dose response of Compound X in DILIsym® (Color table online)

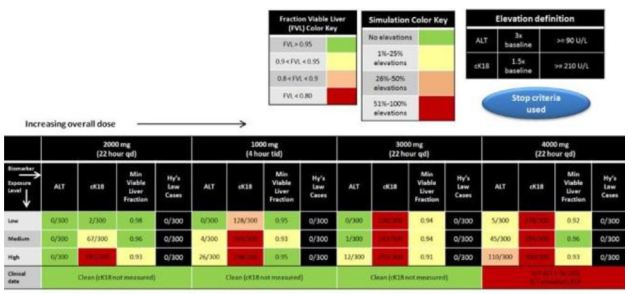

M-26

Preclinical Tumor Dynamic Modeling of an Anti–Fucosyl-GM1 Antibody: Development of a Semimechanistic Model

Jennifer Sheng, Daphne Williams, and Huadong Sun

Bristol-Myers Squibb, Princeton, NJ, USA

Objectives: Fucosyl-monosialoganglioside-1 (Fuc-GM1), a ganglioside expressed on the cell surface of small cell lung cancers (SCLCs), is a potential target for therapeutic approaches. A first-in-class, fully human IgG1 monoclonal antibody (mAb) targeting Fuc-GM1 is under investigation. The objective is to develop a semimechanistic preclinical tumor growth dynamic (TGD) model for this antibody, thus enabling Bayesian estimation of efficacious dose in patients with SCLC.
Methods: Experimental data from tumor growth in xenograft mice that received either placebo or 1 of 5 doses of anti–Fuc-GM1 mAb were analyzed. Commonly reported TGD models [1] were tested and compared using the population nonlinear mixed-effect modeling approach. The final model, derived from the Koch model [2], was selected based on considerations of the tumor-biology rationale such as the nonresponsive tumor fraction, mathematical justification such as Akaike information criterion and Bayesian information criterion, and the visual diagnostic plots. Phoenix 6.4.1 and its NLME 1.3 Quasi-Random Parametric Expectation Maximization (QRPEM) engine were used for data processing and modeling, respectively.
Results: Across the placebo and all 5 administered doses of anti–Fuc-GM1 mAb in xenograft mice, the mean (coefficient of variation, %) tumor exponential growth rate constant, tumor linear growth rate constant, nonresponse tumor volume, and drug potency effect were estimated as 0.114 (51%) 1/day, 122 (171.8%) mm^3/day, 117 (1.16%) mm^3, and 0.0642 (153%) kg/mg/day, respectively. The diagnostic plots suggested that the model adequately decribed the dose-dependent treatment effects of this antibody in the xenograft model (Figure 1). The output of this model is currently used as the prior probability for Bayesian model development.
Conclusion: An improved semimechanistic tumor dynamic growth model was developed to adequately describe the correlation between various doses of this antibody and preclinical efficacy in a xenograft model.

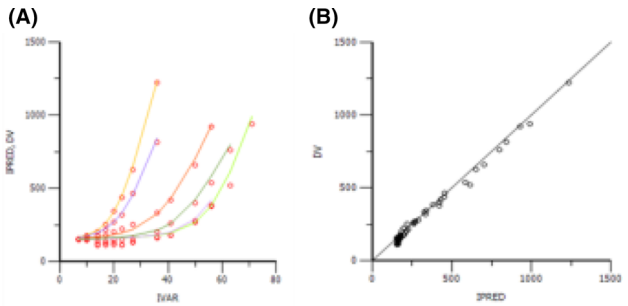

Figure 1 Diagnostic plots of the final semimechanistic model in xenograft mice. (A) Individual predicted tumor volume (mm^3) vs time (days); (B) Observed tumor volume (mm^3) vs individual predicted tumor volume (mm^3) (Color figure online)

References

1. Ribba B, et al. *CPT Pharmacometrics Syst Pharmacol.* 2014;3:e113.
2. Koch G, et al. *J Pharmacokinet Pharmacodyn*. 2009;36:179-197.

M-27

Methodology Advancement on Dose-Scale Analysis to Assess Pharmacodynamic Equivalence

Jia Chen[1], Lanyan (Lucy) Fang[1], Xia Pu[1], Yaning Wang, Yuzhuo Pan, Dongmei Lu, Xiaojian Jiang, Ethan Stier, Bing Li, Liang Zhao[1]

[1]Office of Research and Standards, Office of Generic Drugs, U.S. Food and Drug Administration, Silver Spring, Maryland, USA.

Objectives: To assess the effects of various technicalities on the outcomes of the dose-scale analysis using modeling and simulation approaches.
Methods: The dose-scale method was developed by the FDA to assess bioequivalence (BE) in terms of relative bioavailability (F) of the test to the reference products based on pharmacodynamics (PD) measures that exhibit nonlinear dose-response relationships. The current BE guidance for albuterol inhalaton products recommends in vivo PD study(ies) to assess the relative bronchoprotection ability with PC20 (or PD20) as the PD endpoint. Literature and in house dose-response PD data of albuterol inhalation products were used to fit sigmoidal Emax model in the original or transformed format. Clinical trial simulations were performed to evaluate the nonlinear mixed effect modeling (NLME) approach in the dose-scale analysis. The impact of missing values (missing one or more treatment periods) on F estimate was assessed by deleting simulated observations at random or not at random.
Results: Both log-transformed and raw data followed Emax model structure but transformation of log-normal distributed data is necessary to normalize residual distribution when using ordinary regression. Simulations showed that fitting sigmoidal Emax model with mean PD data without estimating variabilities or with pooled individual PD data with NLME approach can provide similar F estimate when there are no missing values in the dataset. In contract, in the presence of missing values, NLME approach can result in less biased F estimate, as evidenced by F estimate (point estimate and 90% confidence interval) closer to that from the whole dataset.
Conclusions: The modeling and simulation results support fitting pooled individual PD data in a log-transformed format using NLME model in dose-scale analysis to assess PD equivalence of albuterol inhalation products. The impact of missing data on F estimate can be evaluated using a simulation approach.

Reference

1. http://www.fda.gov/downloads/Drugs/GuidanceComplianceRegulatoryInformation/Guidances/UCM346985.pdf (2013) .

M-28

Development of a Universal Pharmacogenetics-guided Warfarin Dosing Nomogram

Jiexin Deng[1], Meghan Arwood[2], Julio Duarte[2], Larisa Cavallari[2], Stephan Schmidt[1]

[1]Center for Pharmacometrics & Systems Pharmacology, Univ. of Florida, Orlando, FL; [2]Pharmacotherapy and Translational Research and Center for Pharmacogenomics, Univ. of Florida, Gainesville, FL
Objectives: Although warfarin is a widely prescribed drug, suboptimal dosing may cause serious complications including bleeding and thrombosis. Genotype-guided algorithms, such as warfarindosing.org, have been primarily developed based on data from Caucasians on stable warfarin dosing. The objective of our study was to develop a dosing nomogram that can facilitate optimal dosing in a diverse population.
Methods: Data from patients of diverse ethnicities (57% African Americans and 17% Hispanics) initiating warfarin with genotype-guided dosing (warfarindosing.org) were used in this study. Data management and exploratory analysis were performed in R (version 3.2.1). The Rosendaal method was used to calculate time in therapeutic range, assuming linear change between two conseceutive INR measurements. A mechanism-based model characterizing warfarin dose/response was developed based on Hamberg et al. in NONMEM® (version 7.3). Initiation nomogram consisting of loading and maintenance dosing were developed based on simulations in virtual individuals of different ages, genotypes (*VKORC1* and *CYP2C9*), and ethnicities.
Results: Exploratory analysis indicates that our patients spent less time in therapeutic range compared to Europeans in the EU-PACT trial (55% vs. 65%) at 70-90 days of therapy, which is consistent with literature reports of suboptimal performance of genotype-guided algorithms in African Americans. To overcome this shortcoming, we developed a dynamic dosing nomogram that could enable patients to reach therapeutic INR within 1 week and remain stable across genotypes and ethnicities (Fig. 1). Furthermore, our maintenance doses were consistent with dose recommendations across different combinations of *VKORC1* and *CYP2C9* as shown on the FDA approved label for warfarin.
Conclusions: We developed the first pharmacogenetic-guided warfarin initiation nomogram that accounts for its dynamic dose -response relationship to facilitate optimal dosing in a diverse population.

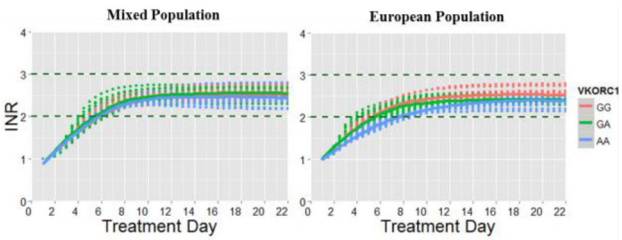

Figure 1 Simulated INR profiles in virtual individuals of different age and genotypes (*VKORC1* and *CYP2C9*) who received warfarin dosing according to our initiation nomogram (Color figure online)

References

1. Rosendaal et al., Thromb. Haemost. 69(3): 236-239, 1993
2. Hamberg et al., CPT 87(6): 727-734, 2010
3. Pirmohamed et al. N Engl J Med 369(24): 2294-303, 2013

M-29

Quality Award Winner (Trainee Category)

Pathogenesis of pneumonia due to *Acinetobacter baumannii*: Using a mechanistic model to describe the pathogen-host interaction

John K. Diep[1], Wojciech Krzyzanski[1], Coen van Hasselt[2], Thomas A. Russo[1], Gauri G. Rao[1*]

[1]SUNY Buffalo, Buffalo, NY; [2]Leiden University, The Netherlands

Objectives: Increasing prevalence of infections due to multi-drug resistant pathogens, such as *Acinetobacter baumannii,* has led to a growing need for better understanding of bacterial pathogenesis. The objective of this study was to develop a mechanistic model capable of describing the pathogen-host immune response interaction during rat pneumonia infection.
Methods: Rat pneumonia data was obtained from Russo et al. [1]. Pulmonary instillation of *A. baumannii* strain 307-0294 was introduced intratracheally in Long-Evans rats to achieve an initial inoculum of $3.5x10^8$cfu/mL. Animals were sacrificed at 3, 6, 24, 48, 72, and 168h for total lung bacterial quantification and assessment of IL-1β and neutrophil counts in bronchoalveolar lavage fluid. ADAPT5 [2] was used for model development.
Results: The model (Figure 1) simultaneously accounted for changes in bacterial concentration (CFU), IL-1β expression (IL-1β), and neutrophil counts (N). Bacterial growth was described by first-order rate constant, k_g. CFU stimulates production of IL-1β which stimulates neutrophil recruitment, each with fitted parameters S_{max}, SC_{50}, and k_{out}. Bacterial killing by neutrophil and neutrophil signaling (represented by two transit compartments: T1, T2) were described by second-order rate constants, k_{dN}, k_{dT1}, and k_{dT2}. T_{max} of CFU was predicted to be 25h. Maximal stimulation of IL-1β and N ranged from ~22-35h and ~12-63h with S_{max} estimates of 36.9 (8.0%CV) and 700 (5.6%CV), respectively. Remaining parameter estimates were within physiological ranges or agreed with values reported in the literature.
Conclusions: The model captures the maximal stimulatory effects of *A. baumannii* on IL-1β and IL-1β on neutrophils providing a reasonable description of the pathogen-host immune response interaction. Increased proinflammatory cytokine expression drives the neutrophil response that is largely responsible for bacterial clearance [3]. The model can be expanded to include additional biomarkers for a more comprehensive description of bacterial pathogenesis.

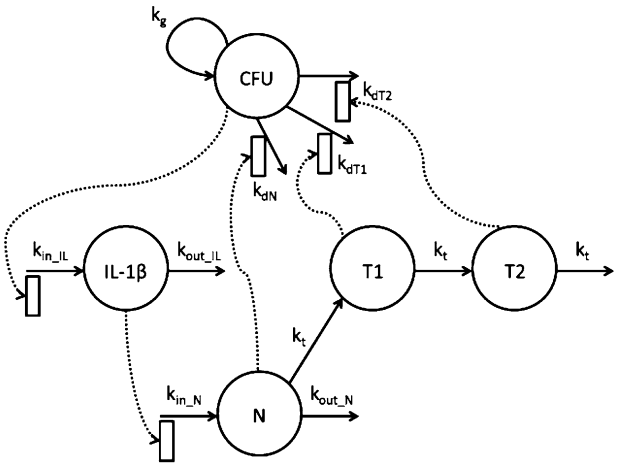

Figure 1 Model structure incorporating bacterial growth and clearance, IL-1β expression, and neutrophil response

References

1. Russo T.A. et al. Infect Immun. Aug.2008;3577-3586.
2. D'Argenio D.Z. et al. BMSR. 2009.
3. Quinton L.J. et al. J Immunol. 2007;178:1896-1903.

M-30

Comparison of Human Tissue Exposure following Partial Destructive Sampling using Bootstrapped Non-Compartmental (NCA) Method vs Non-linear Mixed Effects Models (NLME)

Jon Collins*, Heyward Hull, Julie Dumond

UNC Eshelman School of Pharmacy, Chapel Hill, NC

Objectives: To compare tissue exposures generated from bootstrapped NCA methods and NLME methods, following serial plasma sampling with destructive tissue sampling.
Methods: A four-compartment model developed from observed data after administration of one dose of tenofovir disoproxil fumarate[1] (NONMEM 7.3) was used to simulate plasma and tissue concentrations for two destructive tissue sampling schemes. One scheme consisted of 8 time points, 4 unique samples per time point, and 4 time points in the tenofovir terminal elimination phase (4-8-4). The second consisted of 7 time points, 3 unique samples per time point, and 3 time points in the terminal phase (3-7-3). 100 data sets with densely-sampled individual plasma profiles and one tissue sample per individual were created for both tissue schemes. The bootstrapped NCA was performed in SAS 9.3, using linear-up/log-down trapezoidal method to calculate geometric mean tissue AUC for each dataset. For NLME, individual post-hoc estimates of tissue AUC were determined, then geometric mean from each dataset calculated. Prediction error (PE) and absolute prediction error[2] (APE) were calculated for each method and compared to AUCs from the modeled observed data.
Results: Table 1 shows central tendencies for both methodologies were within 10% of observed geometric mean for all datasets. The results indicate the NLME-generated exposure estimates are biased, but display less variation in prediction error. Bootstrapped NCA PE and APE are quite precise, but had more variation in the prediction errors for both sampling designs.

Sparse Sample Design		Standardized Prediction Error Median (Min, Max)	Standardized Absolute Prediction Error Median (Min, Max)
4-8-4	NLME	−8.7% (−35%, 30%)	13.1% (0.1%, 35%)
4-8-4	Bootstrap NCA	−0.1% (−36%, 115%)	17.1% (0.4%, 115%)
3-7-3	NLME	−9.3% (−45%, 52%)	14.7% (1%, 52%)
3-7-3	Bootstrap NCA	3.5% (−48%, 119%)	17.2% (0.1%, 119%)

Conclusions: Bootstrapped NCA and NLME produce similar tissue exposure estimates following destructive sampling. Overall, NLME PEs/APEs suggest a small under-predicition with fewer extreme outliers over both sampling schemes. The bootstrapped NCA method produced accurrate estimates, particularly with the 4-8-4 scheme, but with some PE/APE >100%. This suggests the optimal methodlogy depends on the nature of the question being asked.

References

1. Patterson KB, et al. Sci Transl Med. 3(112):112re4, 2011
2. Sheiner LB, et al. J Pharmcokinet Biopharm. 9(4):503-12, 1981

M-31

A first application of population pharmacokinetics in feline therapeutics

Jonathan Paul Mochel[1*], Antoine Soubret[1], Jonathan King[2], Jonathan Elliott[3] and Ludovic Pelligand[3]

[1]Pharmacometrics, Novartis Pharmaceuticals, 4056 Basel Switzerland; [2]Elanco Animal Health Inc, Postfach, Basel 4058, Switzerland; [3]Royal Veterinary College, Hawkshead Lane, Hatfield, UK.

Objectives: In veterinary medicine, characterization of the pharmacokinetics is usually performed using a 2 stage approach, thereby limiting most of the analyses to rich datasets. This research aimed to model the PK of the NSAID robenacoxib using a NLME approach thereby leveraging all available information collected from various sparse and rich data sources with different dosing routes. Another objective was to demonstrate that using multiple samples from the posterior distribution of the random effects instead of just the mode leads to robust estimates of correlations between population parameters.
Methods: Data from 83 cats were pooled from 7 preclinical and 1 field robenacoxib PK studies. Cats received robenacoxib subcutaneously and/or intravenously. Data from both routes were modeled simultaneously using NLME in Monolix 4.3.2. The influence of parameter correlations and available covariates on population parameter estimates were evaluated by using the mode vs. multiple samples from the posterior distribution of the random effects.
Results: A two-compartment mammillary model with first-order absorption and elimination best described the PK of robenacoxib in blood. Simultaneous fitting of all dosing routes unveiled the flip-flop kinetics of robenacoxib for which no dosing adjustment seems necessary. Our results further showed that using several samples of the posterior distribution instead of just the mode allows for a more robust estimate of correlations between model parameters.
Conclusions: This work constitutes the first population PK analysis in a large scale of cats. Using several samples of the posterior distribution instead of the EBE allows for a robust estimation of the correlation between model parameters. This research illustrates the value of NLME for the reconciliation of diverse pharmacokinetic data in veterinary drug research and development.

Reference

1. Pelligand L, et al. J Vet Pharmaco Ther 2012, 35(1): 19-32.

M-32

Exploration of the interplay between enterohepatic circulation (EHC) and transport: a physiologically-based pharmacokinetic (PBPK) modeling approach using pravastatin and rosuvastatin as model drugs

Justin D. Lutz, Brian Kirby and Anita Mathias

Department of Clinical Pharmacology, Gilead Sciences, 333 Lakeside Dr. Foster City, CA 94404

Objectives: The pharmacokinetics of pravastatin (PRA) and rosuvastatin (ROS) is dependent intestinal efflux, hepatic uptake and biliary efflux. Contribution of EHC to PRA and ROS disposition further confounds identifiability of these clearance pathways. This work aimed at developing a PBPK modeling approach to address EHC-dependent identifiability issues, allowing the use of this model to predict DDIs for agents with similar complex disposition.
Methods: Full PBPK (with ADAM absorption) models for PRA and ROS were developed in SimCYP (v.14) using available physicochemical, in vitro transport and in vivo renal clearance values based on observed single oral dose clinical data for PRA and ROS in the absence of DDIs. Scaling factors for tissue partitioning (SF_{VD}), hepatic uptake (SF_{HU}) and intestinal efflux (CL_{GE}) were evaluated over 0-100% range of percent of drug reabsorbed (%RA) and optimized based on OFV nadir. The optimized models were then evaluated for their ability to predict observed DDIs with PRA and ROS in the presence of inhibitors of intestinal efflux, hepatic uptake, and biliary efflux.
Results: For PRA and ROS, a %RA of 0% and 50%, respectively, best fit the plasma concentration curves in the absence of DDIs. Increasing %RA from 0 to 100% increased the estimated SF_{HU} approximately 3-fold for PRA (SF_{HU}=28-83) and ROS (SF_{HU}=46-143), resulting in a maximal AUC ratio (due to hepatic uptake inhibition) from 4-9 and 10-27, respectively; consitent with clinical data. Intestinal efflux-to-permeability clearance ratios were large for ROS (range: 7-28) and smaller for PRA (range: 0.2-2). Despite large predicted increases in PRA and ROS C_{max} ($\sim$10-fold), AUC'/AUC after inhibiting gut efflux was minimal; consistent with near complete absorption.
Conclusions: Using PRA and ROS as model drugs, the described sensitivity-estimation method can predict the presence and extent of human EHC. EHC should be accounted for model development because it significantly affects transporter clearance estimates and predicted transporter inhibition liability.

M-33

Application of a Framework Qualifying Fit-for-Purpose Physiological Models to Drug Discovery and Development

Karim Azer[1*], Jeffrey R. Sachs*, Carolyn R. Cho, Thomas Kerbusch[2], Antonio Cabal, Christopher R. Gibson, Sandra Allerheiligen

PPDM-QP2, Merck & Co., Inc., Currently [1]Sanofi Pharmaceuticals, and [2]Quantitative Solutions

Objectives: Physiological models are frequently applied with pipeline. In addition to other quality management systems, it was essential to develop consistent, reliable processes for ensuring models' scientific quality. The processes were used on a physiologically-based pharmacokinetic (PBPK) model for montelukast PK predictions in order to foster support for using PBPK predictions in future decision-making.
Methods: The modeling process was carefully analysed through interviews and literature reviews, including collaborative and organizational steps, and broken into components (Figure). The components include: ▶Communication strategy; ▶Questions that the model will address; ▶Decisions impacted; ▶Model description including relation to questions; ▶Assumptions required and their impact; ▶Data required, used, variability, and limitations; ▶Estimation of parameters, variability and uncertainty predictions, and risks.
These steps were used to investigate the ability of PBPK modeling of montelukast to predict PK in children from adult PK data and known physiological differences (e.g. body size and composition, enzyme ontogeny). The initial SIMCYP [2] model used only *in vitro* data for the known elimination pathways in adults (without fitting to observed PK data) to describe the overall central tendency and variability in the adult PK data. One parameter (hepatic clearance) was then calibrated

using adult IV data. The model was then used to (retrospectively) predict adult PK profiles for *oral* dosing, and *pediatric* PK using enzyme -specific age-dependence.
Results: Adult and pediatric oral-dosing profiles were reasonably predicted (figure). PBPK modeling was accepted for decision-making in pediatric development (such as selecting doses for clinical trials).
Conclusions: Strategic application of a model qualification framework can impact quality and organizational acceptance of models: clear separation of the calibration and (two) data qualification steps (and communicating the intent) was essential to proper model formulation and successful adoption. PBPK models can inform pediatric development.

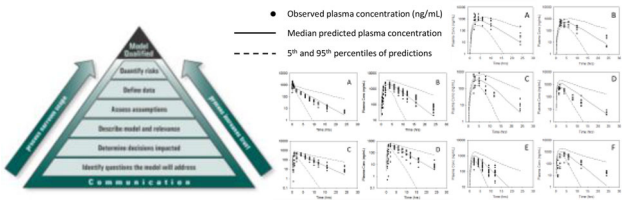

Left: Model qualification for physiological models in which modeler and discovery/development team step from bottom to top. Strategically planned communication at each step is foundational. Modeling steps happen in parallel with those for qualification, and are associated with technical review/qualification. Center (from [1]): Observed adult montelukast data following oral dosing are near the a *priori* predicted plasma concentration-time profiles and (in elimination phase) within the 90% prediction interval. (A) 7 mg IV dose (used for model calibration), (B) 50 mg oral solution, (C) 10 mg film-coated tablet in fasted state, (D) 10 mg film-coated tablet in fed state. *Right* (from [1]): Observed pediatricdata and predicted plasma concentration-time profiles demonstrate that a model based on adult and in vitrodata predicts appropriate dose ranges for pediatric trials. Oral granules 4 mg dose (A) 1-3 months, (B) 3-6 months, and (C) 6 months to 2 years. Film-coated tablet 4 mg oral dose (D) 2-5 years and (E) 6-8 years, and (F) film-coated tablet 10 mg oral dose 9-13 years

References

1. Jones, H.M. *et al., CPT* **97**, 247-62 (2015).
2. Jamei, M. *et al. In Silico Pharmacology* **1**, 9-22 (2013).

M-34

Exploration of Factors Affecting the Activated Partial Thromboplastin Time and Prothrombin Time-International Normalized Ratio Using a Quantitative Systems Pharmacology Model

Koichiro Yoneyama[1,*], Junpei Sugiyama[2], Keisuke Iwa[2], Kazuhiko Hanada[2]

[1]Translational Clinical Research Science & Strategy Dept., Chugai Pharmaceutical Co., Ltd., Tokyo, Japan; [2]Department of Biopharmaceutics, Meiji Pharmaceutical University, Tokyo, Japan

Objectives: To evaluate the identifiability of factors affecting the activated partial thromboplastin time (APTT) and prothrombin time-international normalized ratio (PT-INR) using a quantitative systems pharmacology (QSP) approach.

Methods: The equations used in a previously reported QSP model of the coagulation network [1] were implemented in the MONOLIX software. The impacts of several coagulation and anticoagulation factors, including fibrinogen, factors II, V, VII, VIII, IX, X and XI, and proteins C and S, on APTT and PT-INR were evaluated using model-based simulations of the coagulation tests in which the initial concentration of a factor was varied from 0.01- to 100-fold the normal levels. In addition, the initial levels of vitamin K-dependent factors were simultaneously varied to mimic the anticoagulant effect of warfarin.
Results: The QSP model-based simulations indicated that factors affecting APTT include fibrinogen and factors II, VIII, IX, X and XI, whereas the impacts of factors V and VII, and proteins C and S on APTT were negligible. PT-INR was markedly changed by fibrinogen and factors II, VII and X; no substantial effects of factors V, VIII, IX and XI, and proteins C and S on PT-INR were suggested. A reduction of approximately 80% in the levels of vitamin K-dependent factors from normal was predicted to result in a PT-INR value within a range of 2.0 to 3.0, which is the target of anticoagulant therapy with warfarin.
Conclusions: The QSP approach appears useful for exploring the factors affecting APTT and PT-INR by quantifying their impacts, and for characterizing in a quantitative manner the biological mechanisms underlying the values of therapeutically targeted biomarkers. The simulation-derived findings need to be validated by actual observations to understand how accurately (or inaccurately) the model captures the reality of each component of the system.

Reference

1. Wajima T, et al. Clin Pharmacol Ther. 2009;86(3):290-8.

M-35

Systems Pharmacology of VEGF Splicing in Peripheral Artery Disease

Lindsay Clegg[1,*], Feilim Mac Gabhann[1]

[1]Institute for Computational Medicine & Department of Biomedical Engineering, Johns Hopkins University, Baltimore, MD

Objectives: To understand how changes in VEGF splicing in peripheral artery disease (PAD) lead to impaired angiogenic responses to ischemia. Despite multiple clinical trials, there is not a single approved VEGF-based pro-angiogenic therapy, motivating the need for a deeper understanding of the disease. The $VEGF_{165b}$ isoform, which does not bind to the extracellular matrix (ECM) or to the coreceptor NRP1, activates VEGF receptor 2 (VEGFR2) only weakly [1], and is up-regulated in PAD [2].
Methods: To understand this system, we built a multiscale mechanistic computational model incorporating detailed pharmacodynamics into a whole body compartment model (Figure 1A). We built upon our previous, validated computational model of VEGFR2 ligation, intracellular trafficking, and site-specific phosphorylation *in vitro*, which showed that the binding properties of VEGF isoforms result in signaling changes correlated with distinct endothelial cell phenotypes (proliferative vs. branching) [3].
Results: We used our computational model to study the signaling changes resulting from increased production of $VEGF_{165b}$ in PAD, while free VEGF levels in tissue remain unchanged. Our model explains experimentally-observed large increases in $VEGF_{165b}$ protein in mouse and human tissue, when only small changes in $VEGF_{165b}$ mRNA are measured [2]. Our model predicts that impaired VEGF receptor signaling with increasing $VEGF_{165b}$ expression results

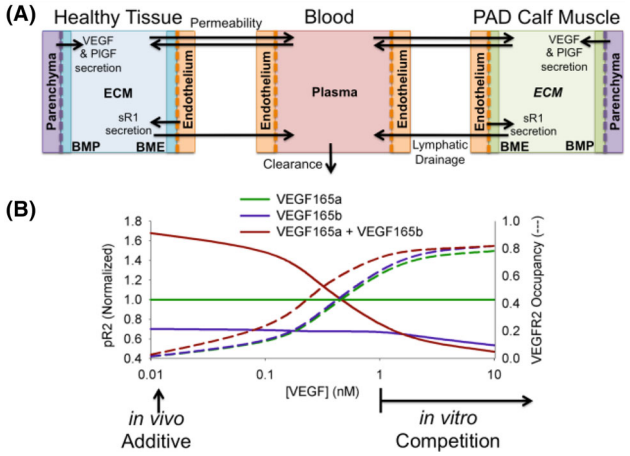

Figure 1 (A) The whole-body compartment model includes: healthy tissue; a calf with peripheral artery diseases (PAD); and blood. Each tissue compartment includes endothelial cells, parenchymal cells, extracellular space, ECM, and basement membrane in physiological proportions. VEGF receptor trafficking and phosphorylation are simulated within endothelial cells to predict VEGFR2 activation. (B) Dose-dependent competition between $VEGF_{165a}$ and $VEGF_{165b}$. Simulations capture experimentally-observed competition in vitro, but predict that competition is not a major factor at in vivo VEGF levels. Solid lines: pR2, normalized by $VEGF_{165a}$ at each concentration. Dashed lines: VEGFR2 occupancy (Color figure online)

from reduced expression of other VEGF isoforms, rather than from competition between VEGF isoforms for receptor binding, as observed *in vitro* (Figure 1B). We are using this model to inform design of antibodies that specifically target $VEGF_{165b}$, a strategy that has shown promise in rodent models [2].

Conclusions: We used a multiscale mechanistic computational model to study the cause of impaired angiogenesis in PAD, and to facilitate translation of experimental observations in cell culture and animal systems into predicted therapy effectiveness in human patients.

References

1. Cébe Suarez S, et al. Cell Mol Life Sci, 63: 2067, 2006
2. Kikuchi R, et al. Nature Med, 20: 1464, 2014
3. Clegg L, et al. PLoS Comp Biol, 11: e1004158, 2015

M-36

Application of Ramucirumab Exposure-Response Modeling to Support Dose Selection for Post Marketing Studies in Patients with Gastric Cancer

Lisa O'Brien[1], Ling Gao[2], Michael Heathman[1]

Eli Lilly and Company, [1] Indianapolis, IN; [2] Bridgewater, NJ

Objectives: Cyramza® (ramucirumab) as a single agent, or in combination with paclitaxel, is indicated globally for the treatment of patients with advanced or metastatic gastric or gastroesophageal junction adenocarcinoma. The approved dose in patients with gastric cancer is 8 mg/kg every two weeks, which has shown to be safe and effective. This analysis was performed to assess the relationship between ramucirumab exposure and measures of efficacy in this patient population, and to evaluate alternative dosing regimens for post marketing commitment studies.

Methods: A total of 335 placebo and 321 ramucirumab treated patients from the Phase 3 RAINBOW study were included in the exposure-response analysis. Estimates of exposure ($C_{min,ss}$) for treated patients were generated using post hoc estimates from an established population pharmacokinetic model previously developed from a pooled analysis of 8 Phase 1/1b, 2, and 3 studies in a variety of cancer indications. Parametric time to event models for overall survival (OS) and progression-free survival (PFS) were subsequently developed, incorporating predicted exposure and patient factors found to be significant. A series of simulations were performed to evaluate the impact of higher dosing regimens on ramucirumab exposure and efficacy.

Results: A combined Weibull and Gompertz model was found to best describe the hazard for both OS and PFS. EC50 based on an 8 mg/kg dose in gastric patients was estimated to be approximately 50µg/mL. Increase in ramucirumab exposure was associated with improvement in efficacy in terms of both OS and PFS.

Conclusions: Higher doses of ramucirumab are predicted to produce greater C_{minss} that may be associated with longer survival. Alternative doses and dosing regimens in patients with advanced gastric cancer are currently being evaluated in ongoing clinical trials.

M-37

A Comprehensive Review of Disease Progression Models (DPM) Across the Entire Spectrum of Alzheimer Dementia (AD)

Mahesh N. Samtani* (1), Partha Nandy (1)

[1]Janssen R&D, NJ, USA.

Objectives: Summarize DPMs across the entire AD spectrum.

Methods: DPMs for the following 4 disease stages are summarized (a) mild to moderate [M2M] AD (b) prodromal AD [pAD] (c) Asymptomatic at Risk for AD [ARAD] (d) Pre-symptomatic AD [PSAD] in Autosomal Dominant AD [ADAD]

Results: The endpoints for DPM include (a) co-primary cognitive and functional endpoints ADAS-cog and ADL for M2M-AD (b) CDRSB for pAD (c) Composite endpoint ADCS-PACC for pre-clinical AD. AD is being studied at earlier stages for secondary prevention and duration of follow-up in the DPMs for disease-modifying-agents is increasing from 1.5 to 4.5 years across M2M-AD to ARAD. Modeling cognitive and functional endpoints in M2M to pAD requires special considerations for bounded outcomes such as (a) structural models with asymptotes e.g. Richard's function (b) data distribution e.g. beta regression (c) drop-out due to long follow-up. DPMs require these structural and distributional considerations to ensure that predictions stay within the boundaries of the scale to allow for floor and ceiling effects. DPM for pre-clinical stages of the disease (ARAD/PSAD) generally employ linear mixed effects modeling with normally distributed data since endpoints are z-scaled composite measures. Key covariates in DPM include amyloid status where amyloid negative subjects exhibit flat disease trajectories and other key factors for progression rate include APOE and age. Finally, one of the underlying processes driving progression rate is disease severity within each stage of AD. DPMs follow an underlying S-shaped disease trajectory; progression rates are slow at earlier and later stages within a disease state and progression rates are fastest around the mid-portion, which represents the dynamic portion of the scale.

Conclusions: Modeling consideration and choice of endpoints for the different disease stages are guided by recent draft guidelines and policies from international bodies and regulatory agencies which are also summarized.

Table 1 Disease Progression Model Characteristics

	AD [1]	pAD [2]	ARAD [3]	PSAD [4]
End-point	ADAS-cog[5] and ADL[6]	CDRSB[7]	ADCS-PACC[8]	
Cognitive composite				
Duration of Disease-Modifying Trials	1.5 year	2 years	3.5 to 4.5 years	4 years
Example of currently ongoing trials	EXPEDITION3[9,12]	AMARANTH[10,12]	A4[11,12]	DIAN-TU[13]
Distributional Assumption	Beta distribution		Normal distribution	
Structural Model	Richard's Function		Linear mixed effects with quadratic terms or cubic splines with knots for accommodating non-linearity	

[1] AD: Alzheimer's disease

[2] pAD: prodromal AD

[3] ARAD: Asymptomatic at risk for AD (pre-clinical stage of AD)

[4] PSAD: Pre-symptomatic AD (pre-clinical stage of AD) due to an autosomal-dominant mutation, also called familial or early onset AD, due to mutations in presenilin 1 (PSEN1), presenilin 2 (PSEN2) or amyloid precursor protein (APP)

[5] ADAS-cog: Alzheimer's disease assessment cognitive scale

[6] ADL: Activities of daily living endpoints such as disability assessment for dementia

[7] CDRSB: Clinical dementia rating sum of boxes

[8] ADCS-PACC: Alzheimer's disease cooperative study-preclinical alzheimer's cognitive composite

[9] EXPEDITION3: Effect of Passive Immunization on the Progression of Mild AD: Solanezumab (LY2062430) Versus Placebo [NCT01900665]

[10] AMARANTH: A 24-month, Multicenter, Randomized, Double-blind, Placebo-controlled, Parallel-group, Efficacy, Safety, Tolerability, Biomarker, and Pharmacokinetic Study of AZD3293 in Early Alzheimer's Disease (The AMARANTH Study) [NCT02245737]

[11] A4: Anti-Amyloid Treatment in Asymptomatic Alzheimer's Disease (A4 Study) [NCT02008357]

[12] Recent studies for treatment or secondary prevention of late onset AD require biomarker enrichment to exclude amyloid negative subjects that exhibit flat trajectories in the DPM

[13] DIAN-TU: Dominantly Inherited Alzheimer Network-Trial Unit [NCT01760005]

M-38

A pharmacokinetic model for drugs undergoing enterohepatic circulation: A sensitivity analysis

Malek Okour, BDS; Richard Brundage, PharmD, PhD

Experimental and Clinical Pharmacology, University of Minnesota

Objectives: Literature modeling strategies of the EHC varies; however, gallbladder-based models provide the best current physiological representation of the process. Regardless, the addition of a gallbladder into the model does not fully depict the physiology of EHC. A more physiological gallbladder-based EHC model is needed. This model should take into account a physiological representation of the bile secretion, gallbladder filling and emptying, duration of gallbladder emptying and irregular mealtimes. With all these considered, the objectives of the current analysis are to propose a gallbladder-based EHC model; to use the model in performing sensitivity analyses to evaluate the effect of the extent of EHC on the pharmacokinetic profile and the non-compartmental analysis (NCA) calculations.
Methods: A gallbladder-based model that describes the EHC process was developed and used to perform determinant simulations assuming various extents of EHC. Next, these simulations were compared to evaluate the effect of the EHC on the pharmacokinetic profiles of orally administered drugs. The influence of the EHC process on the NCA calculations was determined assuming two sampling schemes that differs by the selected sampling times in relation to meal times.
Results: The presence of EHC results in nonlinearity in the system and causes changes in the pharmacokinetic profile. These changes include effects of Cmax, Tmax, and half-life estimates. The comparison of two sampling schemes from a drug undergoing various degrees of EHC demonstrated a major influence of the selected sampling times on the NCA estimations. Bias in the NCA calculations was dependent on the sampling times.
Conclusion: Caution should be taken when designing clinical studies for drugs that undergo EHC. The timing of meals may be an important factor to consider when designing pharmacokinetic studies and defining sampling times. The duration of sampling needs to be extended over a longer duration than what is traditionally done with other drugs. Future studies that attempt to identify best sampling strategies in the presence of EHC are needed.

M-39

Model Based Meta-Analysis of Efficacy in Multiple Sclerosis for Disability Progression Incidence

Matthew Rosebraugh[1], Jaap Mandema[2], Sandeep Dutta[1]

[1]Clinical Pharmacology and Pharmacometrics, AbbVie, North Chicago, IL; [2] Certara, Menlo Park, CA

Objectives: Characterize the efficacy of different multiple sclerosis (MS) drugs in preventing disability progression as defined by the expanded disability status score (EDSS).
Methods: Publically available information were used to create a database comprising summary level efficacy data for 27 drugs evaluated in 91 controlled trials in >41,000 MS subjects. A dataset that includes incidence of progression as defined by increase in EDSS score (31 trials, 13 drugs and 26,205 MS subjects) was used. Analysis was conducted using the generalized least squares method for non-linear models (gnls) within the R nmle package with the odds ratio of progression incidence estimated for the primary clinical trial endpoint. Variability was estimated using the large sample size approximation from a binomial likelihood distribution. Several covariates were tested for statistical significance within the model.
Results: The estimated odds ratios with 90% confidence intervals are presented in the Figure below. One treatment (dirucotide) was excluded due to the small number of total subjects (32) and large confidence intervals. Average age was the only statistically significant covariate at the $p<0.01$ level while the type of MS narrowly missed achieving statistical significance ($p=0.026$).

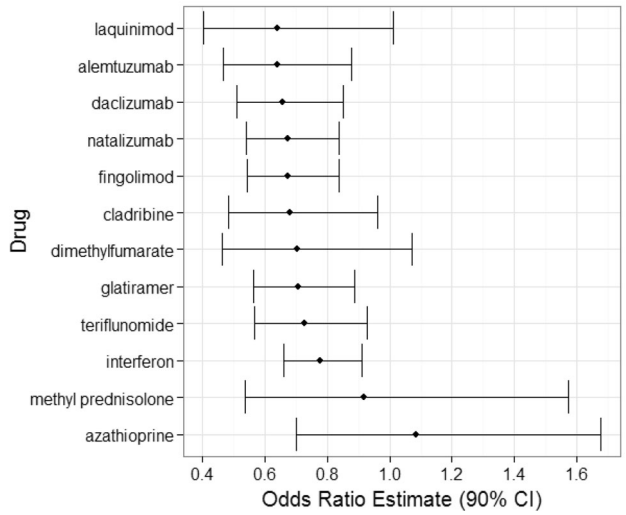

Conclusions: This meta-analysis suggests that most MS treatments have an estimated odds ratio of 0.6-0.8 for incidence of progression relative to placebo. For the approved MS treatments, when adjusting for average age of patients in each clinical trial, alemtuzumab was estimated as the most efficacious drug and interferon was estimated as the least effective. Patient age and type of MS are correlated however; age may have achieved statistical significance since it is a continuous variable while MS type is a discrete patient diagnosis.

M-40

Interactive Shiny Application for Exploratory Data Analysis and Simple Sampling Strategy of Pharmacokinetic Data

Max Tsai[1,*]

[1]Pharmacometrics, Takeda Development Center Americas, Deerfield, IL

Introduction: Exploratory Data Analysis (EDA) is often the first step employed by pharmacometricians to 1) detect errors and check assumptions, 2) evaluate central tendency and variability, 3) determine trends between variables, 4) identify extreme values, 5) provide a direction for selecting appropriate models, and ultimately 6) provide a better understanding of the data.
Objectives: A web-based R application was developed to provide an interactive way to perform EDA and a simple approach for timepoint selection of pharmacokinetic data.
Methods: EDA, typically achieved through graphical or numerical summaries, leverages *ggplot* and *dplyr* packages in the application to efficiently manage large datasets and easily construct figures, layering on appropriate elements as needed. Contextual interactivity is achieved using *shiny* package to provide different links between the user interface and the back-end calculations, based on the user's input. For exploring PK sampling strategies, a brute-force method is applied to traditionally dense Phase I data to create permutations of varying timepoints. The bias of each permutation of timepoints relative to the original sampling scheme is determined and summarized. Suitable sampling strategies are identified, based on the desired number of timepoints and acceptable level of bias.
Results: The graphical interface for the application is organized into multiple tabs: Load: upload data file and a brief data summary is provided; Process: define analysis dataset, using filter and sort conditions and map key data variables; Explore: provide summary statistics of selected variables and generate scatterplot matrix for evaluating correlations; Table: present dataset in a tabular format with sort, filter, and search functions; Plot: present dataset in a graphical format with highlight, zoom, and paneling functions for datapoint identification; Evaluation: analyze dataset and provide sampling recommendations, based on user-defined criteria.
Conclusions: The application provides a dynamic way to explore data, particularly for users unfamiliar with R programming. The modular nature of the application enables components of the application to be inserted to any workflow, utilized across projects, or even expanded upon (e.g.,evaluation of model outputs).

M-41

Using semi-PBPK modeling to explore the impact of route of administration on the metabolic drug-drug interaction (DDI) between midazolam (MDZ) and erythromycin (ERY)

Mengyao Li, Jürgen Venitz

Department of Pharmaceutics, School of Pharmacy, Virginia Commonwealth University

Objectives: To investigate the impact of differences between intravenous (IV) and oral (PO) routes of administration for MDZ, a prototypical CYP3A substrate, and ERY, a CYP3A inhibitor, on the magnitude and time course of their metabolic DDI.
Methods: Semi-PBPK models for MDZ and ERY were developed separately, using PK parameters from clinical/*in-vitro* studies and published physiological parameters. The DDI model incorporated mechanism-based CYP3A inhibition (MBI) of hepatic and gut wall (GW) metabolism of MDZ by ERY, using available *in-vitro/in-vivo* information. The final DDI model was validated by available clinical DDI studies (no IV ERY DDI studies). The IV (1mg)/PO (3mg) MDZ $AUC_{0\text{-}\infty}$ increase in presence of IV/PO ERY (1000 mg) at various post-ERY MDZ administration time intervals were simulated to explore DDI time-dependence. Simbiology toolbox was used for modeling and simulations.
Results: Model-predicted $AUC_{0\text{-}\infty}$ and c_{max} for (IV/PO) MDZ with and without PO ERY are within 30% of their observed values for all available DDI studies, confirming the validity of model and parameters. Prospective simulations demonstrate that, after IV MDZ, IV ERY consistently results in more inhibition than PO ERY (as enteric-coated (EC) tablet), due to its relatively low oral bioavailability ($\sim$40%). However, after PO MDZ, EC ERY increases MDZ $AUC_{0\text{-}\infty}$ more than IV ERY - if MDZ is dosed later than 1 hour after ERY -, due to GW metabolic inhibition. Regardless of ERY route, PO MDZ is more sensitive to metabolic inhibition than IV MDZ, due to presystemic hepatic and GW inhibition. Despite the short ERY $t_{1/2}$ and as result of MBI, maximal DDI occurs when hepatic or GW CYP3A level achieves their nadir ($\sim$2-5 hours), and the DDI lasts about 4 days for IV/PO ERY.
Conclusions: Due to dual hepatic and GW inhibition of MDZ metabolism by ERY, the magnitude and time course of the DDI depends on the administration route for both drugs.

M-42

A physiological-based pharmacokinetic (PBPK) modeling framework to predict antisense oligonucleotide (ASO) distribution in the central nervous system (CNS)

Michael Monine[1], Kumar Kandadi Muralidharan[1], Yanfeng Wang[2], Daniel A. Norris[2] and Ivan Nestorov[1]

[1]Quantitative Clinical Pharmacology, Biogen, Cambridge, MA; [2]PK/Clinical Pharmacology, ***Ionis*** Pharmaceuticals, Carlsbad, CA

Objectives: To develop a general PBPK modeling framework to describe distribution of ASOs in the CNS; to predict how early-time ASO profiles in the cerebral spinal fluid (CSF) following the intrathecal (IT) injection affect the overall exposure in the brain; to evaluate parameter identifiability of the model.
Methods: The model describes the amounts of ASO in different regions of the CNS, as shown in Fig. 1A. ASO transition between the CSF and tissues is assumed to follow the first-order kinetics and the CSF space is discretized into a number of well-stirred compartments. The data was obtained for a range of intrathecally injected ASOs in monkeys, and includes time-dependent PK in the CSF, spinal cord, brain, liver, kidneys and plasma.
Results: Several structural model modifications have been evaluated to mechanistically interpret the observed monkey PK data and select the model that fits the data best (Fig. 1B). The model analysis suggests that the differences in ASO concentrations along the lumbar-thoracic-cervical CSF regions occur on early time scale and have a minor effect on the brain exposure. By testing the models with different numbers of CSF compartments, we concluded that the model with one spinal and one cranial CSF compartments has better parameter identifiability and still fits the data well.
Conclusions: The developed framework enhances the quantitative understanding of complex mechanisms underlying ASO access into specific brain regions. The model will be further optimized for the lead ASOs and linked to biomarker/target expression. Prediction of ASO concentrations and biomarker response in the brain will facilitate the development of ASO therapies in a variety of neurodegenerative diseases.

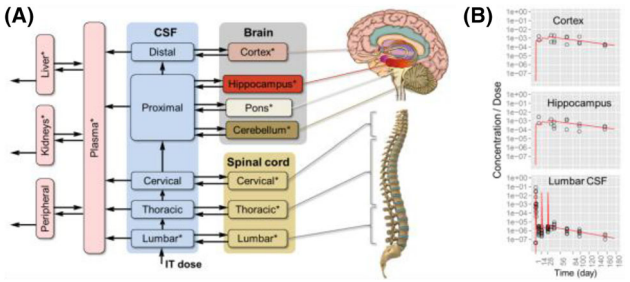

Figure 1 (A) A general PBPK model scheme. Compartments marked with "*" represent regions where the ASO concentrations have been measured in monkeys. (B) Examples of the model fits of the PK data for one of the ASO candidates injected intrathecally to monkeys (Color figure online)

M-43

Predicting Clinical Doses Based on Exposure-Response Modeling of Static Time-Kill Data

N. Mangal[1], J. Hoover[2], J. Wetherington[3], M. Hossain[4], N. Goyal[4], D. Tenero[4]

[1]Center for Pharmacometrics and Systems Pharmacology, University of Florida, Orlando, FL; [2]Preclinical Biology, GlaxoSmithKline, Collegeville, PA; [3]Clinical Statistics, GlaxoSmithKline, Collegeville, PA; [4]Clinical Pharmacology Modeling and Simulation, GlaxoSmithKline, Philadelphia, PA

Background: Antimicrobial dose selection is guided by conventional pharmacokinetic/ pharmacodynamic (PK/PD) indices/targets obtained in *in vivo* animal infection models. We tested whether *in vitro* static time-kill (TK) data could be used for prediction of clinical doses for gepotidacin (GSK2140944).
Methods: A population PK model for gepotidacin was previously developed using Phase I data. *S*tatic TK data were obtained against 6 isolates of *Staphylococcus aureus* at different gepotidacin concentrations and characterized by a PD model. Simulations were run for different dosing regimens and probabilities of target attainment (PTA) were obtained using the PK model and the:

(a) *in vivo* PK/PD index/target (conventional method)
(b) *in vitro* PD model-derived index/target ($\Delta\log_{10}$CFU/mL, change from baseline to 24 hours).

Correlation between PTA derived by the 2 methods were determined based on:

(1) fAUC/MIC>13 (stasis *in vivo*) and $\Delta\log_{10}$ CFU/mL$\geq$0 (at least stasis *in vitro*)
(2) fAUC/MIC>60 (1-log kill *in vivo*) and $\Delta\log_{10}$ CFU/mL$\geq$1 (at least 1-log kill *in vitro*)

Results: A 1-compartment PD model representing the bacterial population, growth saturation, and an E_{max}-type bacterial kill function adequately characterized the *in vitro* TK data. Compelling concordance (r^2=0.96) was found between the TK-derived endpoint ($\Delta\log_{10}$CFU/mL$\geq$0) and the *in vivo* derived endpoint (fAUC/MIC>13) for stasis with weaker concordance (r^2=0.88) between ($\Delta\log_{10}$CFU/mL$\geq$1) and (fAUC/MIC>60), associated with 1-log kill *in vivo*.
Conclusions: The developed *in vitro* PD model reasonably predicted clinical doses for stasis, which is considered the predictive endpoint for less serious infections (e.g., skin). Reliably predicting bacterial killing (considered a more predictive endpoint for serious infections) requires further exploration to widen the model utility. This approach could allow selection of probable clinical doses early in drug development using *in vitro* time-kill data.

M-44

Extension of Multi-Scale Systems Pharmacology Model (MSPM) to Evaluate Effect of Vitamin D3 (D3) Pharmacokinetics (PK) on Bone Health

Ocampo-Pelland AS[1], Gastonguay MR[1,2], French JL[2], Riggs MM[2]

[1]Biomedical Engineering, University of Connecticut, USA; [2]Metrum Research Group, LLC, Tariffville, CT, USA

Objective: To explore the effect of combined D3 plus calcium supplementation (D3CA) on bone-health endpoints.
Methods: A model for D3 and 25OHD3 population PK [2] and a MSPM [1], describing calcium, PTH, and bone remodeling were integrated to describe conversion of 25OHD3 to calcitriol and effects on bone-markers, following D3 or D3CA administration. Using R's *mrgsolve* package [3] a scaling factor for calcitriol production and exponent-gamma term, related to osteoclast bone resorption, were estimated, translating predicted changes in bone-markers to changes in lumbar spine bone mineral density (BMDLS). Population-level

A.

$$AOH0 = \frac{A0_{1,25(OH)_2D3} * 9}{C_{1,25D3,OBS}} \quad (1)$$

$$\gamma = \frac{\theta_1}{A_{1,25(OH)_2D3}} \quad (2)$$

$$C25D3scale = \frac{C0_{25D3}}{\left(\frac{0.1 * A0_{1,25(OH)_2D3}}{AOH0}\right)^{\frac{1}{\gamma}}} \quad (3)$$

$$\frac{d(A_{1,25(OH)_2D3})}{dt} = \left(\frac{C_{25D3}}{C25D3scale}\right)^{\gamma} * AOH - 0.1 * A_{1,25(OH)_2D3} \quad (4)$$

where $A_{1,25(OH)_2D3}$ ($A0_{1,25(OH)_2D3}$ at $t=0$) is serum calcitriol amount (pmol), C_{25D3} ($C0_{25D3}$ at $t=0$) is 25OHD3 concentration (nmol/L), AOH ($AOH0$ at $t = 0$) is the alpha-hydroxylase enzyme production rate (mmol/h), $C_{1,25D3,OBS}$ is the observed calcitriol baseline concentration (pmol/L), and θ_1 was optimized using calcitriol PK data following Vitamin D3 or D3CA administration ; $C25D3scale$ was solved for assuming the steady-state assumption at $t = 0$

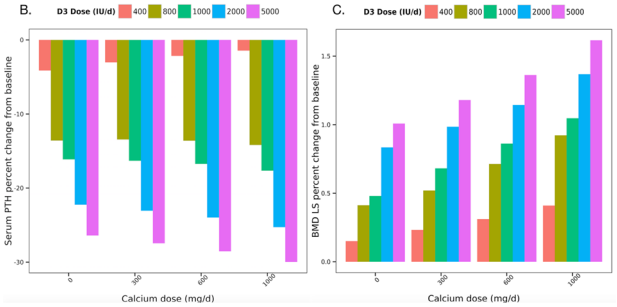

Figure 1 Final model results: (A) final model differential equations, describing change in serum calcitriol (B) change in sPTH following D3CA regimens for 1 year (C) change in BMDLS following D3CA regimens for 1 year (Color figure online)

simulations evaluated changes in BMDLS and PTH, following 1-year regimens of D3CA and quantified the relationship between BMDLS/PTH and 25OHD3 concentration.

Results: A power model structure described 25OHD3-calcitriol conversion and reflected apparent self-inhibition of calcitriol on its own production ($\boldsymbol{\theta_1}$ = 638.1, $\boldsymbol{\gamma}$ = 0.038) (Fig. 1A). Simulations indicated BMDLS/PTH changed by +2%/-52.7% for 25OHD3 concentrations 43-102 nmol/L. For fixed D3 doses, BMDLS/PTH increased/decreased with increasing calcium administration (Fig. 1B-C).

Conclusions: This is the first model-analysis to quantitatively evaluate effect of D3CA administration on bone-health endpoints, as mediated through calcium/PTH homeostatic mechanisms. Following D3 administration, calcitriol inhibited its own production, and D3CA was more effective for increasing/decreasing BMDLS/PTH than D3 alone.

References

1. MC Peterson and MM Riggs, "A physiologically based mathematical model of integrated calcium homeostasis and bone remodeling," *Bone*, vol. 46, no. 1, pp. 49–63, 2010.
2. AS Ocampo-Pelland, MM Gastonguay, JL French, and MM Riggs, "Model-based meta-analysis for development of a population-pharmacokinetic model for D3 and its 25OHD3 metabolite using both individual and arm-level data," *J. Pharmacokinet. Pharmacodyn.* vol. 43, no. 2, pp. 191–206, 2016.
3. KT Baron and MR Gastonguay, "Simulation from ODE-based population PK-PD and systems pharmacology models in R with mrgsolve," in *American Conference on Pharmacometrics 6*, 2015.

M-45

Prediction of treatment efficacy of direct antiviral agent combinations in chronic hepatitis C patients using quantitative systems pharmacology modeling approach

Oleg Demin Jr[1]

[1]Institute for Systems Biology Moscow

Objectives: The aim of this study is to predict results of ongoing clinical trials (CT) of direct antiviral agents (DAA) combinations for chronic hepatitis C patients with genotype 1 (GT1) expressed in terms of primary endpoint "sustained viral response 12" (SVR12) quantifying percent of patients with undetectable hepatitis C virus (HCV) during 12 weeks after treatment completion.

Methods: Model describing chronic hepatitis C progression including HCV dynamics, fibrosis, ALT level, immune response suppression by HCV and effects of 17 DAA compounds (sofosbuvir, daclatasvir etc) was developed. SVR12 simulations were done using the probability of resistant mutation appearance and data on degree of mutation resistance during treatment with different DAA compounds. The progression of chronic hepatitis C was calibrated against data on HCV, ALT, fibrosis score dynamics etc. The parameters of DAA effect was calibrated against data HCV decline during monotherapy.

Results: The model successfully describes the data on HCV decline during treatment with DAA combinations. The model was validated against data on SVR12 of 30 completed CT for genotype 1 treatment-naïve patients without cirrhosis. Examples of model validation and predictions of SVR12 for CT are presented in Table 1.

Table 1 Examples of model prediction of clinical trial results

Treatment	Clinical trial ID	Model predicted SVR12 – mean (range), %	Clinical trial SVR12, %	Number of patients
Sofosbuvir (400 mg QD) + Ledipasvir (90 mg QD) during 24 weeks	NCT01701401	98.83 (98.13–99.53)	99.07	214
Sofosbuvir (400 mg QD) + ACH-3102 (50 mg QD) during 6 weeks	Proxy	95.00 (91.67–100)	100	12
Sofosbuvir (400 mg QD) + Velpatasvir (100 mg QD) + GS-9857 during 8 weeks	NCT02378935	100 (100–100)	100	30

Conclusions: The model satisfactory reproduces SVR12 of CT of different DAA combinations used for treatment of chronic hepatitis C patients with GT1. The predictions of SVR12 for ongoing CT were performed and it allows to test the prediction power of model.

M-46

Pharmacokinetic and Pharmacodynamic Modeling of GPR40 Agonist MK-8666 Proof of Concept Data to Inform Clinical Decisions

Pavan Vaddady[1], Bharath Kumar[1,2], Alexander W. Krug[1], Elizabeth Migoya[1,3], Menghui Chen[1], Elizabeth Ommen[1], Daniel Tatosian[1], Prajakti Kothare[1]

[1]Merck & Co., Inc., Kenilworth, NJ, USA; [2]Biogen Idec, Boston, MA, USA; [3]Shionogi Inc., Florham Park, NJ, USA

Objective: MK-8666 is a partial agonist for the G-protein-coupled receptor (GPR) 40, which was being developed to improve glycemic control in patients with type 2 diabetes mellitus. Pharmacokinetic (PK) and pharmacodynamic (PD) data from the clinical phase 1 and phase 1b studies were modeled to a)predict glycemic efficacy over 12 weeks from short-term glucodynamic data, b) guide dose selection for the phase 2b study and c) compare glycemic efficacy to new or existing oral anti-diabetic agents.
Methods: A population PK and PK-fasting plasma glucose (FPG) model was developed based on single ascending dose (10 to 1000 mg), once-daily multiple ascending dose (50 mg to 800 mg for 10 days) studies in healthy subjects and once-daily multiple dose (placebo, 50, 150 and 500 mg for 2 weeks) phase 1b study in patients with T2DM. A previously published FPG-HbA1c relationship[1] was utilized to extrapolate MK8666 FPG predictions to 12 week HbA1c response. Clinical trial simulations of plausible dose combinations were performed to evaluate the characterization of the overall dose response curve. A previously developed comparator model on dipeptidyl peptidase IV (DPPIV) inhibitors and published TAK-875 clinical results were leveraged to identify a potential clinically efficacious dose with superior glycemic efficacy.
Results: The PK of MK8666 was characterized by a two compartment model with dose dependent central volume of distribution and first order absorption rate constant. An indirect response model with stimulation of glucose elimination well described the PK-FPG relationship. Based on simulations utilizing the PK-FPG model and FPG-HbA1c relationship[1], robust reductions in HbA1c at 12 weeks were feasible at 150 mg QD or higher, with smaller incremental benefits beyond 250-300 mg QD. Doses around 500 mg and above were predicted to be at the Emax. Based on this analysis, doses of 50, 150, 300 and 600 mg QD were predicted to provide an adequate characterization of the overall dose-response curve. A potential clinically efficacious dose of 300 mg had the highest probability for a superior glycemic efficacy in comparison to DPPIV inhibitors and TAK-875.
Conclusion: Integration of modeling and simulation with team strategy allowed extrapolation of two week proof of concept study results to 12 week HbA1C response. The predicted dose-HbA1c curve facilitated decisions on dose selection for a proposed Phase 2b study.

Reference

1. Naik H et. al., Pharmacometric approaches to guide dose selection of the novel gpr40 agonist tak-875 in subjects with Type 2 diabetes mellitus. CPT PSP 2013 Jan; 2(1): e22.

M-47

Evaluation of beta transformation to estimate treatment effect in depression and schizophrenia trials with nonlinear mixed effects analyses

R. Gomeni[1], N. Goyal[2], F.M.M. Bressolle-Gomeni[1]

[1]Pharmacometrica, Longcol, La Fouillade, France; [2]Clinical Pharmacology Modeling and Simulation, GlaxoSmithKline, King of Prussia, PA, USA

Objective: This exercise compares beta transformation of longitudinal bounded PANSS and HAMD clinical scores in schizophrenia and depression trials to estimate treatment effect Vs untransformed (raw) data.
Methods: The data was obtained from a placebo-controlled, 6-week, parallel-group clinical trial in patients with schizophrenia to evaluate an antipsychotic treatment at different doses with olanzapine as a positive control. The longitudinal model was PANS(t)=Baseline*-exp(-k*time)+Slope*time (k is the exponential rate of decrease in PANSS; and Slope is the linear rate of PANSS relapse) (1). The other data was from a clinical trial in patients with depression randomized in an 8-weeks, double-blind, placebo-controlled, parallel-group study evaluating two doses of an antidepressant treatment (2). The longitudinal model was: HAMD(t)=Baseline*exp(-time/td)**b+hrec*time (td is the time corresponding to 63.2% of the maximal change from baseline; b is the sigmoidicity factor; and hrec is the remission rate). The two models were fitted using NONMEM. The mixed-effects beta regression models were implemented using Nemes' approximation to the gamma function.
Results: The treatment effect (TE) for each trial and treatment arm was defined as the change from baseline in the clinical score at the end of the study. Comparisons of the results for PANSS and HAMD indicated that TE estimated using the beta transformed data was statistically higher ($p<0.01$) than that estimated using untransformed data. Furthermore, the drug effect (estimated as change in TE between placebo and drug arms) was statistically higher when this value was estimated using beta transformation (11% for the PANSS and 23% for the HAMD, respectively).
Conclusions: The results of the analyses indicate that the beta transformation approach represents the methodology of choice for analyzing longitudinal bounded data. In fact, this methodology seems to be more efficient in detecting a signal of drug activity.

References

1. Eur Neuropsychopharmacol. 2013; 23(11):1570-1576.
2. Clin Pharmacol Ther. 2008 Sep;84(3):378-84.

M-48

Model Based Approach for Prediction of Human Pharmacokinetic Variability and Efficacy of an Antibody Drug Conjugate from Preclinical Data

Renu Singh (Dhanikula)[1*], Patrice Bouchard[1], Jim Koropatnick[2], Susan Twine[3], Maureen O'Connor-McCourt[4], Ilia Tikhomirov[4]

[1]National Research Council of Canada, 6100 Royalmount Avenue, Montréal Quebec; [2]Lawson Health Research Institute, London, Ontario; [3]National Research Council of Canada, 1200 Montreal Road, Ottawa, Ontario; [4]Formation Biologics, Royalmount Avenue, Montréal Quebec

Objective: Variability in pharmacokinetics of a therapeutic candidate in the patient population is pivotal in understanding the clinical outcome. We have attempted to predict inter-individual variability in pharmacokinetics of an antibody drug conjugate (ADC) using body weight as a covariate. Pharmacokinetics as well as efficacy in different dosing regimens was simulated and tumor regression was compared using different dosing regimens to understand impact of dosing regimen on patient survival.
Methods: A model based approach was used for predicting inter-individual variability in pharmacokinetics of our ADC candidate. Simulations were done in different dosing regimen scenarios in 50 healthy subjects using body weight as a covariate using Berkley Madonna 8.3.18. Two compartment model with linear and non-linear clearance from central compartment was used for this purpose. Hepatic and renal impairment were assumed to not significantly impact systemic clearance of ADC. ADC pharmacokinetics translated from cynomolgus monkey was used for the purpose of simulations. Subsequently, the tumor regression produced in clinic was simulated in 10 patients using Jumbe transduction model. PK/PD parameters estimated from mouse xenograft study were assumed to be the same in human, with the premise that growth rate of human tumor is much slower than xenograft tumor thus parameters that drive tumor-statis in mouse will result in tumor-kill in human. For estimating patient survival tumor volume less than 350 mm^3 was assumed an arbitrary measure of survival.
Results: Minimum systemic exposure was found to vary about 25-30% in the simulated population, however a reasonable coverage of estimated tumor-static concentrations (TSC) was observed. Population average steady state concentrations remained within estimated 95% confidence interval of TSC for all simulated individuals. Remarkably similar therapeutic outcome was observed when doses between 0.5-2.0 mg/kg were given once weekly vs when 1.3 to 3.9 mg/kg were given once every three weeks for 3 or 6 months, resulting in approximately similar patient survival.
Conclusions: The patient survival in simulated conditions was found to be similar in Q1W and Q3W dosing regimens.

M-49

POP PK Quality Control: Data Proofing and Model Verification

Robert Fox[1], Pei Ma[1], Nidal Al-Huniti[1]

[1]Quantitative Clinical Pharmacology, AstraZeneca, Waltham, MA

Objectives: Systematic and thorough data proofing and model verification methods strengthen credibility of POP PK results and allow reviewers to focus on analyses messages and conclusions. Frequently, however, data collection and edit checks are not designed, nor sufficiently developed to clean data related to POP PK analyses. As a result incomplete or erroneous data are arbitrary excluded from analyses. These exclusions can have significant impact on results and interpretation. In addition to data content credibility, tool-specific data formatting requirements can unnecessarily add iterations to the data build process. Slight deviations from the format requirements can prevent analysis from being executed resulting in multiple issue-resolution cycles. Further, NONMEM control streams, outputs, and listings need to be reviewed against the analysis plan. The POP PK report needs to be verified against all data manipulations and modeling methods. Supporting plots, figures, tables and listings need to be verified against the data and analyses. With this in mind, the objective was to develop data proofing and model verification solutions to deliver high-quality, analysis-ready data and to deliver verifiable modeling results.
Methods: A collection of re-useable data proofing programs (using SAS and R) has been created. The data proofing methods facilitate the identification and reconciliation of the data and formatting issues and minimize the iterative data review process.
Manual review steps were initiated to ensure that the modeling and analyses steps from source data to final report are transparent. Simulation models are checked against source descriptive models to ensure accurate translation of model specifications and parameter value transcription. Simulation scenarios are checked to ensure congruity with the modeling and simulation plan.
Results: Data issues and format issues are now more readily identified and corrected. Data review cycles are minimized. Unnecessary interactions are eliminated. Modeling verification activities ensure quality analysis results and conclusion.
Conclusions: By using verification methods, data preparation and modeling activities attain high-quality, fully transparent results allowing the reviewer to focus on the modeling messages and results.

M-50

Physiological modeling of uric acid in man: application to assess benefit-risk of lesinurad in gout

Sergey Aksenov[1,*], Ulf Eriksson[1], Donald Stanski[1]

[1]Quantitative Clinical Pharmacology, AstraZeneca

Objectives: Lesinurad (Zurampic) is a novel selective uric acid reabsorption inhibitor (SURI) recently approved in combination with xanthine oxidase inhibitors (XOI) for chronic treatment of hyperuricemia in gout patients who have not achieved target serum uric acid (sUA) with an XOI alone. Modeling of clinical data can help quantify benefit-risk of alternative dose regimens and treatment strategies [1]. The objectives of this work were to provide further justification of a once daily regimen of lesinurad supported by Phase 3 clinical data; and for using lesinurad in combination with increased allopurinol dosing.
Methods: A model was developed to describe the physiologic turnover of uric acid in man including its production and intestinal and renal clearance. The stimulatory effect of lesinurad on renal clearance of uric acid and the inhibitory effect of allopurinol on its production were described by saturable functions of drug plasma concentration. The model was developed using serial uric acid data in serum and urine in 278 subjects from 9 Phase 1 studies and qualified using data

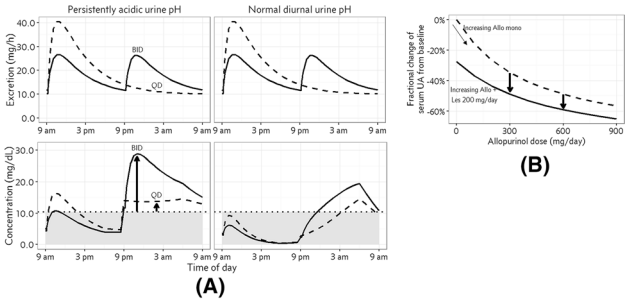

Figure 1 (A) Simulation of concentration of uric acid in urine for twice a day compared with once a day lesinurad 200 mg + 300 mg/day allopurinol. Gray area denotes concentration below solubility limit. (B) Simulation of dose response for fractional reduction of serum uric acid concentration from baseline for increasing doses of allopurinol alone (dashed) and in combination with 200 mg/day lesinurad (solid)

from 6 Phase 3 studies. The model predicts population mean of sUA concentration and excretion of uric acid in urine (uUA).
Results: Simulation showed that twice daily lesinurad results in higher uUA concentration (and the potential to cause adverse events via uric acid precipitation) after the evening than the morning dose because of slower urine flow and lower urine pH at night thus confirming the decision to use once daily dosing in the morning in the lesinurad Phase 3 program. Adding 200 mg lesinurad once a day to allopurinol results in greater lowering of sUA than allopurinol monotherapy. Additional lowering is similar across the range of allopurinol doses used in clinical practice.
Conclusions: Modeling supports improved benefit-risk of once daily over twice daily dosing and additional sUA lowering by lesinurad regardless of the allopurinol dose.

Reference

1. Khanna D, et al. Arthritis Care Res. 64(10): 1431, 2012

M-51

Population pharmacokinetics of trastuzumab emtansine (T-DM1) in patients with HER2-positive advanced gastric cancer (AGC)

Shang-Chiung Chen[1], Matts Kaagedal[1], Yuying Gao[2], Bei Wang[1], Marie-Laurence Harle-Yge [3], Tina van der Horst[3], Jin Jin[1], Sandhya Girish[1], Chunze Li[1]

[1]Genentech, Inc., South San Francisco, CA; [2]Quantitative Solutions, Menlo Park, CA; [3]Roche, Basel, Switzerland

Objectives: A population pharmacokinetic (PK) analysis was performed to characterize T-DM1 pharmacokinetics in previously treated patients with HER2-positive advanced gastric cancer (AGC), and to quantify effects of baseline demographic, laboratory, and disease characteristics on T-DM1 PK.
Methods: 789 T-DM1 serum concentration-time data points from 137 T-DM1 treated patients were fitted using NONMEM® software. Relevant and plausible covariates likely to have an effect on T-DM1 systemic exposure were explored for possible correlation with the key T-DM1 PK parameters of linear clearance (CL) and central volume of distribution (V_c).
Results: T-DM1 PK in HER2 positive AGC patients was best described by a two-compartment model with parallel linear and nonlinear (Michaelis-Menten) elimination from the central compartment. The final population PK model estimated linear CL of 0.79 L/day, Vc of 4.48 L, Q of 0.62 L/day, Vp of 1.49 L, non-linear CL of 2.06 L/day, and KM of 1.63 μg/mL. Parameter uncertainty was low to moderate for fixed effects except for KM, which was estimated with poor precision. Patients with higher body weight and lower baseline trastuzumab concentrations had statistically significant faster CL. Patients with higher body weight also have statistically significant larger V_c. Incorporation of these covariates ($P<0.001$ by likelihood ratio test) decreased IIV of CL and V_c to 26% and 21%, respectively. The model sensitivity analysis suggests <35% PK variability (as represented by T-DM1 AUC) when statistically significant PK covariates were between 5th and 95th percentile of the population.
Conclusions: In HER2-positive AGC population, T-DM1 PK was best described by a two-compartment model with parallel linear and nonlinear (Michaelis-Menten) elimination. Baseline body weight and trastuzumab concentrations were identified as statistically significant covariates influencing the PK in HER2-positive AGC patients. Predicted PK exposure was lower than previously reported for HER2-positive metastatic breast cancer.

M-52

A proof-of-principle example for identifying drug effect from a mechanistic model with a more parsimonious model

Shijun Wang[1, *], Kristin E. Karlsson[1], Maria Kjellsson[1], Mats O. Karlsson[1], Andrew C. Hooker[1]

[1]Dept. of Pharmaceutical Biosciences, Uppsala University, Uppsala, Sweden

Objectives: This work aims to establish a proof-of-principle example for identifying drug effects from complicated mechanistic system using a more parsimonious model. We used the integrated glucose-insulin (IGI) model for oral glucose tolerance tests (OGTT)[1] to simulate virtual drug effects mimicking complex system and the more parsimonious glucose kinetics minimal model for oral absorption[2] for estimation.
Methods: The virtual drug affected either clearance of glucose (CLG) or insulin-dependent clearance of glucose (CLGI) in the IGI model. Drug effect size was measured as decrease in the AUC of the plasma glucose-time curve (1%-15% investigated) after dosing. Minimal models, extended with all potential combinations of drug effects on baseline concentration of glucose (IBSL), sensitivity of glucose (SG), sensitivity of insulin and remote insulin, were used for estimation. AIC values estimated were used to rank the extended models. A geometric distance clustering method based on the estimated parameters was used to identify the type of drug effect.
Results: AIC tests showed that, for data simulated by IGI model with drug effect on CLG, the minimal model where drug effect was on IBSL performed the best in low dose arms, while drug effect on SG was the best in high dose arms; for simulated drug effect on CLGI, estimated drug effect on IBSL or SG performed better than all other models. These models could quantify the simulated drug effect with high accuracy. The clustering analysis based on combination of the estimated AUC decrease, and the SG and IBSL drug effect parameters allowed, using cross-validation, the correct identification of the CLG or CLGI drug effect type was 95% and 61% of the time, respectively.
Conclusions: The size and type of drug effect simulated by a mechanistic model could be properly detected by more parsimonious model in OGTT.

References

1. Silber, *J.Clin.Pharmacol,* 2007.
2. Largajolli, PAGE, 2016.

M-53

Mathematical Modeling to Investigate Pleiotropic TNF-α Activity in Drug-Induced Liver Injury

Shoda, L.K.M[1]., Siler, S.Q.[1], Pisetsky, D.[2], Watkins P.B.[3], Battista, C.[c], Howell, B.[1]

[1]DILIsym Services Inc., 6 Davis Drive, Research Triangle Park, NC 27709-2137; [2]Duke University Medical Center, Durham, North Carolina 27710; [3]University of North Carolina, Chapel Hill, 27299

Objectives: Drug-induced liver injury (DILI) has halted the development of promising drugs and led to the recall of FDA-approved drugs. While drugs can directly induce hepatocyte injury via several mechanisms, injury and outcomes can be influenced by the development of a liver immune response, subsequent to the initial hepatic injury. In fact, plasma acetylated HMGB1, a biomarker of macrophage activation, has been tied with patient outcomes in acetaminophen overdose[1].

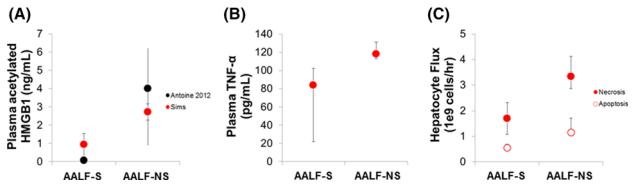

Figure 1 Simulations consistent with the presence of an inflammatory response in some cases of acetaminophen (APAP) overdose. (A) A simulated population sample (n=300) was administered a liver injury inducing 42g APAP. Simulated acetylated HMGB1 was compared with clinical data from patients with APAP liver injury (specific doses not available).[1] Clinical data were differentiated on outcomes: APAP acute liver failure survivors (AALF-S) and non-survivors (AALF-NS). Simulated results were differentiated by degree of liver injury: AALF-S corresponding to 20–55% liver loss; AALF-NS corresponding to 56–85% liver loss. (B) Simulation results indicate more hepatocyte death due to necrosis and apoptosis in simulated patients with more severe injury (Color figure online)

Methods: The DILIsym® software has been developed to support the mechanistic and mathematical evaluation of DILI. It includes (but is not limited to) hepatocyte release of active or non-active forms of non-acetylated HMGB1, depending on mode of hepatocyte death, liver macrophage activation by HMGB1, and macrophage production of acetylated HMGB1, tumor necrosis factor (TNF)-α, and other mediators. Pleiotropic TNF-α activity is reproduced by linking TNF-α-mediated hepatocyte survival/proliferation, apoptosis, or necro-apoptosis to the energetic status, i.e., ATP level, of hepatocytes.
Results: By design, DILIsym® reproduces TNF-α induced survival or proliferation, apoptosis, and necro-apoptosis under alternate starting conditions representative of experiments intended to isolate these responses. Incorporating pleiotropic TNF-α activity permits its investigation in DILI. For example, simulated acetaminophen overdose can extend beyond the finding that the levels of acetylated HMGB1 differentiate outcomes in simulated patients (Figure 1a) to consider the contribution of TNF-α. Higher TNF-α and higher necrotic and apoptotic cell death are associated with poorer outcomes (Figure 1b, c) and can be examined for dynamic changes in TNF-α-mediated hepatocyte proliferation, apoptosis, and necrosis.
Conclusion: Inclusion of immune responses in DILIsym® allows for the systematic investigation of immune contributions to DILI and sets the stage for improved understanding in this complex area.

Reference

1. Antoine DJ, Jenkins RE, Dear JW, et al. Molecular forms of HMGB1 and keratin-18 as mechanistic biomarkers for mode of cell death and prognosis during clinical acetaminophen hepatotoxicity. *J Hepatol*. 2012;56(5):1070-1079. doi: 10.1016/j.jhep.2011.12.019.

M-54

Population pharmacokinetics and exposure-response of filgotinib in patients with moderate to severe Crohn's disease

Shringi Sharma[1], Yan Xin[1], Yuying Gao[2], Florence Namour[3], Anita Mathias[1]

[1]Gilead Sciences, Foster City, CA, USA; [2]Certara Strategic Consulting, Menlo Park, CA, USA; [3]Galapagos NV, Mechelen, Belgium

Objectives: Filgotinib (FIL), a selective janus kinase-1 (JAK-1) inhibitor, has shown a favorable benefit-risk profile in patients with moderate to severe Crohn's disease (CD). The objective was to develop a population pharmacokinetic (PK) model and investigate the exposure-response (efficacy/safety) relationship.
Methods: In a Phase 2, double-blind study, CD patients (N=143) were administered FIL (200 mg versus placebo, once daily [QD]) for 10 weeks. Sparse and intensive PK sampling for FIL and its active metabolite (MET) was performed. Nonlinear mixed-effects models were fitted to FIL/MET plasma concentrations. Covariates screened for influence on FIL/MET PK were baseline age, weight, height, BMI, BSA, sex, race, study region and creatinine clearance. Relationships between model predicted FIL/MET exposures and efficacy (clinical response, remission, endoscopic response) and safety (such as blood count and lipid profile) assessments at Week 10 (primary end point visit), following FIL 200 mg QD, were evaluated.
Results: FIL PK were described by a two-compartment model with first-order absorption, first-order elimination, and a lag time. MET PK were described by a one-compartment model with first-order absorption, first-order elimination, and a lag time. None of the covariates showed a statistically significant effect on FIL/MET PK. The population mean (%IIV) estimate of FIL CL/F was 107.9 (110%) L/hr, Vc/F was 4.17 (139%) L and Ka was 0.18 (72%) 1/h. The population mean (%IIV) of MET CL/F was 3.48 (34%) L/hr, Vc/F was 199.3 (58%) L and Ka was 0.73 (77%) 1/hr. Over the range of FIL/MET exposures (divided into quartiles; > 2 fold range between midpoint of first vs fourth quartile) following FIL 200 mg QD, no association with efficacy or safety was observed.
Conclusions: FIL/MET PK is unaffected by demographic or disease-relevant covariates. No relevant relationship between FIL/MET exposure and efficacy/safety was observed, suggesting that FIL 200 mg QD provided consistent therapeutic effects without any adverse exposure-driven safety trends in CD patients.

M-55

An efficient language for model-based trial simulations

Shuhua Hu, Michael Dunlavey, Kairui Feng, Robert Leary

Certara, Cary, NC

Objectives: Compared to other languages for nonlinear mixed-effect models, Pharsight modeling language (PML) was designed to be good for both model fitting and simulations. The goal is to demonstrate advantages using PML for model-based simulations through an example.
Methods: PML simulation includes two major components. One is for fitted population models and covariate distribution models. The other is for study protocol designs that specify how simulation is conducted and are written in procedures having the capability of "sleep", branching and looping. This allows users to not only directly simulate fitted models but also do individual-level post-analysis (e.g., calculate AUC and Cmin), which avoids outputting a huge amount of data to do such processing/analysis in third party software and hence saves I/O time. PML codes can also be integrated with R to do statistical analysis and visualization.
Results: The example of demonstrating these is based on the antibiotic study [1], where Monte Carlo simulation was used to find optimal dose. This involves multiple endpoint analysis, non-steady-state and steady-state analysis: calculate probability of target attainment for AUC/MIC and probability of Cmin above some value at day 1 and steady-state. We successfully implemented this example in PML with "steadystate" statement used to automatically detect if steady-state is reached. To have some idea of computational savings

for doing individual-level post-analysis in PML, we compared computation times for two methods: one calculates AUC, AUC/MIC and Cmin in PML and does population-level post-analysis in R; and the second method does all the post-analysis in R. We found that the first method integrated PML for post-processing saves over 29% computational time.
Conclusions: We demonstrated how PML can be used to facilitate model-based simulation. This is achieved through seamless integration of fitted population models into simulation and the ability of doing both pre-processing and individual-level post-analysis, and hence avoid manually modifying fitted models for simulation and reduce the need to use different software to do the job.

Reference

1. Tanigawara, et al., Eur J Clin Pharmacol., 68(2012):39-53.

M-56

Simulation of complex population PKPD models with adaptive dosing regimens

Shuhua Hu, Michael Dunlavey, Kairui Feng, Robert Leary

Certara, Cary, NC

Objectives: To demonstrate the capability of Pharsight modeling language (PML) in conducting Monte Carlo simulations of complex PKPD models with adaptive dosing regimens.
Methods: The example of demonstrating this is based on the sedation-study [1]. It includes a PK model, a PK/PD link model, and a PD model with six categorical observations. The dosing regimen involves a loading dose and a sequence of maintenance doses with maximum of 4 allowed and each no sooner than 2 minutes after the previous dose. The time to administer maintenance doses depend on patient's response. Monte Carlo simulation was done in [1] through repeatedly using NONMEM and Excel: NONMEM for simulation, and Excel for identifying when to administer a maintenance dose. We see that this is time-consuming and error-prone. Compared to other modeling languages, PML tries to follow the philosophy of declarative languages, and is designed to be good for both model fitting and simulation. This allows users to directly simulate fitted models and to implement simulations with complicated protocols such as the adaptive treatment feature presented in this example.
Results: The left panel of Figure 1 illustrates PML simulation flow chart, where protocols are written in procedures that can perform "if", "while", "for" and "sleep" statements, use and assign values to model variables, and define local variables. Specifically, whenever a procedure enters a"sleep", it means that it allows some simulation time to pass. With these PML features/functionalities, this example was successfully implemented in PML without using other software to identify when a maintenance dose is needed and to introduce it during an individual run (the right panel of Figure 1 shows a snapshot of the treatment procedure).
Conclusions: We demonstrated the capability of PML in simulating complicated protocols where there is a feedback between treatment and patient's response. This eliminates the need for repeatedly using multiple software during an individual run, and hence greatly improves efficiency and reliability.

Figure 1 (*left panel*) PML simulation flow chart; (*right panel*) a snapshot of the treatment procedure (Color figure online)

Reference

1. Wiltshire, et al., Anesth Analg., 115(2012):284-296.

M-57

A longitudinal PKPD model describing the static Physician Global Assessment (sPGA) Response to ixekizumab in patients with moderate to severe plaque psoriasis

Siak Leng Choi[1], Kimberley Jackson[2], Emmanuel Chigutsa[3], Nieves Velez de Mendizabal[3], Laiyi Chua[1], Leijun Hu[2], Stuart Friedrich[3];

Lilly-NUS Centre for Clinical Pharmacology, Singapore; [2] Global PKPD and Pharmacometrics, Eli Lilly and Company, Windlesham, UK; [3] Global PKPD and Pharmacometrics, Eli Lilly and Company, Indianapolis, IN, USA

Objectives: To develop a PKPD model describing the effect of ixekizumab, an anti-IL-17A monoclonal IgG4 antibody, on the longitudinal sPGA response in patients with moderate to severe plaque psoriasis.
Methods: Ixekizumab or placebo was administered subcutaneously (SC) (10, 25, 75, or 150 mg) at 0, 2, 4, 8,12, and 16 weeks in a Phase 2 study (N=141 patients); and as a 160 mg initial dose, then 80 mg Q2W or Q4W or placebo for 12 weeks, then Q4W or Q12W up to 60 weeks in a Phase 3 study (N=1297 patients). Analyses were conducted using NONMEM 7.3.
Results: A two compartment PK model with first order absorption linked with a semi-mechanistic Type I indirect response latent-variable logistic regression model[1] was adapted to model ordered categorical sPGA scores. The structural model included a weibull-like placebo effect, a mixture model bimodal distribution of EC50, disease progression and a precursor compartment for the latent variable to describe development of tolerance. An adaptive VPC approach demonstrated the model was able to describe the data well. The model simulations were used to support the proposed induction and maintenance dosage regimens for regulatory submission.
Conclusions: The relationship between ixekizumab concentrations and sPGA response over time in patients with moderate to severe plaque psoriasis was described well using a longitudinal latent variable model and supported the proposed dose regimens for registration.

Reference

1. Hu C, Szapary PO, Yeilding N, Zhou H. Informative dropout modeling of longitudinal ordered categorical data and model validation: application to exposure-response modeling of physician's global assessment score for ustekinumab in patients with psoriasis.J Pharmacokinet Pharmacodyn. 2011;38(2):237-260.

M-58

Working Towards a Physiologically-based Mathematical Model for Predicting Treatment Outcomes in a Prostate Cancer Mouse Model

Songmao Zheng, Donald L. Heald, Weirong Wang

Biologics Clinical Pharmacology, Janssen BioTherapeutics (JBIO), Janssen R&D US

Objectives: The objective of our work is to develop a physiologically-based mathematical model to describe the interplay between the key components of the therapeutic agent, host immune system and prostate cancer cells for predicting treatment outcomes.
Methods: The initial step was to first examine a mechanism-based mathematical model developed by Peng *et al.*[1] which had been used to explore the interactions between prostate tumor and immune microenvironment. The model predicted treatment efficacy with androgen deprivation therapy (ADT), dendritic cell vaccines, regulatory T cells (Tregs) depletion and/or Interleukin-2 (IL-2) neutralization in a prostate-specific $Pten^{-/-}$ mouse model. Extensive literature search was conducted to determine the physiological ranges and values of 18 out of the 25 initially model-derived parameters. The updated model was used to fit observed mouse data following various treatments and to examine the biological relevance of other estimated model parameters. First order conditional estimation with interaction (NONMEM® V7.2.0) was used to fit longitudinal mouse data simultaneously from 5 different compartments, including tumor size, Tregs and cytotoxic T cells (CTLs) in prostate tissues and prostate-draining lymph nodes in 7 mono-therapy and combination treatment groups reported by Peng *et al.*[1].

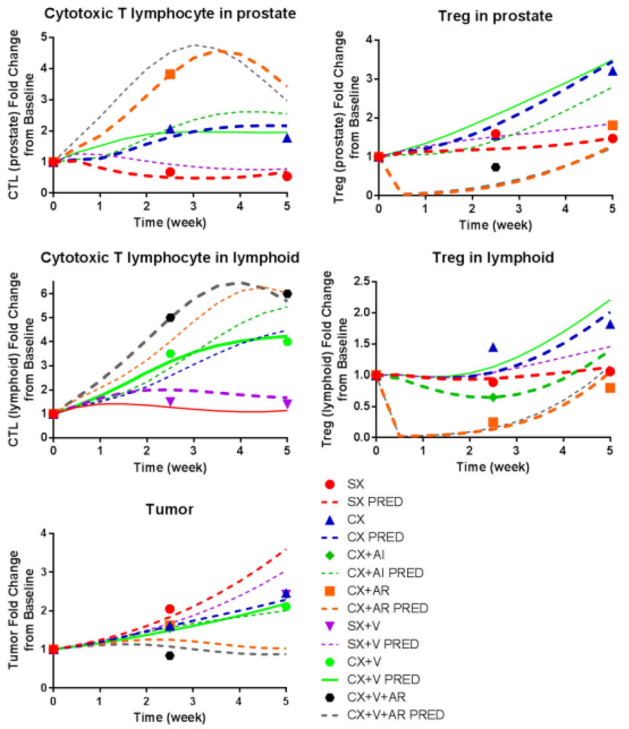

Figure 1 Simultaneous model prediction versus observed using physiological parameter values from literature search. SX: sham-castration (control); CX: castration; AL: anti-IL2 (IL-2 neutralization); AR: anti-Treg (Treg depletion); V: vaccination; "+" means combined treatment (Color figure online)

Results: The Peng *et al.* model was first verified by comparing simulated versus observed data using previously estimated parameter values. Then, the model was updated by replacing over 10 parameters using physiological values from the literature search. The updated model converged successfully with covariance step completed. All treatment groups have reasonable model prediction for all compartments. Next, sensitivity analysis was performed on a series of parameters for determining impact on estimating other parameters and overall model fitting. Further, the established model was used to predict the outcomes for untested combined treatments.
Conclusions: This study highlighted the potential role of physiologically-based mechanistic modeling under a framework of systems pharmacology approach in studying tumor immunotherapy and rational selection of therapeutic interventions.

Reference

1. Peng, H., et al., *Prediction of treatment efficacy for prostate cancer using a mathematical model.* Scientific Reports, 2016. **6**: p. 21599.

M-59

Mechanistic Understanding of the Impact of Loading Dose in the anti-TNFα Biologics Treatment of Inflammatory Bowel Disease in an Adoptive T cell Transfer Mouse Model

Songmao Zheng[1], Jin Niu[1], Damien Fink[1], Brian Geist[1], Zhenhua Xu[1], Honghui Zhou[2], Weirong Wang[1]

[1]Biologics Clinical Pharmacology, JBIO; [2]CPPM, Quantitative Sciences, Janssen R&D US

Objectives: Current biologic treatment for inflammatory bowel disease (IBD) includes various induction phases. Mechanistic understanding of the rationale behind such induction/loading dose is still lacking. Utilizing an adoptive T cell transfer model provided an opportunity to examine the early immunological events associated with gut inflammation and the perpetuation of disease by therapeutic intervention. This study was designed to quantitatively understand the impact of IBD on an anti-TNFα monoclonal antibody (mAb) disposition, the ability of the mAb to neutralize TNFα at the colon and the impact of loading dose on drug efficacy.
Methods: CNTO5408, an anti-TNFα mouse surrogate of SIMPONI® (golimumab), was used in a $CD45RB^{high}$ adoptive T cell transfer model. Total drug, total and free TNFα in mice serum and colon homogenate were measured. A minimal physiologically-based pharmacokinetic (mPBPK) model and a direct response model were developed to characterize drug PK, colon target engagement (TE) and treatment regimen-dependent drug efficacy (PD). Model fitting and simulations were conducted using NONMEM® V7.2.0.
Results: The mPBPK modeling determined that both colon uptake rate and elimination rate of the mAb from the systemic circulation are faster in IBD mice relative to healthy mice. A 10mg/kg loading dose resulted in a near complete target suppression, while sub-efficacious doses (0.3 mg/kg Q3D) were not able to control disease flare. The TE/PD model reasonably captured the observed data, where free TNFα concentrations in colon exhibited dose-dependent suppression and correlated well with histopathology results, such as inflammation scores, neutrophil scores and gland loss. Results from this study also suggested that TNFα production changes with disease status.
Conclusions: This study provided a quantitative understanding of the impact of anti-TNFα mAb loading dose on colon TNFα suppression and its therapeutic efficacy using a physiologically relevant IBD animal model, providing insights on the rationale of administering induction/loading doses for treating IBD patients.

M-60

Development of an Integrated Population Pharmacokinetic Model Characterizing the Tissue Distribution of Azithromycin and Erythromycin in Healthy Subjects

Songmao Zheng[1,2], Shaip Krasniqi[3], Peter Matzneller[3], Markus Zeitlinger[3], Stephan Schmidt[1]

[1]Center for Pharmacometrics & Systems Pharmacology, University of Florida, USA; [2]Biologics Clinical Pharmacology, Janssen R&D USA; [3]Department of Clinical Pharmacology, Medical University Vienna, Austria

Objectives: Emerging evidence suggests that the use of azithromycin triggers macrolide resistance. This effect seems to be less pronounced for other macrolides, such as erythromycin or clarithromycin. The objective of our study was to determine if a causal relationship exists between the physicochemical properties of macrolides, their corresponding pharmacokinetics, and subsequent resistance development.
Methods: Azithromycin (500mg QD) or erythromycin (500mg QID) were administered orally to 6 healthy male volunteers for three days. Free concentrations in the interstitial space fluid (ISF) of muscle and subcutaneous adipose tissue as well as total concentrations in plasma and polymorphonuclear leukocytes (PMLs) were determined on days 1, 3, 5, and 10. All concentrations were modeled simultaneously for both drugs in NONMEM 7.2 using a mechanism-based tissue distribution model that integrates information on the drugs' physicochemical properties, protein binding, unspecific tissue binding and pH differences between tissues to characterize macrolide distribution in tissues in general and in PMLs in particular.
Results: The developed and qualified mechanism-based model enabled describing of drug concentrations across sampling sites. The overall pharmacokinetics of azithromycin is driven by the release of drug from acidic cell/tissue compartments, and the model estimated a more than 30-fold higher distribution factor for the unionized azithromycin concentrations in the cytosol of PMLs ($C_{PML(cytosol,unionized\ AZM)}$) compared to that for erythromycin. Model-predicted $C_{PML(cytosol,unionized)}$ for both drugs were comparable to measured ISF concentrations in muscle and subcutis on day 10, whereas total PML concentrations were more than 1000-fold higher for azithromycin. In contrast to erythromycin, subinhibitory azithromycin concentrations were observed in plasma and interstitial space of both soft tissues through day 10.
Conclusions: The development of a drug class-specific model for macrolides allowed for the characterization of their tissue distribution kinetics on a mechanistic basis with differences in ionization being the main driver. Compared to azithromycin, erythromycin resides much shorter in the body at subinhibitory concentrations, which may explain differences in the emergence of resistance between both drugs.

M-61

A Quantitative Systems Pharmacology Model to Predict the Effects of Warfarin, Rivaroxaban and Enoxaparin on the Human Coagulation Network

Sonja Hartmann[1], Konstantinos Biliouris[1], Lawrence J Lesko[1], Ulrike Nowak-Göttl[2], Mirjam N Trame[1,*]

[1]Center for Pharmacometrics & Systems Pharmacology, University of Florida, Orlando, Florida, USA; [2]University of Schleswig-Holstein, Thrombosis & Hemostasis Treatment Center, Campus Kiel & Lübbeck, Germany

Objectives: To develop a quantitative systems pharmacology (QSP) model describing the coagulation network to monitor anti-coagulation factor levels under warfarin, enoxaparin, and rivaroxaban treatment and to aid in optimization of anti-thrombotic therapy in light of optimal time-to-clot dissolution.
Methods: Individual steady-state coagulation factor level data from therapeutic drug monitoring of 312 subjects on enoxaparin, rivaroxaban, and warfarin/phenprocoumon (Vitamin K antagonists (VKA)) treatment were used to develop a QSP model of the coagulation network in MATLAB®, based on Wajima *et al.*[1] Parameter values for all factor rate constants (V_{max}, K_m) and production rates were estimated and the model was adjusted given the available data. Sobol sensitivity analysis was performed to identify key parameters having the greatest impact on clot dissolution.
Results: Predictions of individual coagulation factor time courses under steady-state VKA, enoxaparin, and rivaroxaban treatment reflected the suppression of the endogenous clot dissolution components PC and PS under VKA compared to rivaroxaban and enoxaparin. The model was used to simulate treatment switch from VKA to enoxaparin or rivaroxaban, and was able to describe the observed 50% increase within 9 and 11 days in PC and PS factor levels, respectively. Treatment switch from enoxaparin to VKA lead to a 50% decrease in PC and PS factor levels within 8 and 10 days, respectively. Sobol sensitivity analysis identified production rates for vitamin K being the most influential parameters to stimulate clot-dissolution.
Conclusion: A QSP model was developed to describe the human coagulation network and time courses of several clotting factors under different treatment regimens. The model may be used as a tool during clinical practice to predict the effects of different anti-coagulant therapies on individual clotting factor time-courses and to optimize anti-thrombotic therapy regimens.

Reference

1. Wajima T. *et al. CPT.* **86**(3):290–8 (2009).

M-62

Safety Exposure-Response Analysis for Daclatasvir /Asunaprevir/ Beclabuvir Regimen in Hepatitis C Virus Infected Subjects

Takayo Ueno[1], Mayu Osawa[1], Tomomi Shiozaki[1], Hiroki Ishikawa[1], Hanbin Li[2], Phyllis Chan[3], Brenda Cirincione[3], Frank LaCreta[3], Tushar Garimella[3]

[1]Bristol-Myers Squibb K.K, Tokyo, [2]Quantitative Solutions, CA, [3]Bristol-Myers Squibb, NJ

Objectives: The combination regimen of daclatasvir, asunaprevir and beclabuvir (DCV/ASV/BCV regimen) is being developed as fixed-dose-combination for the treatment of HCV infection in Japan. The objectives of this analysis were to characterize the relationship between the exposure of DCV, ASV, and BCV and liver-related laboratory abnormalities (Grade3/4 ALT, AST and total bilirubin), and to evaluate the impact of selected covariates on the exposure-response (E-R) relationships.
Methods: The E-R analysis was performed with data from one Phase2 and three Phase3 studies in HCV infected-subjects. The probability of Grade3/4 liver-related laboratory abnormalities were modeled using linear logistic regression. Selected covariates (eg, demographic, baseline laboratory, disease related and treatment) were tested using a forward-addition ($p<0.05$) and backward-elimination ($p<0.01$) approach. Model evaluations were conducted by comparing

the observed incidence rates with the final model simulations stratified by covariates and visual predictive checks.

Results: The final model for ALT elevations included the effect of Asian race and ASV exposure, and the effect of body weight in non-Asian subjects. Similar to ALT, Asian race was the most important factor contributing to Grade3/4 AST elevation; no other covariate or exposure effect tested was significant. The final model for total bilirubin elevation included the effect of Asian race, fibrosis-category and ASV exposure.

Conclusions: Higher ASV exposure was associated with increases in Grade3/4 ALT and total bilirubin elevations rates, but the impact on the ALT elevation was not clinically relevant and the effect on the total bilirubin elevation in the range of observed ASV exposure was smaller than the other significant covariates. The impact of ASV exposure on Grade3/4 AST elevation rate was not significant. Asian subjects had greater Grade3/4 ALT, AST and total bilirubin elevation rates than non-Asians. In addition, Grade3/4 ALT rates increased with decreasing body weight in non-Asian subjects and subjects with fibrosis-category4 had a higher rate of total bilirubin elevations compared to subjects with fibrosis category0-3.

M-63

Efficacy Exposure-Response Analysis for Daclatasvir / Asunaprevir/Beclabuvir Regimen in Hepatitis C Virus Infected Subjects

Takayo Ueno[1], Mayu Osawa[1], Tomomi Shiozaki[1], Hiroki Ishikawa[1], Michelle Green[2], Phyllis Chan[3], Brenda Cirincione[3], Frank LaCreta[3], Tushar Garimella[3]

[1]Bristol-Myers Squibb K.K, Tokyo, [2]Quantitative Solutions, CA, [3]Bristol-Myers Squibb, NJ

Objectives: The combination regimen of daclatasvir, asunaprevir and beclabuvir (DCV/ASV/BCV regimen) is being developed as fixed-dose-combination for the treatment of HCV infection in Japan. The objectives of this analysis were to characterize the relationship between DCV, ASV, and BCV exposure and sustained virologic response at post-treatment week 12 (SVR12) in HCV infected-subjects, and to evaluate the impact of demographic covariates and clinical factors on the exposure-response (E-R) relationship.

Methods: The efficacy E-R analysis was performed with data from one Phase2 and three Phase3 studies in HCV infected-subjects treated with DCV/ASV/BCV regimen. The relationship between the probability of achieving SVR12 and exposure for DCV, ASV and BCV was described using a logistic regression model, and included assessments of the potential covariate effects. The impacts of the covariates related to demographic, laboratory, disease and treatment on the rate of SVR12 and interactions of covariates with the individual drug effects were tested using a univariate-covariate-screening process ($p<0.05$), followed by a stepwise-forward-addition ($p<0.05$) and backward-elimination ($p<0.01$) approach. Model evaluation was conducted using visual predictive checks of the final model and presented stratified by covariates of interest.

Results: The final model for SVR12 included: effects of non-genotype-1a status, resistance-associated NS5A Q30 variant in genotype-1a subjects, and baseline RNA level on the intercept, and effect of prior peg-interferon failure on the BCV slope. The 95% confidence intervals for the slope of the relationships between DCV, ASV, and BCV and SVR12 included zero. Subject gender, race, age, weight, fibrosis score, ALT, and cirrhosis status had no statistically significant impact on the rate of SVR12.

Conclusions: The individual E-R relationships with DCV, ASV, and BCV, administered as the DCV/ASV/BCV regimen, were relatively flat and the effects of expousre were not significant. With the exception of the Q30 variant in genotype-1a subjects, statistically significant covariate effects had little impact on SVR12 rates. Overall the E-R model supported the high SVR12 rates for DCV/ASV/BCV regimen in HCV infected-subjects.

M-64

PK/PD Modeling of Soluble Ligand and Tumor Growth Inhibition for Anti-GITR Antibody mDTA-1 in Syngeneic Mouse Tumor Models

Tao Ji[1], Yan Ji[2], Debbie Liao[3] and Deborah A Knee[3]

[1]DMPK, [2]Oncology Clinical Pharmacology, East Hanover, NJ, [3]GNF, San Diego, CA, Novartis

Objectives: To characterize the PK/PD relationship of the soluble ligand, soluble glucocorticoid-induced TNFR-related protein (sGITR), and tumor growth inhibition for the anti-GITR antibody, murine DTA-1 (mDTA-1), in a Colon26 syngeneic mouse tumor model.

Methods: The relationship between serum mDTA-1 exposure and serum sGITR levels was evaluated in Colon26 syngeneic tumor mice following a single intravenous (i.v.) dose of 0.3, 1, 3, 10 or 15 mg/kg of mDTA-1. A one-compartment PK model with linear and non-linear (Michaelis-Menten) clearance was used to describe the PK of mDTA-1. The relationship between mDTA-1 exposure and sGITR was described using an Emax model. Tumor growth inhibition was described by an exponential model with first-order growth and second-order killing driven by mDTA-1 concentration, with first-order transit capturing delay of tumor cell death [1].

Results: The model-estimated maximal response (E_{max}) was 132 ng/mL sGITR. The mDTA-1 exposure to produce 50% of E_{max} (AUC_{50}) was 516 h·μg/mL, and the estimated baseline level of sGITR was 11.4 ng/mL. The linear clearance (CL), maximal elimination rate (V_{max}) and the Michaelis-Menten constant (K_m) of mDTA-1 were estimated to be 0.0082 mL/h, 0.38 μg/mL/h and 2.17 μg/mL, respectively. The estimated first-order growth rate (K_g), second-order tumor death rate (K_{kill}) and first-order rate constant of transit (k_1) were 0.0059 h^{-1}, 0.0078 $(h\cdot\mu g/mL)^{-1}$and 0.012 h^{-1}, respectively. The tumor stasis concentration (TSC), derived from the model, was estimated to be 0.742 μg/mL.

Conclusions: The exposure-response relationship for sGITR and tumor growth inhibition following i.v. administration of mDTA-1 in tumor bearing mice were well described by Emax and tumor kinetic PK/PD models, respectively. The results were used in part to predict the minimal anticipated biological effect level (MABEL) and efficacious dose in patients.

Reference

1. Simeoni M, et al. Cancer Research 64: 1094, 2004

M-65

Quantitative systems pharmacology model of amyloid pathology allows for clinical endpoint prediction and hypothesis testing

Tatiana Karelina[1], Oleg Demin[1], Sridhar Duvvuri[2], Tim Nicholas[2]

[1]Institute for System Biology, Moscow, Russia, [2]Pfizer Worldwide Research and Development, Groton, CT, USA

Objectives: Different treatments of Alzheimer's disease (AD) targeting amyloid (Ab) are under development and in clinical trials now. We apply QSP model of amyloid pathology for quantitative simulation of longitudinal biomarker dynamics for validation of different Ab toxicity hypothesis using trial data.
Methods: The translational model of Ab pathology describes Ab production, clearance and distribution in brain, CSF, plasma and other tissues, as well as aggregation in brain. It was calibrated and validated on multiple dynamic and steady state data for mouse, monkey and human. PET data were used for external verification. Three assumptions of relationship between Ab and Adas-cog score are used: (i) proportional or (ii) threshold Ab influence on Adas-cog score and (iii) Ab functional obligatoriness for neurons [1]. Formulation of hypotheses as explicit algebraic functions of model predicted Ab concentration allows for description of the disease progression corresponding to the observed longitudinal sporadic AD data.
Results: Amyloid secretion inhibition (SI) by 20 and 50 % and activation of insoluble Ab destruction (DA) to 150% were simulated for two ages of therapy start: 70 (early) and 75 (late) years. Model predictions revealed that for early therapy start no significant difference with placebo group would be seen for at least two years for all toxicity hypotheses. Amyloid obligatoriness assumption predict cognitive decline at the beginning of late start SI compensated only after two years with toxic form depletion. Destruction activation is less dangerous in this respect, but requires a year to observe at least 4 points of Adas-cog score diff vs placebo. Under the proportional toxicity and Ab obligatoriness hypothesis model predictions approximately correspond to the published results of avagacestat [2] and bapineusumab [3] trials.
Conclusions: Mechanistic model allows framework for amyloid toxicity hypothesis formulation and prediction of clinical trial results.

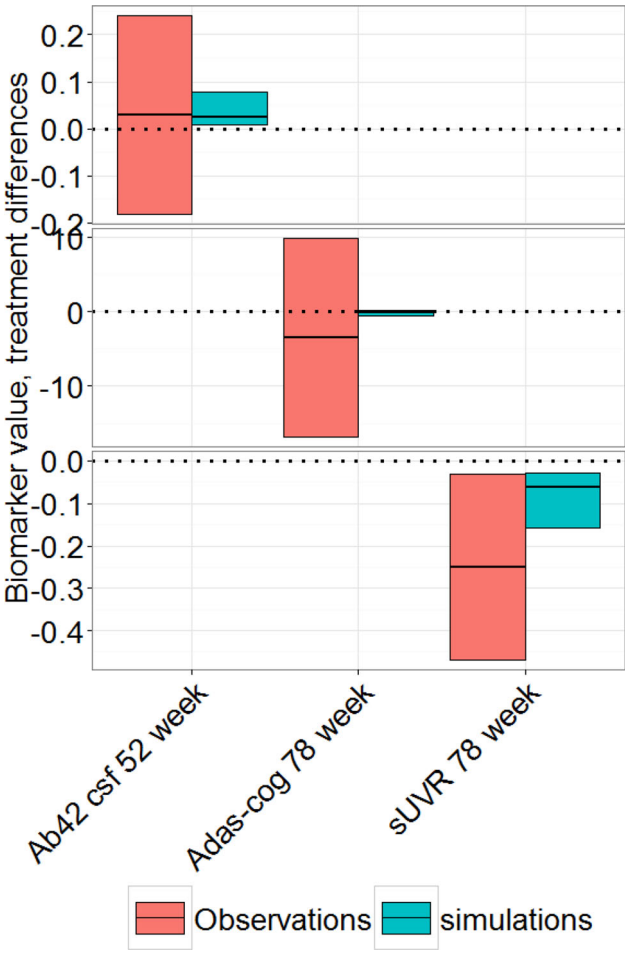

Figure 1 Comparison of model simulations (validation) with bapineusumab trial results: 95% confidence intervals for observations and model simulations (Color figure online)

References

1. J Neurosci. 2008;28(53):14537-14545. 21.
2. Arch Neurol. 2012;69(11):1430.
3. Lancet Neurol. 2010;9(4):363-372.

M-66

Dalbavancin Population Pharmacokinetic Modeling and Target Attainment Analysis

TJ Carrothers[1,*] and Jason Chittenden[2]

[1]Allergan, Jersey City, NJ; [2]qPharmetra LLC, Andover, MA

Objectives: To evaluate single dose population pharmacokinetics and support determination of a PK/PD breakpoint for dalbavancin.
Methods: Population pharmacokinetic (popPK) modeling, exploratory exposure-response analysis, and target attainment simulation were conducted following the conclusion of a pivotal single dose study in patients. This study compared a single IV dose of 1500 mg to the previously approved two-dose regimen of 1000 mg (Day 1) and 500 mg (Day 8). The popPK dataset utilized the current study as well as three prior Phase 2/3 studies. Covariate analysis was conducted to characterize the impact, if any, of intrinsic factors on dalbavancin exposures. Exploration of exposure-response used logistic regression. Using the final popPK model, target attainment was simulated for the non-clinical free AUC/MIC stasis target of 27.1 h.
Results: A three compartment distribution model with first-order elimination provided an appropriate fit to the observed data. Inter-individual variability for clearance and central volume were low, at 22% and 24%, respectively. Statistically significant ($p<0.05$) covariate relationships with total clearance were found for creatinine clearance, weight, and albumin, although their clinical importance was limited. Dose-adjustment is only indicated for creatinine clearance under 30 mL/min. The efficacy endpoints showed no statistically significant relationships with any PK/PD indices (e.g., cumulative AUC/MIC), which was unsurprising given the high success rates and

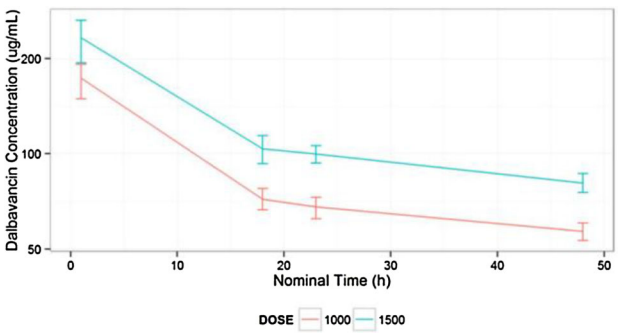

Figure 1 Mean Concentrations after Day 1 Dose (mg) (Color figure online)

low PK variability. Nonclinical target attainment simulations projected more than 90% of simulated subjects to achieve the nonclinical target at MIC <= 2 mg/L, although relatively few isolates above 0.25 mg/L have been observed in clinical studies or surveillance.
Conclusions: The pharmacokinetic profile (Figure 1) of dalbavancin was well-characterized, with low intersubject variability and a limited impact of intrinsic factors, other than severe renal impairment, observed. Clinical exploration of exposure-response was limited by the high rate of clinical success observed for dalbavancin in the ABSSSI pivotal studies. Nonclinical target attainment simulations supported a PK/PD breakpoint up to 2 mg/L for both approved dosing regimens.

M-67

Relationship between nintedanib exposure, clinical efficacy and adverse events in patients with idiopathic pulmonary fibrosis (IPF)

U. Schmid[1], B. Weber[1], C. Dallinger[1], L. Richeldi[2], C. Hallmann[1], G. Raghu[3], M. Freiwald[1]

[1]Boehringer Ingelheim Pharma GmbH & Co. KG; 2National Institute for Health Research Southampton Respiratory Biomedical Research Unit and Clinical and Experimental Sciences, University of Southampton, Southampton, UK; 3University of Washington, Seattle, Washington, USA

Objectives: To explore the relationship between nintedanib exposure and absolute change in forced vital capacity (FVC) and adverse events.
Methods: Data from 1403 IPF patients receiving nintedanib doses of 50-150 mg bid (N=895) or placebo (N=508) for up to 52 weeks in one phase II (TOMORROW) and two phase III trials (INPULSIS®-1 and INPULSIS®-2) were analyzed. A longitudinal disease progression modeling framework was used to describe the natural FVC decline in patients over time in dependence of nintedanib exposure. A parametric time-to-first event modeling approach was applied to investigate the relationship between nintedanib exposure and the probability of experiencing diarrhea or ALT and/or AST elevation to $\geq$ 3x ULN. Observed and pharmacokinetic (PK) model predicted predose plasma concentrations at steady-state (Cpre,ss) were selected as exposure metrics.
Results: The FVC data were described by a linear disease progression model with a disease-modifying drug effect. An Emax relationship was established for both observed and PK model predicted Cpre,ss with EC80 estimates of 10 and 13 ng/mL, respectively. . A reliable association between nintedanib exposure and the risk to develop diarrhea could not be established; results rather indicate that dose is a better predictor for diarrhea than exposure. A weak relationship between nintedanib exposure and ALT and/or AST elevations was found with a trend towards increased hazard with increasing nintedanib exposure based on limited data (i.e. 41 safety events).
Conclusions: The exposure-efficacy/safety analyses provide a modelling framework for a quantitative benefit-risk assessment in patients with IPF with altered nintedanib exposure due to comedication or patient characteristics.
Disclaimer: The results in this abstract have been previously presented in part at ATS (San Francisco, CA, May 2016) and ERS (London, UK, September 2016).

M-68

Development of a Physiologically Based Pharmacokinetic Model to Predict the Exposure of Itopride in Flavin-Containing Monooxygenase 3 Extensive and Poor Metabolisers

Wangda Zhou[1,*], Helen Humphries[2], Sibylle Neuhoff[2], Iain Gardner[2], Eric Masson[1], Nidal Al-Huniti[1] and Diansong Zhou[1]

[1]Quantitative Clinical Pharmacology, AstraZeneca, Waltham, MA; [2]Simcyp (A Certara Company), Sheffield, UK

Objectives: Itopride was approved for the symptomatic treatment of various gastrointestinal disorders in Asian countries and is mainly metabolized by Flavin-Containing Monooxygenase 3 (FMO3). The objective of this study was to develope a physiologically based pharmacokinetic (PBPK) model to capture itopride PK in FMO3 extensive metabolisers (EM) and poor metabolisers (PM).
Methods: Simcyp simulator version 14 release 1 (Certara, Sheffield, UK) was used to conduct all simulations. The Asian population library files within the modeling platform were further developed by incorporating FMO3 enzyme abundance/activity and genotype frequencies which were derived from *in vitro* human liver microsomes data and clincial pharmacogenetic studies of multiple drugs metabolized by FMO3. A full body distribution model was used to describe tissue-plasma partitioning for itopride with partition coefficients and Vss predicted by the method of Rodgers et al. A first order oral absorption model was applied, using an optimized absorption constant value of 4 /h and an absorption lag time of 0.4 h to recover the clinically observed Tmax. The kinetics of itopride N-oxygenation by FMO3 were obtained from *in vitro* pooled human liver microsomes studies and verified using clinical observed data. The model was first verified with multiple itopride clinical studies conducted in Japanese and Korean subjects following administration of 150 mg single dose or 50 mg TID itopride, then was applied to predict itopride exposure in Chinese FMO3 EM and PM subjects.
Results: The meta-analysis of relative enzyme activities suggested that FMO3 activity in PM is 47% lower than EM. In a combined Asian population, EMs account for about 5% of the total population. The predicted plasma concentration-time profiles of itopride in Chinese FMO3 EMs and PMs were compared with observation (Figure 1). The PBPK predicted AUC of itopride in Chinese FMO3 PM is 1.6 fold higher than FMO3 EM, which is slightly lower than clinical observation (2.2 fold). The difference is likely caused by the small sample sized in the clinial trial (6 subjects in each group).

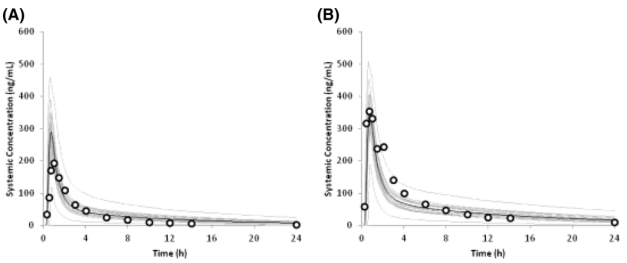

Figure 1 Mean simulated (*solid line*) and observed (data points) concentration of itopride after oral administration of a single 50 mg dose to healthy male Chinese FMO3 EMs (A) and PMs (B). The *grey lines* represent individual trials (20 trials, 6 subjects in each trial) and the *solid black line* is the mean of the population (n = 120)

Conclusions: The system components describing FMO3 phenotype frequency and relative activity were derived in Asian populations and applied to predict the pharmacokinetics of Itopride. The developed itopride PBPK model could reasonably capture the drug exposure of FMO3 EMs and PMs in a Chinese population.

M-69

Application of Physiologically Based Pharmacokinetic Modeling to Predict Raltegravir Pharmacokinetics in Children

Wangda Zhou[1,*], Trevor Johnson[2], Khanh Bui[1], S.Y. Amy Cheung[3], Jianguo Li[1], Hongmei Xu[1], Nidal Al-Huniti[1], Diansong Zhou[1]

[1]Quantitative Clinical Pharmacology, AstraZeneca, Waltham, MA; [2]Simcyp (A Certara Company), Sheffield, UK; [3] Quantitative Clinical Pharmacology, AstraZeneca, Cambridge, UK

Objectives: Raltegravir is a potent human immunodeficiency virus 1 (HIV-1) integrase strand transfer inhibitor and is mainly metabolized by UDP-glucuronosyltransferases (UGT) 1A1 and UGT1A9. The objective of this study was to develop a physiologically based pharmacokinetic (PBPK) model to predict Raltegravir PK in pediatric patients across all age groups.
Methods: Simcyp simulator version 15 release 1 (Simcyp, (A Certara Company), Sheffield, UK) was used to conduct all simulations. A full PBPK models with first order absorption was constructed for raltegravir based on physicochemical properties and clinical observations. Absorption rate constants of three formulations (tablet, chewable tablet and suspension) were optimized using PK data observed in clinical studies in adults. Following appropriate verification in adult populations, pediatric PK was predicted for raltegravir across all age groups using Simcyp pediatric module with application of physiological-based ontogeny. The predicted AUC, CL and Cmax were then compared with available clinical data in pediatric subjects for each age group.
Results: Pediatric PBPK models reasonably predicted the AUC values of raltegravir in infants (1∼6 months), toddlers (6 month - 2 years), young children (2 - 6 years), school-aged children (6 - 12 years) and adolescents (12 - 19years). All predicted AUC values are within 2-fold of observed values (Figure 1). Large inter subject variability was observed in children and adults taking tablet formulation.

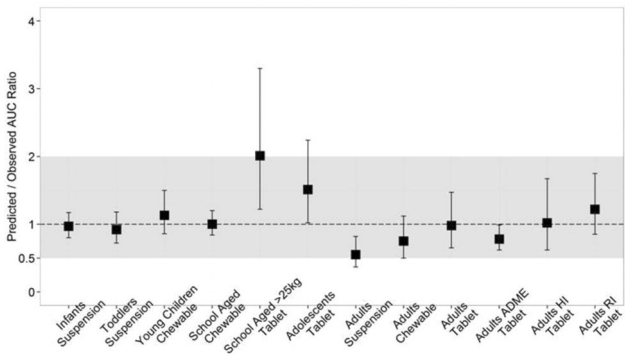

Figure 1 Predicted over observed ratios of mean AUC ± 90% CI for raltegravir in different age and adult studies following oral administration of suspension, chewable tablet or tablet. The *dashed line* represents line of unity and *grey shading* the 0.5 to 2-fold window. For the last two studies in hepatic (HI) and renal (RI) impairment, data is only presented from the control arms

Conclusions: Pediatric PK of raltegravir can be reasonably described using the developed PBPK model by considering ontogeny profiles of UGT1A1 and UGT1A9 built in the Simcyp pediatric model. This approach represents a general strategy for projecting drug exposure in children, *a priori* to guide pediatric clinical trial design.

M-70

Population Pharmacokinetics and Pharmacodynamics of Bivalirudin in Chinese Subjects

Wenfang Liu[1], Xiaoxing Wang[2], Yang Lin[1], M Rose Feng[2]

[1]Beijing Anzhen Hospital, Beijing, China; [2]College of Pharmacy, University of Michigan, Ann Arbor, MI, USA

Objectives: Bivalirudin is used as an anticoagulant agent for the treatment of thrombosis associated with heparin-induced thrombocytopenia (HIT) and for patients at risk of HIT undergoing percutaneous coronary intervention (PCI). In this study, bivalirudin population pharmacokinetics and the correlation between bivalirudin plasma concentration and the activated clotting time (ACT) in Chinese subjects was characterized to support the proper dosing and drug monitoring in Chinese patients.
Methods: Twenty healthy male Chinese subjects were enrolled and randomly assigned to two groups. Individuals in the group 1 received a bolus intravenous (IV) dose of 0.75 mg/kg bivalirudin, and in the group 2 received the same bolus IV dose of 0.75 mg/kg followed by a one hour IV infusion of 1.75 mg/kg/hr of bivalirudin. Population pharmacokinetic (PK) and pharmacodynamic (PD) modeling were performed using nonlinear mixed effects modeling (NONMEM). The final models were selected based on the likelihood ratio test, goodness-of-fit plots, and visual predictive check.
Results: Plasma bivalirudin concentration-time profiles in both groups were best described by a two-compartment PK model, and the model estimated systemic plasma clearance (CL±SE), volume of distribution in the central (V1±SE) and peripheral compartments (V2±SE), were 11.2 (±1.5) L/hr, 3.17 (±0.31) and 1.99 (±0.25) L, respectively. The relationship between bivalirudin plasma concentration and ACT was best characterized by a sigmoid E_{max} model. Model estimated maximum increase of ACT (E_{max}±SE), the plasma concentration associated with 50% of E_{max} (EC_{50}±SE), and the sigmoidicity factor ((γ±SE, steepness of the curve) were 269% (± 63%), 5040 (±2810) μg/L, and 0.824 (±0.096), respectively.
Conclusions: There was a strong direct correlation between the plasma bivalirudin concentrations and the ACT prolongation. The POPPK and PK/PD models developed in the present study could provide very useful information for dose optimization and individualization in Chinese patients.

M-71

Population Pharmacokinetics and Dose Proportionality of Aranidipine Sustained-release Capsules in Healthy Subjects

Wenfang Liu[1], Xiaoxing Wang[2], Yang Lin[1,*], M Rose Feng[2,*]

[1]Institute of Clinical Pharmacology, Anzhen Hospital of Capital Medical University, Beijing, China; [2]Department of Pharmaceutical Sciences, College of Pharmacy, University of Michigan, Ann Arbor, MI, USA

Objectives: Aranidipine (AR) is a dihydropyridine-type calcium channel blocker used for the treatment of hypertension. In this study, the population pharmacokinetics (POPPK) and dose proportionality

of AR was characterized using nonlinear mixed effect modeling (NONMEM) to support the proper dosing and drug monitoring of AR in Chinese patients.
Methods: The AR plasma-concentration data were collected from two Phase I clinical studies (n=47) in healthy subjects receiving a single oral dose of sustained-released AR capsules of 5, 10, or 20 mg in fasted state. POPPK modeling was performed using nonlinear mixed effects modeling (NONMEM) and the contribution of physiological factors (e.g., BW, AGE, and SEX) was assessed. The final models were selected based on the likelihood ratio test, goodness-of-fit plots, and visual predictive check.
Results: The model estimated AR exposure (AUC) at 5 mg, 10 mg and 20 mg were 6.72, 14.8, and 31.2 μg·hr/L respectively, suggesting that AR exposure increased dose-proportionally over the dose range of 5 - 20 mg. Plasma AR concentration-time profiles were best described by a two-compartment PK model with 1st-order absorption, and the model estimated AR absorption rate constant (Ka), apparent clearance (CL/F), volume of distribution in the central (V2/F) and peripheral compartments (V3/F) were 0.670 hr^{-1}, 728 L/hr, 299 L, 792 L respectively. No significant contribution of physiological factors was observed.
Conclusions: The present study demonstrated dose proportionality for sustained-release AR capsules at 5 – 20 mg in healthy subjects in fasted state. The POPPK model developed in the present study could provide valuable information for dose individualization and optimization in Chinese patients.

M-72

Development of Time to Event Models for Exposure-Response Analysis of Peginterferon Beta-1a in Subjects with Relapsing Remitting Multiple Sclerosis

Xiao Hu[1] Shifang Liu[1] Yaming Hang[1]

[1]Biogen Inc

Objectives: To compare semi-parametric models and parametric models for peginterferon beta-1a (PEG-IFN) exposure and time to relapse, and explore covariates that impacted time to relapse.
Methods: PK and relapse data were obtained from a double-blind placebo-controlled Phase 3 study in RRMS patients (n=1512), in which 125 mcg subcutaneous PEG-IFN every 2 (Q2W) or 4 (Q4W) weeks reduced ARR (primary endpoint) significantly [1]. Using post-hoc PK parameters derived from a population PK model developed using NONMEM [2], PEG-IFN exposure was represented by monthly cumulative AUC for each subject. The data was modelled using semi-parametric approach (cox proportional model) and parametric approach, including exponential, Weibull, Gaussian, logistic, loglogistic, lognormal models. The survival analysis was carried out in R [3].
Results: Based on Cox proportional hazard analysis, the AUC showed statistically significant impact on time to relapse ($p<0.001$), with increased exposure reducing hazard to relapse. Additionally, the following covariates were also significant ($p<0.001$): baseline relapse rate in the past 3 years, baseline Gadolinium enhanced lesion count, and baseline relapse rate in the past 1 year. With regards to parametric models, loglogistic model provided the best fit based on its log-likelihood values using placebo data. The covariates identified as significant in the parametric models were consistent with those identified in Cox proportional model, with baseline relapse rate in the past 3 years as the most significant covariate. The significant covariates were not sensitive to model selected.
Conclusions: Exposure-response models were developed for PEG-IFN. Greater exposure was associated with lower hazard to relapse. Other significant covariates included baseline relapse rate in the past 3 years, baseline Gadolinium enhanced lesion count, and baseline relapse rate in the past 1 year.

References

1. Calabresi PA, Kieseier BC, Arnold DL, Balcer LJ, Boyko A, Pelletier J, Liu S, Zhu Y, Seddighzadeh A, Hung S, Deykin A; ADVANCE Study Investigators, Pegylated interferon β-1a for relapsing-remitting multiple sclerosis (ADVANCE): a randomised, phase 3, double-blind study. Lancet Neurology (2014), 13:657-65.
2. Beal SL, Sheiner LB, Boeckmann AJ & Bauer RJ (Eds.) NONMEM Users Guides. 1989-2011. Icon Development Solutions, Ellicott City, Maryland, USA.
3. R Core Team (2015). R: A language and environment for statistical computing. R Foundation for Statistical Computing, Vienna, Austria. URL http://www.R-project.org/.

M-73

Population Pharmacokinetics and Food Effect of the Antihypertensive Drug Aranidipine in Healthy Subjects

Xiao-Xing Wang[1], Wenfang Liu[2], Yang Lin[2,*], Meihua Rose Feng[1,*]

[1]College of Pharmacy, University of Michigan, Ann Arbor, MI, USA. [2]Institute of Clinical Pharmacology, Anzhen Hospital of Capital Medical University, Beijing, China

Objectives: Aranidipine (AR) is a dihydropyridine-type calcium channel blocker used for the treatment of hypertension. In this study, the population pharmacokinetics (PK) of AR, the food effect, and the contribution of physiological factors (e.g., body weight, age, gender) were assessed using nonlinear mixed effect modeling (NONMEM).
Methods: The AR plasma-concentration data were collected from a clinical study in healthy Chinese subjects (n=9) receiving a single oral dose of sustained-released AR capsules of 10 mg under fasted or fed conditions with a cross-over design. Population PK modeling was performed using nonlinear mixed effects modeling (NONMEM). The final models were selected based on the likelihood ratio test, goodness-of-fit plots, non-parametric bootstrap analysis and visual predictive check. No significant contribution of physiological factors was observed.
Results: The AR plasma maximum concentration (C_{max}) and area under the curve ($AUC_{(0\text{-}inf)}$) at 10 mg were 4.2 ± 0.5 μg/L and 11.4 ± 1.4 μg·hr/L for the fasted group, and 6.8 ± 1.5 μg/L and 15.9 ± 2.0 μg·hr/L for the non-fasted group respectively, suggesting that food increased AR exposure. Plasma AR concentration-time profiles were best described by a two-compartment PK model with 1st-order absorption. The model estimated AR absorption rate constant (Ka), apparent clearance (CL/F), volume of distribution in the central (Vc/F) and peripheral compartments (Vp/F) were 0.59 ± 0.02 hr^{-1}, 714 ± 648 L/hr, 210 ± 112 L, and 2151 ± 33 L for the fasted group; 0.64 ± 0.02 hr^{-1}, 484 ± 58 L/hr, 573 ± 395 L and 2340 ± 35 L for the non-fasted group, respectively.
Conclusions: The absorption and disposition of AR was successfully characterized by population PK models. AR exposure was higher and CL/F was lower in subjects under non-fasted condition. The population PK model developed in this study is useful for dose optimization and study design in Chinese population.

M-74

Semi-Mechanistic Physiologically-Based Pharmacokinetic Modeling of L-Histidine Disposition and Brain Uptake in Wildtype and *Pht1* Null Mice

Xiao-Xing Wang, David E Smith, Meihua R Feng

University of Michigan, Ann Arbor, MI, US

Objectives: PHT1, a member of the peptide transporter superfamily, is responsible for translocating various di/tripeptides, peptide-like drugs and L-histidine (L-His) across biological membranes. Based on our preliminary results, PHT1 is located in brain parenchyma, however, its relative significance in brain bio-disposition of its substrates is unknown. With this in mind, we developed a semi-mechanistic physiologically-based pharmacokinetic (PBPK) model to describe the quantitative contribution of PHT1 in the disposition of L-His in brain.
Methods: [^{14}C]L-His was administrated to wildtype and *Pht1* null mice via tail vein injection. Serial samples from plasma, cerebrospinal fluid (CSF) and brain parenchyma were collected. The concentration-time profiles of these samples were then analyzed using non-linear mixed effects modeling with NONMEM v7.3.
Results: The disposition kinetics of L-His in plasma, CSF and brain parenchyma was best described by a four-compartment model (Figure 1). We observed that the plasma and CSF pharmacokinetic profiles of L-His were comparable in wildtype and *Pht1* null mice. However, a more rapid uptake of L-His occurred in the brain parenchyma of wildtype mice due to active transport by PHT1, which was modeled using a single Michaelis-Menten term (V_{max}=1.0 nmol/min and K_m=16.9 μM). In addition to uptake by PHT1, the influx of L-His into brain parenchyma and CSF was mediated by first-order processes. Blood flows and tissue volumes were obtained from the literature, and partition coefficients between the brain or CSF and plasma were estimated at 0.293 or 0.077, respectively. Simultaneously, L-His was drained from the brain to CSF through bulk flow.
Conclusions: In the present study, a semi-mechanistic PBPK model was developed to compare the disposition of L-His in the plasma, CSF, and brain of wildtype and *Pht1* null mice. We were able to quantitatively determine the contribution of PHT1 in the uptake kinetics of L-His in brain, which may provide insight into the role of PHT1 in brain histidine-histamine homeostasis and the disposition of other neural-active compounds.

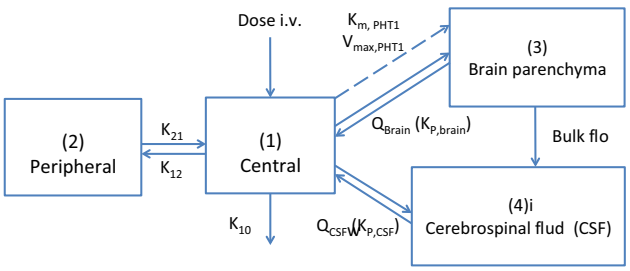

Figure 1 Schematic structural model of L-histidine disposition in mice after an intravenous (iv) bolus dose. Vmax,PHT1 represents the maximum rate of active transport; Km,PHT1 the Michaelis-Menten constant; K10, K12 and K21 the first-order micro-rate constants; QBrain and QCSF the blood flows to the brain parenchyma and CSF compartments; and KP,brain and KP,CSF the partition coefficients in brain-to-plasma and CSF-to-plasma. The *dashed line* indicates a process existing only in wildtype mice (Color figure online)

M-75

Mathematical modeling of temporal proteomic profiles in response to gemcitabine on pancreatic cancer cells

Xin Miao[1], Gilbert Koch[4], Shichen Shen[2,3], Jun Li[1,3], Xiaomeng Shen[2,3], Xue Wang[2,3], Robert M. Straubinger[1], Jun Qu[1,3], William J. Jusko[1]

[1]Department of Pharmaceutical Sciences, University at Buffalo, SUNY, Buffalo, New York; [2]Department of Biochemistry, School of Medicine and Biomedical Sciences, University at Buffalo, SUNY, Buffalo, New York; [3]New York State Center of Excellence in Bioinformatics & Life Sciences, Buffalo, New York; [4]Pediatric Pharmacology and Pharmacometrics Research Center, University of Basel, Children's Hospital, Basel, Switzerland

Objectives: This study utilized a high-throughput and sensitive proteomic methodology to assess gemcitabine effects on the proteomic responses in pancreatic cancer cells. Mathematical models were developed to characterize gemcitabine effects on the dynamics of the proteomic changes.
Methods: In vitro experiments were performed in the pancreatic cancer cell line MiaPaCa-2. Cells were cultured in 10 cm dishes and were exposed to the IC_{50} concentration of gemcitabine for 0, 12, 24, 36, 48 and 72 h. Cells (n=3 per group) were lysed at each time point. A highly reproducible and sensitive LC-MS method permitted proteomic profiling of all biological replicates (n=45). Immunoassays for selected proteins were performed together with proteomics. Mathematical models were developed with >100 ordinary differential equations (ODE) to describe the time course of all observed proteins expressed in the signaling pathways.
Results: The proposed integrated pharmacodynamic (PD) model of proteomic changes was built for numerous signaling pathway components. The PD model characterized well all protein expression profiles in various pathways. Compared to the control group, gemcitabine down-regulated proteins such as EGFR, P130CAS, which are responsible for cell growth and migration, and anti-apoptotic protein P53, and mediated protein changes that correlate with cell cycle arrest.
Conclusions: A systems proteomic PD model was developed and very well characterized gemcitabine effects on signal transduction pathways in pancreatic cancer cells. The proteomic PD model enables the characterization of 'big data' from different sources in the dimensions of time, sub-populations, and biochemical space.

M-76

Covariate Test Using Empirical Bayes Estimates May be better than Likelihood Ratio Test for Population Pharmacokinetic Modeling: Why We Don't Have to be Concerned about Shrinkage (too much)

Xu Steven Xu[1]*, Min Yuan[2]*, Haitao Yang[3], Yan Feng[4], Jinfeng Xu[5], Jose Pinheiro[1]

[1]Janssen Research & Development, 920 Route 202, Raritan, NJ 08869 USA; [2]Department of Mathematics, University of Science and Technology of China, Hefei, China; [3]University of Florida, FL, USA; [4]Bristol-Myers Squibb, Princeton, NJ, USA; [5]Department of Statistics & Actuarial Science, University of Hong Kong, Hong Kong

*These authors contributed equally

Objectives: Covariate analysis based on population pharmacokinetics (PPK) is increasingly used to identify clinically relevant factors impacting exposure. The likelihood ratio test (LRT) based on fits of nonlinear mixed-effects models is currently recommended for

covariate identification, whereas individual empirical Bayesian estimates (EBEs) are considered unreliable for that purpose, due to the presence of shrinkage. The objectives of this research were to compare EBE- and LRT-based approaches for covariate analysis in PPK.
Methods: Limiting ourselves to the context of a simple one-compartment PK model with only a single covariate on the clearance, we conducted simulations for a wide range of scenarios according to a 2-way factorial design, and compared the false positive rate, power, and estimation accuracy between the EBE- LRT-based covariate analysis. We attempted to identify influential factors as well as to investigate the impact of shrinkage of the EBEs.
Results: The EBE-based regression approach not only provided almost identical power for detecting a covariate effect, but also controlled the false positive rate better than the LRT. Number of subjects, value of covariate coefficient, and inter-individual variability were the primary factors affecting the power, while residual variability and number of samples per subject mainly affected the estimation accuracy. Shrinkage of EBEs is likely not the root cause for decrease in power or inflated false positive rate as both LRT- and EBE-approaches were affected. The EBE-based approach tends to underestimate the size of the covariate effect, and the relative bias of the estimation proportionally increased with the amount of shrinkage.
Conclusions: Contrary to the current practice, EBEs may be a better choice for statistical tests in PPK covariate analysis compared to LRT.

M-77

Optimal sampling design for a pediatric pharmacokinetic study of an anti-influenza A monoclonal antibody, MHAA4549A, with prior information from adults

Yaping Zhang, Mauricio Maia, Jeremy Lim, Leonard Dragone, Jorge Tavel, Elizabeth Newton, Rong Deng*

Genentech, South San Francisco, CA

Objectives: MHAA4549A is a human monoclonal IgG1 antibody being developed for the treatment of hospitalized patients with severe influenza A infection. The objective of this study was to design an optimal sampling scheme for a pediatric pharmacokinetic (PK) trial of MHAA4549A, using prior serum PK data from adults.
Methods: MHAA4549A serum PK data from three clinical studies in adults were used to build an adult population PK model. The covariate effects of body weight (BW), age, sex, creatinine clearance, albumin, total protein and infection status were evaluated. Similar body-size-adjusted PK parameters were observed in pediatrics and adults for mAb with linear PK [1]. Therefore, the established adult PK model, together with the pediatric BW distribution from oseltamivir pediatric trials, were implemented in the software PFIM [2] to identify optimal sampling scheme for age groups of 0 to 23 months and 2 to 12 years old. Pediatric trials with sampling times corresponding to the design scheme were then simulated to further evaluate the design, by re-estimating PK parameters and calculating relative bias and relative standard errors for each PK parameter.
Results: A two-compartment PK model with BW as a covariate on clearance and volume of distribution of the central compartment was established. A sparse sampling design (0.5 hour after the end of IV infusion on day 1, days 4, 15 and 120) was proposed for pediatric patients in both age groups. With this design, the pediatric PK parameters were well estimated in simulated trials with adult PK parameters as a prior.
Conclusions: Appropriate sampling design is critical for precisely characterizing PK parameters in a pediatric population with limited number of samples. This study illustrates an example of leveraging adult PK information to design a sampling scheme for a pediatric PK study.

References

1. Xu, et al., Pharmacology & Therapeutics, 2012.
2. Bazzoli, et al. Computer Methods and Programs in Biomedicine, 2010.

M-78

Development of a quantitative systems pharmacology model of drug-induced renal proximal tubule injury for benchmarking and translation

Yeshitila Gebremichael[1], James Lu[2], Harish Shankaran[2], Jerome Mettetal[2], Gabriel Helmlinger[2], Melissa Hallow[1]

[1]University of Georgia; [2]Astrazeneca Pharmaceuticals

Objectives: To develop a quantitative systems pharmacology model of drug-induced renal injury that uses novel structural biomarkers to predict functional/pathophysiologic renal responses.
Methods: We employed a systems pharmacology model to predict pathophysiological responses to drug-induced proximal tubule (PT) injury. Cisplatin is a known nephrotoxicant that produces localized PT damage and is used as a test compound for the model. To inform the mathematical model, we utilized multiple urinary biomarker timecourse data (including KIM-1, αGST, albumin, glucose, urine volume, creatinine, etc.) from rats treated with cisplatin. Time profiles for biomarkers indicative of structural/cellular damage were used as input signals to the mathematical model (cf. Figure below).
Results: The time-course of urine biomarkers exhibited unique patterns that elucidated two groups of biomarkers with distinct timecourses: one group of expressed or up-regulated biomarkers with a broad peak at day 7, and another group of filtered and pre-formed biomarkers with a steep narrow peak at day 5. The two classes were hypothesized to represent distinct injury mechanisms and to reflect associated changes in PT function (water, sodium, glucose, albumin

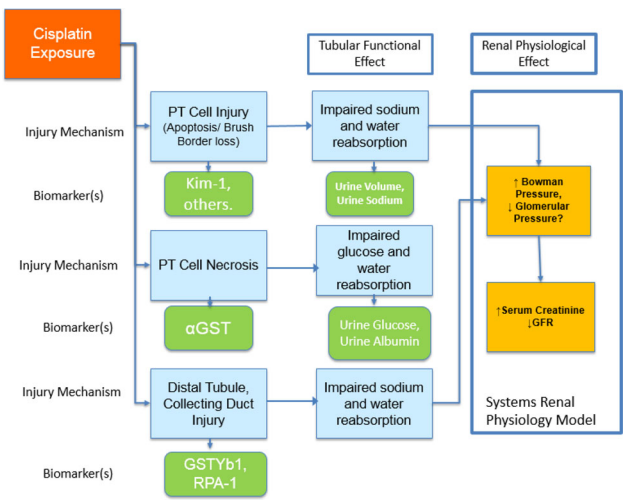

Figure 1 Overview of a quantitative systems pharmacology model of drug-induced renal injury (Color figure online)

reabsorption). Under this hypothesis, αGST and KIM-1 timecourses were used to reflect changes in PT function in the model, and the model predicted the magnitude and timecourse of functional urinary biomarker responses including albumin and glucose. The sharp rise and decline exhibited by these biomarkers also correlated with qualitative histopathological data indicating the timecourse of necrosis and regeneration of PT epithelial cells.
Conclusion: The developed model quantifies changes in PT reabsorption and allows simulation of functional biomarkers based on measurement of two biomarkers (αGST and KIM-1) which represent distinct injury processes. Future work includes mapping drug-induced renal injury across additional tubular segments and the glomerulus. Such a model will facilitate benchmarking safety signals of new drugs, as well as translating to human injury in the setting of chronic kidney disease.

M-79

Population PK-tumor size dynamic modeling and survival analysis of EGF816, a third generation, mutant-selective EGFR TKI, in patients with advanced NSCLC harboring T790M

Ying Hong, Xiaoming Cui, Eugene Tan, Susan Moody, Mike Roy, Shu-Fang Hsu Schmitz, Charles Davis

Novartis Pharmaceuticals Corporation, East Hanover, NJ, USA

Objectives: To investigate the relationship between EGF816 exposure and tumor growth inhibition (TGI) in patients with advanced NSCLC harboring an EGFR T790M mutation. The predictability of progression free survival (PFS) using tumor size (TS) response metrics was also evaluated.
Methods: Data were obtained from a phase 1, dose escalation study (NCT02108964), in which patients were treated with oral EGF816 from 75 mg to 350 mg QD in either capsule or tablet formulations. The analyses were performed sequentially using NONMEM v7.2. First the population PK model was developed to estimate the individual daily AUC (AUCtau). A semi-mechanistic AUCtau-driven TGI model was then fit to the longitudinal TS data to predict individual TS metrics, namely TS ratio to baseline at week 8, time to tumor growth (TTG), and tumor growth rate (G). The risk of progression or death with TS metrics was assessed using a parametric survival model.
Results: EGF816 PK was described with a linear two-compartment disposition model and with an absorption process characterized by a transit model [1]. The TS data were best described by a TGI model which incorporated a first-order tumor growth rate, the drug effect on tumor cell killing, and resistance to drug effect [2]. The AUCtau producing 50% of maximal TGI was 1.94 mg·hr/L, which when converted to a daily average concentration (i.e., 81 ng/mL), was similar to the human equivalent tumor stasis concentration (99 ng/mL) determined using the H1975 xenograft model. The lower TTG corresponded to higher risk of progression or death.
Conclusions: Tumor growth inhibition was achieved at all dose levels and increased with EGF816 dose up to 300 mg QD. Further, TTG was a predictor of PFS in patients with EGFR T790M mutant NSCLC receiving EGF816.

References

1. Savic RM, et al. J Pharmacokinet Pharmacodyn. 34(5) : 711-726, 2007
2. Claret LC, et al. J Clin Oncol. 27(25) : 4103-4108, 2009

M-80

Development of a Quantitative Systems Pharmacology (QSP) Toolbox and Virtual Population (VPop) for Affinity-Drug Conjugate (ADC) Research

Yougan Cheng[a], Heather E. Vezina, Manish Gupta, Chin Pan, Tarek A. Leil, Brian J. Schmidt[a]

Bristol-Myers Squibb, Princeton, NJ, USA

[a]Contributed equally.

Objectives: ADCs combine the affinity and specificity of biological targeting agents (eg, antibodies or adnectins) with cytotoxic payloads. Previously, we reported the development of a QSP platform to interpret mechanistic data from disparate assays in pharmaceutical R&D [1]. We integrated these data sets stepwise while exploring trade-offs between modeled processes and impact on readouts (eg, tumor uptake measured by ^{89}Zr-PET). Our objective is to simultaneously optimize parameters across all assays to comprehensively generate alternate mechanistic hypotheses that are in quantitative agreement with experimental data.
Methods: We developed the QSP Toolbox, a set of functions, data structures, and objects that implement critical elements of QSP workflows [2,3] for MATLAB® SimBiology® models. An objective function evaluated virtual xenografts against multiple time-series data sets across all in vitro and in vivo experiments. The virtual cohort of xenografts was developed by optimization methods and by adding stochastic variability in over a dozen mechanistic parameters governing processes such as antigen shedding, internalization, tumor growth, vessel permeation, and label loss. VPops of xenografted mice were created using a modification of a previously described prevalence-weighting algorithm [4], matching mean, variance, and binned distributions from each data set.
Results: The virtual cohort of 1,000 xenografted mice exhibited agreement with cell culture antibody internalization, in vivo antigen shedding, xenograft growth, and radiolabel accumulation. VPops had an acceptable goodness-of-fit (Fisher's combined test [4]).
Conclusion: The QSP Toolbox successfully integrated data sets across interventions and serves as a generalized tool for QSP platform calibration and application. The ADC platform and VPop will enable integration of dose-response data in a mechanistic framework, translational predictions, and extrapolation between indications.

References

1. Schmidt BJ, et al. *J Pharmacokinet Pharmacodyn*. 2015;42:S66-S67.
2. Schmidt BJ. *CPT Pharmacometrics Syst Pharmacol*. 2014;3:e106.
3. Gadkar K, et al. *CPT Pharmacometrics Syst Pharmacol*. 2016;5:235-249.
4. Schmidt BJ, et al. *BMC Bioinformatics*. 2013;14:221.

M-81

A Disease Progression Model of Longitudinal Lung Function Decline in Idiopathic Pulmonary Lung Fibrosis Patients

Youwei Bi[1], Miya O. Paterniti[2], Banu A. Karimi-Shah[2], Badrul A. Chowdhury[2], Yaning Wang[1], Dinko Rekić[1]

[1]Office of Clinical Pharmacology, OTS, CDER, FDA, Silver Spring, MD; [2]Division of Pulmonary, Allergy, and Rheumatology Products, OND, CDER, FDA, Silver Spring, MD

Objectives: To quantify and explain the variability in longitudinal lung function decline in patients with idiopathic pulmonary fibrosis (IPF).
Methods: The clinical development programs for pirfenidone and nintedanib included 1,132 patients in the placebo-controlled arms in 6 clinical trials (1-4). Observed repeated individual measures of %p-FVC from time of randomization to time of last observation collected over an average of 58.5 weeks were analyzed with parametric linear and nonlinear mixed effects models using NONMEM 7.3. Potential covariates were selected based on prior knowledge from literature as well as regulatory and medical practice and were tested in a stepwise manner.
Results: An empirical Weibull model was found to best describe longitudinal lung function decline in IPF. Covariate analyses have shown that patients who have lower DLCO, who weigh less or who used oxygen at baseline tend to have a faster decline in lung function. Acute exacerbation during the study period was also found to be highly associated with a faster lung function decline.
Conclusions: The developed model may be of use for clinicians who treat individual patients as well as drug developers who wish to optimize their IPF drug development programs.

References

1. King TE, Jr., et al. A phase 3 trial of pirfenidone in patients with idiopathic pulmonary fibrosis. N Engl J Med. 2014;370(22):2083-92.
2. Noble PW, et al. Pirfenidone in patients with idiopathic pulmonary fibrosis (CAPACITY): two randomised trials. Lancet. 2011;377(9779):1760-9.
3. Richeldi L, et al. Efficacy of a tyrosine kinase inhibitor in idiopathic pulmonary fibrosis. N Engl J Med. 2011;365(12):1079-87.
4. Richeldi L, et al. Design of the INPULSIS trials: two phase 3 trials of nintedanib in patients with idiopathic pulmonary fibrosis. Respir Med. 2014;108(7):1023-30.

M-82

A Semi-mechanistic Pharmacokinetic-Enzyme Turnover Model for Dichloroacetic Acid Auto-inhibition in Rats

Yu Jiang[1], Gary Milavetz[1], Margaret O James[2], Peter W. Stacpoole[3], Guohua An[1]

[1]College of Pharmacy, University of Iowa, IA; [2]College of Pharmacy, University of Florida, FL; [3]College of Medicine, University of Florida

Objective: Dicholoroacetic acid (DCA) is a pyruvate dehydrogenase kinase (PDK) inhibitor that has been used to treat congenital or acquired lactic acidosis in children and is currently in early phase clinical trials for cancer treatment. DCA was found to inhibit its own metabolism by irreversibly inactivating glutathione transferase zeta (GSTZ1-1), resulting in non-linear kinetics and abnormally high accumulation ratio after repeated dosing. The aim of this analysis was to develop a semi-mechanistic pharmacokinetic-enzyme turnover model for DCA to characterize the unusual nonlinear pharmacokinetic of DCA observed in rats.
Methods: 20 rats received oral doses of 50 mg/kg DCA once daily for one or two days. Blood samples were collected 0.25, 0.5, 0.75, 1, 1.5, 2, 3, 4, 6, 8, 12 and 24 hours post dose. Population pharmacokinetic analysis was performed in NONMEM 7.3 to characterize the observed plasma concentration-time profiles of DCA in rats. A one compartment disposition model combined with an enzyme turnover model was used to describe the dramatic reduction in clearance after repeated DCA dosing. To account for the double peaks observed in DCA absorption phase possibly caused by gastrointestinal region-dependent absorption, a sequential first order absorption model was implemented.
Results: The intrinsic DCA hepatic clearance decreased from 1.26L/h after first dose to 0.017L/h dose after second dose. The rate constant for DCA induced GSTZ1-1 inactivation (0.85 /h) is 97 times that of the rate constant for GSTZ1-1 natural degradation (0.00875 /h). The DCA concentration that corresponds to 50% of maximum enzyme inhibition (EC50) is 3.44 mg/L. 98.7% of the total clearance is inhibited by DCA according to model estimates. The remaining clearance that is unaffected by DCA indicated alternative metabolic pathways for DCA apart from GSTZ1-1 mediated metabolism.
Conclusions: The proposed semi-mechanistic pharmacokinetic-enzyme turn over model was able to capture DCA auto-inhibition, gastrointestinal region-dependent absorption, and time dependent change in bioavailability in rats. The constructed PK-enzyme turnover model, when scaled up to human, could be used to predict the accumulation of DCA after repeated oral dosing, guide selection of dosing regimens in clinical studies, and facilitate clinical development of DCA.

T-01

A Multiscale Physiologically Based Pharmacokinetic Model for Doxorubicin: Scale-up from Mouse to Human

Hua He[1, 2], Yun Wu[3], Xinyuan Zhang[4], Yanguang Cao[1*]

[1]DPET, School of Pharmacy, University of North Carolina at Chapel Hill, NC,USA; [2]China Pharmaceutical University, Nanjing, China; [3]Department of Biomedical Engineering, University at Buffalo, State University of New York, Buffalo, NY, USA; [4]Division of Quantitative Methods and Modeling, Office of Research and Standards, OGD, FDA, Silver Spring, Maryland, USA

Objectives: Doxorubicin used either alone or in combination is the most widely applied chemotherapeutic agent. The aim of this study was to develop a state-of-art physiologically based pharmacokinetic model (PBPK) for doxorubicin to describe its multiscale (system, tissue, cellular, and subcellular) disposition in animals and then scale up to human.

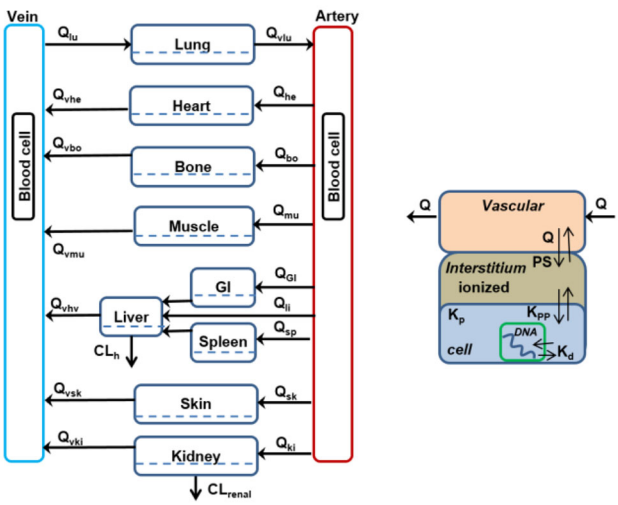

Figure 1 Schematic of multiscale PBPK model of doxorubicin (Color figure online)

Methods: A multiscale PBPK model was developed that divided tissue into four sub-compartments: vascular, interstitial, tissue cellular, and nucleus DNA bound. Drug-associated parameters in the model include cell/interstitial partition coefficient (K_p), ionization effect (K_{pp}), cell membrane-limited permeability (PS), and affinity to extensive DNA intercalation (K_D). Equilibrium binding was assumed between doxorubicin and nuclear DNA and tissue DNA content was used to predict doxorubicin extensive tissue distributions. Various sources of data were obtained in the literature about doxorubicin PK and tissue distribution. Hepatic clearance (CL_h), DNA binding affinity (K_D), and K_p for each tissue were parameters optimized using ADAPT 5. The developed PBPK model based on mice data was further extrapolated to rats and humans.
Results: The concentration-time profiles of doxorubicin in plasma and 9 tissues (liver, spleen, lung, heart, etc) were well characterized by the developed multiscale PBPK model of doxorubicin. The model was optimized successfully based on mice data resulting in precise estimations of 12 parameters (CL_h, K_D, and K_p). The PBPK model was then scaled up to well predict PK and tissues distribution of doxorubicin in rats and human. Sensitivity analysis suggested the importance of hepatic clearance in shaping concentration-time profiles and DNA binding as the key determinant of broadly tissue distribution of doxorubicin.
Conclusions: The present study developed a multiscale PBPK model of doxorubicin. The model could be applied to predict doxorubicin PK and multiscale disposition across species.

T-02

Exposure-Response Analyses of C1 Esterase Inhibitor in Adult and Pediatric Patients for the Prevention and Treatment of Hereditary Angioedema Attacks

JF Marier[1], Grygoriy Vasilinin[1], Jennifer Schranz[2], Patrick Martin[2], and Yi Wang[2]

[1]Certara Strategic Consulting, Canada, [2]Shire, Lexington, MA

Objectives: CINRYZE® (C1 esterase inhibitor [human]; C1INH) is a highly purified, viral-inactivated, nanofiltered concentrate of C1 inhibitor (C1 INH) produced from human plasma. The objectives of this project were to perform exposure-response analyses to support dosing of intravenous Cinryze in pediatric patients for the prevention and treatment of HAE attacks.
Methods: Exposures to C1INH derived with a population PK model previously constructed were merged with the probability of preventing HAE attacks (whereby response was defined as $\leq$1.0 HAE attack/month) to ultimately assess exposure-response relationships (n=166). Logistic regressions for the probability of response and time-to-event modeling of the first HAE attack as a function of exposure was performed for the prevention of HAE. For subjects treated with Cinryze for an acute HAE attack, dose- and exposure-response relationships were explored. Exposure-response analyses (i.e., logistic regression and time-to-event) were performed using R® version 3.2.2.
Results: A positive relationship was observed between minimum concentrations (C_{min}) of functional C1INH and the probability of preventing HAE attacks (p=0.0004). Typical C_{min} values of 0.285, 0.425 and 0.955 U/mL (corresponding to 1st, 2nd, and 3rd tertiles, respectively) were associated to 85.5%, 86.8%, and 90.9% probabilities of preventing HAE attacks, respectively. Time to a 50% probability of HAE attack for the 1st, 2nd and 3rd tertiles of C_{min} were 2.43, 9.79, and 15.7 weeks, respectively. For treatment of an acute attack, relief of defining symptoms within 4 h of dosing (1000 U) was observed in 95.2% of patients. No exposure-response relationship was observed. For patients who did not show improvement within 1 h of dosing, an additional dose (1000 U) resulted in symptom relief within 4 h in 84.2% of patients.
Conclusions: A 500 U dose of CINRYZE in patients 2–5 years of age and 1000 U dose in patients 6-11 years of age are expected to result in optimal prevention and treatment of HAE attacks.

T-03

Exposure-Response Analyses to Assess Lack of QT Prolongation by VS-6063 in Healthy Subjects or in Patients with non-Hematologic Malignancies

Ajit Chavan[1,*], Mahesh Padval[1], Brian Sadler[2], Farell Colm[2] and Maria Pitsiu[2]

[1]Clinical Pharmacology, Verastem Inc, Needham, MA, USA; [2]PK M&S Icon Plc, Dublin, Ireland

Objectives: Defactinib (VS-6063) is an anti-tumor agent being developed for the treatment of non-hematological cancers. The work was undertaken to evaluate the lack of QT prolongation based on exposure-response analyses utilizing data at different dose levels from a dose escalation Phase 1 oncology study and healthy subjects study evaluating food effect.
Methods: In Study B0761001 (n=46), the safety, pharmacokinetics (PK) and pharmacodynamics of single and multiple-doses of VS-6063 administered orally at increasing dose levels (12.5 mg to 750 mg BID) under fasted conditions (12.5 mg to 750 mg BID) and fed conditions (300 mg and 425 mg BID). Triplicate electrocardiograms (ECGs) were taken at PK-matched time points. For Study VS-6063-105, healthy subjects were given 400 mg as a single dose in a cross-over design and time-matched ECGs were collected on Day -1 and Day 1 of each period. Linear mixed-modeling was performed to analyze relationship between plasma exposure and heart-rate-corrected QT intervals.
Results: In the VS-6063 exposure-ddQTc model for the combined Study B0761001 and Study VS-6063-105 data the typical baseline ddQTc in the absence of drug administration was determined not to be significantly different from zero while the slope (95% CI) relating serum or plasma defactinib concentration to ddQTc was -5.43 (-9.43, -1.43) msec/μg/mL. Covariate analyses evaluating gender, age, weight or BMI and fasting/fed administration did not influence the QT interval or defactinib and exposure-QTc relationships in the exposure-QTc analysis.
Conclusions: As assessed in patients with advanced solid tumors and healthy subjects, VS-6063 does not affect ventricular repolarization. Early assessments of cardiac safety at ascending doses of VS-6063 suggest lack of QT prolongation and therefore, dedicated and thorough QT study may not be necessary.

T-04

Proper Number of Subjects and Study Design for Evaluation of Ethnic Difference of Oral Clearance: Use of Inter-individual and Inter-study Variability Obtained from Meta-analysis

Akihiro Hisaka[1,*], Hiromi Sato[1], Rika Matsunami[2], and Hiroshi Suzuki[2]

[1]Clinical Pharmacology and Phamacometrics, Graduate School of Pharmaceutical Sciences, Chiba University, Japan; [2]Department of Phamacy, The University of Tokyo Hospital, Japan.

Objectives: Ethnic difference in pharmacokinetics is one of the most critical concerns in the international new drug development. However, statistical detectability and proper number of subjects of clinical studies for evaluation of the ethnic difference have not been fully investigated. This is probably because variability of the oral clearance (CL_{oral}) is highly variable, and is hence unpredictable. Previously, we have performed a meta-analysis of CL_{oral} of 80 drugs reported in 662 clinical studies to elucidate the ethnic difference in CL_{oral} between Japanese and Western subjects considering clearance pathways. In this study, proper number of subjects and study design for evaluation of the ethnic difference are considered based on outcomes of the meta-analysis.
Methods: For the meta-analysis of ethnic difference, CL_{oral} values of 80 drugs in Japanese and Wester subjects were collected mainly from literatures and product labels. Drugs were classified by their clearance pathways (eight groups) based on contribution ratio (CR) determined *in vivo*. Ethnic difference of CL_{oral}, inter-individual variability, and inter-study variability were estimated by Gibbs sampling method. Based on outcomes of the meta-analysis, statistical powers to detect ethnic difference were calculated for various conditions.
Results: In addition to inter-individual variability, significant and consistent inter-study variability was detected in the meta-analysis. When the observed variability was considered, it was estimated that significant ethnic difference might be detected in 22% of studies incorrectly (i.e. false-positive) for drugs cleared by hepatic metabolism. On the other hand, ethnic difference can be detected as significant if the difference is more than 2.5-fold, although this degree of difference does not exist for usual type of drugs. In order to detect ethnic difference reasonably, it is suggested that sufficient subjects of both reference and target ethnicities need to be included from this study.

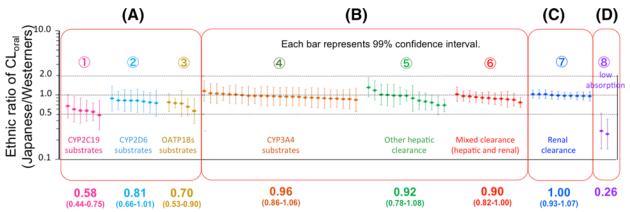

Figure 1 Ethnic differences of oral clearance of 80 drugs (Color figure online)

T-05

Tofacitinib Dose Selection by Extrapolation of Efficacy from Adult RA to Polyarticular Juvenile Idiopathic Arthritis (pJIA) and Optimal Design to Select PK Sampling Times for a Phase 3 (P3) Study in Children

Anasuya Hazra[1,3,*], Camille Vong[2,3], Thomas Stock[3], Sriram Krishnaswami[1,3], Mark Peterson[2,3]

[1]Clinical Pharmacology, [2]Global Pharmacometrics, Clinical R&D[3], Pfizer Inc.

Objectives: Select tofacitinib (oral JAK-inhibitor), doses and evaluate/optimize tofacitinib PK sampling windows that reduce patient burden using optimal experimental design (OED) in a P3 pJIA study.
Methods: A nonlinear mixed-effects population PK (POPPK) model was constructed using tofacitinib PK data from 26 pJIA patients (2 to <18yrs, open-label, multiple-dose study). Doses across a wide body weight (BW) range (5-80Kg) were selected based on simulations providing steady state (SS) exposures shown efficacious in RA patients. OED (method=D-optimality) of the PK-sampling schedule/windows was investigated in PopED. Sampling times were discretized to be consistent with reasonable clinical execution and several sampling windows were evaluated using the efficiency metric based on the determinant of the Fisher information matrix (det(FIM)). Various sampling schemes were evaluated via simulation/re-estimations.
Results: The POPPK model was one-compartment with 1st order absorption. Inter-individual variability (IIV) on CL/F and Ka were described by exponential error models. Power coefficients (mean[95% CI]) relating BW to CL and V/F were 0.292[0.125-0.525] and 0.843[0.621-0.993], respectively. Figure 1 displays simulated tofacitinib $C_{avg,SS,\ pJIA}$ (relevant exposure metric for efficacy in RA), across a BW range (5-80kg) for the proposed P3 dosing regimen in pJIA. Substantial difference in det(FIM) was observed when comparing 2 vs. 3 sampling times and differing terminal sampling times. Final design provided the highest expected efficiency conditional on clinical execution constraints (sample number and clinic visit-time) at 0.25 hr±5min, 0.75 hr±10min, 3h[-15min;+30min]. Relative root mean squared errors were 13.77% and 14.24% for $CL/F_{tofacitinib,pJIA}$ and $V/F_{tofacitinib,pJIA}$, respectively.
Conclusions: Selected tofacitinib-doses for pJIA patients with BW <40 kg were based on BW while for BW >40 kg were capped at 5mg BID. Predicted concentrations at these proposed doses were equivalent to those of adult RA doses of 3-5mg BID. Implementation of OED allowed sample number reduction and shortened stay duration at investigator sites.

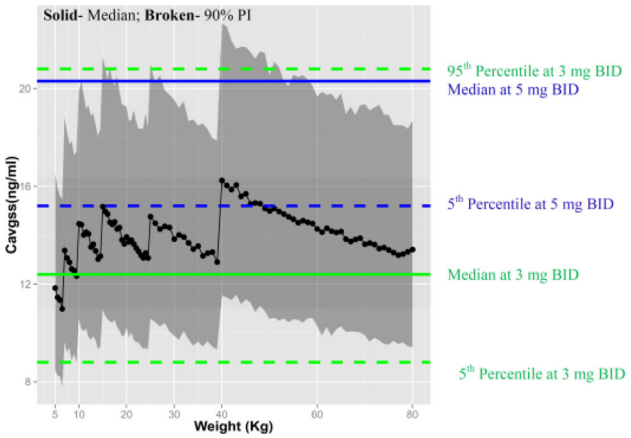

T-06

Quality Award Winner (Trainee Category)

A Minimal Physiologically-Based Pharmacokinetic Model to Investigate FcRn-Mediated mAb Recycling: Effect of K_{on}, K_{off}, Endosome Trafficking, and Animal Species

Brian Maas, Yanguang Cao

University of North Carolina Eshelman School of Pharmacy

Objectives: Neonatal Fc receptor (FcRn)-mediated IgG salvage is an important mechanism to protect monoclonal antibodies (mAbs) from systemic degradation. However, it is still challenging to translate FcRn binding affinity to mAb half-life. Herein, we proposed a minimal physiologically-based pharmacokinetic (mPBPK) model that accounts for mAb-FcRn binding, endosomal trafficking, and species differences to improve the understanding of critical factors in this translation.

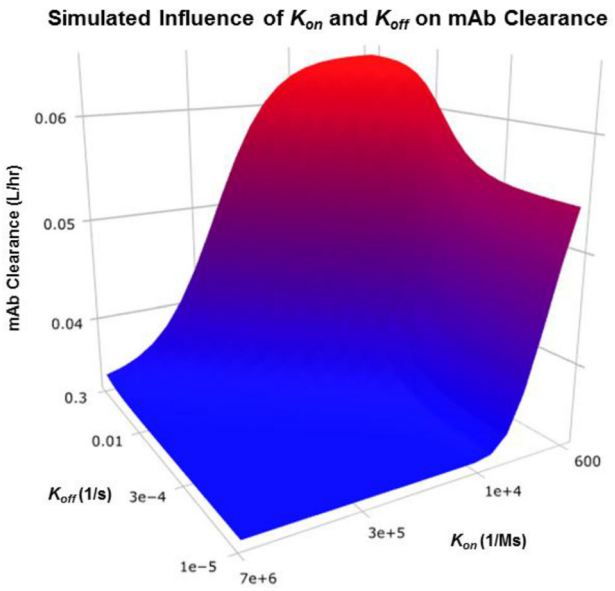

Methods: The binding kinetics between FcRn and mAb in trafficking endosomes were quantitatively analyzed. The influence of IgG-FcRn association (K_{on}) rate, disassociation (K_{off}) rate, and endosome transit time on mAb nonspecific clearance (CL_{ns}) were simulated. Their quantitative relationship was further integrated into our previously developed mPBPK model, which supported the estimation of fluid-phase endocytosis rate (CL_{up}) based on the pharmacokinetics (PK) data of 11 IgG variants in various species from the literature. Species differences in CL_{up} were also explored.
Results: The mAb CL_{ns} was successfully predicted as a function of K_{on}, K_{off}, and endosome transit time. Simulations suggested that decreasing K_{off} beyond endosome transit duration would lose its sensitivity in further reducing mAb CL_{ns} (Figure), where increasing K_{on} would become important but it is largely limited by mAb-FcRn diffusion rate. The quantitative relationship of these factors was successfully integrated into the mPBPK model. The final model described the observed data well with estimations of CL_{up} by incorporating K_{on} and K_{off} ranging from 1.2 to 6.5 (10^6/Ms) and 0.000065 to 0.297 (1/s), respectively. CL_{up} (mL/h) was estimated as 6.51e-3 for mice, 6.38e-1 for monkeys, and 2.65e-2 L/hr for humans. CL_{ns} of mAbs demonstrated allometric relationships across species, but CL_{up} did not.
Conclusions: Our proposed model is capable of predicting the PK of mAbs with known FcRn binding kinetic parameters in several different species. It will serve as a useful tool throughout drug development for optimizing the physical properties of engineered antibodies to achieve desirable PK profiles.
Support: University of North Carolina Start-up for Yanguang Cao

T-07

QSP model of Niemann Pick B Disease and Olipudase Alpha ERT is an innovative tool for extending the value of clinical data and disease knowledge, and filling the gap through computer simulation

Chanchala Kaddi[1], Paul Jasper[2], Bradley Niesner[2], John Pappas[2], Jing Li[1], Rena Baek[3], John Tolsma[2], Shayne Watson[1], Jason Williams[1], Sharon Tan[3], Ana Cristina Puga[4], Gerald Cox[3], Edward Schuchmann[5], Jeffrey S. Barrett[1], Karim Azer[1]

[1]Translational Informatics, TMED, Sanofi, Bridgewater, NJ; [2]RES Group Inc., Needham, MA; [3]Sanofi Genzyme, Cambridge, MA; [4]Sanofi Genzyme, Chilly-Mazarin, France; [5]Genetics & Genomic Sciences, Mount Sinai School of Medicine, New York, NY

Objective: We describe a QSP model supporting late-stage development of olipudase alfa, an enzyme replacement therapy for acid sphingomyelinase deficiency (ASMD). ASMD, clinically known as Niemann-Pick disease types A and B, is a lysosomal storage disorder resulting in sphingomyelin accumulation and other complex lipid abnormalities. This leads to heterogeneous clinical effects affecting multiple organ systems. Through a multi-scale, semi-mechanistic description of ASMD, the QSP model can provide insight into the variability among patient characteristics, clinical disease markers, and treatment response.
Methods: The multi-scale model framework includes mechanistic and empirical sub-models (Figure 1A). These sub-models describe olipudase alfa effects on clinical disease markers, including ceramide, hepatosplenomegaly, and pulmonary decline. The model was informed by natural history, preclinical, and clinical studies for non-neurological ASMD [1,2,3,4].
Results: The model was calibrated using single- and multiple-dose (78 weeks, Q2W) clinical data. By using patient-specific PK profiles and indicators of disease severity, the model reproduced transient and long-term responses of molecular-level markers (Figure 1B), and changes in organ volume and lung function.
Conclusions: The QSP model captures molecular- and organ-level clinical responses to olipudase alfa. By quantifying systemic treatment responses in a heterogeneous disease like ASMD, the model provides insight into how the treatment affects the overall disease burden. The model also provides a platform for studying different dosage regimens and pediatric extrapolation.

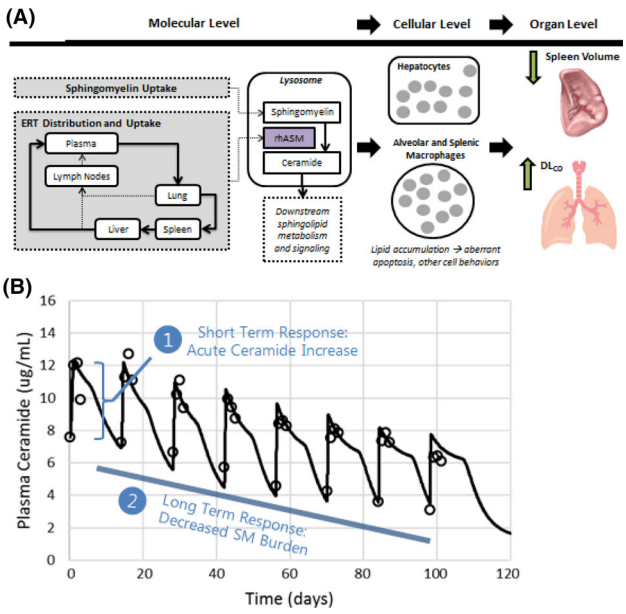

References

1. McGovern et al. (2016) Genet Med 18(1):34-40
2. Wasserstein et al. (2015) Mol Genet Metab 116(1-2):88-97
3. Murray et al. (2015) Mol Genet Metab 114(2):217-25
4. McGovern et al. (2008) Pediatrics. 122(2):e341-9

T-08

A continuous-time Markov model to describe the occurrence and change in severity of diarrhea events over time in metastatic breast cancer patients treated with Lumretuzumab in combination with Perjeta and Paclitaxel

Chao Xu[1], Francois Mercier[1], Patanjali Ravva[1], Jun Dang[1], Johann Laurent[1], Celine Adessi[2], Christine Mcintyre[1], Georgina Meneses-lorente[1]

Clinical Pharmacology[1], Pharma drug safety licensing[2], Pharma research and early development, Roche

Objectives: To model the incidence and duration of the diarrhea events with various grades of severity in metastatic breast cancer patients treated with a combination therapy of Lumretuzumab (a novel anti-HER3 mAb) in combination with Perjeta and Paclitaxel.
Methods: The data from 3 clinical trials (Lumretuzumab monotherapy n=47, Perjeta monotherapy n=78, and the combination therapy of Lumretuzumab, Perjeta and Paclitaxel n=34) were pooled together for model building. The higher severity of diarrhea events in the combination therapy was hypothesized to mainly result from the interaction of Lumretuzumab and Perjeta. A continuous-time Markov model implemented in NONMEM was developed to describe the time dynamics of diarrhea events. A compartmental structure was used (Fig. 1) with four compartments, each representing a severity grade of diarrhea. Drug concentration effect on the forward and backward rate constants that connect the four compartments were evaluated. Synergistic effect of the two mAbs in the combination therapy was tested on EC50. Visual Predictive checks (and other GoF metrics) were used for model diagnostics.
Results: The continuous-time Markov model was able to capture the time course of different severities of diarrhea reasonably well. Drug effect was best described with the increase of the forward rate constants that leads to more severe diarrhea. The magnitude of change of EC50 was estimated to be 130 folds, suggesting strong synergy between the two mAb drugs. The prophylactic effect of Loperamide in a subset of patients was also well captured.
Conclusions: The continuous-time Markov model incorporating interactions between the two mAbs was able to describe the incidences of different severities of diarrhea reasonably well. Further refinement may be achieved including the effect of Paclitaxel.

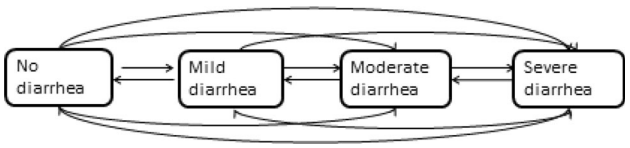

Figure 1 Continious-time Markov model for the incidence of diarrhea events

References

1. Suleiman A et al, A Modeling and Simulation Framework for Adverse Events in Erlotinib-Treated
2. Non-Small-Cell Lung Cancer Patients. *AAPS J*, Vol. 17, No. 6, 2015

T-09

Stan Functions for Bayesian Pharmacometric Modeling

Charles Margossian, William R. Gillespie

Metrum Research Group, Tariffville, CT

Objectives: Stan is a very flexible open source probabilistic programming language designed primarily to perform Bayesian data analysis (1). The Stan No U-Turn Sampler (NUTS), an adaptive Hamiltonian Monte Carlo simulation algorithm, is more efficient than more commonly used MCMC samplers for complex high dimensional problems. Stan also includes a penalized maximum likelihood method. The primary objective of the presented work is to develop new Stan functions to perform pharmacometric modeling tasks including implementation of compartmental PKPD models and schedules of discrete events, e.g., dosing.
Methods: New Stan functions for pharmacometric applications are programmed in C++. They are integrated with Stan software so that the new functions may be used in a manner identical to built-in Stan functions. Use of the new functions is illustrated by analysis of simulated data for plasma drug concentrations and 2 different PD responses: one from an effect compartment model, the other from an indirect action model.
Results: The current prototype Stan functions include one and two compartment models with first-order absorption, and general compartment models described by systems of first order ODEs. The latter uses the CVODES solver (2). The functions incorporate discrete event handling based on NONMEM conventions including recursive calculation of model predictions, bolus or constant rate inputs into any compartment, and dosing histories that include single, multiple and steady-state dosing. Implemented data items include TIME, EVID, CMT, AMT, RATE, ADDL, II, and SS.
Conclusions: The prototype Stan pharmacometric functions facilitate Bayesian pharmacometric modeling by simplifying user implementation of a wide range of pharmacometric models in Stan.

References

1. AC Hindmarsh, PN Brown, KE Grant, SL Lee, R Serban, DE Shumaker, CS Woodward. SUNDIALS: Suite of nonlinear and differential/algebraic equation solvers. ACM Transactions on Mathematical Software, 31:363–396, 2005.
2. B Carpenter, A Gelman, M Hoffman, D Lee, B Goodrich, M Betancourt, MA Brubaker, J Guo, P Li, A Riddell. Stan: A Probabilistic Programming Language. Journal of Statistical Software, 2016 - in press.

T-10

Indirect response model for pharmacokinetic-pharmacodynamic (PK/PD) relationship between synthetic high density lipoprotein (sHDL) and cholesterol efflux

Dan Li[1, 2], Jie Tang[1, 2], Wenmin Yuan[1, 2], David Smith[1], Anna Schwendeman[1, 2]

[1]Department of Pharmaceutical Science, [2]Biointerfaces Institute, University of Michigan, Ann Arbor, MI 48109, USA

Objectives: It has been clinically proven that direct infusions of synthetic high-density lipoproteins (sHDL) composed of apoA-I mimetic peptide and phospholipids are capable of removing the excess cholesterol from arterial plaques. The aim of this study is to establish a PK/PD model describing the different effect of free apoA-I mimetic peptide (22A) and sHDL on cholesterol efflux through intravenous (IV) or Intraperitoneal (IP) injection.
Methods: Pharmacokinetic/pharmacodynamics (PK/PD) analysis were performed by least-squares regression using WinNonlin® software. Indirect response model was established by relating serum concentrations of either 22A or phospholipid component of sHDL to free cholesterol (FC) level. Standard PK and PD parameters were obtained using the group mean (n=4) of concentration and FC levels at each time point by one-step fitting. All final models were chosen and compared based on best fit in terms of sum of squared residual and diagnosis plots.
Results: sHDL has a significant lower 22A EC_{50} value than free peptide for IV injection (60.9 mg/dL versus 139.2 md/dL), indicating lipidation of 22A increased the cholesterol efflux potency of free peptide. Besides, the smaller value of phospholipids EC_{50} in 22A-sHDL IV group compared to IP group (32.5 mg/dL versus 67.8 mg/dL) showed phospholipids in sHDL trigger higher cholesterol efflux after IV injection. In sHDL IP group, the phospholipid-FC PK/PD model appears to provide better fit for the data relative to 22A-FC PK/PD model as highlighted by larger LogLik value. The better quality of fit indicates that FC mobilization is likely elicited by serum presence of cholesterol-free lipid membrane of sHDL and to a less degree by peptide mediated cholesterol efflux.
Conclusion: This PK/PD model reasonably characterizes the relationship between 22A or phospholipids concentration and FC levels. Lipidation of 22A in sHDL increases its cholesterol efflux ability and FC mobilization in vivo is elicited by a greater extent by sHDL's phospholipids rather than peptide. Further PK-PD model validation by administration of various dose levels of sHDL is needed to improve predictive ability.

T-11

Evalulation of parallel efficiency for NONMEM, using multi-core processors and Intel Xeon Phi Co-processors

Dooyeon Jang[1,*], Seunghoon Han[1], Min-gul Kim[2], Dong-seok Yim[1]

[1]PIPET (Pharmacometrics Institute for Practical Education and Training), College of Medicine, The Catholic University of Korea, Seoul, Korea [2]Clinical Pharmacology Unit, Biomedical Research Institute, Chonbuk National University Hospital, Jeonju, Republic of Korea

Objectives: The long computation time spent at model estimation has been a burden to pharmacometricians. So, there is a need to develop methods to reduce the computation time by optimizing the performance of software and/or hardware system. The aim of this study was to identify the parallel-run efficiency of NONMEM (Ver. 7.3)when using the multi-core x86_64 architecture CPU and Intel MIC architecture(Xeonphi) co-processor.
Methods: Two PK models and five different-sized datasets with 500 $\sim$ 3000 subjects were made up for this study. All estimation steps were run on a Linux operating system. The Massage Passing Interface(MPI) method was used for all of the tests used in this study. First, three types of X86_64 architecture processors (4, 8 and 24-core CPU) were used as host environments to explore the influence of adding –maxlim option on the running speed of parallel-optioned NONMEM (-parafile). Second, The performance of Xeon-phi (60-core co-processor) with or without SIMD vectorization installed at the 8-core CPU system was also tested in comparison with the performance of the 8-core system before installing Xeon-phi. The SIMD vectorization to accelerate the co-processor performance was done by modifiying the Fortran source codes and compile options of NONMEM. The speedup ratio and parallel efficiency were employed as parameters of the computation speed.
Results: The maxlim option accelerated the computing speed of the three host environment systems by about 1.9 times when the subject number of the dataset were more than 1000. The co-processor with SIMD vectorization accelerated the computing speed of the 8-core CPU system by about 30$\sim$40%.
Conclusions:We found that the -maxlim option was helpful to speed up NONMEM running of large data (> 1000 subjects) under multi-core desktop computer environments. Additionally, next generation co-processors that support the advanced vector extensions (AVX) is expected to further improve the speed.

T-12

Does birth have an effect on UGT2B7 activity in neonates?

Farzaneh Salem[1], Khaled Abduljalil[1], Trevor N Johnson[1], Edmund Cappareli[3], Raeesa Taylor[2], Janak Wedagedera[1] and Amin Rostami-Hodjegan[1,2*]

[1]Simcyp Limited, Sheffield, UK; [2]Manchester School of Pharmacy, The University of Manchester, Manchester, UK; [3]Department of Pediatrics, University of California, San Diego, USA

Objectives: To derive an *in vivo* ontogeny function that accounts for differences in activity of UGT2B7 in preterm and full-term neonates by considering gestational age (GA) at birth and postnatal age (PNA) using clearance values of zidovudine and morphine as substrates of UGT2B7.
Methods: A literature review was undertaken to collect intravenous clearance data for zidovudine and morphine. The values were deconvoluted back to intrinsic clearance ($CLu_{int,H}$) values (per mg of liver microsomal protein) as described previously[1]. The 'best-fit' model for ratio of paediatric to mean adult $CLu_{int,H}$ with age for zidovudine was determined to obtain an *in vivo* ontogeny function for UGT2B7 using the Phoenix software.
Results: The ontogeny function for UGT2B7 describes an increase in relative $CLu_{int,H}$ during neonatal life as a function of both GA and PNA. UGT2B7 activity in very preterm neonates showed little difference during the post-natal period, however for subjects born at higher weeks of GA the difference in the activity becomes more pronounced post-birth (See Table below). Applying the new UGT2B7 function to predict morphine $CLu_{int,H}$ ratios showed some under-prediction of morphine $CLu_{int,H}$ ratios in neonates. This under-prediction could be due to renal clearance.

Table 1 Fraction of adult activity of UGT2B7 in neonates born at 24, 32 and 40 GA weeks on days 1 and 28 PNA

GA (weeks)	Fraction of adult on day 1	Fraction of adult on day 28
24	0.00169	0.00301
32	0.00692	0.01383
40	0.02871	0.05612

Conclusions: When implementing enzyme ontogeny functions in PBPK models, it is important to consider the GA of premature neonates on the speed of maturation of pathways and also the PNA at which differences in development are no longer apparent. This ontogeny function requires further validation in a preterm PBPK model.

Reference

1. Salem, F., et al. Clin Pharmacokinet, 2014; 53: 625-636.

T-13

Performance and Scalability of Parallel Computing in Biosimulation/modeling Platforms for Pharmacometric Solutions

Fred Soltanshahi, Michael Tomashevskiy, *Kairui Feng

Certara/Pharmacometric Solutions

Purpose: The continued growth of PK/PD modeling in pharmaceutical industry is creating a challenge for all PK/PD software industry. The performance and scalability of software and hardware is always a constraint [1,2]. To improve performance of computationally intensive algorithms by parallel computing and to take full advantage of available computing resources, a few platforms (Figure 1) were explored for remote execution of Phoenix® NLME^{TM} 7.0 jobs.
Methods: Parallel computing platforms investigated include Linux Grid servers (TORQUE and SGE), Window's MPI Cluster, and Amazon Elastic Compute Cloud. Phoenix® NLME^{TM} engine is farmed to these parallel computing platforms to evaluate scientific validation, performance and scalability. Multiple job submission to these computing nodes validated the scalability issues. Examples include some long-running jobs such as bootstrap analysis and covariate search. The parallel computing platforms include: 1) Windows single core, 2) Windows 4 core MPI, 3) 24 core Windows MPI cluster, 4) 32 core Linux Grid, 5) 48 node Amazon cloud.
Results: The execution time recorded for scenarios running on the above platform include: bootstrap analysis using 100, 250, 1000 and 5000 replicates and covariate search including 8, 64, 256 scenarios. The ratio of the execution time between multiple cores and single run was calculated for the analysis on the trend of increasing nodes with different platform setups.
Conclusion: Performance improves proportional to the number of compute nodes employed, with execution times reduced from a few hours to a few minutes.Multiple runs show that: 1) The Linux grid (Torque or SGE) gets best performance. 2) Windows MPI cluster suffers from latency and bandwidth problems. 3) Smaller runs such as 8 covariate search or 100 replicate bootstrap jobs do not gain from increasing the number of nodes. 4) Amazon Cloud has best scalability capability for multiple jobs in contrary to other platform setups.

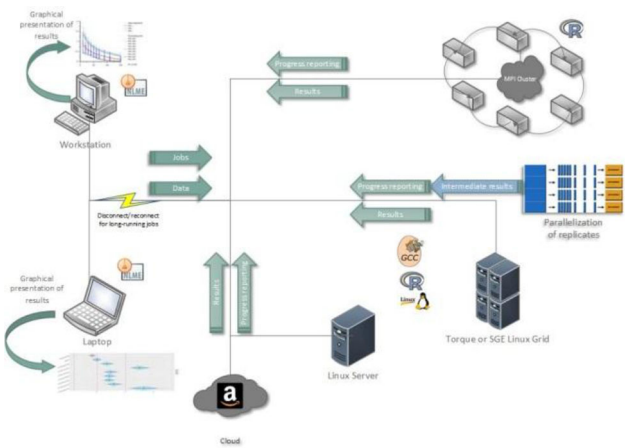

Figure 1 Parallel computing framework (Color figure online)

Reference

1. Sanduja, Cloud computing NONMEM., CPT-PSP, 2015,4 537-546

T-14

Comparison of estimation methods for modelling aggregated survival data

Helena Edlund[1,*], Sergey Aksenov[1], Nidal Al-Huniti[1]

[1]Quantitative Clinical Pharmacology, AstraZeneca

Objectives: Meta-analyses of oncology trials entail modeling of aggregate survival data as fraction (F) of subjects alive (overall survival, OS) or progression-free (progression-free survival, PFS) as a function of time [1]. The impact of covariance (if any) between PFS and OS on inferences using PFS from short-term trials has not been established. This requires characterization of distributions of these two variables. Objective of this work was to investigate the impact of data transformations on how these distributions evolve with time on therapy.
Methods: Individual survival times were sampled from a Weibull distribution with shape=1 and scale=0.5. Between-trial variability was modeled with a log-normal distribution, standard deviation of log(scale)=0.3. We simulated 20 trials with n=500 subjects/trial. Data from each trial were aggregated into fractions. Fractions 1 and 0 were removed. Fractions were modeled with a mixed-effect model [$\exp(-a*\exp(\eta)*time)+\varepsilon$, $\eta \sim N(0,\omega^2)$, $\varepsilon \sim N(0,\sigma^2)$] using three approaches: untransformed data a) constant residual variance σ^2, b) variance $\sigma^2/n*|F*(1-F)|^{2*P}$, c) logit-transformed data and model, constant variance. We simulated 1000 values of F sampling a from asymptotic distribution of its estimate, η and ε using the estimates of ω, σ and p, to represent the population distribution of fractions.
Results: Parameter estimates were similar across models. All models showed acceptable goodness-of-fit for fractions away from boundaries (0 and 1). For fractions closer to boundaries, the logit-transformed model showed asymmetric residuals vs predicted. The three models showed similar predicted distribution of fractions away

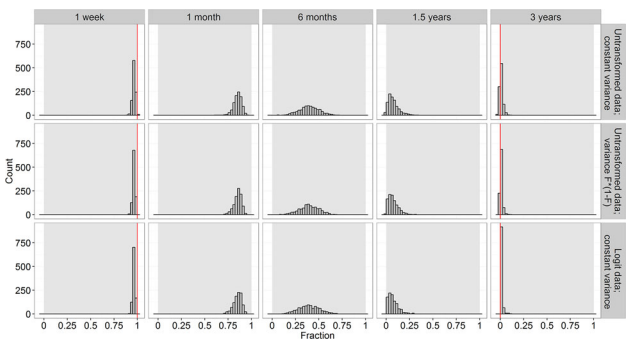

Histograms of simulated distributions of fraction (F) at selected time (columns) for three models (rows). Gray boxes and red lines delimit the range of variable F

from boundaries. Untransformed models show implausible values (<0 and >1) at early and late times. Mathematically the logit transformation is unable to predict exact fractions 0 or 1 that arise in survival data. Distributions are symmetric around F=0.5 and asymmetric closer to boundaries.

Conclusions: None of the models and transformations were adequate to describe the binomial nature of the data (ignoring censoring). The analysis suggests that aggregate survival data (PFS and OS) should be treated as a joint correlated binomial distribution.

Reference

1. Lu D, et al. CPT Pharmacometrics Syst. Pharmacol. 3: e115, 2014.

T-15

The impact of modelling and simulation in oncology: a survey of all drugs approved in oncology by the FDA 2005-2015.

Helena Edlund, Tylee Lin, Kaitlyn Minchella, Hongmei Xu, Robert C. Penland, Eric Masson, Nidal Al-Huniti

Quantitative Clinical Pharmacology, Astrazeneca, Waltham, MA

Objectives: Pharmacometric (PM) analysis is critical for understanding the dose-exposure-response relationship throughout drug development. We surveyed PM analyses and their impact on the approval and labelling of all New Molecular Entities (NMEs) in oncology that were approved by FDA from 2005 to 2015. The objectives are to systematically present an overview of the PM analysis impacting the approval and labeling of NMEs approved for oncology use from 2005 to 2015.

Methods: PM analysis information was obtained from the "Clinical Pharmacology & Biopharmaceutics Reviews" of each NME (http://www.accessdata.fda.gov/scripts/cder/drugsatfda/index.cfm). Results from both the FDA and Sponsor were included. Impact was assigned to one of four categories based on any reported PM details and supported dose adjustments. Dosage information was collected from the approved and revised labels. The impact was compared over two time periods, 2005-2009 and 2010-2015.

Results: From 2005 to 2015, FDA approved 69 NMEs in oncology consisting of 51 small and 18 large molecule drugs. Overall, a large increase in approved drugs was seen between the two time periods (Table 1). A shift was observed in the use of PM analysis (66% vs. 82 %) and more importantly in the impact on the labelling (22% vs. 67%). The impact on the label for large molecules (2010-2015) mirrored that for small molecules. PM analysis supported dose adjustment without support of a dedicated study (renally impaired) in only one label.

Conclusions: Pharmacometric analysis is playing an increasingly important role in supporting dose labeling for oncology drugs. It now impacts over 60% of recently approved small and large molecule therapeutics, a level on par with that of non-concology drugs reviewed earlier[1]. Even when no dose adjustment is recommended, PM efforts play a strong and expanding supportive role in that determination.

Table 1 Summary of pharmacometrics impact on oncology NME approvals and labels, 2005-2015

	Small molecules (N=51)				Large molecules (N=18)				All (N=69)			
	A	B	C	D	A	B	C	D	A	B	C	D
2005–2009	6	7	3	0	0	1	1	0	6	8	4	0
2010*–2015	7	5	22	1	2	3	11	0	9	8	33	1

Categories: A) No PM performed, B) PM performed but no mention in the label, C) PM performed and mentioned in the label – no dose adjustment, D) PM performed and mentioned in the label – dose adjustment supported

* Only 2 drugs were approved in 2010

Reference

1. Lee et al. Clin Pharmacokinet 2011; 50 (10): 627-635.

T-16

Evaluation of body weight descriptors in modeling of cefoxitin and cefazolin pharmacokinetics in the normal and obese populations

Helene Chapy[1], Luigi Brunetti[1,2], Leonid Kagan[1]

[1]Department of Pharmaceutics and [2]Department of Pharmacy Practice and Administration, Ernest Mario School of Pharmacy, Rutgers, The State University of New Jersey, Piscataway, NJ

Objectives: The estimated prevalence of overweight and obese individuals >20 years in the US is 154.7 million (nearly double since the early 1960s). Our previous study and other works indicate that current antibiotic dosing strategies result in inadequate tissue concentration of antibiotics in obese patients.[1,2] The overall goal is to develop approaches for optimization of antibiotic dosing in the obese population. Specifically, we have investigated the relationship between the pharmacokinetic parameters of two cephalosporin antibiotics and several body weight descriptors of obese and normal-weight patients.

Methods: Plasma concentration-time profiles of cefoxitin and cefazolin in normal-weight, overweight, and obese subjects were extracted from published studies. Two- and three- compartment models were constructed and evaluated. The volume of the central compartment and the peripheral compartment(s) were expressed as a function of the total body weight (TBW), lean body weight (LBW), or extra fat (calculated as TBW-LBW). Mean data from different population were fitted simultaneously, and parameters were estimated using maximum likelihood method in Matlab.

Results: For both compounds, three-compartment model provided a good description of cefazolin and cefoxitin data sets. For each compound, the parameters were estimated with good precision. The best

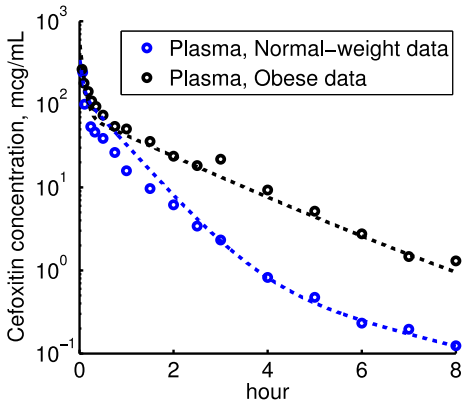

Figure 1 Pharmacokinetic profiles of Cefoxitin (Color figure online)

fit was obtained when volumes of the central and one of the peripheral compartments were set proportional to LBW, and the volume of the second peripheral compartment was set proportional to the size of the extra fat tissue (TBW-LBW).
Conclusion: Biodisposition of antibiotics and other drugs can be significantly altered in obese subjects. The prevalence of obesity continues to increase and approaches for optimization of drug dosing in this population is urgently needed. Utility of indirect and direct measures of body size and body composition for describing drug pharmacokinetics should be evaluated in future studies.

References

1. Brunetti, L., *et al.*(2016).Clin Ther 38(1):204-210.
2. Toma, O., *et al.*(2011).Anesth Analg 113(4):730-737.

T-17

Population Pharmacokinetics and Exposure-Response Relationships of Belimumab Following Subcutaneous Administration in Subjects with Systemic Lupus Erythematosus

Herbert Struemper[1], Mita Thapar[2], David Gordon[3], David Roth[3]

[1]Quantitative Clinical Dev., PAREXEL, Durham, NC; [2]ICON, Marlow, UK; [3]GlaxoSmithKline, Collegeville, PA

Objectives: To characterize the population pharmacokinetics (popPK) and exposure-response of belimumab following subcutaneous (SC) administration in patients with SLE.
Methods: Serially sampled Phase 1 PK data in healthy volunteers (n=134, BEL114448/NCT01583530, BEL116119/NCT01516450) and Phase 3 PK (n=554, BEL112341/NCT01484496) and clinical response data in systemic lupus erythematosus (SLE) patients were analyzed with a non-linear mixed effects modeling approach using NONMEM. Following popPK model development, a logistic regression model for efficacy response (SRI; SLE Responder Index) was developed using a hybrid full model/back ward eliminate approach.
Results: The PK of belimumab administered SC was best described by a linear 2-compartment model with first order absorption and absorption lag time. The bioavailability of belimumab was estimated to be 74%. The population estimates for CL, Vss and terminal half-life were 204 mL/day, 4950 mL, and 18.3 days, respectively. In addition to allometric body weight scaling of CL, Q, Vc, Vp, significant covariate effects (α=0.001) in the final model included BMI on Vc, and the neonatal Fc-receptor related effects of albumin and IgG on CL (Fig.1). Simulations with PK parameters from this and the intravenous (IV) [1] popPK analysis, demonstrated that weekly 200 mg SC dosing results in steady-state Cavg equivalent to 10 mg/kg IV Q4Wk regimen. In the final SRI logistic regression model Cavg was not significant (α=0.05); only baseline disease activity, proteinuria and race were significant predictors of response.
Conclusions: The final SC popPK model parameters were consistent with results for the belimumab IV popPK analysis [1] and other IgG1 mAbs without substantial target-mediated disposition. These PK and PK/PD results indicate that 200 mg qw belimumab dosing is appropriate for subcutaneous administration to SLE patients and that no dose adjustments based on subject characteristics are required.

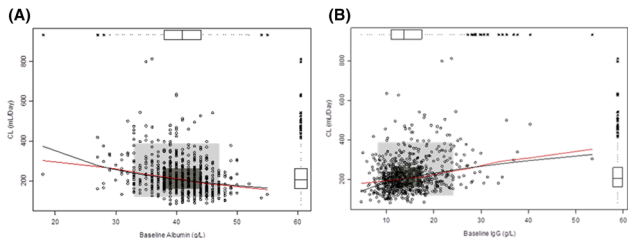

Figure 1 Covariate Effect of Baseline Albumin (A) and IgG (B) on CL (Color figure online)

Reference

1. Struemper H, et al. J. Clin. Pharmacol. 2013;53:711–720.

T-18

Maximum Tolerated Dose or Low-Dose Metronomic Regimen: Implication by A Cellular Pharmacodynamics Model Based on in vitro Cytotoxic Data

Hua He[1, 2], Yanguang Cao[1*]

[1]DPET, School of Pharmacy, University of North Carolina at Chapel Hill, NC, USA; [2]China Pharmaceutical University, Nanjing, China.

Objectives: The dosing regimen of traditional maximum tolerated dose (MTD: high dose, low frequent) is often challenged by low-dose metronomic (LDM: low dose, high frequent) dosing in many chemotherapies. However, it remains unclear which types of chemotherapies would significantly benefit from LDM dosing. The aim of the present study was to develop a cellular pharmacodynamics (PD) model that analyzed *in vitro* cytotoxic data to select the favorable dosing regimen between MTD and LDM.
Methods: The developed PD model divided cancer cells into two subpopulations that were assumed susceptible to either concentration- or time-dependent cytotoxicity. The cellular PD model was taken to analyze various types of in vitro cytotoxic data. The model was further used to simulate tumor suppressive effects of paclitaxel at two commonly dosing regimens. MTD and continuous constant infusion (an extreme LDM) were extensively compared based on the developed model to explore critical factors that largely determine the optimal dosing regimen between MTD and LDM.
Results: The developed cellular PD model adequately captured various patterns of concentration-tumor survival curves obtained in *in vitro* toxicity assay. The ratio of drug concentrations (C_{ss}) to cytotoxic sensitivity (KC_{50}) and the fraction of time-dependent subpopulation (f_u) were found two critical factors. A Cellular PD model Predicted Dosing System (CPPDS) was then developed, where four classes of chemotherapies were defined: Class I (high C_{ss} /KC_{50}, low

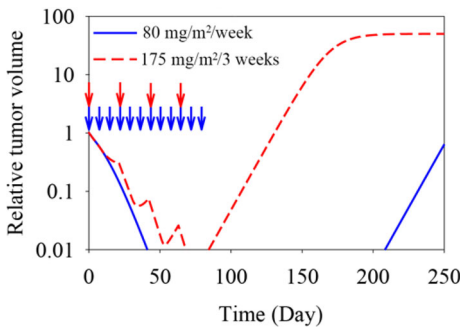

Figure 1 Simulation of the antitumor effect of paclitaxel at different clinical dosing schedules (Color figure online)

f_u), Class II (high C_{ss} /KC_{50}, high f_u), Class III (low C_{ss} /KC_{50}, high f_u), and Class IV (low C_{ss} /KC_{50}, low f_u). Our results indicated that only chemotherapies in Class IV favor MTD with all other Classes in preference of LDM, among which Class I highly benefit from LDM. **Conclusions**: The developed cellular PD model and CPPDS presented a simple and innovative approach to guide the selection of optimal dosing regimen in chemotherapy.

T-19

Quality Award Winner (Non-Trainee Category)

Systems Pharmacology Modeling to Support Clinical Development of Anti-CD20/CD3 T-Cell Dependent Bispecific Antibody

Iraj Hosseini[1,*], Kapil Gadkar[1], Eric Stefanich[1], Chi-Chung Li[1], Laura Sun[1], Yu-Waye Chu[1], and Saroja Ramanujan[1]

Genentech Inc., South San Francisco, CA

Objectives: To develop and apply a quantitative systems pharmacology (QSP) model to support clinical trial design for anti-CD20/CD3 TDB in non-Hodgkin lymphoma (NHL).
Methods: We developed a mechanistic model to describe the dynamics of B- and T-lymphocytes and their interactions in multiple physiological compartments (peripheral blood, tumor, and lymphoid tissues including the spleen, lymph nodes, and bone marrow) in the presence of an anti-CD20/CD3 T-cell dependent bispecific antibody (CD20-TDB) and the CD19-targeting bispecifc T-cell engager blinatumomab (a molecule with similar mechanism, approved for ALL). The model is based on physiological, mechanistic, pharmacokinetic, and pharmacodynamic data and includes: 1) multiple activation states of CD8+ T-cells; 2) CD19+CD20- (pro-B), and CD19+CD20+ (pre- to mature-B) B-lymphocytes; and 3) the pharmacokinetics of CD20-TDB and blinatumomab and their mechanistic effects (activation of CD8+ T-lymphocytes and consequent killing of CD20+ and CD19+ B-lymphocytes, respectively).

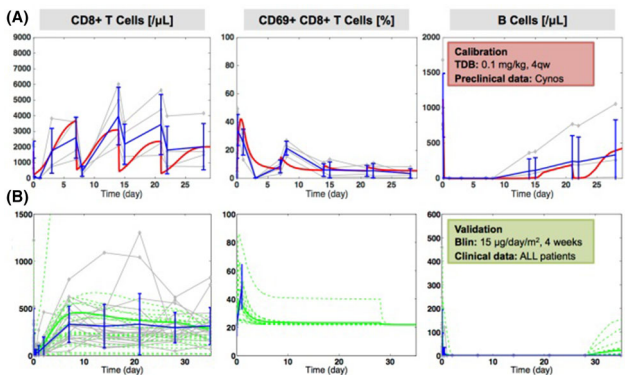

Figure 1 Time profiles of CD8+ T cells, activated T cells (CD8+CD69+) and B cells (A) calibrated using data from cynomolgous monkeys treated with CD20-TDB and (B) validated against clinical data from ALL patients treated with continuous infusion of blinatumomab. *Gray* and *blue*: individual and mean data; *red*: model calibration results; *green*: validation results (Color figure online)

Results: The model was calibrated using *in vitro* potency data and circulating cell measurements in cynomolgous monkeys treated with CD20-TDB [1]. Preclinical and translational validation was performed using additional CD20-TDB preclinical data and blinatumomab clinical data [2, 3]. The model replicated the effects of CD20-TDB on cell dynamics in circulation, and predicted CD20-TDB preclinical data at lower doses and in tissues, and blinatumomab clinical data in patients with ALL and NHL (Fig. 1). The model will be used to evaluate and propose dosing strategies for CD20-TDB in patients with NHL and to inform other clinical development considerations.
Conclusions: The mechanism-based systems model accurately captures and predicts the pharmacodynamics of CD20-TDB in cynomolgous monkeys and in patients with ALL and NHL. The model provides a novel approach for evaluation of clinical dosing strategies for CD20-TDB and can be extended to related molecules and/or other B cell malignancies.

References

1. Sun LL, et al. Sci Transl Med. 2015; 7(287): 1-10.
2. Klinger M, et al. Blood. 2012;119(26):6226-3.
3. Hijazi Y, et al. Abstract: 3051. ASCO; May 31-June 4, 2013.

T-20

Prediction of SVR rates in HCV GT-3 non-cirrhotic patients with 8 weeks of Daclatasvir + Sofosbuvir ± Ribavirin treatment using a viral kinetics model

J. Zhang[*], T. S. Garimella, P. Narasimhan, T Leil

Bristol-Myers Squibb, Princeton, NJ

Objectives: Treatment of Hepatitis C virus (HCV) genotype (GT) 3 is more challenging than other genotypes. In the ALLY-3 Phase 3 study, AI444218, 12 weeks of Daclatasvir (DCV) + Sofosbuvir (SOF) demonstrated a 96% sustained virologic response rate at 12 weeks after completion of therapy (SVR12) in HCV GT-3 non-cirrhotic patients. We investigated if HCV GT3 patients would benefit from a shorter treatment duration and the addition of ribavirin (RBV).
Methods: A non-linear mixed effects (NLME) viral kinetics (VK) model was used to reproduce the viral load measurements with 12 weeks DCV+SOF to optimize model parameters. The model included a wild type strain and a drug resistant strain. A Markov chain Monte Carlo (MCMC) Bayesian Laplacian algorithm was used for parameter estimation. Stochastic simulations using the posterior MCMC Bayesian samples were performed to predict SVR12 for 8 weeks for treatment with and without RBV.
Results: The VK model adequately captures the observed SVR12 results for 12 weeks of treatment with DCV + SOF. The model predicted that SVR12 would be 82% for a 8 week DCV+SOF treatment. The addition of RBV is predicted to increase the SVR12 to 96% following 8 weeks of treatment.
Conclusions: A mechanistic population viral kinetics model was used to characterize the 12 week DCV+SOF treatment efficacy data, and then to predict the efficacy of 8 weeks DCV+SOF±RBV treatment. We find that 8 weeks DCV+SOF treatment is suboptimal for HCV GT-3 non-cirrhotic patients, while 8 weeks DCV+SOF+RBV treatment would be expected to be more efficacious.

T-21

Predicting kinase inhibitor induced cardiotoxicity using transcriptomics and clinical risk scores

J.G.C. van Hasselt, J. Hansen, D. Meretzky, M.R. Birtwistle, E.U. Azeloglu, E.A. Sobie, R. Iyengar

Department of Pharmacology and Systems Therapeutics, Icahn School of Medicine at Mount Sinai, New York, NY, USA.

Objectives: A major side effect of several kinase inhibitors (KIs) is cardiotoxicity (CT), manifesting as loss of contractile function and heart failure [1]. There is an urgent need to minimize KI-associated CT risk in individual patients, and for newly developed KIs. However, the underlying mechanisms KI-associated CT are still poorly understood [1]. We aimed to derive predictive signatures for CT risk, based on regression analyses of transcriptomic and clinical CT risk data.
Methods: Human primary cardiomyocyte cell lines (n=4) were treated with 24 KIs, followed by mRNAseq profiling. Z-scores for the relative risk of hypertrophic cardiomyopathy (HCM), dilated cardiomyopathy (DCM), ventricular dysfunction (VD) and undefined cardiotoxicity (CTU) were derived through mining of the FDA Adverse Event Reporting System database. Individual gene expression based metrics (IGEMs) and weighted correlation network derived signatures (WCNMs) were computed for each drug. These metrics were then and associated with CT clinical risk scores using elastic net regression and leave-one-out (LOO) cross-validation.
Results: IGEM based metrics best predicted HCM with a LOO R^2 of 0.78, and WCNM-based metrics best predicted DCM with a LOO R^2 of 0.92. Predictive WCNR clusters ranged from 12 to 61 genes and distinctly enriched for various cytoskeletal processes, cell shape regulation, insuline-like growth factor receptor signaling, oxidative phosphorylation, and different metabolic processes.
Conclusion: We have generated quantitative expression based signatures associated with clinical risk for cardiotoxicity. The biological mechanisms associated with the individual predictors may provide global insights in mechanisms underlying KI-associated CT, and its mitigation.

References

1. Force *et al. Nat. Rev. Drug Discov.*10, 111–126 (2011)
2. Langfelder *et al. BMC Bioinformatics* 9:559 (2008)

T-22

Prediction of Metabolic Interactions with Atazanavir through UGT1A1 Inhibition using a Physiologically Based Pharmacokinetic Model

J.S. Macwan*, G. Fraczkiewicz, M. B. Bolger, V. Lukacova, W. S. Woltosz

Simulations Plus, Inc. Lancaster, California, USA

Objectives: The objective of this study was to develop a physiologically based pharmacokinetic (PBPK) model of atazanavir following oral administrations. The predictive performance of the model for UGT1A1 inhibition was assessed using a validated raltegravir PBPK model.
Methods: A mechanistic absorption/PBPK model of atazanavir was developed using GastroPlus™ 9.0 (Simulations Plus, Inc.).The program's Advanced Compartmental Absorption and Transit™ (ACAT™) model was used in conjunction with the PBPKPlus™ module to describe the absorption and pharmacokinetics of atazanavir. Human physiologies were generated by the program's internal Population Estimates for Age-Related (PEAR™) Physiology™ module. Data describing the drug's physicochemical properties, enzyme kinetic inputs, and plasma concentration-time profiles were obtained from literature. All tissues were modeled as perfusion-limited tissues. The Lukacova method was used for tissue/plasma partition coefficient estimation. The model was validated by comparing simulated and observed plasma concentration-time profiles for atazanavir across different dose levels following single and multiple oral administrations. The drug-drug interactions mediated via UGT1A1 inhibition [1] were predicted with the GastroPlus DDI module through dynamic simulations using the validated atazanavir and raltegravir PBPK models.
Results: The PBPK model correctly described observed plasma concentration-time profiles of atazanavir for different doses in healthy subjects after single and multiple oral administrations. Dynamic simulations adequately predicted the effect of UGT1A1 inhibition by atazanavir on raltegravir PK. The predicted increase in $AUC_{0\text{-}t}$ and C_{max} of raltegravir in the presence of atazanavir was approximately 2-fold, which was in close agreement with observed values.
Conclusions: The absorption and pharmacokinetics of atazanavir were accurately predicted using the proposed PBPK model. The model demonstrated excellence performance for the prediction of drug-drug interactions related to inhibition of UGT1A1-mediated raltegravir metabolism by atazanavir. New guidance issued by the US-FDA recommends assessing drug interactions for UGT substrates. This model can be successfully used to predict quantitative drug interactions for UGT1A1 substrates.

Reference

1. Iwamoto M, et al. Clin Infect Dis. 2008;47:137-40

T-23

Population Pharmacokinetics of Trametinib in Combination with Continuous or Intermittent Dosing of a PI3K inhibitor, GSK2126458 in Patients with Advanced Solid Tumors

Jafar Sadik B. Shaik*[1, 2], Bela Patel[1], Deborah A. Smith[3], Rajendra P. Singh*[1]

[1]Clinical Pharmacology Modeling Simulation, GlaxoSmithKline, King of Prussia PA USA; [2]Department of Pharmaceutical Sciences, University of Florida, Gainesville, FL USA; [3]Quantitative Clinical Development, PAREXEL International, Durham, NC, USA

Objective: To characterize the pharmacokinetics (PK) of MEK1/2 inhibitor trametinib and dual pan-PI3K/mTOR inhibitor GSK2126458 administered together in patients with advanced solid tumors and to identify potential covariates influencing their PK.
Methods: Population PK analysis was performed using NONMEM version 7.1.2 (ICON, Ellicott City, MD). Subjects (n=65) received escalating doses of GSK2126458 (BID, continuous or intermittent) and trametinib (QD). Covariates were included in the base model based on improvement in objective function value using the likelihood ratio. Final model selection was based on evaluation of goodness-of-fit plots, biological plausibility and precision of parameter estimates. Visual predictive checks (VPC) were implemented for final model evaluation.
Results: A two-compartment model with first order absorption and linear elimination described the GSK2126458 PK with CL/F and Q/F of 3.25 and 2.71 L/h, Vc/F and Vp/F of 8.95 and 38.4 L. WT and ALT levels were predictors of CL/F. WT and age were predictors of Vc/F.

The inter-individual variability (IIV) on CL/F and Vc/F was 53% and 97%. For trametinib, a two-compartment model with rapid and slow absorption components (with MTIME) and first order elimination described PK with CL/F and Q/F of 5.46 and 85.3 L/h, Vc/F and Vp/F of 107 and 348 L respectively. The population estimates of slow and rapid absorption rates and MTIME were 0.135, 0.906 h^{-1} and 0.42 h, respectively. The IIV on CL/F, Q/F, Vc/F, Vp/F, KA1 were 29.6%, 84%, 84%, 72%, and 34%. WT and gender were predictors of CL/F. WT was predictor of Q/F. The VPC plots suggested that the model adequately predicted the concentrations of both agents in this patient population.

Conclusions: The two-compartment model with linear elimination adequately described the PK of both trametinib and GSK2126458. There was no significant difference in the PK estimates of both agents when coadministered as compared to the estimates when administered alone.

T-24

Population Pharmacokinetics/Pharmacodynamics of anti beta-Amyloid Monoclonal (BAM) Antibody GSK933776 in Patients with Geographic Atrophy Secondary to Age related Macular Degeneration

Jafar Sadik B. Shaik[1, 2], Mindy H. Magee[1], Rajendra P. Singh[1], Megan M. McLaughlin[3], Amy Loercher[4], Scott Hottenstein[5], Trish McBride[6], Renee Kurczewski[7], Angela Gress[3]

[1]Clinical Pharmacology Modeling & Simulation, GlaxoSmithKline, King of Prussia, PA USA; [2]Department of Pharmaceutical Sciences, University of Florida, Gainesville, FL USA; [3]Alternative Discovery and Development, GlaxoSmithKline, King of Prussia, PA USA; [4]Immunogenicity and Clinical Immunology, GlaxoSmithKline, King of Prussia, PA USA; [5]Bioanalysis, GlaxoSmithKline, King of Prussia, PA USA; [6]Global Clinical Sciences & Operations, GlaxoSmithKline, King of Prussia, PA USA; [7]Clinical Pharmacology Science & Study Operations, GlaxoSmithKline, King of Prussia, PA USA

Objective: GSK933776 is a humanized IgG1 monoclonal antibody with high affinity for the N-terminal amino acid residues of β-amyloid protein (Aβ). A Proof of Concept study (NCT01342926, GSK-funded study BAM114341) was conducted to evaluate the effects of GSK933776 on patients with geographic atrophy (GA) a form of age-related macular degeneration leading to blindness with no current therapy. This interim analysis is aimed to characterize the PK and the concentration-response relationship between plasma GSK933776 and free Aβ (FBAM) in GA patients.

Methods: Patients (n=191) were randomized 1:1:1:1 to receive placebo or 3, 6, 15 mg/Kg of GSK933776 intravenously every 28±3 days for 18 months. On selected visits at pre-determined time points, plasma samples were collected for the analysis of GSK933776 and FBAM concentrations. Population PK/PD analysis was performed using NONMEM. Final model selection was based on evaluation of goodness-of-fit plots, biological plausibility and precision of parameter estimates. Visual predictive checks (VPC) were implemented for final model evaluation.

Results: A two compartment model adequately described the PK of GSK933776 in GA patients. The inter-individual variability on CL and Vc decreased after adjusting for WT and gender. The exposure parameters (AUC, Cmin, Cmax) at steady-state showed dose proportionality over the range of 3–15 mg/Kg. A sigmoidal Emax inhibition model described the concentration-response relationship in GA patients with moderate variability. The VPC plots suggested that the model adequately predicted the observed GSK933776 effects on FBAM levels in GA patients.

Conclusions: The two-compartment model with linear elimination adequately described the PK of GSK933776. WT and gender were significant predictors of variability in PK. A sigmoidal inhibition model adequately described the effects of GSK933776 on reduction of plasma FBAM levels.

T-25

Model of energy balance predicts body weight and food intake in obesity/diabetes clinical trials

Jangir Selimkhanov[1, *], W. Clayton Thompson[1], Cynthia J. Musante[1]

[1]Cardiovascular and Metabolic Diseases Research Unit, Pfizer Inc, Cambridge, MA USA

Objectives: To develop a mathematical model of food intake (FI) that, along with an energy balance model, can be used to predict long-term body weight (BW) changes in response to various individual clinical pharmacotherapies trials and their combinations.

Methods: A differential equation model of energy balance and BW, which relates change in BW to the change in FI, was adapted from Chow and Hall [1]. Expanding on work in Gobel et al. [2], we incorporated a two-phase FI model, which describes the weight-loss and weight-regain stages of most anti-obesity clinical trials, into the energy balance model. The model captures the dose-dependent effects of individual drugs and their combinations on FI. We embed the combined FI/BW model in a two-level mixed effects statistical framework and fit it to BW data from published anti-obesity and diabetes clinical trials. In total, 80+ clinical trials containing 20+ various drugs were used for non-linear mixed effects model fitting and leave-p-out cross-validation.

Results: The model adequately captured BW changes across a majority of clinical trials. Identified proportionality and transition parameters allow for prediction of the magnitude of initial BW loss as well as its long-term durability. The model also identifies the changes in FI that ultimately lead to the predicted BW loss.

Conclusions: The longitudinal mixed effects model presented here provides an attractive approach to identifying a set of existing therapies that have the greatest potential for combination and to estimating their BW and FI effect sizes in the future. Additionally, the mechanistic model of FI and BW allows for prediction of long-term BW and FI dynamics based on the observed/predicted initial BW loss.

References

1. Chow CC and Hall KD. PLoS Computational Biology. 2008;4(3):e1000045–11.
2. Göbel B, et al. Obesity. 2014; 22(10): 2105–8.

T-26

Population PK and Exposure-Response Analyses of Icatibant in Pediatric Patients for the Treatment of Hereditary Angioedema

JF Marier[1], Claudia Jomphe[1], Jennifer Schranz[2], Patrick Martin[2], and Yi Wang[2]

[1]Certara Strategic Consulting, Canada, [2]Shire, Lexington, MA

Objectives: Icatibant is a synthetic decapeptide with a structure similar to bradykinin that acts as an antagonist of the bradykinin B2 receptor. Population PK and exposure-response analyses were

performed to support dosing of icatibant in pediatric patients for the treatment of HAE.
Methods: Population PK modeling of icatibant was performed based on data collected in 172 subjects enrolled in four Phase I studies (healthy subjects), a Phase IIa study in adults with HAE, and a Phase III study in children and adolescents with HAE. Sources of variability (weight, age, sex, race, HAE attacks) were explored and tested using a full model approach (NONMEM V7). Exposure-response analysis of time of onset of symptom relief (TOSR) was performed (R® version 3.2.2).
Results: A 2-compartment model with first-order absorption and lag-time resulted in an adequate quality-of-fit. The population PK model included the effect of body weight on apparent clearance (CL/F) and volume of distribution (Vc/F). Typical CL/F and Vc/F were 15.4 L/h and 20.4 L, respectively. Maximum concentration in children (2-<12 years old) and adolescents with HAE (12-17 years old) following a single 0.4 mg/kg dose (capped to 30 mg) were similar (737 and 734 ng/mL, respectively) but approximately 34% lower than those derived in adults less than 75 kg (1116 ng/mL). The clinical relevance of the lower icatibant exposure in pediatric patients was evaluated in light of the exposure-response of TOSR. Patients with exposure in the lower tertiles displayed the slowest onset of symptom relief. Overall, median Time to Onset Symptom Relief (TOSR) was 1.0 h (95% CI 1.0-1.1) and all subjects displayed resolution of symptoms within 4 h of dosing.
Conclusions: The exposure to icatibant in children and adolescents was generally lower than that observed in adults. The lower exposure did not affect clinical response, based on the TOSR and complete symptom resolution within 4 hours of icatibant administration.

T-27

Evaluation of Power of Linear Mixed Effect (LME) and Linear Median Quantile Mixed (LMQM) Modeling to Predict Through-QT (TQT) Study Outcomes Using a Single Dose Arm (SDA) Data of Phase I Stduies

Jianguo Li and Nidal Al-Huniti

Quantitative Clinical Pharmacology, AstraZeneca, Waltham, MA

Objectives: To evaluate the power of LME and LMQM in predicting TQT study outcomes using the typical sample size of a SDA data of Phase I studies.
Methods: Simulation studies were conducted for 2 scenarios: one is for a moxifloxician-like positive TQT study with the maximum upper bound of 90% confidence of baseline- and placebo- subtracted QTcF across sampling times (MΔΔQTcF)>10 msec, the other is for a negative TQT study with MΔΔQTcF < 5 msec. QTcF and concentration (CONC) data of 60 subjects from a cross-over TQT study of AZD5672 with positive control of 400 mg moxifloxician (MΔΔQTcF =12 msec) and negative QTcF prolongtion of AZD5672 150 mg (MΔΔQTcF =2 msec) were used for simulations. 1000 SDA data sets of QTcF and CONC data were simulated for each scenario. For each simulated data set, 9 subjects (3 for placebo and 6 for active treatment) were sampled without replacement from 60 subjects to mimic the typical design of the SDA of Phase I studies. R packages LME4 and LQMM were used to model the relationship between CONC and ΔQTcF for each simulated data set. QTcF prolongation was calculated as the 95th percentile of 3000 bootstrapping replicates for the mean QTcF prolongation at the geometric mean CONC for each replicate. The power was calculated as % 1000 simulated SDA data sets that concluded the correct positive or negative TQT study outcomes.
Results: The estimated power to predict moxifloxician-like positive TQT study are 94.4 % and 98% for LME and LMQM, respectively, while the estimated power to predict the negative TQT study are 96 % and 97.5% for LME and LMQM, respectively.
Conclusions: For a compound with moxifloxician-like positive or little ΔΔQTcF prolongation, both LME and LMQM provide high power to predict correct TQT study outcomes using typical SDA data. LMQM provides further improvemnet to the power.

T-28

Population Pharmacokinetic (PK) and Exposure Simulation Analyses for Cediranib (AZD2171) in Pooled Phase I/II Studies in Patients with Cancer

Jianguo Li[1], Nidal Al-Huniti[1], Anja Henningsson[2], Weifeng Tang[1], Eric Masson[1]

[1]Quantitative Clinical Pharmacology, AstraZeneca, Waltham, MA; [2]qPharmetra, LLC, Stockholm, SE

Objectives: To develop a population PK model for cediranib, and simulate cediranib exposure for different doses in cancer patients.
Methods: Cediranib plasma concentration and covariate data from 625 cancer patients after single or multiple oral dose administration (ranging from 0.5 to 90 mg) with the majority of patients treated in the dose range of 20 to 45 mg in 19 Phase I and II studies were used for analyses. A stepwise covariate modelling procedure with forward selection and backwards elimination was used for covariate screening. The final population PK model was used to simulate cediranib exposure for 20 or 15 mg dose alone or for 30 mg dose co-administered with 400 mg rifampicin to evaluate cediranib target coverage, potential need for dose adjustment due to covariate effects or co-administration with rifampicin. NONMEM (Version 7.3) and R3.03 were primarily used for analyses.
Results: A two-compartment disposition model with a sequential zero and first order absorption and first order linear elimination from the central compartment adequately describes cediranib concentration time courses. Body weight and age were identified with statistically significant impact on apparent clearance or apparent volume of central compartment. However, the effects of body weight and age on the area under plasma concentration-time curve and maximum cediranib concentration were <21%. The simulated lower bound of 90% prediction interval or median of unbound cediranib concentrations after 20 or 15 mg doses at steady-state overall exceed the IC_{50} for vascular endothelial growth factor receptors (VEGFR-1,-2 and -3). Simulations supported an increase of dose to 30 mg when cediranib is co-administered with rifampicin.
Conclusions: No covariate was identified to require *a priori* dose adjustment for cediranib. Cediranib exposure following 20 or 15 mg multiple dose administration is overall adequate for the inhibition of VEGFR-1, -2 and -3 activities. Increase in cediranib dose may be needed for cediranib co-administered with strong UGT/Pgp inducers like rifampicin.

T-29

PK/PD model of plasma ceramide in patients with acid sphingomyelinase deficiency following enzyme replacement therapy with olipudase alfa

Jing Li[1], Vanaja Kanamalaru[1], Kerry Culm-Merdek[2], Jason H. Williams[1]

Translation Medicine and Early Development, [1]Sanofi, Bridgewater, NJ; [2]Sanofi Genzyme, Cambridge, MA

Objectives: Plasma ceramide, a catabolite of sphingomyelin, transiently increased in patients with acid sphingomyelinase deficiency (ASMD) who received treatment with olipudase alfa (rhASM), an investigational enzyme replacement therapy. A novel within-patient dose-escalation strategy was employed in a Phase 1b clinical trial of olipudase alfa to successfully control the release of ceramide. Pre-infusion ceramide levels declined with each successive dosing step, and remained below pre-treatment levels at completion of dose escalation. Our objective was to develop a population PK/PD (popPK/PD) model to characterize the time course of plasma olipudase alfa and ceramide in patients with ASMD receiving olipudase alfa.
Methods: The pooled modeling database included 16 adults with nonneuronopathic ASMD who were treated with olipudase alfa – 11 received a single dose (0.03 to 1.0 mg/kg) and 5 were dose-escalated from 0.1 mg/kg to 3 mg/kg. A sequential PK/PD modeling approach using NONMEM software was applied to describe plasma concentrations of olipudase alfa and ceramide. Estimated individual PK parameters were used as an input function on the rate parameter that represented the catabolism of sphingomyelin to ceramide (k_{ASM}).
Results: The final model consisted of a 5-compartment popPK/PD model with saturable response on the rate of catabolism as a function of enzyme concentration changing over time. The model adequately described the individual PK and PD time courses observed in single and multiple dose trials. Nearly maximal increase in enzyme rate was achieved at peak concentrations of olipudase alfa following a single dose of >0.1 mg/kg, and repeat doses of olipudase alfa resulted in a cumulative reduction in the predicted sphingomyelin levels.
Conclusions: A popPK/PD model has been developed to characterize the time course of plasma olipudase alfa and ceramide responses in patients with ASMD. The model could be used to guide late stage clinical development of olipudase alfa and to serve as an important tool for pediatric extrapolation.

T-30

Population pharmacokinetic modeling of long-acting microsphere formulations of risperidone

Jing Niu[1], Harish Kaushik Kotakonda[2], Narsimha Reddy Yellu[3], Jogarao Gobburu[1]

[1]Center for Translational Medicine, University of Maryland, Baltimore, MD; [2]Dept of Pharmacy, IST, Jawaharlal Nehru Technological University Hyderabad, India; [3]PPDM Lab, University College of Pharmaceutical Sciences, Kakatiya University, India

Objective: Risperidone, a benzisoxazole-type atypical antipsychotic, is currently marketed as oral therapy and an injectable depot formulation (Risperdal consta®). In order to address the compliance issue with marked product, five novel long-acting formulations of risperidone are under development. The objective of the present study is to characterize the pharmacokinetics of five novel long-acting microsphere formulations of risperidone as well as Risperdal consta® in rats.
Methods: Five novel microsphere formulations of risperidone were developed, including four polylactide-co-glycolide (PLGA) microsphere (SFA, SFB, SFC and SFD) and one polycapro lactone (PCL) microsphere (F5) formulations. PK samples (11–15 samples per rat) were collected from five groups (n=6) of male Sprague-Dawley rats (weighing approximately 300 g) after single subcutaneous administration of SFA, SFB, SFC, SFD and F5, respectively. PK samples from an additional group of six rats after single intramuscular injection of Risperdal consta® were collected as well. Population pharmacokinetic analysis was performed using Phoenix® NLME for all six formulations. Final PK model with covariates was validated by visual predictive check.
Results: A one-compartment model described was selected for risperidone disposition, while a combined zero order-transit compartment and a sequential zero order-zero order with lag time model adequately described the absorption phase in Risperdal consta® and F5, respectively. A sequential first order-transit compartment absorption model was employed for SFA, SFB, SFC and SFD formulations. Population mean apparent clearance (CL/F) and volume of distribution (V/F), derived from Risperdal consta®, were used for all five novel microsphere formulations and the relative bioavailability with respect to Risperdal consta® was estimated for each novel formulation.
Conclusions: The population PK models adequately described the observed risperidone PK in rats after receiving five novel microsphere formulations as well as Risperdal consta®. The established models will be further extrapolated to human in simulation for purpose of dose selection.

T-31

Pharmacokinetic/pharmacodynamics analysis of hydrocortisone in pediatric patients with congenital adrenal hyperplasia

Johanna Melin[1,2], Thi Truong[1], Peter Hindmarsh[3], Zinnia P Parra-Guillen[1], Charlotte Kloft[1]

[1]Dept. of Clinical Pharmacy and Biochemistry, Institute of Pharmacy, Freie Universitaet Berlin, Germany; [2]and Graduate Research Training Program PharMetrX, Germany; [3]Developmental Endocrinology Research Group, Institute of Child Health, University College London, UK

Objectives: Patients with congenital adrenal hyperplasia (CAH) have no/low synthesis of cortisol. Optimisation of hydrocortisone (synthetic cortisol) therapy in this population is important, since too low or high concentrations increase the risk of adrenal crisis or Cushinǵs syndrome, respectively [1]. 17-hydroxyprogesterone (17-OHP, cortisol precursor) concentrations are elevated in these patients and may serve as a disease-specific marker to evaluate therapy [1, 2]. This analysis aimed to characterise the pharmacokinetics/pharmacodynamics (PK/PD) of cortisol by using 17-OHP as a biomarker in paediatric patients with CAH.
Methods: CAH patients (n=30, age: 7-17 years) received standard hydrocortisone replacement (tablet, 5-20 mg) twice (n=17) or thrice (n=13) daily. Plasma samples were collected pre-dose and every 20 minutes up to 24 h post-dose [2]. The PK model was first developed and sequentially fixed when estimating the PD parameters using NONMEM 7.3. Use of mixture models was evaluated. Model selection was based on plausibility and goodness of fit plots. Predictive performance and parameter precision were assessed by visual predictive checks and bootstraps, respectively [3].
Results: The cortisol concentration-time profiles were accurately described by a two-compartment disposition model with sequential zero- and first-order absorption. An indirect response model with a cortisol-mediated inhibition (sigmoidal I_{max} effect model) of the 17-OHP synthesis described the data most adequately. A mixture model was used to estimate different baseline concentrations of 17-OHP for two subpopulations (5.3 and 280 nmol/L).
Conclusions: An initial PK/PD model for cortisol has been established, and additional aspects such as circadian rhythm may be included to improve model performance. When final, simulations can be performed to evaluate cortisol substitution therapy.

References

1. Speiser PW, et al. J Clin Endocrinol Metabol, 2010
2. Charmandari E, et al. J Clin Endocrinol Metabol, 2001
3. Lindbom L, et al. Comput Methods Programs Biomed, 2005

T-32

Pharmacometrics "Thoughtflow": Standards for provenance capture and workflow definition

Jonathan Chard[1], Justin Wilkins[2], Amy Cheung[3], Evan Wang[4], Mike K Smith[5], Phylinda Chan[5], Maria Luisa Sardu[6]

[1]Mango Solutions, [2]Occams, [3]Astra Zeneca, [4]Eli Lilly, [5]Pfizer, [6]Merck Serono

Objectives: To develop a standard, implemented with a workflow software tool, for capturing the full range of activities and entities that are performed during a pharmacometric analysis, based on existing standards. Capturing the provenance of task outputs (how was this created) as well as providing knowledge management for the pharmacometrics workflow (how did we get to this model) facilitates reproducibility, sharing, and communication of results with others. Using this standard, we can visualise the steps taken during the analysis, reproduce analysis steps, and capture decisions, assumptions, and support the process of quality control

Methods: Several tools and standards were evaluated, but the PROV-O ontology was selected due to its wide adoption, extensibility and suitability for capturing the provenance and relationships between activities and entities within and across projects. Analysis artefacts and relationships were mapped onto PROV-O concepts. Tools were developed to support the pharmacometric workflow; storing files in Git, generating the provenance information representing the steps taken by the pharmacometrician, and querying the captured information to report on and regenerate the artefacts in an analysis.

Results: The standard allows tracking of tools and files in an analysis, while capturing assumptions, decisions and relationships beyond input to output. Information is captured at multiple levels of detail, allowing a reviewer to understand key decisions taken during an analysis. It is possible to identify project artefacts that are out of date (e.g. a plot that should be recreated due to dataset change), and re-run activities. Analysts can apply this information to generate documentation, from run records to complete reports. Knowledge shared between team members is enhanced, avoiding duplication of work, increasing quality and reproducibility. Traceability assists reviewers and regulators to evaluate assumptions, results and conclusions.

Conclusions: Capturing structured information with software tools helps to ensure data integrity, facilitating QC and adoption of MID3 concepts.

T-33

Raltegravir PK in neonates – An adaptive trial design to define an appropriate regimen for neonates from birth to 6 weeks of age.

Jos Lommerse[1], Diana Clarke[2], Anne Chain[3], Han Witjes[1], Hedy Teppler[3], Edward P Acosta[4], Edmund Capparelli[5], Matthew L. Rizk[3], Larissa Wenning[3], Thomas Kerbusch[1], Stephen Spector[6], Betsy Smith[7], Mark Mirochnick[8]

[1]Certara Strategic Consulting, Oss, The Netherlands, [2]Boston Medical Center, MA, [3]Merck Research Laboratories, Rahway, NJ [4]University of Alabama at Birmingham, AL, [5]University of California at San Diego, CA, [6]San Diego and Rady Children's Hospital, CA [7]National Institute of Health, NIAID, Division of AIDS, Bethesda, MD, [8]Boston University School of Medicine, MA

Objectives: Evaluate a 6-week dosing regimen during an adaptive trial design.

Methods: The rapid maturation of UGT-1A1, a hepatic enzyme clearing raltegravir (RAL), was characterized in a population PK-model [2] using data from 6 neonates (P1110, cohort-1). The model was applied to design a safe and efficacious 6-week dosing regimen (P1110, cohort-2) and evaluated using an optimized sampling scheme (13 samples/subject).

Results: RAL UGT-1A1 clearance was near-nil at birth and becomes fully maturated around 4 months ($t_{½}$=2.8 weeks). The oral absorption rate was 0.08 (1/hr) at birth and increased 9-fold within one week. The updated PK model validated the 6-week regimen (1.5 mg/kg QD week 1; 3 mg/kg BID weeks 2-4; 6 mg/kg BID weeks 5-6) attaining the therapeutic window (trough>75 nM and AUC24<90 uM.hr, Figure). PK parameters remained within 20% from the original model estimates, but the peripheral volume (V3) was reduced by 50% (3.2 L for 4 kg neonate), which is analogous to prior pediatric PK-model where V3 ≅ body weight.

Conclusions: Significant accumulation of RAL in the first few days of life was well predicted and no adjustment of the 6-week dosing regimen was required.

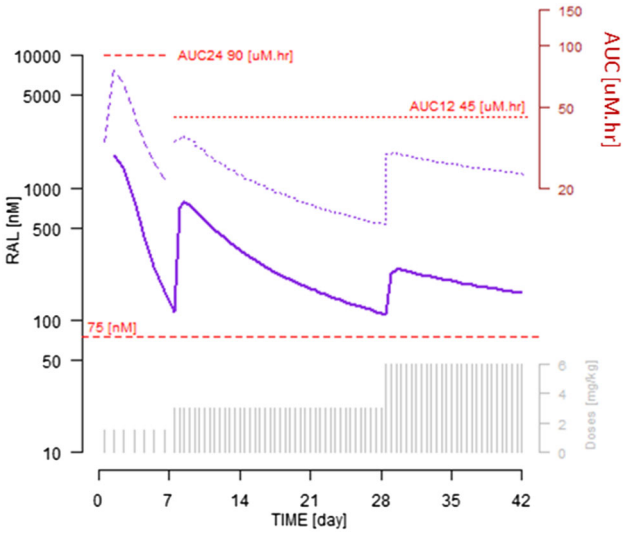

Figure 1 Assessment of 6-week dosing regimen of raltegravir administered to neonates (*week 1*: 1.5 mg/kg QD; *weeks 2–4*: 3 mg/kg BID; *weeks 5–6*: 6 mg/kg BID). The graph shows that C-trough levels are maintained above 75 nM, AUC24 below 90 μM h (QD dosing) and AUC12 below 45 μM h (BID dosing) throughout the full 6-week period (Color figure online)

References

1. IMPAACT-P1110, A PHASE I TRIAL TO EVALUATE THE SAFETY AND PHARMACOKINETICS OF RALTEGRAVIR IN HIV-1-EXPOSED NEONATES AT HIGH RISK OF ACQUIRING HIV-1 INFECTION. http://impaactnetwork.org/DocFiles/P1110/P1110V110DEC12_CM1LoA1CM2CM3_15Jan15.pdf
2. Lommerse J et al. Raltegravir dosing in neonates (IMPAACT-P1110). Use of allometry and maturation in PK modeling to develop a daily dosing regimen for investigation during the first weeks of life. PAGE-24 (2015) Abstr 3627.

T-34

Raltegravir PK in neonates – Modeling rising and declining PK profiles of newborns exposed to raltegravir in-utero

Jos Lommerse[1], Diana Clarke[2], Anne Chain[3], Han Witjes[1], Hedy Teppler[3], Edward P Acosta[4], Edmund Capparelli[5], Matthew L. Rizk[3], Larissa Wenning[3], Thomas Kerbusch[1], Stephen Spector[6], Betsy Smith[7], Mark Mirochnick[8]

[1]Certara Strategic Consulting, Oss, The Netherlands, [2]Boston Medical Center, MA, [3]Merck Research Laboratories, Rahway, NJ [4]University of Alabama at Birmingham, AL, [5]University of California at San Diego, CA, [6]San Diego and Rady Children's Hospital, CA [7]National Institute of Health, NIAID, Division of AIDS, Bethesda, MD, [8]Boston University School of Medicine, MAAIDS, Bethesda, MD, [8]Boston University School of Medicine

Objectives: To develop a population PK model for neonates exposed to RAL in-utero.
Methods: The RAL clearance maturation profile in neonates develops from near-nil at birth to a maximum in approximately 4 months representing development of UGT-1A1 activity, which was implemented in a 2-compartment population PK-model for newborns exposed to RAL first time (naïves) [1]. Neonates exposed to RAL via the mother in-utero (non-naïves) [2], but without post-birth administration, showed striking PK with either declining (Figure, right-panel) or rising (left-panel) RAL levels during the first 36 hours of life. A non-naïve neonate PK-model was built mimicking fast RAL transport via the umbilical cord between mother (receiving RAL) and fetus assuming all RAL-clearance via the mother.
Results: The non-naïve PK-model elegantly explained that neonates could have rising or declining concentrations by tissue redistribution. Upon birth, the Vc mother-Vc neonate link is broken resulting in possible peripheral tissue back-flow where RAL cannot be cleared from Vc neonate.
Conclusions: A PK-model was developed explaining rising or declining RAL levels in non-naïve neonates through redistribution phenomena without having to assume a RAL depot (e.g. formation of RAL-glucuronides [2]).

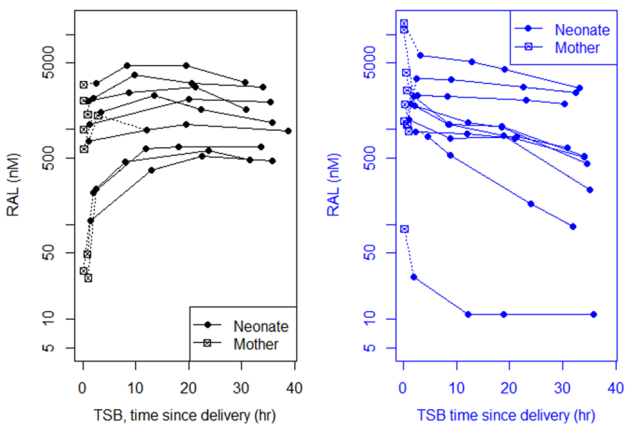

Figure 1 Observed rising and declining non-naive neonate PK profiles after birth from trial P1097: 19 mother-neonate pairs, 1 sample mother shortly after birth and up to 4 samples per neonate. *Left panel* for the 9 rising and the *right panel* for the 10 declining non-naive neonate PK profiles (Color figure online)

References

1. Lommerse J et al. Raltegravir dosing in neonates (IMPAACT-P1110). Use of allometry and maturation in PK modeling to develop a daily dosing regimen for investigation during the first weeks of life. PAGE-24 (2015) Abstr 3627.
2. Clarke DF et al. International Maternal Pediatric Adolescent AIDS Clinical Trials (IMPAACT) P1097 Study Team. Raltegravir pharmacokinetics in neonates following maternal dosing. J Acquir Immune Defic Syndr. 2014 Nov 1;67(3):310-5

T-35

Use of PBPK Modeling to Identify Unexpected Ferroquine Pharmacokinetics in a Phase 1 Study and to Support a Phase IIb Study

Jun Chen[1], Cathy Cantalloube[2], Stephan Beilles[3], Xavier Boulenc[4]

[1]PKDM, Sanofi, Bridgewater NJ; [2]PKDM, Alfortville, France; [3]LGCR, [4]DSAR, Sanofi, Montpellier, France

Objectives: To understand reasons for the unexpected ferroquine pharmacokinetics (PK) in a Phase I study in healthy volunteers (HVs), and predict ferroquine PK to support a Phase IIb study in patients with malaria.
Methods: A physiologically based pharmacokinetic (PBPK) model was established for HVs and patients with malaria. The model performance was evaluated using observed PK data. Ferroquine PK parameters such as bioavailability (F), fraction absorbed (Fa), fraction escaped through the gut (Fg) and clearance (CL) were predicted to understand the super proportional exposure-dose response occurred in the Phase I study.
Results: Both PBPK models for HVs and patients demonstrated good performance with simulated over observed exposure ratio of 0.80 – 1.54x for HVs, 0.84 – 1.32x for patients. In the Phase I study, extended drug precipitation time (Tp) of ferroquine (15620s) was measured in vitro mimicking drug intake medium i.e. milk plus OZ439 re-suspended in 0.8% v/v polysorbate 80 in water & Orasweet. A complete absorption (Fa), dose dependent Fg (38.6-72.1%) and linear clearance were predicted over the dose range of 300-1200 mg. As a result, dose dependent oral bioavailability was predicted from 35.9 to 66.4%. In the phase IIb study, ferroquine capsules are taken with water and OZ439 is administered with vitamin E-TPGS plus sucrose. The measured Tp in the intake medium was 1120s as a model input. From 400 to 1200 mg, the predicted Fa was from 96 to 85%, Fg increased from 57 to 74%, and the overall bioavailability was predicted to be from 50 to 57%. Thus, ferroquine exposure in patients at the highest dose i.e. 1200 mg is anticipated to be similar to that observed at 1200 mg in HVs.
Conclusions: This modeling result supports the phase IIb study for combination therapy of ferroquine and OZ439 in patients with similar ferroquine exposure predicted at the highest dose of 1200 mg as compared to the previous well tolerated study in HVs at 1200 mg.

T-36

A Pharmacokinetic-Pharmacodynamic (PKPD) Model Describing Irreversible Inhibition of Bruton's Tyrosine Kinase by GS-4059

Justin D. Lutz[1], Cara Nelson[1], Helen Yu[2], Albert Liclican[2], Joy Feng[2], Andrew Billin[3], Brian E. Schultz[2], Mark Bresnik[4] and Anita Mathias[1]

Departments of [1]Clinical Pharmacology, [2]Biology, [3]Biomarker Sciences and [4]Clinical Research, Gilead Sciences, 333 Lakeside Dr. Foster City, CA 94404

Objectives: GS-4059 is a covalent inhibitor of Bruton's Tyrosine Kinase (BTK) under development for the treatment of rheumatoid arthritis (RA) and cancer. This work aimed at characterizing the in vitro and in vivo binding kinetics of GS-4059 and exploring the relationship between dose and BTK occupancy to provide a framework for dose selection in clinical studies.
Methods: In vitro, BTK inactivation kinetics of GS-4059 was characterized using the Omnia Kinase assay. Ex vivo BTK binding was investigated in samples from healthy volunteers who received single 100mg or multiple QD 20mg doses of GS-4059. Free and total (free+drug bound) BTK in peripheral blood mononuclear cells (PBMCs) was measured. A PKPD model (NONMEM v.7.3) incorporating BTK inactivation and turnover in PBMCs was developed. BTK occupancy in PBMCs and splenocytes after multiple ascending daily doses (1.25-160mg) were simulated based on model derived BTK binding kinetics to predict the optimal dose(s) to explore in future studies.
Results: GS-4059 exhibited efficient BTK inactivation in vitro with a time-dependent inactivation rate over affinity constant ratio (k_{inact}/K_I) of $86\mu M^{-1}*h^{-1}$. Significant BTK occupancy was observed after single 100 mg and multiple once daily 20mg GS-4059 dosing and this occupancy persisted following GS-4059 washout. The PKPD model estimated in vivo population k_{inact}/K_I ($69\mu M^{-1}*h^{-1}$) was in agreement with the in vitro data. The BTK degradation half-life in PBMCs was estimated to be 64h (k_{deg} value of $0.011h^{-1}$) explaining the persistence of BTK occupancy following drug washout. Simulations suggested that once daily 10mg GS-4059 provides >80% BTK occupancy in PBMCs over a 24h period at steady-state; higher doses may be needed to obtain comparable occupancy in the splenocytes.
Conclusions: This analysis provides a mechanistic understanding of in vivo time- and concentration-dependent BTK inactivation and presents a valuable tool in guiding GS-4059 dose selection for RA and oncology patients.

T-37

A mechanistic model describing the effect of respiratory syncytial virus (RSV) kinetics on clinical symptom score, and disease attenuation by presatovir (GS-5806)

Justin D. Lutz[1], Kashyap Patel[2], Patrick Smith[2], Jason W. Chien[3], Robert Jordan[4], Yan Xin[1], Srini Ramanathan[1] and Anita Mathias[1]

Departments of [1]Clinical Pharmacology, [3]Clinical Research and [4]Biology, Gilead Sciences, Foster City, CA; [2]d3-Medicine, Parsippany, NJ

Objectives: RSV infection causes potentially fatal disease in infants and immunocompromised adults. Unfortunately, options for management of RSV infection are limited. The objective of this work was to characterize the dynamics between RSV load, clinical symptom score (CSS) and the exposure of presatovir, a potent viral fusion inhibitor.
Methods: Data from healthy adult volunteers challenged with RSV (Memphis 37b) and then administered either presatovir or placebo were previously reported[1]. RSV kinetics was described using a mechanistic target-cell limited model[2], which includes an eclipse phase (k) between epithelial cell infection (β) and viral production (p) rates. An indirect response model described the relationship between viral load and CSS, a sum of 10 symptoms each assessed on a 4-point scale. Viral transition and cell mortality rates were fixed based on reported estimates[3]. Based on mechanism of action, it was assumed that presatovir would decrease viral load by inhibiting β. Model evaluation was based on biological plausibility of parameters and Visual Predictive Checks (VPCs).
Results: Diagnostic plots and VPCs indicate that the model accurately described viral load and CSS. Between-subject variability (160–600%) was well estimated (% relative standard error of 5–32%). After placebo the model estimated reproductive number (R_0) was in a biologically realistic range (5–36) providing additional confidence in model performance. A simple E_{max} model best described presatovir inhibition of β, with an EC_{50} of 20ng/mL, in agreement with in vitro data (11ng/mL).
Conclusions: The developed model provides a quantitative link between RSV viral load and CSS and further mechanistic insight into the impact of fusion inhibitors on RSV infection.

References

1. DeVincenzo JP et al. N Engl J Med (2014)
2. Baccam P et al. J Virol (2006)
3. Gonzalez-Parra G et al. Comput Math Methods Med (2015)
The results in this abstract are planned to be presented in part at the RSV Symposium in Patagonia, Argentina, September 28th to October 1st, 2016, and published in the conference proceedings (abstract number T.B.D.)

T-38

Application of A Physiologically-Based Subcutaneous Absorption Model to Estimate Bioavailability of Monoclonal Antibodies Using Subcutaneous Data Only

Lanyi Xie, Yaowei Zhu, Alice Zong, Heald Donald, Honghui Zhouand Weirong Wang

Biologics Clinical Pharmacology, Janssen R&D, 1400 McKean Road, Spring House, PA 19477, USA

Objective: To estimate the subcutaneous (SC) bioavailability of therapeutic monoclonal antibodies (mAbs) using a physiologically-based SC absorption model.
Methods: A physiologically-based mathematical model has been previously developed to describe the SC absorption of mAbs [1]. One implication of this model, though not explicitly stated in the original report, is that SC bioavailability (F) of a mAb can be estimated with the model using SC data only. This hypothesis was examined by applying the model to golimumab, ustekinumab, sirukumab and guselkumab using Phase 1, 2 or 3 clinical study data following single or multiple SC administrations of those mAbs. The F values estimated using the model were compared with those obtained from the traditional non-compartmental analyses (NCA) with both intravenous (IV) and SC data. The physiologically based SC absorption model was developed using Monolix 4.3.
Results. The physiologically based SC absorption models were successfully developed for golimumab, ustekinumab, sirukumab and guselkumab with SC data only. The model estimated F values were in good agreement with those obtained from NCA with both IV and SC data. Mena F values obtained from the model vs. NCA were 0.44 vs. 0.51 for golimumab, 0.58 vs. 0.57 for ustekinumab, 0.60 vs. 0.59-0.87 for sirukumab and 0.50 vs. 0.50 for guselkumb.
Conclusions: The results provided evidence to support the application of the physiologically-based SC absorption model to estimate the F values of mAb using SC data only.

Reference

1. Zhao L, Ji P, Li Z, Roy P, Sahajwalla CG. The antibody drug absorption following subcutaneous or intramuscular administration and its mathematical description by coupling physiologically based absorption process with the conventional compartment pharmacokinetic model. J Clin Pharmacol. 2013;53(3):314-325.

T-39

Model-based Meta-analysis of Bortezomib Exposure–Response Relationships in Multiple Myeloma Patients

Li Zhang and Donald E. Mager

University at Buffalo, SUNY, Buffalo, NY

Objectives: Multiple myeloma (MM) is an incurable bone marrow plasma cell malignancy that accounts for 20% of hematological malignancy related deaths in the United States. Bortezomib, a reversible proteasome inhibitor, shows potent antineoplastic activity by inhibiting the constitutively elevated proteasome activity in myeloma cells and is approved as a first-line therapy for MM. Although clinically successful, drug resistance and dose limiting toxicities (e.g., thrombocytopenia) remain unmet challenges for the clinical use of bortezomib. This study aims to develop a quantitative and predictive pharmacodynamic model to investigate bortezomib dosing-regimens.
Methods: Mean temporal profiles of bortezomib pharmacokinetics, proteasome activity, M-protein concentrations, and platelet counts following bortezomib monotherapy were extracted from published clinical studies. A model–based meta-analysis of bortezomib anti-myeloma activity and thrombocytopenia was conducted sequentially with the Stochastic Approximation Expectation Maximization algorithm in Monolix. The final model was further used to simulate the clinical response and risk of thrombocytopenia during bortezomib monotherapy in myeloma patients under several regimen scenarios.
Results: A small systems model linking drug exposure to response was developed by integrating major regulatory mechanisms, including: target-mediated disposition of bortezomib, proteasome inhibition, modulation of apoptotic intracellular signaling, and subsequent regulation of myeloma progression with proteasome-mediated platelet turnover. Bortezomib pharmacokinetics, myeloma progression, and platelet dynamic profiles were well characterized in myeloma patients. Local sensitivity analysis suggested that increased target density may alter bortezomib PK and attenuate cytotoxic effects, with decreased bortezomib exposure leading to the rapid recovery of proteasome activity, diminished apoptosis signal activation, and accelerated disease relapse and progression (Figure 1). In addition, model simulations indicate that a once-weekly dosing schedule represents an optimal therapeutic regimen with comparable antineoplastic activity but reduced risk of thrombocytopenia.
Conclusions: A pharmacodynamic model was successfully developed, which provides a quantitative, mechanism-based platform for exploring bortezomib dosing-regimens. Further research is needed to apply this model to maximize antineoplastic efficacy and minimize thrombocytopenia for individual MM patients.

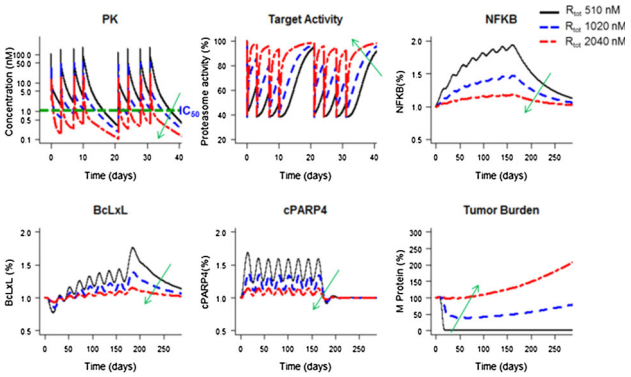

Figure 1 Model simulated profiles of bortezomib plasma exposure, proteasome activity (%), apoptosis signals (NFκB, BclxL, and cPARP), and myeloma tumor burden or M-protein (%) in MM patients with varying basal proteasome density (Rtot) values after bortezomib multiple-dosing (1.3 mg/m2 IV administration on Days 1, 4, 8, and 11 for up to eight 21-day cycles). IC50 represents the model estimated bortezomib potency of proteasome inhibition. *Lines* represent model-simulated mean profiles and arrows indicate the direction of increasing R_{tot} values (Color figure online)

T-40

Model-based Meta-analysis of GLP-1 Agonist Liraglutide Intervention of Obesity and Glucose Intolerance Disease Progression in Type 2 Diabetes

Li Zhang, Christopher Rubino

ICPD, Schenectady, NY

Objectives: Type 2 Diabetes Mellitus (T2DM) is a chronic metabolic disorder that is characterized by a progressive loss of insulin sensitivity and resultant chronic hyperglycemia. Obesity has been recognized as a major risk for T2DM through deterioration of insulin resistance. The ability to simultaneously target deteriorated glycemic control and obesity represents the ideal approach for treating T2DM; unfortunately conventional glucose-lowing therapies commonly result in weight gain. Liraglutide, a GLP-1 agonist that promotes insulin secretion and accelerates weight loss simultaneously, has been approved for treatment of T2DM and obesity. This study aims to develop a model to quantitatively describe liraglutide effects on glycemic control and weight management simultaneously in T2DM.
Methods: A database of study-level aggregate data of body weight, fasting plasma glucose (FPG) and HbA1c in T2DM patients after placebo or liraglutide monotherapy (daily dose ranged from 0.9 to 3.0 mg) was constructed from published clinical studies. Model-based meta-analysis of liraglutide weight reduction effects and glycemic control activity was conducted sequentially with a Stochastic Approximation Expectation Maximization algorithm in NONMEM.
Results: A mechanism-based model was developed by integrating temporal cascades of liraglutide PK, inhibition of β-cell deterioration, induction of pancreatic insulin secretion, and inhibition of weight gain-associated insulin resistance with FPG and HbA1c homeostasis. This model adequately described the time-course of body weight, FPG and HbA1c dynamics following placebo and liraglutide monotherapy, where liraglutide decreased weight and reduced FPG and HbA1c concentrations in a dose-dependent manner. The model-predicted HbA1c dynamics reasonably replicated external data, illustrating the robustness of this model. Furthermore, the good agreement between model-predicted insulin resistance index and literature reported HOMA-IR assessments supported the applicability of this model (Fig.1).
Conclusions: A quantitative model was developed and successfully characterized the time-course of glycemic and obesity biomarkers following liraglutide monotherapy in T2DM patients. This model is based on codifying multiple regulatory mechanisms of liraglutide

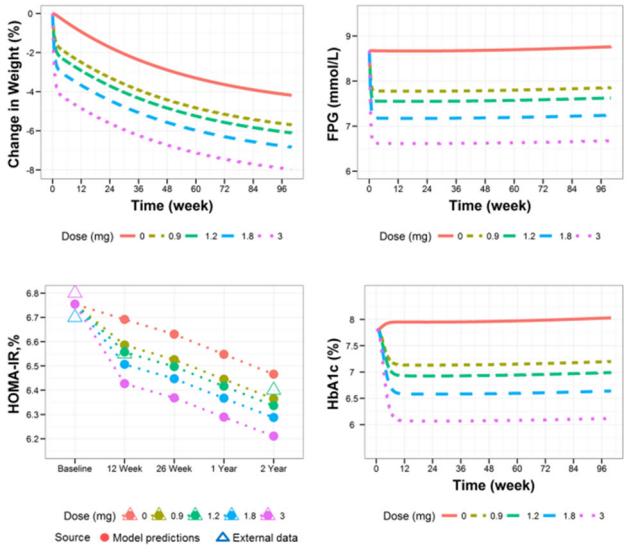

Figure 1 Model-predicted mean profiles of changes in weight, fasting serum glucose (FPG), homeostasis model assessment of insulin resistance (HOMA-IR) and HbA1c after placebo or liraglutide monotherapy in patients with T2DM (Color figure online)

action and should provide a platform for probing optimized liraglutide-based combination therapy in T2DM.

T-41

A mathematical model of tumor-immune interactions for evaluating mono- and combination cancer immunotherapy

Liang-Hui Chu, Weirong Wang, Songmao Zheng

Biologics Clinical Pharmacology, Janssen BioTherapeutics, Janssen R&D US

Objectives: Use mathematical modeling to explore the interplay between T cells and tumor cells in the tumor microenvironment and the impact of various treatment conditions.
Methods: A mathematical model was developed to incorporate key players in cancer immunotherapy, i.e. CD4+ helper cells, CD8+ cytotoxic T cells (CD8+ CTLs), T regulatory cells (Tregs), unlicensed and licensed dendritic cells, NK cells, tumor cells, and cytokines critical for T cell activity regulation (i.e. IL-2, IL-10 and TGF-β). Matlab 2015b SimBiology was utilized to implement the model and generate model simulations. Ordinary differential equations were used to represent the tumor-immune interactions. Perturbations to the CD8+ CTLs and Tregs were introduced. Under different T cell and tumor cell baseline conditions, dynamics of tumor without or with various treatment conditions were examined. Sensitivity analysis of variables and all model parameters was conducted.
Results: Modeling and simulation results illustrated the anticipated differential tumor elimination and dynamic regulation of various T cells and cytokine expression without treatment or with treatments that lead to CD8+ CTL or Treg cell perturbations. Baseline and different initial values of CD8+ CTLs and Tregs were shown to affect tumor progression. In addition, perturbations to CD8+ CTLs and Tregs identified the circumstances when combinations and specific dosing regimens that can lead to significantly faster tumor cell elimination when compared with monotherapy. Sensitivity analysis identified factors such as IL-2 that are of the most importance to tumor cell growth.
Conclusions: This preliminary work illustrated the potential use of system pharmacology models for rational design of combination therapy for cancer immunotherapy. It also provides guidance in designing mechanism-based PK/PD studies to collect key datasets to support further development of the model.

References

1. Robertson-Tessi, M., A. El-Kareh, and A. Goriely, *A mathematical model of tumor-immune interactions.* J Theor Biol, 2012. **294**: p. 56-73.
2. Kim, K.S., G. Cho, and I.H. Jung, *Optimal treatment strategy for a tumor model under immune suppression.* Comput Math Methods Med, 2014. **2014**: p. 206287.

T-42

Modeling and Simulation of the Six Minute Walk Test (6MWT) during Disease Progression in Duchenne Muscular Dystrophy (DMD)

Lora Hamuro, Phyllis Chan, Giridhar S. Tirucherai,, Tushar Garimella and Malaz AbuTarif

Clinical Pharmacology and Pharmacometrics, Bristol-Myers Squibb, Princeton NJ 08543

Objectives: To develop a model that characterizes the natural history progression of the 6MWT in DMD subjects .
Methods: A linear-mixed effect model was developed in Phoenix-NLME that estimated two slopes/intercepts simultaneously for both the improvement and decline in the 6MWT performance with age. Literature data from two sources were digitized using Plot Digitizer and used to build the model (Goemans and McDonald) [1, 2]. The model was assessed using goodness of fit plots and visual prediction checks. Model robustness and parameter estimate confidence intervals were evaluated using bootstrapping. Predictive performance of the model was evaluated by comparing model predictions with results from the datasets used to build the model and a 3rd data set (Mazzone) [3].
Results: The mean age of decline in the 6MWT was estimated at 9.8 years. A 20 meter/year improvement during developmental and an 85 meter/year decline during disease progression was estimated with similar interpatient slope variability ($\sim$23% CV). Model simulations (N=100) were performed to predict the 6MWT change from baseline over 1 year using the age demographics from two datasets used to build the model (Goemans and McDonald) and a validation dataset (Mazzone) (**Table**). The model had a slight bias to underpredict the decline in performance, but the predicted values were within the SD of the observed data.

Table 1 Change from Baseline 6MWT (meters) at 1 year Mean (SD)

	All Age Groups	≤7 years old	>7 years old
McDonald Predicted	−20.4 (33.4) n=57	13.3 (9.5) n=23	−43.2 (22.6) n=34
McDonald Observed	−44.1 (88) n=55	34.1 (53.9) n=6	−58.9 (81.9) n=33
Goemans Predicted	−36.6 (34.4) n=65	12.0 (11.5) n=9	−44.4 (30.2) n=56
Goemans Observed	−42.9 (89.9) n=25	8.6 (84.2) n=3	−50.0 (90.2) n=22
Mazzone Predicted	−23.1 (27.3) n= 106	11.0 (10.2) n=28	−35.4 (20.2) n=78
Mazzone Observed	−25.8 (74.3) n= 106	−7.8 (63.9) n= 35	−42.3 (73.9) n= 71

Conclusions: A model describing the improvment and decline in 6MWT performance with age was developed using literature data. Simulations using age demographics from the literature could reasonably predict the trend in improvement and decline in the 6MWT during DMD diseae progression. Due to the nature of the available data, additional variables that could further impact disease progression could not be evaluated, but is the focus of ongoing work.

References

1. Goemans, et al., Neuromuscul Disord, 2013. **23**(8): p. 618-23.
2. McDonald, et al., Muscle Nerve, 2013. **48**(3): p. 343-56.
3. Mazzone,et al., Neurology, 2011. **77**(3): p. 250-6.

T-43

Leveraging Pharmacometrics in Selecting Proper Dose Regime for Nulojix in Pediatric Patients

Man Melody Luo[1], Sun Ku Lee[1], Bindu Murthy[1], Ihab Girgis[1*]

[1]Clinical Pharmacology and Pharmacometrics, Bristol-Myers Squibb Company, Princeton, NJ 08540

Objectives: Nulojix® (Belatacept) is a selective T-cell costimulation blocker indicated for prophylaxis of organ rejection in adults receiving a kidney transplant. The objective of the present study was to characterize the pharmacokinetic (PK) profile of belatacept in pediatric subjects age 12 to 17 years old using a population pharmacokinetic (PPK) approach.
Methods: A phase 1 belatacept pediatric study is currently ongoing to guide future pediatric dose selection. A single-dose of 7.5 mg/kg was administered to 7 subjects in the on-going study, which was based on the allometric exploration of the adult PPK model [1]. The available pediatric PK data, collected by semi-intensive serial blood sampling, were compared with the PPK model simulations using pediatric demographics. The pediatric PPK model were further optimized to describe the observed pediatric PK data, and assess the effects of individual-specific covariate factors (e.g., demographics, disease status) on variability of belatacept disposition.
Results: The modeling results show that the adult PPK model underestimates the exposure in pediatric subjects. The best pediatric PPK model was identified when the age covariate on clearance was removed from the established adult model. The external predictive check suggested that this updated model adequately predicted the median observed belatacept PK in pediatric subjects aged 12 to 17 years old. This alteration to the model is also physiologically reasonable considering the age effect on clearance in addition to body weight was meant to describe an older aged transplant population, which may not be relevant to a pediatric population.
Conclusions: Available belatacept pediatric concentration data were well described by a linear, two compartment, zero-order infusion, and first-order elimination model. Body-weight and disease status are significant covariates on the clearance and volume of belatacept PK thereby adequately explaining the observed variability in serum concentrations.

Reference

1. Z Zhou, J Shen, Y Hong, S Kaul, M Pfister, A Roy. Clin Pharmacol Ther. 2012; 92:251-7

T-44

A Systems Pharmacology Approach for Translational Learning and Pharmakokinetic Predictions across Patient Populations

Markus Krauss[1], Christian Mueller[2], Jan Schlender[1], Andreas Schuppert[3], Michael Block[1], Lars Kuepfer[1]

[1]Systems Pharmacology ONC, Bayer Technology Services GmbH, Leverkusen, Germany; [2]Applied Mathematics, Bayer Technology Services GmbH, Leverkusen, Germany; [3]Technology Development, Bayer Technology Services GmbH, Leverkusen, Germany

Objectives: The goal of the presented work is to develop a translational approach that enables the identification and transfer of (patho-) physiological and drug-specific knowledge across distinct patient populations.
Methods: Physiological and physicochemical parameters are extracted from experimental data by a Bayesian-PBPK analysis, thereby taking into account available initial literature information [1]. The Bayesian approach in combination with mechanistic modeling enables the translation of knowledge, as the conserved underlying model structure and model parameters across populations allow the transfer of assessed parameter distributions as initial knowledge in subsequent Bayesian-PBPK analyses.
Results: In the translational approach (Fig. 1), a Bayesian-PBPK analysis is performed using study data of a probe drug in a cohort of healthy volunteers (1). Next, the physiological knowledge acquired in

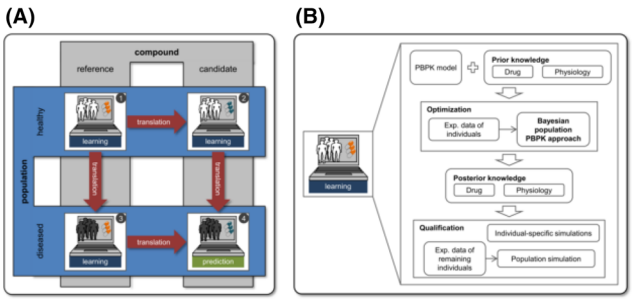

Figure 1 Schematic illustration of the translational approach. (A) A learning step involves a full Bayesian-PBPK analysis, using initial knowledge in combination with new experimental data to refine and acquire knowledge about physiological and drug-specific parameters. A translation step transfers the acquired knowledge to a new investigation, and the acquired knowledge is used as initial knowledge in a new Bayesian-PBPK analysis. (B) PBPK model assessment for each learning step in the translational approach (Color figure online)

step one is refined in combination with study data of a candidate drug in the same cohort of healthy volunteers (2). The acquired physicochemistry of the probe drug is used with study data of a diseased patient cohort to identify pathophysiological changes in this population (3). The acquired physicochemistry of the candidate drug and the assessed pathophysiology from step three are combined for a de novo prediction of the population PK of the candidate drug in the diseased cohort (4). Notably, the Bayesian-PBPK analyses generate individual-specific information in the three learning steps and simultaneously allow to quantify the population-specific interindividual variability.
Conclusions: The presented systems pharmacology approach is a prototype for model-supported translation across the stages of pharmaceutical development programs. Potentially, it can improve the forecasting power in drug development programs by systematically incorporate and translate results of clinical trials to subsequent studies.

Reference

1. Krauss, M., et al., *Bayesian Population Physiologically-Based Pharmacokinetic (PBPK) Approach for a Physiologically Realistic Characterization of Interindividual Variability in Clinically Relevant Populations.* PLoS One, 2015. **10**(10): p. e0139423.

T-45

Selection of exposure metrics AUC, Cmax or Cmin in exposure response analyses – a simulation study.

Matts Kågedal, Qi Liu, Jin Yan Jin

Genentech Inc

Introduction: The relation between drug exposure and response (ER) is often described based on AUC, Cmax or Cmin. This approach ignores time, but makes the analysis efficient and it is commonly used in drug development and regulatory reviews. This simulation study was performed to understand the consequences of ignoring time and to understand when AUC, Cmax or Cmin correlates better with response. These results have been previously presented at PAGE, Lisbon, 2016, abstract 5707.
Methods: Longitudinal PK and PD data were simulated based on a PK model combined with an indirect response PD model[1] with drug effect on the rate constants Kout or Kin. Different underlying models for the relation between drug concentrations and the effect on rate constants were tested. AUC, Cmax and Cmin were derived and correlated with response
Results: The exposure metric that correlated best with response was dependent on the underlying relationship and also varied between doses for the same assumed relationship. AUC was the best metric (highest correlation with response) in the linear range and across doses spanning a wide range. Cmin correlated best in the exposure range approaching saturation. Cmax correlated best when exposures were mostly below the EC50 for an on/off like effect. Only when the model was truly linear and when AUC was used as the exposure metric, were the results consistent across doses. In most other cases, there was a discrepancy between the ER relations derived based on each dose separately. I.e. the expected response differed between doses even at the same exposure.
Conclusions: - This simulation study suggests that the best exposure metric varies with dose and the underlying PK-PD relation.
- The ER relationship derived based on one dose group may not be predictive of the response of another dose. This complication may need special attention when ER assessment and dose justification is based on a single dose group.

Reference

1. Jusko WJ, Ko HC. Clinical Pharmacology and Therapeutics [1994, 56(4):406-419]

T-46

Quality Award Winner (Non-Trainee Category)

Identifying Optimal Dose Combinations of Anticancer Agents via Simultaneous Clinical Exposure-Toxicity and Preclinical Exposure-Efficacy Modeling

Mayankbhai Patel[1], Ekta Kadakia[1], Jilai Zhou[2], Chirag Patel[1], Karthik Venkatakrishnan[1], Arijit Chakravarty[1], Dean Bottino[1]

[1]Millennium Pharmaceuticals, Inc., a wholly-owned subsidiary of Takeda Pharmaceutical Company Limited, 40 Landsdowne Street, Cambridge, MA 02139, USA [2]Thayer School of Engineering, Dartmouth College, 14 Engineering Drive, Hanover, NH, 03755

Objectives: When developing a two-drug anti-cancer combination, the maximum tolerated exposure (MTE) (and therefore maximum tolerated dose) is not a unique number but rather a curve in combination space. Therefore we can think of recommended phase 2 dose-dose ($RP2D^2$) determination as a constrained optimization problem, where the constraint is clinical tolerability and the objective function to be maximized is antitumor effect. We sought to develop methodology whereby clinical toxicity data and preclinical efficacy data could be combined to determine $RP2D^2$ combination most likely to provide clinical antitumor effects and tested this methodology on clinical and preclinical data from a combination of drugs "X" and "Y".
Methods: First we determined via regression analysis that the free-fraction-corrected average concentrations $[X]_{ave}$ and $[Y]_{ave}$ were the primary PK drivers of single-agent preclinical efficacy and clinical toxicity. Next, we characterized the preclinical efficacy surface (green in figure) as a function of free-fraction corrected $[X]_{ave}$ and $[Y]_{ave}$, allowing for nonlinear interactions between the two exposures. Then we fit another surface via 2D logistic regression to the clinical toxicity outcomes, which were treated as binary variables indicating whether each patient experienced a dose-limiting toxicity (DLT). The maximum tolerated exposure (MTE) curve (black in figure) was then defined to be the set of (X,Y) points giving a probability of DLT of

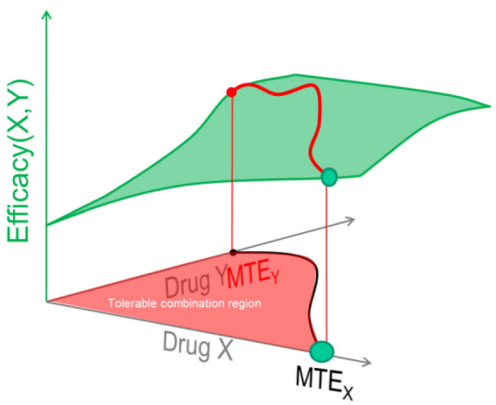

25%. Finally we calculated the predicted antitumor effect along this curve (red curve in figure) to determine the optimal $RP2D^2$.
Results: The toxicity constraint curve determined from early clinical data resulted in the prediction that the most efficacious tolerable combination was not likely to result in higher antitumor effect than the single agents if administered alone.
Conclusions: We believe this is a general and principled method for evaluating and choosing optimal recommended phase 2 dose combinations in oncology.

T-47

Development of an interactive tool to explore paediatric doses and sample size for paediatric trials

Michael Cheng[1], David McDougall[1], Allan Rae[1], Bruce Green[1]

Model Answers Pty Ltd, Australia

Objectives: To develop an interactive tool for: (1) exploration of paediatric dose levels that provide similar exposure as predicted for an adult reference population, and (2) calculation of sample size [1].
Methods: A virtual demographic database of subjects aged ≥1 month to ≤65 years was created based on the Continuous NHANES database [2] and the WHO weight-for-age tables for paediatrics aged ≤10 years [3]. Age-dependent maturation functions for renal and hepatic elimination pathways were implemented [4-5]. Required inputs include: a reference dose; clearance (CL), volume of distribution (Vc) and their variability in adult subjects. Typical CL values are simulated for adult and paediatric populations randomly sampled from the database; taking allometry, enzymatic and renal maturation into account.
Results: A bodyweight-based paediatric dose range is explored in the exposure simulations. Using the simulated CL values, AUCs are calculated at each dose level as: AUC=Dose/CL. For each paediatric age group, the bodyweight-based dose-level best matching the exposure at the reference dose in adults is determined. The percentage of paediatric subjects with exposures falling within the 95% prediction interval of the adult exposure is used as the decision criterion (Figure 1).
The paediatric PK sample size is determined as the minimum number of subjects to achieve "a 95% confidence interval within 60% and 140% of the geometric mean estimate of CL and Vc for the drug in each paediatric group with at least 80% power" [1]. Virtual paediatric PK trials for each age group are generated by sampling from the database. Individual CL and Vc values are then simulated. The power to fulfil the FDA requirement is explored for each sample size across all simulated trials.
Conclusions: An interactive tool was developed to facilitate paediatric drug development.

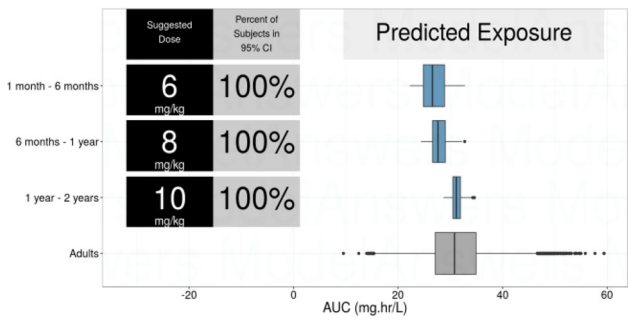

References

1. FDA. Guidance for Industry: Considerations for pediatric studies for drugs and biological products. 2014.
2. National Center for Health Statistics. http://wwwn.cdc.gov/nchs/nhanes/search/nhanes_continuous.aspx.
3. World Health Organization. The WHO Child Growth Standards.
4. Salem et al. Clin Pharmacokinet. 2014;53:625-636.
5. Rhodin et al. Pediatr Nephrol. 2009;24:67–76.

T-48

IQM Tools – Efficient State of the Art Modeling across Pharmacometrics and Systems Pharmacology

Mikael Sunnåker[1], Henning Schmidt[1]

[1]IntiQuan GmbH, Basel, Switzerland

Objectives: Increased demand for support of model-based drug development through pharmacometric and systems pharmacolgy type of analyses requires tools that meet requirements regarding user-friendliness, flexibility, efficiency, compliance, and state of the art methodology. It can be argued that there is no single tool, currently used in the pharmaceutical industry, that fulfills all of these requirements, but that each individual modeler must maintain an own set of partly inherited and subsequently adapted scripts. The personal preferences of a modeler regarding software may lead to the adaptation of an analysis problem to the software, rather than adapting the tool and methodology to the project at hand.
Methods: IQM Tools [1] has been developed as a software package for the well-established mathematical analysis software MATLAB [2]. Guiding principles for the implementation have been user-friendliness, flexibility, extensibility, and compliance. IQM Tools enables a seamless access to available pharmacometric parameter estimation tools, such as NONMEM [3] and MONOLIX [4], enables a straight forward transition from mechanistic systems pharmacology to descriptive pharmacometric models, and efficiently supports reproducibility and compliance, including automated report generation in the Microsoft Word format.
Results: IQM Tools is designed in a modular fashion and consists of three main packages; IQM Lite, IQM Pro, and IQM Report. IQM Lite offers an environment for model building, simulation, optimization, and statistical functions, whereas IQM Pro provides resources for data analysis, NLME modeling, and trial simulations. IQM Report adds automated report generation.

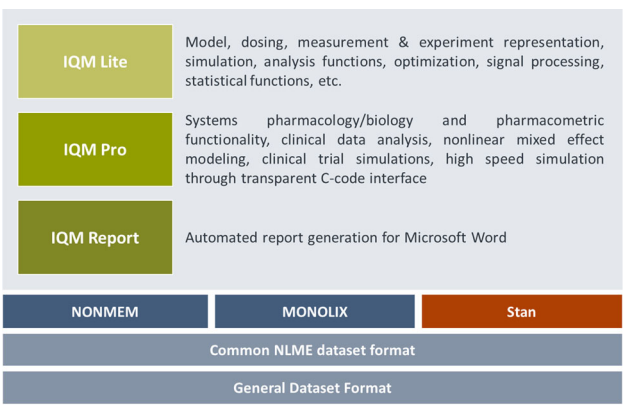

Conclusions: IQM Tools supports and increases the efficiency, quality, and compliance of model-based analyses in pharmacometrics, systems pharmacology, and systems biology by incorporting and extending the capabilities of existing tools. The user-friendliness of the package considerably lowers the threshold for the conduct of pharmacometric analyses, which also makes it useful both for complex analyses and for educational purposes. IQM Tools is published as open source software and available for download [1].

References

1. http://www.intiquan.com/iqm-tools/
2. http://www.mathworks.com
3. http://www.iconplc.com/innovation/solutions/nonmem/
4. http://lixoft.com/

T-49

Quality Award Winner (Trainee Category)

Effect of supplemental formula milk on physiological weight changes in neonates

Mélanie Wilbaux[1], Severin Kasser[2], Tania Coscia[2], Julia Gromann[2], Isabella Mancino[2], Sven Wellmann[2], Marc Pfister[1,3]

[1]Paediatric Pharmacology and Pharmacometrics, University Children's Hospital Basel (UKBB), Basel, Switzerland; [2]Division of Neonatology, UKBB, Basel, Switzerland; [3]Quantitative Solutions LP, Menlo Park, CA, USA

Objectives: Feeding problems can occur in breastfed newborns, leading to dehydration and excessive weight loss, associated with increased morbidity. Goal was to describe effects of supplemental formula milk on weight changes during the first week of life, expanding an existing semi-mechanistic model characterizing physiological weight changes in neonates [1].
Methods: Longitudinal weight data from 887 healthy term neonates exclusively breastfed and 809 breastfed neonates receiving additional formula were available up to 7 days of life. A Kinetic-Pharmacodynamic (K-PD) component was added to the existing semi-mechanistic model to characterize effects of supplemental formula milk on weight changes in neonates. Exclusively breastfed neonates were compared to those receiving supplemental formula. A population analysis was performed with NONMEM7.3. Model selection was based on predefined statistical criteria, goodness-of-fit plots and simulations. Advanced evaluation was performed on data from 829 additional neonates.
Results: Weight changes during the first week of life were described as a balance between time-dependent rates of weight gain (Kin) and weight loss (Kout); Fig.1. A saturable effect of supplemental formula feeding was included on an additional weight gain rate (Kin_{Add}). A population effect (neonates exclusively breastfed vs. neonates receiving supplemental formula) was found on Kin with faster basal rate of weight gain in neonates exclusively breastfed. Visual predictive check (VPC) demonstrated good predictive performance of the expanded model; Fig.1.
Conclusions: We report here the first pharmacometric model that describes effects of supplemental formula milk on weight changes in breastfed neonates during first days of life. An online tool permits caregivers to forecast individual weight changes, and with that to personalize and optimize monitoring and feeding of neonates.

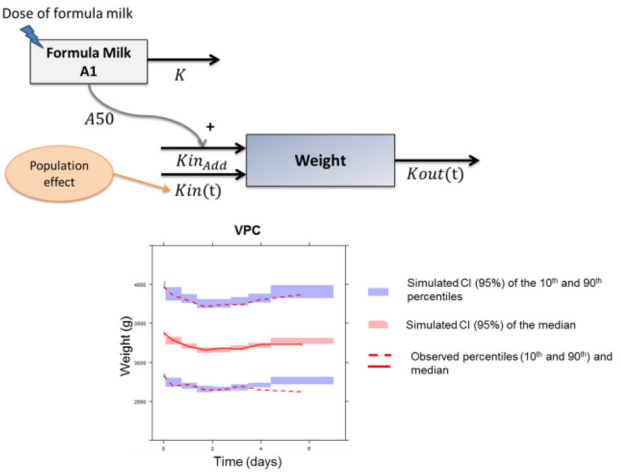

Figure 1 Developed model and VPC (Color figure online)

Reference

1. Wilbaux M. et al. Characterizing and forecasting individual weight changes in term neonates. Journal of Pediatrics 173: 101-107. 2016

T-50

The Use of Animations in Describing Underlying Quantitative Systems Pharmacological Processes

Mohamed Ismail[1], Michael Trang[1], Chris Rubino[1]

[1]ICPD, Schenectady, NY

Objective: Animations can be used as a visual aid to illustrate dynamic processes such as the transfer of mass in the body, tumor size reduction, etc., and can be especially useful in explaining these processes to team members not familiar with pharmacokinetic/pharmacodynamic (PK/PD) principles. The objective of this work was to demonstrate the use of animations in describing the underlying quantitative systems model and to make it simple for pharmacometricians to generate such animations.
Methods: An open source R package is being developed to facilitate the creation of both static and animated schematic PK/PD diagrams using R packages "Ggplot2"[1] and "animation"[2]. Animated schematic diagrams can be created by specifying the type of model (two compartment, PBPK, etc.) and a dataframe containing time points and concentrations or masses within each compartment at each time point. Static schematic diagrams are generated as ggplot objects, and thus can be seamlessly incorporated into Shiny applications and rMarkdown reports, or outputted as images. Animations can be created as .gif, .html, .mp4, or .svg files.
Results: Two examples of pharmacokinetic animations were created using the R package in development. Data from a physiologically-based pharmacokinetic (PBPK) model simulation were animated to show the transfer of mass of drug between compartments. A similar animation was generated for a simpler three compartment model. The creation of animations from common PK and PD simulations and experiments have been or are in the process of being fully automated, requiring only a data table and model type specification as input.
Discussion: The animations developed served as a strong visual aid in describing the underlying pharmacokinetic system, especially for the

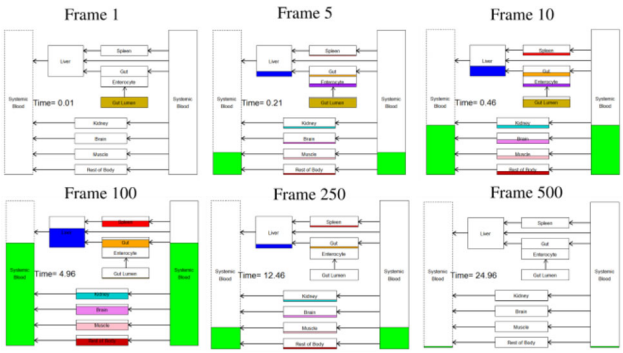

Figure 1 Frame captures of animation of a PBPK simulation. Drug mass is administered into the gut lumen, travels in series to enterocyte, gut tissue, liver, then systemic blood, and subsequently travels in parallel to the various body compartments (Color figure online)

more complex PBPK model. They were able to be easily incorporated into a PowerPoint presentation. These animations can be useful in educational environments and when describing PK/PD processes to non-pharmacometrician stakeholders.

References

1. Yihui Xie, Christian Mueller, Lijia Yu, Weicheng Zhu (2015). animation: A Gallery of Animations in Statistics and Utilities to Create Animations.
2. H. Wickham. ggplot2: Elegant Graphics for Data Analysis.

T-51

Automation of Population Pharmacokinetic-Pharmacodynamic Modeling Reports Using the RShiny Application: TFL Generator

Murad Melhem[1], Dan Polhamus[3], Thomas Lau[2], Ping Chen[1], Adimoolam Narayanan[1], John D Clements[1], John Gibbs[1], George Seegan[2]

[1]Clinical Pharmacology, Modeling and Simulation, Amgen, Thousand Oaks, CA, USA; [2]Research and Development Informatics, Amgen, Thousand Oaks, CA, USA; [3]Metrum Research Group, Tariffville, CT, USA

Objectives: Population pharmacokinetic–pharmacodynamic modeling has become a mainstream tool for supporting internal decision making and regulatory submissions. Appropriate workflow and automation will significantly maximize the productivity of pharmacometricians. In formal reports, tables, figures and lists (TFL) are usually associated with time-consuming quality checks. The objectives of this work were to develop a qualified RShiny [1] tool to efficiently generate TFLs in templated reports and minimize quality checks.
Methods: The developed application was created using RShiny, writing output to rich text format. For submission-quality products, GGgplot2 and GridExtra drive most graphics, while LaTex drives tables and listings. This tool was designed to reliably access to input and output datasets, reporting of pre- and post-processing graphical/tabular results.
Results: The TFL Generator was designed to be efficiently applied across projects/programs with minimal modification. The development of the first version of TFL Generator is complete and further improvements are ongoing. The application provides flexible options

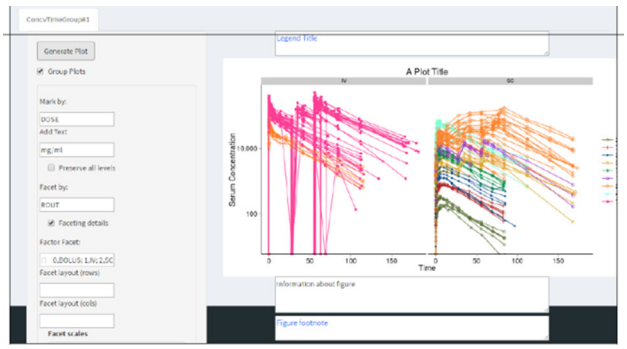

Figure 1 An example of the TFL Generator user-friendly generation of exploratory plots (Color figure online)

for modifying elements of the TFLs, create new TFL templates from the app; download, modify, and share these templates for TFLs with other users through the interface. To enhance flexibility of the for data manipulation, an R script parser is also included. The full R script producing the report is generated from QC'ed R script, saved and can be supplied to regulators.
Conclusions: Pharmacometric analyses play an important role in model-informed drug development for better decision making. The PharmacometricsTFL Generator provides pharmacometricians with a qualified tool for formal reporting of analysis results. This is expected to allow more time to focus on the scientific challenges.

Reference

1. Winston Chang, Joe Cheng, JJ Allaire, Yihui Xie and Jonathan McPherson (2015). shiny: Web. Application Framework for R. R package version 0.12.1. http://CRAN.R-project.org/package=shiny

T-52

Information gain in considering individual tumor size lesion dynamics for future model developments: classification and clustering are the 1st step forward

N. Terranova[1], P. Girard[1], U. Klinkhardt[2,3], A. Munafo[1]

[1]Merck Institute for Pharmacometrics, Merck Serono S.A., Lausanne, Switzerland; [2]Merck KGaA, Darmstadt, Germany; [3]Current affiliation: CureVac GmbH, Tübingen, Germany

Objectives: Developing a methodology to evaluate the gain in classifying individual tumor lesions (iTLs) into different tissues, to be used further in modelling of resistance to anticancer drugs, rather than the sum of tumor sizes.
Methods: A novel methodological approach for the non-parametric analysis of iTLs has been defined by integrating knowledge from signal processing and machine learning. Specifically, the proposed workflow uses (i) a rule-based algorithm to classify iTLs based on functional and location criteria, (ii) the cross-correlation to estimate the similarity among classified TL dynamics by also considering potential delays, (iii) K-means clustering on cross-correlation measures to obtain a straightforward result interpretation. Thanks to the defined classification, the assessment of similarity of TL dynamics can be then performed both at the inter-class level (i.e., among TLs differently classified) and intra-class level (i.e., among iTLs similarly classified) (Figure 1).

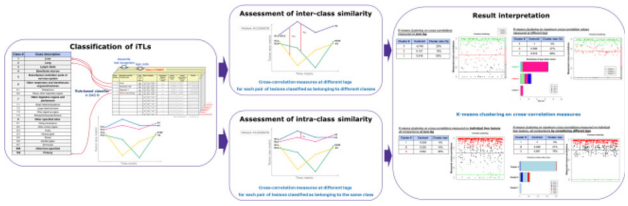

Figure 1 Steps of the proposed methodology, simplified on one subject data are shown for both inter-class analyses. Classification of iTLs is automatically performed through a rule-based classifier based on keywords recognition in the lesion description and on the type code reported by physicians in the Case Report Form (CRF). Once iTLs have beeb classified, the similarity of their dynamics can be assessed by calculating cross-correlation measures for each pair of lesions classified in different classes in case of inter-class analysis, or within the same class in case of intra-class analysis. As cross-correlation measures also calculated at different lags, maximum cross-correlation values can be used to assess at which delay the degree of similarity among lesion dynamics is maximized. Result interpretation is then facilitated by the adoption of the k-means algorithm for clustering cross-correction measures at zero lag as well as maximum cross-corrections obtained by considering different lags (Color figure online)

Results: We have classified 2038 individual target lesions of 642 mCRC patients from two Phase II studies. Different dynamics of classified TLs were highlighted in 30% of patients involved in the inter-class analysis. In particular, 35% of cross-correlation measures computed without considering any delay indicated poor similarity. The degree of similarity substantially increased when considering delays between lesion dynamics. Similarity of iTLs dynamics was mainly indicated by results of the intra-class analysis.
Conclusions: The proposed approach, flexible enough to be applied to many cases and at different levels, provides a deeper understanding of available data and guides next modelling steps [1] by coupling the information on target TLs along with the lesion dynamics.
Results in this abstract have been previously presented in part at PAGE 24, Hersonissos, Crete, 2-5 June 2015 and published in the conference proceedings as abstract 3399.

This work was supported by the DDMoRe project (www.ddmore.eu).

Reference

1. Sardu M-L, et al. PAGE 25 (2016) ISSN 1871-6032, Abstr 5901

T-53

Modeling of Relationships of Cediranib Exposure to Hypertension and Diarrhoea for Cediranib Phase I and II Studies in Patients with Cancer

Nidal Al-Huniti[1], Jianguo Li[1], Klas Petersson[2], Weifeng Tang[1], Eric Masson[1]

[1]Quantitative Clinical Pharmacology, AstraZeneca, Waltham, MA; [2] qPharmetra, Stockholm, SE

Objectives: To establish relationships of cediranib exposure to safety endpoints of diastolic and systolic blood pressures (DBP&SBP) and diarrhoea events in cancers patients with cediranib monotherapy, and apply models to predict DBP&SBP and diarrhoea outcomes for the proposed cediranib dose regimen in cancer patients.
Methods: Paired DBP&SBP data, and diarrhoea events with grades of mild, moderate and severe from 631 subjects in 10 Phase I and II cediranib monotherapy studies were pooled for this analysis. DBP&SBP were simultaneously modelled with an indirect response model for predicted cediranib concentrations from the cediranib population PK model. Diarrhoea was modelled through an ordered categorical proportional odds model incorporating a Markov element and with probabilities of observing none, mild, moderate or severe diarrhoea on a given day being predicted by average cediranib concentrations on the day of the observation. NONMEM (Version 7.3) was primarily used for the analysis.
Results: Increase of DBP&SBP can be described by Emax models with typical increase in DBP&SBP for 20 mg cediranib being predicted to be 7 and 8 mmHg respectively. Probabilities of observing none or any grade diarrhoea was described by an Emax model, and predicted to be highly dependent on the grade on the previous day. At the 20 mg dose, the probability of mild diarrhoea was predicted to increase overtime but not the severity, and the probability of severe diarrhoea was predicted to resolve to grade none approximately 5 days upon discontinuing the cediranib treatment. No demographic covariates were identified to impact the relationships of DBP&SBP or diarrhea to cediranib exposure.
Conclusions: Cediranib increases DBP&SBP with Emax relationships to cediranib concentrations with a predicted small mean increase in DBP&SBP for 20 mg cediranib. The frequency but not the severity of diarrhoea increases with mean cediranib concentration but is far more dependent on the status of diarrhoea on the previous day.

T-54

Interactive Exploration and Quality Control of NONMEM Data Using R Shiny

Nina X. Wang[1,*], Qi Liu[1], Tong Lu[1], Dale Miles[1], Shweta Vadhavkar[1], Priya Agarwal[1], Jin Jin[1], Xiaobin Li[1]

[1]Clinical Pharmacology, Genentech, Inc., Sourth San Francisco, CA

Objectives: To provide initial guidance for the model development, an interactive web-based application was developed to allow end users to explore NONMEM data, examine the correlation among covariates, and identify potential outliers and issues with the source data.
Methods: R Shiny's infrastructure was used to create an interactive web application to explore and examine NONMEN data. Several advanced open-source packages including "ggvis", "ggplot2" and "DT" were used to enhance additional interactive functionality.
Results: Upon loading single or multiple files in csv or tab-delimited format, the end user can review NONMEM data by individual PK profiles, population PK profiles and mean PK profile with error bars. High degrees of freedom are provided in this platform to improve the flexibility and efficiency of data review. End users can select any available stratification variables (e.g. gender, dose, regimen, etc.) and time segments of any subset data to investigate and compare drug effects. Multiple options of PK concentration scales, error bar statistics, and time segments are also implemented, which allows for increased versatility. This R shiny product also provides the following features to assist abnormal data detection: 1) a scroll over feature where patient id, concentration and time information are displayed when hovering over a particular data point of interest, 2) an option for end user to apply multiple outlier detection rules on different subset of data (e.g. each treatment) to identify potential concentration outliers automatically, 3) the ability to display the relationship between dosing and concentration in both actual time and nominal time on a single graph, which will help to identify discrepancies in the data collection.

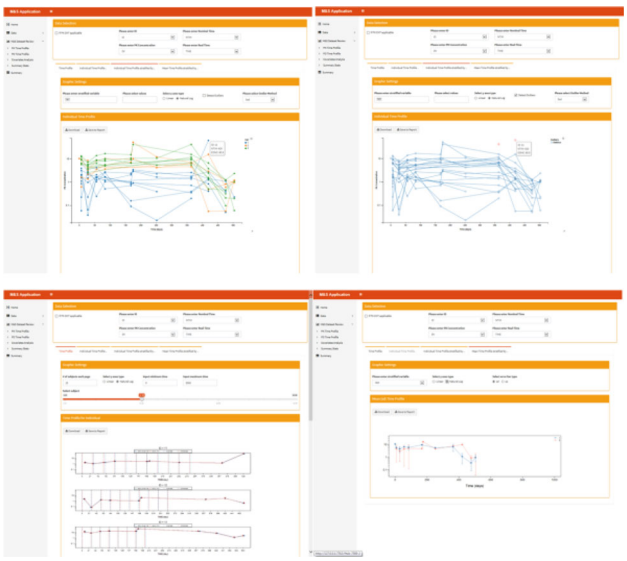

Figure 1 Snapshot of the user interface of R shiny product (Color figure online)

Conclusions: This R Shiny application offers flexibility and versatility to explore NONMEM data and provides a visual-friendly and interactive communication tool for effective team discussions on data related topics. This also improves first step towards efficient model development.

T-55

Exploration of differences between mechanism-based PK/PD and systems pharmacology models

Oleg Demin[1]

[1]Institute for Systems Biology Moscow

Objectives: Both "mechanism-based PK/PD" and "systems pharmacology" models are typically applied to describe PK and PD of a drug and explore translational problems. The aim of the study is to address following questions: are there any principles underlying model structure and ODE system construction which are different for "mechanism-based PK/PD" and "systems pharmacology" models?
Methods: Published "mechanism-based PK/PD" and "systems pharmacology" model were analyzed to find out differences in model structure. Mechanism-based PK/PD model of recombinant human erythropoietin (rHuEPO) in rat [1] was transformed to systems pharmacology model of rHuEPO in rat. Parameters of the systems pharmacology model were fitted against available *in vivo* "rat" data using the Hook-Jeeves method as implemented in the DBSolve Optimum package [2] and then allometrically scaled it to monkey and human.
Results: Our analysis revealed that "mechanism based PK/PD" models described PD in terms of variables potentially located in different "physical compartments" but did not take into account volumes of the "physical compartments" and mass transfer between them. In contrast, "system pharmacology" models described PD in terms of variables potentially located in different "physical compartments" and took into account volumes of the "physical compartments" and mass transfer between them. Basing on the finding of the difference we transformed "mechanism based PK/PD" model of rHuEPO [1] to corresponding "systems pharmacology model" introducing physiologic volumes of the "physical compartments" and mass transfer between them. The such constructed "system pharmacology" model was successful in translational prediction of effect rHuEPO in monkey and human (Fig. 1).
Conclusions: "Systems pharmacology" models can be distinguished from "mechanism-based PK/PD" models in following way: "systems pharmacology" models take into account physiological volumes of the "physical compartments" and mass transfer between them but "mechanism-based PK/PD" models do not.

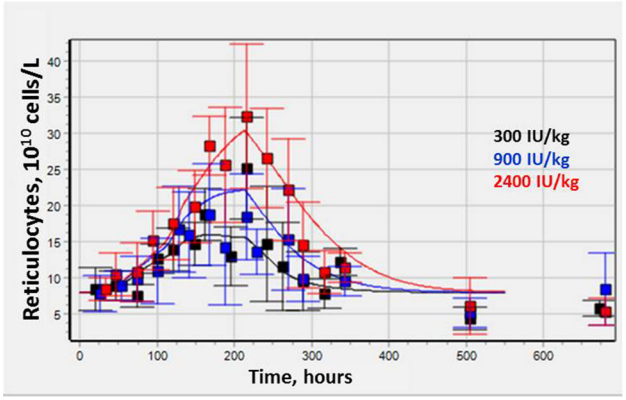

Figure 1 Prediction of effect of different dosages of rHuEPO on human with "systems pharmacology" model scaled from rat. Data taken from [3] (Color figure online)

References

1. Woo S, et al. J Pharmacology Experimental Therapeutics, 2006, 319: 2971-1306
2. Gizzatkulov N, et al. BMC Systems Biology, 2010, 4 (109): 1-11
3. Ramakrishnan R, et al. J Clin Pharmacol 2004, 44:991-1002

T-56

Modeling of immune response suppression by hepatitis C virus and nivolumab treatement in chronic hepatitis C patients using quantitative systems pharmacology approach

Oleg Demin Jr[1]

[1]Institute for Systems Biology Moscow

Objectives: To describe suppression of immune response by hepatitis C virus (HCV) and treatment of chronic hepatits C patients with PD-1 inhibitor nivolumab.
Methods: Model describing chronic hepatitis C progression including HCV dynamics, fibrosis, ALT level, immune response suppression by HCV. The effect of HCV on immune cells was implemented as dependence of immune cell mediated death of infected hepatocytes on HCV level in blood. Nivolumab effect was described as increase in death of hepatocytes (bith infected and normal) in accordance with mechanism of action of PD-1 inhibitors. The progression of chronic hepatits C was calibrated against data on HCV, ALT, fibrosis score dynamics etc. The parameters of nivolumab effect was calibrated asgainst data HCV decline during therapy.
Results: Immune response suppression by HCV was calibrated against data on immune cell (CD8 and CD4 T cells, myeloid-derived suppressor cells) dynamics during treatment of chronic hepatitis C patients with PEG-interferon/ribavirin therapy. The model

successfully describes the dynamics of HCV during treatment with nivolumab as well as response of different patients at follow-up. It was shown that the effect of nivolumab should be very strong to completely eliminate the HCV and infected hepatocytes.
Conclusions: Despite only very small part of patients are completely cured after nivolumab treatment, PD-1 inhibitors could be used in combination with direct antiviral agents to decrease the treatment duration and increase the percent of reposnders. Immunotherapy (including PD-1 inhibitors) is the one of possible options to treat patients with chronic hepatitis C.

T-57

Minimal Physiological Model of Trastuzumab and Rituximab Subcutaneous Absorption Across Species

Edward Pyszczynski[1], Kuan-ju Lin[1], Weiyan Zhang[1], Yanguang Cao[1, 2], William J. Jusko[1], Leonid Kagan[3], and Donald E. Mager[1]

[1]Department of Pharmaceutical Sciences, University at Buffalo, SUNY, Buffalo, New York; [2]Division of Pharmacotherapy and Experimental Therapeutics, University of North Carolina at Chapel Hill, Chapel Hill, North Carolina; [3]Department of Pharmaceutics, Rutgers, The State University of New Jersey, Piscataway, New Jersey

Objectives: To investigate the relative contribution of kinetic processes at the subcutaneous (SC) site on the overall absorption kinetics of trastuzumab, develop a general pharmacokinetic model for simultaneously describing SC absorption of trastuzumab across species, and to examine the capabilities of predicting human SC PK from preclinical data.
Methods: Trastuzumab serum concentrations were measured following intravenous (1, 10, and 40 mg/kg) and subcutaneous (1 and 40 mg/kg) injection at the back and abdomen of rats. The effect of co-administration with human nonspecific IgG was also examined. A minimal physiologically-based pharmacokinetic (mPBPK) model was constructed in ADAPT5 (BMSR, USC, LA) and used to characterize the absorption and disposition of trastuzumab in rats. The model was then scaled across species (rat, minipig, and man) using allometric methods to predict the concentration-time course in man. Rituximab and belimumab PK in humans were used as external validation of the mPBPK model.
Results: Trastuzumab bioavailability in rats was inversely related to dose level (with greater bioavailability at low doses) and varied among injection sites. Decreases in the area under the concentration-time curve were obtained after co-administration with IgG in rats, showing greater reductions following back injection (2.4-fold decrease). The final mPBPK model characterized trastuzumab pharmacokinetics across all species and includes allometric relationships for linear non-specific clearance and the apparent capacity of carrier-mediated uptake. Human rituximab and belimumab pharmacokinetic profiles following SC injection were predicted well after scaling the final model.
Conclusions: A pharmacokinetic model was successfully developed that describes the absorption and disposition of several subcutaneously dosed monoclonal antibodies. The model and approach may prove useful in predicting the concentration time-course of monoclonal antibodies in humans from preclinical species.

T-58

Leveraging a Quantitative Systems Pharmacology Model to Explore the Mechanism of Action of a Novel Basal Insulin Analog

Parag Garhyan[1], Rukmini Kumar[2], Jeanne Geiser[1]

[1]Eli Lilly and Company, Indianapolis, USA; [2]Vantage Research, Chennai, India

Objectives: To mechanistically evaluate, using a Quantitative Systems Pharmacology [QSP] model, the plausible range of differential tissue distribution and insulin receptor binding of novel basal insulin analog [BIL] and its impact on glucose metabolism (endogenous glucose production [EGP] and glucose disposal rate [GDR]) in healthy subjects [HV] and patients with type 1 diabetes [T1DM].
Methods: A QSP model of glucose regulation was developed previously [1]. Data from a clinical euglycemic clamp study [2, 3] that evaluated EGP and GDR in HV and T1DM receiving intravenous infusion of Glargine [GL] for 8 hours was used to incoporate study design in the model. A range of values for two important mechanistic parameters that differentiated BIL from GL: tissue distribution (periphery:liver, [P:L]) and insulin binding affinity relative to GL (relative potency, [RP]) were used to simultaneously simulate the observed EGP and GDR of BIL.
Results: Plausible range of tissue distribution of BIL (P:L from 0.1 to 1) and relative potency (RP between 0.01 to 0.5) were used to simulate the clamp experiment in HV and T1DM subjects [2, 3]. Simulated EGP and GDR profiles were in agreement with clinical data for a select combinations of the 2 parameters – P:L ratio was estimated to be lower than 0.5 and RP between 0.05 and 0.1, based on simulating GDR and EGP data in HV simultaneously. Estimates from HV were confirmed in T1DM subjects. Additional hypotheses (e.g. different potency at liver and muscle, dose dependent tissue distribution etc.) were also examined. The estimated differential tissue distribution and relative potency of BIL was used to predict glucose responses for BIL in long term trials in T1DM subjects.
Conclusions: A QSP model with physiological parameters that can be modulated is a useful tool to aide the understanding of the mechanisms of action of a novel therapeutic agent. Attenuated peripheral activity of BIL with approximately 3-fold lower activity than in liver and potency relative to GL of 0.06, described the clinical data well.

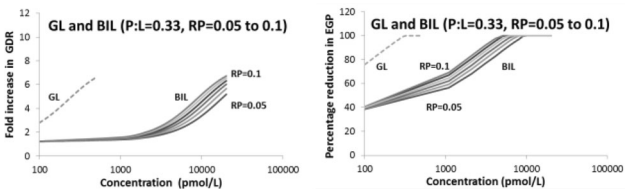

Figure 1 Basal insulin concentration vs. GDR and EGP relationships for BIL and GL in HV after 8 h of primed intravenous infusion

References

1. Kumar R et al, JPKPD, M-028, Volume 41, Issue 1 Supplement, October 2014.
2. Henry, RR et al, Diabetes. 63(Suppl 1):A226, 2014.
3. Mudaliar S et al, Diabetologia, 58: S1 2015.

T-59

Mechanistic Population Pharmacokinetics of Oseltamivir in neonates to young adult patients with normal renal function

Patanjali Ravva[1], Stefan Sturm[2], Neil John Parrott[2], Rajinder Bhardwaj[3], Barry Clinch[4], Leonid Gibiansky[5]

[1,2,3]Roche Innovation Centers: [1]New York, USA; [2]Basel, Switzerland; [3]d3 Medicine, New Jersey, USA; [4]Roche Products Ltd, Welwyn, UK; [5]QuantPharm LLC, Maryland, USA

Objectives: To develop a predictive mechanistic population pharmacokinetics (PK) model for oseltamivir (OP) and its active metabolite, oseltamivir carboxylate (OC) in term neonates and young adults (≤40 years) with normal renal function accounting for the developmental physiological changes taking place in the first 2 years after birth. Additionally, to evaluate various dosing regimens in term neonates and infants providing exposures established in adults.
Methods: The analysis included 3100 OP and 3560 OC concentrations from 436 subjects (13 trials; ages 2 weeks-40 years; post-menstrual age, PMA>38.6 weeks; weight 2.9-128 kg) following oral (346 subjects) or intravenous (90 subjects) OP. A more mechanistic PK model was developed based on previous models [1, 2] for oseltamivir by including effects such as renal maturation with post-menstrual age (PMA) on the systemic exposure of OC. Extensive model evaluations across all ages and simulations for PK bridging to adults were performed.
Results: The estimates (RSE%) of clearance for OP and OC for a typical subject (with WT ≥ 43 kg) were 197 L/hr (4.6%) and 27.4 L/hr (3.6%), respectively. Maturation of renal OC clearance CL_M was described by the Hill function of post-menstrual age (PMA) [3]: $CL_{M,AGE}=PMA^{\gamma}/(PMA_{50}^{\gamma}+PMA^{\gamma})$ with PMA_{50}=45.6 weeks (4.5%) and sigmoidicity parameters γ=2.35 (14.9%). Incorporation of hepatic maturation did not improve the model. Posthoc estimates indicated that variability of exposure in term neonates and infants administered 3 mg/kg doses was higher than in adults administered 75 mg doses, median exposure was higher, but the lowest percentiles of exposure distributions were comparable.
Conclusions: The developed model supported a dose of 3 mg/kg BID in children 0-1 years.

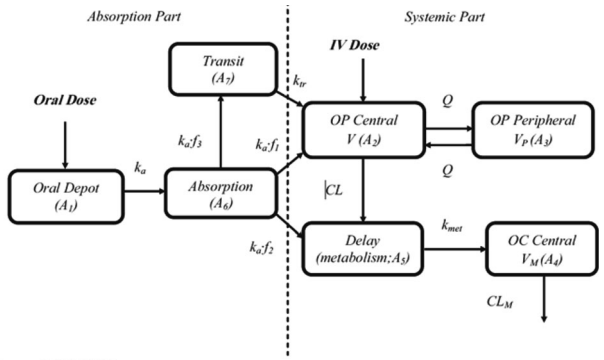

Figure 1 Schematic representation of the Oseltamivir population PK model

References

1. Gibiansky, L et al. J Pharmacokinet Pharmacodyn. (2015) 42:225–236
2. Kamal, M et al. Antimicrob Agents and Chemother. (2013) 57: 3470–3477
3. Rhodin, MM,et al. Pediatr Nephrol. (2009) 24:67–76

T-60

Population Pharmacokinetics and Pharmacodynamics (PK/PD) of Etelcalcetide for Secondary Hyperparathyroidism (sHPT) in Subjects with Chronic Kidney Disease (CKD) on Hemodialysis

Ping Chen[1], Adimoolam Narayanan[1], Benjamin Wu[1], Per Olsson Gisleskog[2], Andrew T.Chow[1], John Gibbs[1], Murad Melhem[1]

[1]Amgen Inc. [2]SGS Exprimo NV

Objectives: Etelcalcetide is a novel calcium-sensing receptor (CaSR) activator currently in development for the treatment of sHPT. The objectives of this analysis were to develop a population PK/PD model relating etelcalcetide exposure to markers of efficacy (intact PTH, iPTH) and safety (corrected serum calcium, cCa); to evaluate covariate effects on PK/PD parameters; and to perform PK-PD simulations to support intravenous TIW administration of etelcalcetide.
Methods: Plasma etelcalcetide, serum iPTH and cCa concentration-time data were collected from 5 clinical studies including phase 1, 2, and 3 clinical trials following the administration of etelcalcetide as single or multiple intravenous doses (2.5 to 60 mg). Population PK/PD modeling of etelcalcetide was performed using NONMEM 7.2. A semi-mechanistic model, implementing allosteric activation, was use

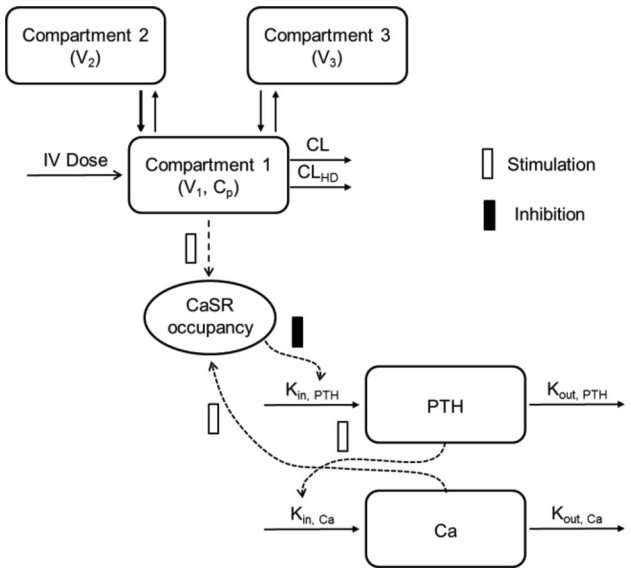

Figure 1 Semi-mechanistic PK/PD Model Structure. $K_{in,PTH}$ and $K_{out,PTH}$: the zero-order production rate of PTH and the first-order elimination rate constant for iPTH, respectively. $K_{in,Ca}$ and $K_{out,Ca}$: the zero order production rate of Ca and the first order elimination rate for Ca, respectively. C_p: the etecalcetide plasma concentration. V_1, V_2 and V_3: central compartment, shallow and deep peripheral compartments, respectively

to describe the relationship between etelcalcetide, iPTH and cCa (Figure 1). Impact of relevant covariates (weight, sex, race, age, phosphorus, time on dialysis and vitamin D) was evaluated by stepwise forward/backward selection. Model evaluation was based on standard goodness-of-fit plots and prediction-corrected visual predictive checks (pcVPC).

Results: The exposure-response profiles between etelcalcetide, iPTH and cCa were well described by the model. Estimates of the turnover half-lives of iPTH and cCa were 0.36 hr and 23 hours, respectively. The estimated cooperativity constant to 3.41 confirming allosteric activation effects of etelcalcetide on CaSR. The extent of inter-individual variability in model parameters was low to moderate (6-67%). No covariates were identified as significant predictors of PD variability. pcVPC confirmed the predictive ability of the model. Simulations suggested that the titration algorithm is needed to provide effective PTH and minimal Ca lowering.

Conclusions: The current model incorporates the major components of the PTH-Ca homeostatic system, and describes the etelcalcetide allosteric activation effects of CaSR. Dose adjustment by relevant covariates was deemed unwarranted.

T-61

Predictive Performance of Early Phase 1 Studies in Assessing Thorough QT Outcome Across 12 Compounds - Application of a Novel Analysis Method

Puneet Gaitonde[1], Yeamin Huh[1,2], Guenter Heimann[3], Jianguo Li[4], Kaifeng Lu[5], Charles Benson[6], Borje Darpo[7], Georg Ferber[8], Jim Keirns[9], Bernard Sebastien[10], Kuenhi Tsai[11], Yaning Wang[12], Meijian Zhou[7], Steve Riley[1]

[1]Pfizer Inc., [2]A2PG, [3]Novartis, [4]AstraZeneca, [5]Allergan plc, [6]Eli Lilly and Co., [7]iCardiac Technologies, [8]Statistik Georg Ferber GmbH, [9]Astellas Pharma Inc., [10]Sanofi, [11]Merck & Co., [12]US Food and Drug Administration

Background: Cardiac safety assessment is a key regulatory requirement for almost all new drugs. Thorough QT (TQT) studies are expensive and resource intensive. Efficiencies can be appreciated through use of Phase 1 single ascending dose (SAD) and multiple ascending dose (MAD) data to evaluate QT liability. Application of a standardized exposure-response methodology to quantify QT effects based on early clinical studies is demonstrated.

Methods: Twelve compounds with SAD/MAD and TQT data having time-matched drug concentrations and ECG measurements were selected. The change from baseline Fridericia-corrected QT interval (ΔQTcF) vs. drug concentration relationship was evaluated using linear mixed-effects (LME) model with known covariance structure based on the number of baseline time points. Drug concentrations and nominal time post first dose were modeled as fixed effects and subject as random effect. Heteroscedasticity was allowed across studies. Estimated slope and CIs were used to determine placebo-adjusted ΔQTcF (ΔΔQTcF) at the TQT supratherapeutic C_{max}. Predicted ΔΔQTcF was compared with TQT study results. Analyses were performed in R and SAS.

Results: A LME model appropriately described the SAD/MAD data. QTc effects < 10 msec were detected for 9 compounds and > 10 msec for 1 compound. Results were discordant for 2 compounds. Predictions for 10 of 12 compounds were consistent with TQT study outcomes. R and SAS provided similar results.

Conclusion: Application of a standardized methodology to quantify QT effects was implemented in two widely used statistical softwares. Results from exposure-response analyses of early clinical data and TQT data were generally in agreement, and consistent with and supportive of conclusions from previous prospective analyses [1].

Reference

1. Darpo B. et al., CPT 97 (4); 326-335; 2015

T-62

Population Pharmacokinetic model of trebananib in pediatric patients with relapsed solid tumors

Ramy A. Abdelrahman[1], Sarah E. S. Leary[2], Joel M. Reid[1], Charles G. Minard[3], Elizabeth Fox[4], Brenda Weigel[5]

[1]Mayo Clinic, Rochester, MN; [2]Seattle Children's Hospital, Seattle, WA; [3]Baylor College of Medicine, Houston, TX; [4]Children's Hospital of Philadelphia, Philadelphia, PA; [5]University of Minnesota, Minneapolis, MN

Objectives: Trebananib is a first-in-class peptibody (peptide-Fc fusion protein) that selectively inhibits Angiopoietin 1 and Angiopoietin 2 to inhibit interaction with the Tie2 receptor tyrosine kinase and prevent angiogenesis by a VEGF independent mechanism. The aim of this study was to develop a population pharmacokinetic (PK) model for trebananib in pediatric patients from a phase 1 trial with relapsed solid tumors.

Methods: A total of 361 trebananib plasma concentrations from 35 patients (age 2-20 years, body weight 11.7-105.6 kg) were analyzed simultaneously using nonlinear mixed-effects modeling with NONMEM and Pirana software to develop a population PK model. Trebananib was administered as a weekly 30-60 minute IV infusion. Three dose levels (10, 15 or 30 mg/kg/dose) were evaluated in a dose escalation study using a rolling-six design. Blood samples were obtained both prior to and at the end of infusion on Days 1, 8, 15 and 22. Additional samples were obtained at 2, 6-8, 24±2, 48±4, 96 ±4 and 168 hours after the drug administration on Day 22. The model was evaluated with goodness-of-fit plots and visual predictive check.

Results: A 2-compartment model with exponential interindividual variability and proportional residual error models was used to describe trebananib concentration data. Five baseline variables (weight, sex, age, serum creatinine, and dose level) were tested with forward selection ($p<0.05$) and backward elimination ($P<0.001$) approaches for their effects on CL and V1. Weight was the only significant covariates. Table 1 provides the final parameter estimates and covariate effects. GOF and VPC plots were adequate.

Table 1 Parameter estimates and bootstrap results from the final model

Parameter (Units)	Estimate (%RSE)	Bootstrap Estimate (95% CI)
CL (L/hr)	0.0723 (4%)	0.0723 (0.0664–0.0781)
Body weight effect on CL	0.526 (11%)	0.522 (0.405–0.642)
V1 (L)	2.15 (3%)	2.15 (2.02–2.29)
Body weight effect on V1	0.803 (7%)	0.803 (0.694–0.911)
Q (L/hr)	0.0635 (13%)	0.0647 (0.0501–0.0769)
V2 (L)	2.93 (15%)	2.95 (2.25–3.83)
Between Subject Variability (BSV)		
BSV CL	0.0432, %CV = 20.8%	0.0387 (0.0166–0.0643)

Table 1 continued

Parameter (Units)	Estimate (%RSE)	Bootstrap Estimate (95% CI)
BSV V1	0.0317, %CV = 17.8%	0.0293 (0.0127–0.048)
BSV Q	0.19, %CV = 43.6%	0.19 (0.0445–0.357)
BSV V2	0.449, %CV = 67%	0.433 (0.201–0.764)
Residual Unexplained Variability (RUV)		
Proportional error (RUVp)	0.0166, %CV = 12.8%	0.0165 (0.0133–0.0202)

Conclusions: A linear 2-compartment model best described the pharmacokinetics of trebananib in pediatric patients. Body weight was the only covariate included in the final model.
Supported by UM1 CA097452, P30 CA15083, and T32 GM008685.

T-63

Simplifying Data Builds for Pharmacometric Modeling: A Generalized Dataset Format Approach

Robert Fox[1], Henning Schmidt[2], Nidal Al-Huniti[1]

[1]Quantitative Clinical Pharmacology, AstraZeneca, Waltham, MA. [2]IntiQuan, 4057 Basel, Switzerland

Objectives: In the context of model-based drug development, many different pharmacometric activities need to be performed. The effort and time to construct multiple data builds to support these activities often clash with resource and time constraints. Consequently, the modelers must necessarily reduce their decision making support.
With this in mind, the objective was to develop a systematic data build approach that would support various modeling activities, eliminate the data build redundancies and minimize programming resource requirements.
Methods: A generalized and sufficiently robust dataset format was defined that could be used across projects, compounds, and indications. The format also needed to be independent of modeling activity and modeling tool. The format needed to contain a minimum level of redundancy and to include contextual variables: names for different record type, units, etc. The contextual data was considered important for rendering the subsequent datasets more understandable without additional documentation, for reducing mistakes, and for facilitating project hand-over processes.
Results: A robust modeling tool and methodology-independent (generalized) dataset format was developed. Mapping programs were written to translate the generalized format into tool-specific, methodology-specific, and data or graphical summary datasets. This approach simplified the data preparation activities, reduced resource requirements and retained previously lost information (units, names of observations, decoded values, etc.).
Conclusions: The implementation of a generalized dataset format for pharmacometric analyses allows a more systematic data preparation approach which is less resource intensive and requires far fewer iterations between data programmer and modeler. The captured information in the generalized dataset is also more complete, meaning that 1) the same generalized dataset can contain all relevant information for different analyses and modeling activities and 2) the information contained in the generalized dataset is self-explaining, compared to typical and very cryptic NONMEM datasets. Ultimately, the generalized dataset format leads to higher-quality analyses in support of pharmaceutical decision making.

T-64

A Knowledge Management Solution for Pharmacometric Analysis

Robert Fox[1], Henning Schmidt[2], Nidal Al-Huniti[1]

[1]Quantitative Clinical Pharmacology, AstraZeneca, Waltham, MA. [2]IntiQuan, 4057 Basel, Switzerland

Objectives: Providing submission deliverables in the regulated pharmaceutical industry, sharing knowledge across regions in a global environment, and effectively leveraging institutional memory demand the ability to reproduce results, ensure data/information security, and demonstrate traceability. However, pharmacometric knowledge management systems are frequently burdensome to navigate or are fractured across multiple solutions. These systems and issues jeopardize reproducibility, security and traceability, lead to potential loss of institutional memory, and can elevate the risk for regulatory noncompliance. Developing and maintaining a knowledge management system that satisfies regulatory requirements and is sufficiently nimble to facilitate utilization is the objective of this work.
Methods: We investigated several options from over-the-counter products to cloud-based solutions. We concluded that the capabilities already available in our current computing infrastructure, a Linux High Performance Cluster (HPC) would work best.
The file server (data and analysis files) and NONMEM application operate on the same Linux system minimizing network traffic and performance issues. A samba connection to our windows environment was established for easy cross-environment file access (protocols, CRF, analysis plans, etc.).

Using the Linux environment, we were able to define user roles and responsibilities (Associate, Reviewer, Approver, and Administrator). Each of these roles was granted appropriate access and read-write privileges. Naming conventions were mandated to control directory structures and to define analysis runs. Preprogrammed directory setup scripts established and ensured accuracy and consistency of directory hierarchy across projects. Analysis naming conventions, which were enforced via reviewer signoff, simplified file searches across time interruptions and across modeler handoffs. With the methods and tools in place, traceability was established from source data through analysis and modeling results.
Results: Using our established infrastructure hardware, a knowledge management system has been implemented with minimal cost. It is easy to use and maintain from both the administrator and analyst perspectives. Automated scripts and approval processes ensure compliance to regulatory requirements.
Conclusions: A validated knowledge management system balanced for utilization and regulatory compliance is possible.

T-65

A mechanistic target-mediated drug disposition model to select an optimal biweekly dosing regimen for GC1118, a novel monoclonal antibody against the epidermal growth factor receptor

Sang-In Park[1], Keun-Wook Lee[1], Do-Youn Oh[1], Sae-Won Han[1], Jin Won Kim[1], Jung-Won Shin[1], Seong-Jin Jo[1], Na Hyung Kim[2], Ahmi Woo[2], Jonghwa Won[2,3], Seokyung Hahn[1], Woo Ho Kim[1], Yung-Jue Bang[1], Howard Lee[1]

[1]Seoul National University College of Medicine, Seoul, Korea; [2]Green Cross Corp., Yongin, Korea; [3]Mogam Institute for Biomedical Research, Yongin, Korea

Objectives: To develop a mechanistic population pharmacokinetic (PK) model of GC1118, a novel monoclonal antibody inhibiting the epithelial growth factor receptor (EGFR), using concentration-time data obtained from the clinical trial with GC1118 after repeated once-weekly intravenous administration and to select an optimal biweekly dosing regimen based on the model for further clinical development.
Methods: GC1118 was intravenously infused over 2 hours once weekly for four consecutive weeks at 0.3-5.0 mg/kg. Serial blood samples for PK analysis were collected up to 504 hours after the last dose of GC1118. A mechanistic target mediated drug disposition (TMDD) model was developed using NONMEM (version 7.3, ICON Development Solutions, Hanover, MD, USA), and qualified by visual predictive checks. The final population PK model was used to simulate concentration-time data for various biweekly dosing regimens to choose from one for further development in the second part of the FIH study with GC1118.
Results: A total of 22 patients with advanced solid tumors completed the PK study. A mechanistic TMDD model adequately described the observed concentration-time data of GC1118. Based on a series of simulation experiments using the final PK model, a loading dose of 12.0 mg/kg followed by a biweekly maintenance dose of 8.0 mg/kg was expected to yield a trough concentration comparable to that seen after once weekly administration at 4.0 mg/kg, a recommended phase 2 dose. Furthermore, the maximum concentration after this biweekly dosing regimen was anticipated not to exceed that noted in patients experiencing dose limiting toxicities after receiving 5.0 mg/kg once-weekly regimen.
Conclusions: A mechanistic TMDD model of GC1118 was adequately developed and used successfully to select an optimal biweekly dosing regimen for further development.

T-66

Application of Population Pharmacokinetics/Pharmaco-dynamics (PopPK-PD) for Selection of Optimal Dose of Amiselimod

Shinsuke Inoue[1], Pascal Chanu[2], Mathilde Marchand[3], François Mercier[2], Himanshu Naik[4], Atsuhiro Kawaguchi[1]

[1]Mitsubishi Tanabe Pharma Corporation; [2]Pharsight Consulting Services, now with Genentech/Roche; [3]Certara Strategic Consulting; [4]Biogen, Inc.

Objectives: Amiselimod is an oral selective S1P receptor modulator currently being developed for the treatment of various autoimmune diseases, which prevents S1P receptor-dependent lymphocyte egress leading to subsequent decrease in peripheral lymphocyte count. The objective of the analysis is to characterise the pharmacokinetics and pharmacodynamics of amiselimod's active metabolite, amiselimod-P, using population PK and PK-PD models models and to use the models to guide selection of doses for future studies.
Methods: PK and PD data obtained from three Phase1 studies (dose range from 0.125 to 4 mg) were analysed using NONMEM 7.2 PK model development started with a 2-compartment model based on PK profile. Covariate analysis was performed. Relationship between amiselimod-P plasma concentration and lymphocyte count was evaluated using an indirect response model accounting for circadian rhythm. The final PK and PK-PD models were used to simulate the lymphocyte count at steady state. The uncertainty associated with each typical parameter was taken into account along with individual and residual error using Trial Simulator^{TM} for simulations.
Results: The amiselimod-P concentration vs time profiles were best described by a 2-compartment model with parallel zero- and first-order absorption and body weight allometric scaling on volumes and clearances. The PK-PD model consisted of an indirect response model which inhibits lymphocyte production mediated by a Hill-Emax relationship driven by amiselimod-P concentrations. Circardian changes were modeled using a cosine function impacting baseline lymphocyte count (estimated parameter as below). Simulation conducted with the final PK-PD model predicted average 65% reduction in lymphocyte count with 0.4 mg dose of amiselimod at steady state relative to placebo.

Parameter	Estimate
Base (10^9/L)	2.06
K_{out} (/h)	0.285
Logit-E_{max}	4.33
IC_{50} (ng/mL)	3.16
Hill	1.19
Amplitude (%)	14.2
Shift (h)	10.2
IIV Base	0.0272 (16%)
IIV IC_{50}	0.144 (38%)
Additive residual (SD, 10^9/L)	0.098 (0.31)
Proportional residual (SD)	0.135 (14%)

Note: Base ly,phocyte levels at baseline; K_{out}, rate of disappearance; Logit-E_{max}, logit-transformed maximum inhibition; IC_{50}, concentration required to achieve half the maximum inhibition; Amplitude, amplitude of circadian rhythm; Shift, shift of circadian rhythm; IIV, inter-individual variability expressed as variance estimates and (CV%)

Conclusions: The relationship between amiselimod-P concentration and lymphocyte count was well described by an indirect response model. Considering lymphocyte count as biomarker, the dose of 0.4 mg of amiselimod is expected to show clinical efficacy for various autoimmune diseases, in light of results obtained with other S1P receptor modulators.

T-67

Physiologically Based Pharmacokinetic Modeling of Metformin and Prediction of Pharmacokinetics in Geriatric Population

Su-jin Rhee[1], Hyewon Chung[1], SoJeong Yi[2], Kyung-Sang Yu[1], Jae-Yong Chung[3]

[1]Department of Clinical Pharmacology and Therapeutics, Seoul National University College of Medicine and Hospital, Seoul, Korea; [2]Division of Clinical Pharmacology 3, OCP, CDER, FDA, Silver Spring, MD, USA; [3]Department of Clinical Pharmacology and Therapeutics, Seoul National University College of Medicine and Bundang Hospital, Seongnam, Korea

Objectives: Developing and validating geriatric PBPK models shall enrich our knowledge about their limitations and lead to a better use of the generated data. This study was conducted to investigate how PBPK models describe the pharmacokinetics of metformin in geriatric population.
Methods: A first-order absorption/PBPK model for metformin was built in the Simcyp simulator version 14 release 1 (Certara USA, Inc., Princeton, USA). Full PBPK model was constructed for metformin based on physicochemical properties and clinical observations. The model was refined and validated across several different dose levels using clinical plasma concentration data obtained in healthy adults aged 20-45 years following single oral administrations of metformin. Following appropriate optimization of the metformin PBPK model, geriatric (65-85 years) pharmacokinetics was predicted using Simcyp geriatric module. The predicted T_{max}, C_{max}, AUC, and CL/F were then compared with geriatric clinical data obtained in healthy elderly subjects.
Results: The metformin pharmacokinetic profiles obtained from PBPK model were comparable to the observed clinical plasma concentration data for healthy adults aged 20–45 years. Geriatric PBPK model reasonably predicted the CL/F of metformin in elderly population. The predicted T_{max}, C_{max}, AUC, and CL/F values were within 1.5-fold of the observed data of metformin.
Conclusions: The geriatric PBPK model of metformin adequately characterized the pharmacokinetics of metformin in elderly population. PBPK modeling and simulation might be used as a powerful tool to guide geriatric clinical trial design.

T-68

Population Pharmacokinetics and Pharmacodynamics of Sorafenib in Acute Myelogenous/B-Type Leukemia Patients

Tao Liu[1], Philip Sabato[1], Vijay Ivaturi[1], John J. Wright[2], Jacqueline M. Greer[3], Keith W. Pratz[3], B. Douglas Smith[3], Michelle A. Rudek[3]

[1]Center for Translational Medicine, University of Maryland Baltimore [2]National Cancer Institute, Investigational Drug Branch, Bethesda, MD [3]The Sindey Kimmel Comprehensive Cancer Center at Johns Hopkins, Baltimore, MD

Objectives: To characterize the pharmacokinetics and pharmacodynamics of sorafenib in patients with Acute Myelogenous Leukemia (AML) and to optimize the dosing regimen in further clinical trials.
Methods: Sorafenib and its N-oxide metabolite plasma concentration and FLT3/ERK activity from 15 patients with leukemia given 400mg or 600mg BID oral administration of sorafenib were analyzed using sequential PKPD approach in Phoenix NLME v1.4. Sorafenib structural PK model was adopted from a previous publication. Bound and unbound plasma concentrations were modeled simultaneously using an unbound fraction parameter. A one-compartment model of the N-oxide metabolite was added to the parent drug model. The relationship between sorafenib exposure and FLT3/ERK activities were described by Emax model. Different dosing regimens (200mg BID and 400mg BID) were simulated based on the PK/PD relationship.
Results: A one-compartment model with transit absorption compartment and enterohepatic recirculation successfully described the PK profile in leukemia patients. Body weight was modeled as a covariate on both volume of distribution and clearance using an Allometric scaling approach. Sorafenib could inhibit FLT3 activity by 100% with an IC_{50} of 133.7ng/mL and ERK activity by 90% with an IC_{50} of 169.6ng/mL.
Conclusions: 200mg BID dosing regimen showed similar FLT3 and ERK inhibitory activity at steady state compared to 400mg BID which is the approved dose for patients with hepatocellular carcinoma or renal cell carcinoma.

References

1. Jain L, et al. Br J Clin Pharmacol 72:2 /294–305
2. Villarroel MC, et al. Invest New Drugs 30:6 /2096-102

T-69

Predicting the safety and efficacy of inhibition of diacylglycerol transferase 2 for the treatment of non-alcoholic fatty liver disease

Theodore Rieger[1], Scott Siler[2], Grant Generaux[2], Brett Howell[2], Richard Allen[1], Cynthia Musante[1]

[1]Cardiovascular and Metabolic Research Unit, Pfizer Inc, Cambridge, MA; [2]DILIsym Services Inc., Research Triangle Park, NC

Objective: With no effective treatment, non-alcoholic fatty liver disease (NAFLD) decreases patient quality of life and leads to increased healthcare costs. Here we assess the efficacy and safety of a novel approach to reversing hepatic steatosis, inhibition of diacylglycerol transferase 2 (DGAT2). We utilized a systems pharmacology approach to test if we should expect a better clinical benefit for NAFLD from DGAT2 inhibitors versus their metabolic "next-door neighbors" in VLDL synthesis: microsomal triglyceride transfer protein (MTP) inhibitors. While MTP inhibitors have previously been reported to cause lipotoxicity in the liver (1), preclinical data indicate that DGAT2i may not (2).
Methods: We utilized DILIsym, a systems pharmacology model of liver metabolism to represent NAFLD pathophysiology, including liver triglyceride synthesis, storage, and release as VLDL and effects of lipotoxicity on hepatocellular health (3). We simulated MTP and DGAT2 inhibition to differentiate their effects on liver TG and hepatocellular apoptosis. We tested the pharmacodynamics of the DGAT2 inhibitor with and without reported gene expression changes in fatty acid synthesis, esterification, and oxidation (2).
Results: In contrast to the MTP inhibitor, the DGAT2 inhibitor was predicted to reduce liver triglycerides (up to 90%), without exacerbating lipotoxicity. MTP, however, elicited increases in liver TG and lipotoxicity. Performing a sensitivity analysis on the pharmacodynamics of the DGAT2 inhibitor demonstrated that adaptations by fatty acid uptake pathway were the most important to minimize lipotoxicity.
Conclusions: A systems pharmacology model has provided insight into DGAT2 inhibition as a strategy for the treatment of NAFLD and established its differentiation from the failed MTP inhibitors. However, the predicted patient response is sensitive to critical adaptive responses and should be verified in follow-on studies.

References

1. Cuchel M et al. NEJM. 2007.
2. Choi CS, et al. JBC. 2007.
3. Siler SQ. Drug Discov. & Toxicol. Pgs. 114 - 117. 2016.

T-70

Population Pharmacokinetics for Atezolizumab in Cancer Patients

Mathilde Marchand[2], Helen Winter[1], Laurent Claret[2], Rene Bruno[2], Steve Eppler[1], Jane Ruppel[1], Jin Jin[1], Sandhya Girish[1], Mark Stroh[1]

[1]Genentech, South San Francisco, CA, USA; [2]Certara Strategic Consulting, Marseille, France

Objectives: Atezolizumab, a humanized immunoglobulin G1 (IgG1) monoclonal antibody that targets human programmed death-ligand 1 (PD-L1) on tumor cells and immune cells, was recently approved in the US in bladder cancer and is being developed to treat patients with various solid tumors. The aim of the analysis was to characterize atezolizumab pharmacokinetics (PK) and evaluate impact of clinically relevant covariates on atezolizumab pharmacokinetics.
Methods: The PK of atezolizumab in serum was evaluated in 472 PK evaluable patients with 4563 samples from the two Phase I studies (PCD4989g and JO28944) who received 1 to 20 mg/kg of atezolizumab every 3 weeks (q3w) single agent, or the fixed 1200 mg dose q3w. NONMEM was used for pharmacokinetic analysis. The impact of about 20 covariates (i.e. body size, gender, disease characteristics, organ function markers) on the PK of atezolizumab was investigated. Covariates were selected using forward addition followed by backward elimination method.
Results: Atezolizumab exhibited linear pharmacokinetics over a dose range of 1 – 20 mg/kg, including the 1200 mg dose. The population clearance (CL), volume of distribution (V1), and terminal half-life estimates of 0.200 L/day, 6.91 L, and 27 days, respectively, were consistent with expectations for an IgG1. Body weight was identified as a statistically significant covariate on both CL and V1. In patients who were positive for anti-therapeutic antibodies (ATA), CL was estimated to be 16% higher than in patients with negative ATA. Albumin and tumor burden were also identified as statistically significant covariates on CL. In females, V1 and V2 would be 13% and 27% lower than in males, respectively. No covariate effect resulted in more than 32% change in exposure (i.e., AUCss) from the typical patient receiving 1200 mg q3w.
Conclusions: A population PK model was developed for atezolizumab in cancer patients. Covariates had minimal impact on steady-state exposure. The data support the recommended 1200 mg fixed dose q3w for all patients.

T-71

Population Pharmacokinetic (PK)/Pharmacodynamic (PD) Modeling and Simulation for ASP5094, an Anti-alpha-9-integrin Monoclonal Antibody in a First-in-Human Trial

Tianli Wang and Robert Townsend

Astellas Pharma Global Development, Inc. Northbrook, IL, USA

Objectives: To develop a population PK/PD model that describes the time course of ASP5094 serum concentration and quantitatively evaluates the relationship between PK and receptor occupancy (RO) of alpha-9 integrin on neutrophils (PD) in human peripheral blood using data from the single-ascending-dose study. ASP5094 is a recombinant humanized anti-alpha-9 integrin IgG1 monoclonal antibody (mAb) under development for the treatment of rheumatoid arthritis.
Methods: A nonlinear mixed-effects population model was developed to describe the PK of ASP5094 in healthy subjects. The relationship between PK and alpha-9 integrin RO in neutrophil was also explored. Data were modeled using NONMEM 7.3.
Results: ASP5094 PK can be adequately described by a two-compartment model with saturable elimination described by Michaelis-Menten kinetics. The relationship between plasma concentration and RO was analyzed with a direct-response Sigmoidal Emax model since no significant evidence of hysteresis was demonstrated. PK and PD model parameters are shown in the table. The linear clearance (CL(linear)) and volumes of distribution (Vc and Vp) estimates of ASP5094 were similar to those reported in literature for mAbs [1]. PK profiles after once every 28 days dosing were simulated to support a multiple-ascending-dose study. Full RO was predicted to be achieved for 3 months after 3 mg/kg once every 28 days dosing and for 4 months after 10 mg/kg once every 28 days dosing.
Conclusions: ASP5094 PK exhibited nonlinear target-mediated drug disposition. The developed population PK and PK/PD models will be utilized to determine an optimal dosing regimen for multiple dose administration.

Table 1 Parameter Estimates of ASP5094 PK and PK/PD Models

Parameter	Estimate (%CV)	Inter-Individual Variability
CL (linear) (L/h/kg)	0.000121 (14.1%)	48.4%
Vc (L/kg)	0.0451 (fixed)	17.9%
Vp (L/kg)	0.0313 (11.8%)	–
Q (L/h/kg)	0.000249 (7.0%)	–
Vmax (μg/h/kg)	1.99 (11.4%)	18.5%
Km (ng/mL)	252 (22.7%)	–
Baseline (%)	9.8 (15.1%)	8.97 (additive)
EC50 (ng/mL)	23.3 (30.9%)	–
Emax (%)	82.5 (3.1%)	19.3%
Hill coefficient	0.781 (19.8%)	–

Reference

1. N Dirks and B Meibohm, Clin Pharmacokinet 2010; 49(10):633-659

T-72

Network-Based Analysis of Pharmacodynamic Heterogeneity in Multiple Myeloma Cells

Vidya Ramakrishnan and Donald E. Mager

Department of Pharmaceutical Sciences, University at Buffalo, SUNY

Objectives: The purpose of this study is to develop a Boolean logic-based network representing important intracellular signaling pathways regulating cell growth, proliferation, and apoptosis in multiple myeloma (MM) to explain differences in pharmacodynamic sensitivities of MM cell lines to bortezomib exposure.
Methods: A genetically diverse panel of four MM cell lines were chosen: U266, RPMI8226, MM.1S, and NCI-H929. Concentration-effect (CE) and cell proliferation dynamics (CPD) were obtained by treating cells with bortezomib (0.01–100 nM for CE study; 2, 4, 10, and 20 nM for CPD study) and measuring viable cells using the WST-

1 assay. Data from the CE study were modeled using a standard inhibitory Emax function. A network model, built by extensive literature review, was implemented using Odefy (MATLAB® compatible toolbox), and used to simulate dynamic profiles. A model reduction algorithm identified critical system proteins, and the expression time-course of these proteins were measured in control (untreated) and bortezomib (2 and 20 nM) treated MM.1S, RPMI8226, and NCI-H929 cells using the MAGPIX® multiplex platform. Finally, a cellular pharmacodynamic model of bortezomib in RPMI8226 cells was developed.

Results: The CE study identified MM.1S as most sensitive to bortezomib, with estimated IC_{50} values of 2.28, 3.60, 4.71, and 4.75 nM for MM.1S, NCI-H929, RPMI8226, and U266 cells at 24 h. The CPD study also classified cell lines as more sensitive (MM.1S, NCI-H929) and less sensitive (RPMI8226, U266) to bortezomib based on time to complete cell death. The more sensitive cell lines exhibited protein dynamic profiles with relatively greater expression and earlier onset of intracellular signaling activation. The final cellular pharmacodynamic model, driven by RPMI8226 intracellular protein dynamics, adequately described *in vitro* cell death.

Conclusions: Selected cell lines were significantly different in their responses to bortezomib. The magnitude of relative expression of intracellular proteins was associated with bortezomib sensitivity in these MM cells. The cellular pharmacodynamic model for RPMI8226 will be extended to describe xenograft tumor dynamics using intracellular signaling as a tool to translate across experimental systems.

T-73

Population Pharmacodynamic and Markov Modeling Approach for Clinical Trial Outcome Predictions in Anti-obesity Drug Development

Vishnu Sharma[1], Francois Combes[1], Majid Vakilynejad[2], Gezim Lahu[2], Lawrence J. Lesko[1], Mirjam N. Trame[1]

[1]Centre for Pharmacometrics & Systems Pharmacology, University of Florida, Orlando, FL; [2]Takeda Pharmaceuticals International GmbH, Zurich/Chicago

Objectives: Development of anti-obesity drugs is continually challenged by high dropout rates during clinical trials [1]. The objective of this analysis was (i) to develop a population pharmacodynamic (PopPD) model to describe time-courses of bodyweight (BW) changes, accounting for disease progression (DP), lifestyle intervention (LSI) and drug effects; and (ii) to predict, using a Markov Model (MM), Responder (R), Non-responder (NR) and Dropout (D) rates during clinical trials based on longitudinal % BW changes.

Methods: Subjects (n=4591) from 6 Contrave® trials were included in this analysis. An indirect-response model, developed by van Wart et al. [2] was used as a starting point. Inclusion of drug effect was dose driven using a Kinetic-Pharmacodynamic (KPD) model. Additionally, a Population-PK Parameters and Data (PPPD) model was developed using the final KPD model structure and final parameter estimates from a Pharmacokinetic (PK) model based on available Contrave® PK concentrations. Lastly, MM was developed to predict transition rate probabilities between R, NR and D states driven by the PD effect resulting from the KPD or PPPD model.

Results: The developed KPD and PPPD models described the BW changes over time adequately well. Some of the covariates included in the models were diabetes (on K_{out}, K_{pro}, BW, and E_{max}) and race (on LSI). The linked KPD-MM and PPPD-MM models were able to predict transition rates between R, NR and D states well. The PPPD-MM model had slightly better predictions as compared to KPD-MM model.

Conclusions: In this study, BW change is an important factor influencing dropout rates and the MM model has depicted that overall a KPD model driven approach is as good in predicting clinical trial outcome probabilities as a PK driven approach such as the evaluated PPPD model.

References

1. Gadde KM. Expert Opin Pharmacother. 2014; 15(6):809–22.
2. Van Wart S, et al. ACOP, 2011, San Diego, CA, USA

T-74

Use of a Model Based Approach for Evaluation of partial Area Under the Curve for Bioequivalence Assessment of Methylphenidate Transdermal products

Vittal Shivva[1], Lanyan Fang[1*], Xiaoyan Yang[1], Nan Zheng[2], Hao Zhu[2], Sam G Raney[1], Liang Zhao[1]

[1]Office of Research and Standards, OGD, CDER, FDA; [2]Office of Clinical Pharmacology, OTS, CDER, FDA

Objectives: To evaluate the value of additional bioequivalence (BE) metrics for Methylphenidate (MPH) transdermal products using a model based approach.

Methods: Methylphenidate is a central nervous system stimulant used in the treatment of attention-deficit hyperactivity disorder in children. A population pharmacokinetic (PK) model was developed for MPH transdermal products using internally available datasets from Abbreviated New Drug Applications (ANDAs). This population PK model was linked to the previously published pharmacodynamic (PD) model [1] to study the impact of formulation changes on PK and PD (SKAMP-Composite score). Several clinically plausible PK profiles corresponding to potential formulation changes of MPH patch were simulated and were subsequently explored to study the impact on predicted PD response. One thousand cross-over BE studies were simulated for two hypothetical test formulations (change in lag time for release/absorption and change in rate of absorption) to detect the power of various BE metrics (such as AUC, C_{max} and partial AUCs) in detecting clinically meaningful PK differences associated with formulation changes.

Results: PK of MPH following patch application was best described by a one-compartment model with zero-order input and first-order elimination. PK model linked to the PD model that describes time-dependent placebo effects and a direct effects E_{max} model for drug induced response. For practical purpose, clinically meaningful PK differences associated with formulation changes are defined as PK changes that resulted in greater than 20% difference in the predicted PD response, at clinically relevant time windows. Clinical trial simulations showed that partial $AUC_{2\text{-}9h}$ was the most sensitive metric that could detect clinically relevant and meaningful PK differences with formulations changes.

Conclusions: A strong PKPD correlation has been well documented in literature for all MPH products. Since PD is highly correlated with MPH concentrations, PK profile similarity is recommended in evaluation of ANDAs of MPH patch. This work supports recommendation of $pAUC_{2\text{-}9h}$ as an additional evaluation metric to ensure BE and therapeutic equivalence among formulations of MPH patch products.

Reference

1. Kimko H et al., J Pharmacokinet Pharmacodyn. 2012, 39(2):161-76

T-75

Improving priors for human mAb linear PK parameters by using half-lives from pre-clinical species

Vittal Shivva[1*], Philip J Lowe[2], Martin Fink[2]

[1]University of Otago, Dunedin, New Zealand; [2]Novartis Pharma AG, Basel, Switzerland

Objectives: Obtaining a good prior for the linear pharmacokinetic (PK) parameters of new monoclonal antibodies (mAb) is essential for designing first-in-man (FIM) studies but also for stabilising the fitting of non-linear target-mediated disposition observed in these studies.
Methods: FIM studies for five mAbs were fitted with a 2 compartment PK model, both separately and together using a simple pool, a model with a 3rd hierarchical random effects ($LEVEL, NM7.3+) and one with non-human-primate (NHP) half-lives as a covariate for between mAb differences. Two other mAbs with slightly nonlinear PK were included for comparison.
Results: There was good agreement between compounds for the central volume (reflecting the rapidly accessible plasma volume V_p of 2.9L for 70kg human), but the tissue volume (V_{ti}) and clearance (CL) differed substantially, leading to terminal half-lives ranging from 15 to 28 days (plausibly reflecting differences in FcRn binding, charge distribution, glycosylation, etc. [1,2]). Inter-compartmental flow estimates were variable but mostly had lower precision. One of the two nonlinear compounds showed, despite similar typical parameter values, greater inter-individual variability (IIV) in V_{ti} (44 %CV) whereas the other showed much larger CL, V_p and V_{ti}, perhaps due to rapid binding to readily available membrane-bound receptors. The simple pool of human studies (similar to [3]) gave larger IIV estimates (CL - 32 %CV, V_{ti} - 33 %CV) than separate fits (CL 13-26 %CV, V_{ti} 15-35 %CV). The pool using a 3rd hierarchical random effects and adding drug specific covariates gave IIV estimates close to those of the separate fits (CL - 24 %CV, V_{ti} - 16 %CV). The between-mAb differences were predictable using body weights and terminal half-life estimates from NHP.
Conclusions: Ignoring inter-mAb variation leads to inflated estimates of IIV. However, by using just body weights and terminal half-life estimates from NHP data one can account for between-mAb-differences and thus provide non-inflated priors for the linear PK parameters of new mAbs.

References

1. Suzuki et al., J Immunol. 2010; 184(4):1968-76.
2. Datta-Mannan et al., MAbs. 2015; 7(6):1084-93.
3. Davda et al., MAbs. 2014; 6(4):1094-102.

This work was previously presented (as oral presentation) at the Population Approach Group Europe (PAGE) 2016 meeting being held at Lisbon, Portugal during June 7th-10th 2016 (http://www.page-meeting.org/default.asp?abstract=5736).

T-76

Best Statistical Practices for Concentration-QT Modeling: Quality Assessment of ECG Data, Model Sensitivity, Specificity and Evaluation

Winnie Weng, Lu Wang, Cara Nelson, Srini Ramanathan, Liang Fang

Gilead Sciences, Foster City, CA

Objectives: Concentration-QT (c-QT) modeling of early phase ECG data is recognized as a viable alternative to thorough-QT (TQT) study for assessing QT/QTc-interval prolongation. However, multiple statistical characteristics have to be assessed before reliable modeling results can be produced. Herein, we develop a comprehensive set of statistical methods to assess modeling characteristics such as, model fitting, robustness of results to assumption violations, sensitivity and specificity of the modeling approach in detecting QT/QTc-interval prolongation. Statistical methods are also developed to address issues related to the lack of positive control arm.
Methods: ECG data quality is assessed using variance component and variability analysis. Variability statistics are compared to those in TQT studies. The sensitivity and specificity of c-QT modeling approach are confirmed by Monte Carlo simulation studies. Goodness-of-fitting is evaluated by AIC parameter and diagnostic plots. Model robustness is assessed through sensitivity analyses with alternative model structure and independent variable terms.
Results: Through rigorous statistical testing, ECG data quality is confirmed to be comparable with TQT standard. Adequate model sensitivity and specificity assures ability of the method to detect true positive or negative QT prolongation. Consistent QT-RR relation validates selection of dependent variable. Goodness and robustness of model fitting ensures excellence of final model, providing a concrete foundation to conclude the c-QT relationship. This set of statistical methodology was successfully applied to c-QT of 3 different investigational compounds to monitor data quality and to ensure correctness of model fitting. One compound was granted TQT waivers from US FDA and EMA based on c-QT analysis [1]. Waiver submission for the other two compounds is ongoing.
Conclusions: With a thorough evaluation of model characteristics, reliable and robust results can be produced using c-QT modeling approach, as a viable alternative to TQT for QT/QTc prolongation assessment. Lack of positive control in early phase studies can be addressed by the proposed statistical analyses.

Reference

1. Nelson CH, et al. Clin Pharmacol Ther. 2015 Dec; 98(6):630-8

T-77

Exploring maternal-infant linked influenza antibody kinetics using a unified population model

Xiaoxi Liu[1], Casey Tak[2], Catherine M.T. Sherwin[1], Julie H. Shakib[3]

[1]Division of Clinical Pharmacology, Department of Pediatrics, School of Medicine, University of Utah, Salt Lake City, Utah; [2]Pharmacotherapy Outcomes Research Center, Department of Pharmacotherapy, College of Pharmacy, University of Utah, Salt Lake City, Utah; [3]Division of General Pediatrics, Department of Pediatrics, School of Medicine, University of Utah, Salt Lake City, Utah

Objective: Inactivated influenza vaccine is recommended during pregnancy to provide passive immunity against influenza to the infant. However, the kinetics of transplacentally acquired immunity have not been assessed in a comprehensive quantitative manner. Our objectives were to 1) develop a physiological model that describes the effects of vaccination in increasing maternal influenza antibody levels; 2) model infant influenza antibody kinetics and evaluate the influence of maternal vaccination; 3) develop a unified maternal-infant physiological model that simultaneously describes influenza antibody transfer and the effects of maternal immunization.
Methods: Pregnant women 18 – 45 years of age were enrolled from 01/2012 through 05/2014 (three influenza seasons) from University of Utah Health obstetric clinics. Antibody data from the A/California

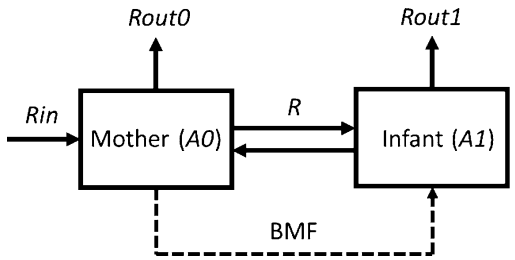

Figure 1 Model structure of maternal/infant influenza antibody level association. *A0*: maternal antibody level; *A1*: infant antibody level; *Rin*: rate of maternal antibody generation; *Rout0*: rate of maternal antibody decay; *Rout1*: rate of infant antibody decay; *R*: transplacentally antibody exchange ratio; BMF: breast milk feeding influence

strain (01/2012 – 05/2014) was analyzed. Infant serum samples were collected at delivery, and 2 and 6 months of age. Influenza antibody levels were determined by hemagglutination inhibition (HAI) assay. Population models were developed using NONMEM 7.3 (ICON Development Solutions, Ellicott City, MD, USA). Demographic characteristics including birth weight, gestational age, sex and ethnicity, together with maternal vaccination status (yes=1, no=0), were evaluated as potential covariates. Covariate screening was conducted in a stepwise (forward inclusion, $p<0.05$; backward elimination, $p<0.01$) manner using PsN modules.

Results: A total of 70 pairs of mother/infant subjects were included in analysis. Infant subjects had a median (5^{th} - 95^{th} quantiles) gestational age of 39.3 (38 – 41) weeks, birth weight of 3240 (2760 – 3903) grams. 60% (42/70) of infants were male and 31% (22/70) were Hispanic/Latino. Maternal antibody kinetics and vaccination influence were best described by a one-compartment model with constant rate generation (*Rin*) and first-order elimination (*Rout0*). The initial antibody amount was parameterized with a log normally distributed parameter *A0*. The vaccine effect was parameterized by an amplification factor (*VAC*) that immediately increases *A0* upon vaccination. The parameter estimates were as follows: *A0*, 9.2 (95% CI: 6.7 – 11.6) titer; *Rout0*, 0.005 (95% CI: 0.001 – 0.01) day^{-1}; *VAC*, 2.7 (95% CI: 1.9 – 3.6). Infant immunity kinetics were best described by a one-compartment model with first order elimination. The model was parameterized with the initial antibody level at delivery (*A1*) and the elimination rate (*Rout1*). The parameter estimates were as follows: *A1*, 48.9 (95% CI: 24.6 – 73.2) titer; *Rout1*, 0.018 (95% CI: 0.016 – 0.021) day^{-1}. Vaccination status was detected as a significant covariate on *A0* ($p<0.005$), while the incorporation of other covariates did not improve model fitting significantly.

Conclusions: Maternal influenza antibody kinetics were described by a one-compartment model with constant rate generation and first-order elimination. Infant influenza antibody kinetics were described by a one-compartment model with first-order elimination. Maternal vaccination significantly increased infant influenza antibody levels at delivery. Future analyses will link the infant and maternal models and evaluate the impact of breast feeding on infant influenza immunity.

T-78

A population Pharmacokinetic Analysis of Telaprevir in Healthy Korean and Japanese Subjects

Yewon Choi, MD[1], Seonghae Yoon, MD, PhD[1], SeungHwan Lee, MD, PhD[1], Kyung-Sang Yu, MD, PhD[1], In-Jin Jang, MD, PhD[1]

[1]Department of Clinical Pharmacology and Therapeutics, Seoul National University College of Medicine and Hospital, Seoul, Korea

Objectives: Telaprevir is a reversible selective inhibitor of viral protease and a potential blocker of viral replication, which is indicated for treatment of hepatitis C virus genotype 1 infection. The purpose of this study was to develop a population pharmacokinetic (PK) model of telaprevir in healthy Korean and Japanese subjects and to compare the PK characteristics between the two ethnic groups.

Methods: A population PK analysis was performed using 936 telaprevir concentrations in 42 subjects (24 Koreans and 18 Japanese), who received 500, 750 or 1250 mg of single-dose oral telaprevir in fasted state or 750 mg of multiple-dose oral telaprevir in fed state. Plasma concentrations of telaprevir were analysed using nonlinear mixed-effect modelling in NONMEM (ver 7.3). The first-order conditional estimation (FOCE) with interaction method was used to fit the plasma concentration-time data. Standard goodness-of-fit (GOF) diagnostics and visual predictive checks were used to evaluate the adequacy of the model fit and predictions.

Results: A one-compartment model using first-order absorption with lag time and proportional residual error best described the data. The typical population estimates of the apparent clearance (CL/F), volume of distribution (Vd/F), the absorption rate constant (Ka) and the lag time of absorption were 318 L/h, 789 L, 0.13 h^{-1} and 0.21 h respectively. The inter-individual variabilities were 9.1 % for the CL/F and 11.3 % for the Vd/F. Food intake significantly increased Ka and relative bioavailability by 1.34- and 4.50-fold. Ethnicity had no statistically significant effect on the PK parameters. Model evaluation by GOF plot and VPCs indicated that the proposed model adequately described the data.

Conclusions: The population PK model for oral telaprevir was developed in healthy Korean and Japanese subjects, and the population PK parameters of telaprevir were not different between two ethnic groups.

T-79

Population pharmacokinetic modeling of gentamicin in pediatric patients and assessment of age influence

Yuhuan Wang[1], Xiaoxi Liu[1], E Kent Korgenski[2], Catherine M.T. Sherwin[1]

[1]Division of Clinical Pharmacology, Department of Pediatrics, School of Medicine, University of Utah, Salt Lake City, Utah, United States; [2] Intermountain Healthcare, Pediatric Clinical Program, Salt Lake City, Utah, United States

Objectives: The population pharmacokinetics (popPK) of gentamicin in pediatric patients have previously been investigated in several relatively small cohorts. Such small studies are prone to be underpowered and sometimes fail to detect clinically relevant covariates. Separate studies of specific age group (or age groups with unbalanced sample size) have evaluated the influences of potential covariates such as body weight, age, sex, creatinine clearance, etc. However, published popPK models vary significantly in model structure, covariate selection, and covariate - parameter relationship. This study aims to investigate the popPK of gentamicin in a large pediatric cohort that is well balanced in age groups. We also aim to develop a unified population model that systemically describes the gentamicin PK and covariate structure across all age groups.

Methods: The gentamicin concentration-time data and clinically relevant covariates were retrieved from the Enterprise Data Warehouse (EDW) maintained by Intermountain Healthcare (IH). Pediatric patients (from birth to 18 years of age) from January 2006 to December 2014 received intravenous gentamicin ($\geq$2 doses). A population PK model was developed using NONMEM® version 7.3.0 (ICON Development Solutions, Ellicott City, MD, USA).

Patient covariates examined included body weight, height, sex, age, race, ethnicity, serum creatinine, and creatinine clearance (calculated using Modified Schwartz method). Patients were categorized as: neonates (AGEG1, <28 days, n=1507), infants (AGEG2, 28 days to 23 months, n=1309), children (AGEG3, 2 to 11 years, n=899), and adolescents (AGEG4, 12 to 18 years, n=760). The stepwise covariate search (forward addition $p<0.05$, backward elimination $p<0.01$) was performed to identify the potential impacts of covariates on the PK of gentamicin.

Results: A total of 4812 observations from 4475 pediatric patients were included with mean (5^{th} - 95^{th} quantiles) body weight of 16.04 kg (4.05-68 kg) and creatinine clearance of 96.80 mL/min/1.73 m^2 (81.67-208.89 mL/min/1.73 m^2). The gentamicin PK data were best described by a one-compartmental model with an additive error model structure. Stepwise covariate search returned body weight (BW) and creatinine clearance (CL_{CR}) as significant covariates. A power relationship was assumed relative to median BW and CL_{CR} and expressed mathematically as below:

$$CL_{ij} = 0.286 \times \left(\frac{BW}{4.25}\right)^{\alpha_{jCL}} \times \left(\frac{CL_{CR}}{83.33}\right)^{\beta_{jCL}} \times \exp(\eta_{CL})$$

$$V_{ij} = 1.75 \times \left(\frac{BW}{4.25}\right)^{\alpha_{jV}} \times \exp(\eta_{V})$$

where CL_{ij} and V_{ij} are the plasma clearance and volume of distribution for the i^{th} subject in age group j (AGEG j), respectively. η is the random between subject variability. $\alpha_{jCL,}$ $\beta_{jCL,}$ and α_{jV} are the power exponents that were estimated with different sets of values across age groups. The PK parameters are summarized in Table 1.

Table 1 Summary of PK parameter

	Parameter	Description	Final model		
			Estimate	RSE	95% CI
	CL(L/H)	Clearence	0.286	2%	0.275–0.297
	V(L)	Volume of distribution	1.75	2%	1.681–1.819
AGEG1	α_{1CL}:CL-BW1	BW influence on CL	1.14	4.2%	1.047–1.233
	β_{1CL}:CL-CL_{CR}1	CL_{CR} influence on CL	0.333	17.5	0.219–0.447
	α_{1V}:CL-BW1	BW influence on V	0.781	5.1%	0.703–0.859
AGEG2	α_{2CL}:CL-BW2	BW influence on CL	0.741	5%	0.699–0.813
	β_{2CL}:CL-CL_{CR}2	CL_{CR} influence on CL	0.483	10.7%	0.381–0.585
	α_{2V}:CL-BW2	BW influence on V	0.755	4.2%	0.712–0.838
AGEG3	α_{3CL}:CL-BW3	BW influence on CL	0.831	3.3%	0.777–0.885
	β_{3CL}:CL-CL_{CR}3	CL_{CR} influence on CL	1.03	11.7%	0.795–1.265
	α_{1V}:CL-BW3	BW influence on V	0.771	4.2%	0.708–0.834
AGEG4	α_{4CL}:CL-BW4	BW influence on CL	0.849	2.2%	0.812–0.886
	β_{4CL}:CL-CL_{CR}4	CL_{CR} influence on CL	0.624	13.7%	0.456–0.792
	α_{4V}:CL-BW4	BW influence on V	0.788	1.9%	0.759–0.817
	Parameter	Description	Estimate	RSE%	
	ω^2 CL	Variance of CL BSV	0.0559	8.3	
	ω V	Variance of V BSV	0.063	17.6	
	σ^2	(additve)			
	Variance of addtive	residual error	0.276	9.2	

Conclusions: The popPK of intravenous gentamicin was best described by a one-compartment model with first order elimination. Clearance was predicted by body weight and creatinine clearance, while volume of distribution was predicted by body weight. The influence of creatinine clearance significantly varied across age groups. The current model provides an alternative angle of examining gentamicin PK in different age groups to traditional covariate model structure.

T-80

Interactive Concentration-QTc Analysis and Automatic Report Generation Using R Shiny and Knitr

Rui Zhu, Qi Liu, Jin Y Jin, Nageshwar Budha

Clinical Pharmacology, Genentech, Inc. South San Francisco, CA

Objectives: To facilitate internal standardization of concentration-QTc (C-QTc) analyses and reporting, an interactive web based Shiny application as well as an automatic report generation system via Kintr were developed using R. This combined system allows users to efficiently perform C-QTc exploratory analyses, conduct model development, comparison, evaluation, and automatically generate a report.

Methods: Several R packages including 'shinydashboard', 'DT', 'ggplot2', and 'rmarkdown' were adopted to improve interactive functionality of the R-Shiny application. The 'Knitr' package under R Sweave system was used to link R with LaTex to create the automatic report generation template. Resulting figures and tables within the R shiny interface can be selectively downloaded to users' local file folder and directly combined with the template to generate a report in PDF format.

Results: R shiny interface snapshots are shown in Figure 1. Upon loading the dataset, standardized exploratory plots will be generated for multiple purposes, including underlying assumption assessment (eg,

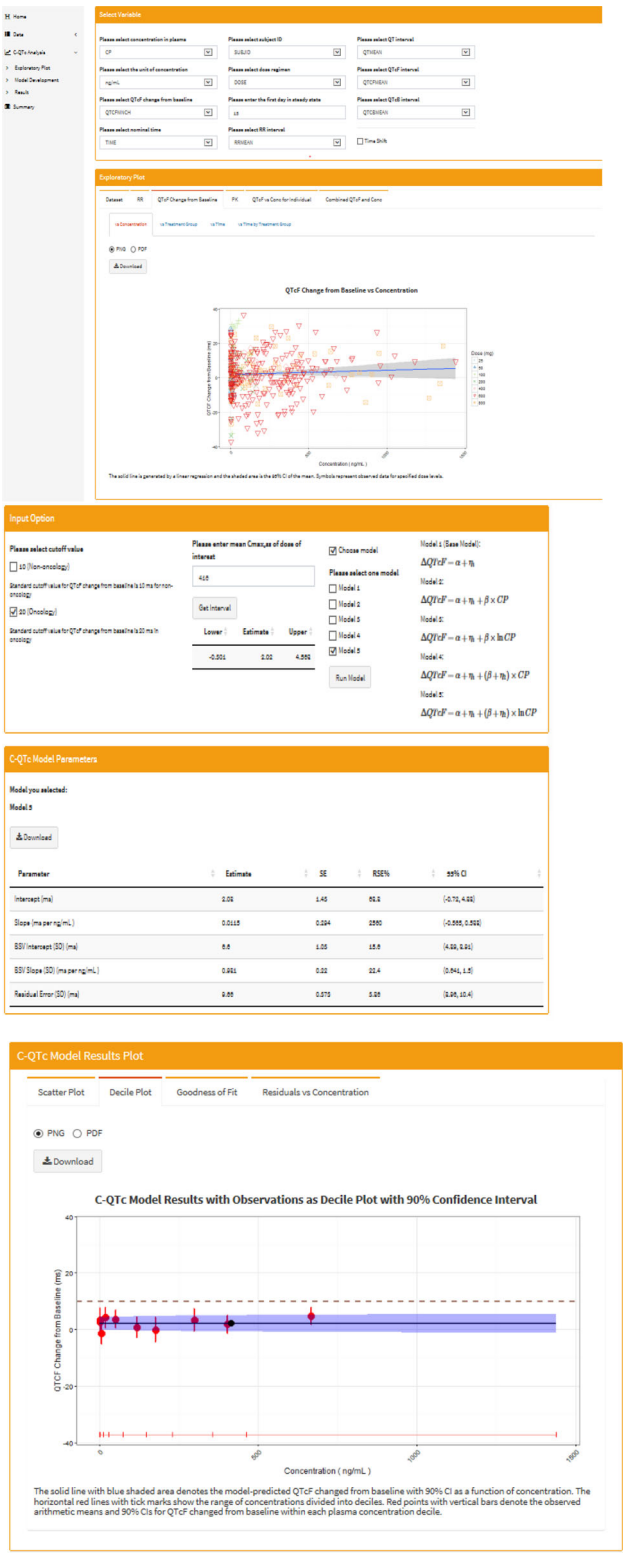

Figure 1 Snapshots of the R shiny user interface for C-QTc analysis (Color figure online)

time delay/hysteresis), QT interval correction method selection, outlier detection, categorical analysis, and dose/concentration-QTc and QTc change from baseline (ΔQTc) relationship exploration, etc. User can select between linear and nonlinear mixed effect model categories in model development. Further, multiple different models (eg, linear or lognormal concentration, with or without random effect, etc) can be tested under each category. Standard diagnostic plots and a table summarizing details of all the tested models will be provided for model comparison. With user inputted steady-state maximum concentration (C_{max}) at dose of interest, developed C-QTc model can be utilized within the platform to simulate mean ΔQTc and 90% confidence interval at that C_{max} of interest. User also has the flexibility to download any resulting tables and figures in R-shiny interface and include them in the report automatically generated in R Sweave.

Conclusions: This combined R Shiny interface and automatic report generation system provides a user-friendly platform to efficiently perform C-QTc analysis and dynamic report generation. This also provides a visual-friendly and interactive communication tool for effective team discussions of the analysis.

T-81

Exposure Response Analysis of Safety of Elotuzumab in Patients with Multiple Myeloma

Chaitali Passey[1,*], Leonid Gibiansky[2], Jennifer Sheng[1], Akintunde Bello[1], Amit Roy[1], Manish Gupta[1]

[1]Clinical Pharmacology and Pharmacometrics, Bristol-Myers Squibb, Princeton, NJ; [2]QuantPharm LLC, North Potomac, MD

Objectives: Elotuzumab (ELO) is a humanized anti-SLAMF7 IgG1 monoclonal antibody approved in combination with lenalidomide/dexamethasone (Len/Dex) for treatment of relapsed/refractory (R/R) multiple myeloma (MM). Exposure-response (E-R) analyses was conducted to describe relationship between ELO exposure and safety, and impact of covariates in R/R MM patients.

Methods: E-R analysis of time to first occurrence of Grade 3+ AEs and time to AEs leading to discontinuation/death was conducted in MM patients from study CA204004 who received Len/Dex with/without 10 mg/kg ELO with estimates of ELO exposure from PPK analysis (N = 629)[1]. The E-R was characterized by two separate semi-parametric Cox Proportional Hazards (CPH) models relating ELO exposures (measured by individual predicted time-dependent average concentrations over dosing interval). A full covariate model was developed by incorporating following predictor variables in the base CPH model: body weight, age, race, gender, lactate dehydrogenase (LDH), ECOG score, albumin, absolute lymphocyte count, serum M-protein, and β2-microglobulin. E-R models were evaluated by visual predictive check.

Results: Risk of Grade 3+ AEs and AEs leading to discontinuation/death does not increase with increasing ELO exposure. Risk of Grade 3+ AEs and AEs leading to discontinuation/death is higher for patients with elevated levels of baseline 2-microglobulin and baseline LDH. Risk of Grade 3+ AEs is higher in patients with baseline ECOG score of 2 compared with patients whose ECOG score is 0 or 1, and in patients with lower baseline albumin. Risk of AEs leading to discontinuation/death is higher in patients with lower baseline serum M-protein.

Conclusion: Risk of Grade 3+ AEs and AEs leading to discontinuation/death do not increase with increasing ELO exposure over the range of exposures achieved with the 10 mg/kg dosing regimen.

Reference

1. Gibiansky, L *et al*. Model-based pharmacokinetic analysis of elotuzumab in patients with relapsed/refractory multiple myeloma. *J Pharmacokinet Pharmacodyn*. 2016.

T-82

QSP-SIG Student Award Winner

Integrated analysis for quantitative predictions of drug-induced toxicity

Jaehee Shim, Evren Azeloglu, Yuguang Xiong, Jens Hansen, Marc Birtwistle, Ravi Iyengar, Eric Sobie

Drug Toxicity Signature Generation Center, Icahn School of Medicine at Mount Sinai, New York, NY 10029; Department of Pharmacological Sciences, Icahn School of Medicine at Mount Sinai, New York, NY 10029

Objectives: Cardiotoxicity is a common adverse event caused by tyrosine kinase inhibitors (TKIs), a class of chemotherapeutic agent. Reported toxicities include left ventricular dysfunction, heart failure, and arrhythmias[1]. TKI cardiotoxicity is thought to be induced by dysregulation of cardiomyocyte survival signaling cascades via both on- and off-target effects, but the mechanistic details remain unclear[2]. Given the effectiveness of many TKIs in cancer treatment, elucidating molecular interactions behind these toxicities would be critical in alleviating these detrimental side effects to maintain treatment efficacy. The Drug Toxicity Signature Generation (DToxS) Center at Mount Sinai has started a large-scale project that aims to address this issue by providing a bridge between molecular changes in cells and the prediction of pathophysiological effects.

Methods: In our ongoing work we use high-throughput transcriptomic measurements using mRNA-Seq as the basis for computational analysis to generate "signatures" for TKIs. Primary human cardiac myocytes in culture are treated with TKIs, and drug-induced changes in gene expression are quantified. The gene expression profiles are then used to identify pathways involved in the drug response, to build networks of interacting cellular components, and as inputs to dynamical mathematical models that predict pathophysiological responses. My PhD project involves simulating the effects of TKI-induced changes in gene expression in several models to obtain signatures related to cellular signaling dynamics. The models that we implement are chosen based on the relevance to cardiomyocyte survival/growth/death signaling network. These include a logic-based model of cardiac hypertrophy that simulates 193 biochemical reactions with 106 ordinary differential equations (ODEs)[3]. To simulate how TKIs may influence apoptosis susceptibility, an ODE-based model with 67 species and 118 reactions is implemented[4]. This approach has generated novel predictions about the mechanisms underlying TKI-induced cardiotoxicity.

Results: For the initial analyses, changes in gene expression in a single cell line due to three TKIs (trastuzumab, sunitinib, and sorafenib) were used. These three drugs were chosen based on the literature availability of cardiotoxicity reports.

The simulations for hypertrophy and apoptosis models were examined separately to delineate the differences in the degree of the toxicity. Results from the hypertrophy model indicated that the overall risk index is in the order of sorafenib>trastuzumab>sunitinib in both basal activity (i.e. no stimulus) and when stretch is given as a stimulus. Apoptosis model result also had the same order of risk index –i.e. sorafenib as the most apoptotic inducing. To examine the mechanistic details, time course plots of selected network nodes for each model were generated. Mechanistic hypotheses that result from these simulations are as follows:

Sorafenib: Simulations suggest that the predicted strong pro-hypertrophic signaling caused by sorafenib results from the regulation pattern of the metabolic enzyme GSK3β. Originally identified as an enzyme in glycogen metabolism, GSK3β was also found to play an important role in hypertrophy prevention in cardiomyocytes. The down-regulation of GSK3β predicted by the simulations (Fig. 1A) causes an exaggerated response of other pro-hypertrophic signals in the model, as shown.

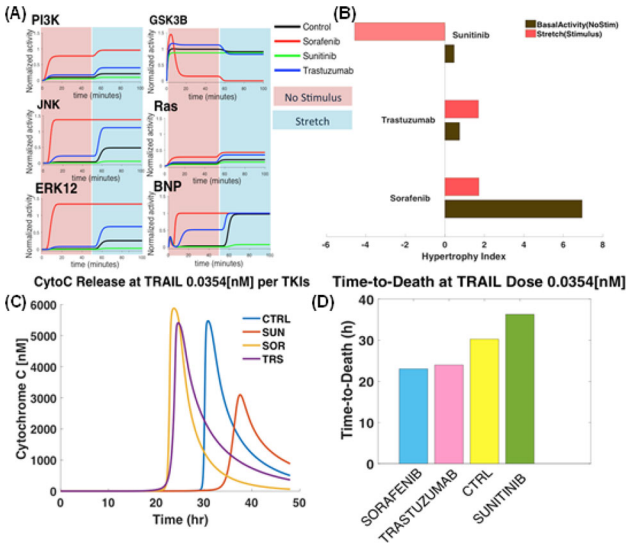

Figure 1 Simulation Results of Hypertrophic/Apoptotic Tendencies of TKI network Perturbation (A) Time course plot for 6 species in hypertrophy network. First 50 minutes are for basal level activity or no stimulus state and the next 50 minutes are simulated for stretch-induced state. (B) Hypertrophy index for the drugs per given stimulus. (C) Apoptosis time course plot based on the peak time of cytochrome C release given 0.0354nM of TRAIL. TRAIL concentration was arbitrarily chosen based on the amount required for control simulation to commit death in 30 hours. (D) Based on cytochrome C release simulation, time to death bar plot is generated (Color figure online)

Trastuzumab: While trastuzumab is mildly pro-hypertrophic as well, the results suggest that the difference in hypertrophic tendency between sorafenib and trastuzumab could result from the maintained levels of GSK3β activity in trastuzumab.

Sunitinib: Unlike sorafenib and trastuzumab, sunitinib was predicted to be somewhat protective against both hypertrophy and apoptosis, which suggests that the toxicity could occur through some other mechanism such as dysfunction of energy homeostasis. We are currently implementing mathematical models of mitochondrial metabolism and myocyte contraction to potentially uncover mechanisms underlying sunitinib toxicity.

In addition to these novel insights in mechanistic details, this approach also allowed us to validate known mechanisms of cardiotoxicity for these TKIs. For instance, sorafenib and trastuzumab are both known to induce cell death via intrinsic apoptotic pathway. In both drugs, we have confirmed elevated JNK expression (Fig1A) which can lead to JNK-mediated cytochrome C release. The commitment of apoptosis was further validated with apoptosis model simulation shown in Fig1C&D where sorafenib and trastuzumab show higher tendency to commit cell death given the death signaling ligand (TRAIL).

Conclusion: In conclusion, we have demonstrated a robust quantitative systems approach in predicting drug toxicity by integrating transcriptomic data with mathematical modeling. Using this approach, we have both validated known mechanisms of cardiotoxic TKIs and generated novel insights into other possible mechanism which can be validated experimentally. In particular, we plan to apply TKIs in combination with physiological stimuli such as stretch and test model predictions using western blot or immunofluorescence. We

are confident that this analyses pipeline will be an invaluable tool in delineating differences in toxicity between TKIs with similar targets as well as predicting possible toxicity of drugs in development.

References

1. Chen MH, Kerkel R, Force T. Mechanisms of cardiac dysfunction associated with tyrosine kinase inhibitor cancer therapeutics. *Circulation*. 2008;118(1):84–95.
2. Force T, Kolaja KL. Cardiotoxicity of kinase inhibitors: the prediction and translation of preclinical models to clinical outcomes. *Nat Rev Drug Discov*. 2011;10(2):111–126.
3. Ryall KA, Holland DO, Delaney KA, Kraeutler MJ, Parker AJ, Saucerman JJ. Network reconstruction and systems analysis of cardiac myocyte hypertrophy signaling. *J Biol Chem*. 2012;287(50):42259–42268.
4. Albeck JG, Burke JM, Spencer SL, Lauffenburger DA, Sorger PK. Modeling a snap-action, variable-delay switch controlling extrinsic cell death. *PLoS Biol*. 2008;6(12):2831–2852.
5. Kuramochi Y, Guo X, Sawyer DB. Neuregulin activates erbB2-dependent src/FAK signaling and cytoskeletal remodeling in isolated adult rat cardiac myocytes. *Journal of molecular and cellular cardiology*. 2006;41(2):228–35.

W-01

Repeated Dose Pharmacokinetics in Rats for Identification of Novel Drug-Induced Nephrotoxicity Biomarkers

Abdul Naveed Shaik[1], Deborah Altomare[2], Barbara Teets[3], Lawrence J Lesko[1], Mirjam N Trame[1]

[1]Center for Pharmacometrics and Systems Pharmacology, University of Florida, Orlando, FL; [2]Burnett School of Biomedical Sciences, University of Central Florida, Orlando, FL; [3]Agilent Technologies, Raleigh-Durham, NC

Objectives: Nephrotoxicity is monitored using serum creatinine (SCr) and blood urea nitrogen (BUN). However, kidney damage is not detected until significant changes in levels of SCr and BUN are observed due to the time lag between kidney damage and increase in biomarker levels. This led to identification of novel biomarkers using proteomics and metabolomics, which show early signs of kidney damage in rodents. However, translating the findings to humans is lacking. The objective of this project was to identify biomarkers to detect early drug-induced nephrotoxicity in rodents using cisplatin as an exemplar and to translate those changes to humans using quantitative modeling approaches.
Methods: An LC-MS/MS method was developed and validated using Agilent-QQQ-6460 for quantitative determination of cisplatin. Pharmacokinetic (PK) studies were performed in Sprague–Dawley rats (n=4-7) and doses of 0.5, 3.5, and 7.0 mg/kg of cisplatin/blank-saline were administered via jugular vein. On days 1,7,14 and 21, blood and urine was collected. Rats were sacrificed on different days to extract kidney tissues. Samples were aliquoted into two, one for analysis of cisplatin, other for metabolomics using Agilent-QTOF-6540.
Results: Developed cisplatin method was validated to meet FDA guidelines for bioanalytical method validation, LOD was 1 ng/ml, calibration range 5-3000 ng/ml, and parameters such as accuracy, precision were within ±15% deviation. The method was applied to analyze plasma, urine and kidney samples from rats. PK parameters were determined by non-compartmental analysis using Phoenix64, resulted in AUC of 0.35±0.02 µg/mL*h and CL of 1676±231 ml/h/kg.
Conclusions: PK parameters obtained in-house were similar to reported literature values of different dosing groups. Furthermore, a PBPK model will be developed using cisplatin concentrations obtained in plasma, urine and kidney in rats linked to metabolomic changes. This model will be applied and evaluated in humans using literature data to predict early drug induced nephrotoxicity.

W-02

Evaluation of the Performance of Modified Chi Square Ratio Statistic for Cascade Impactor Profiles Equivalence Testing

Abhinav Kurumaddali[1,*], Li Zhao[1], David Christopher[2], Beth Morgan[3], Dennis Sandell[4], Helen Strickland[3], Steve Stein[5], Christopher Wiggenhorn[5], Lyapustina Svetlana[2], Guenther Hochhaus[1]

[1]Department of Pharmaceutics, University of Florida, Gainesville, FL, [2]Merck, West Point, PA, [3]GSK, Raleigh-Durham, NC, [4]S5 Consulting, Blentarp, Sweden, [5]3M, Greater Minneapolis, MN

Objectives: A Modified Chi Square Ratio Statistic (mCSRS) for comparison of aerodynamic particle size distributions of Test (T) and Reference (R) inhaled drug products was proposed earlier. In this paper, the effect of various factors viz. mean deposition, critical value level, variance ratio, high vs low deposition sites, sample size and bootstrap number on the performance of mCSRS was evaluated.
Methods: Cascade Impactor (CI) profiles were generated by Monte Carlo simulation in R assuming multivariate normal distribution of amount of drug deposited on different stages of cascade impactor. A thousand pairs of R and T CI profiles each of defined sample size without intersite correlation were generated. Generally, the percent of the 1000 pairs resulting in equivalence (PE) was calculated.
Results: As the mean difference between R and T increased, PE decreased at a given variability and critical value level. As the critical value level increased, PE increased at a given variability and mean difference. PE decreased as the R/T variance ratio decreased at a

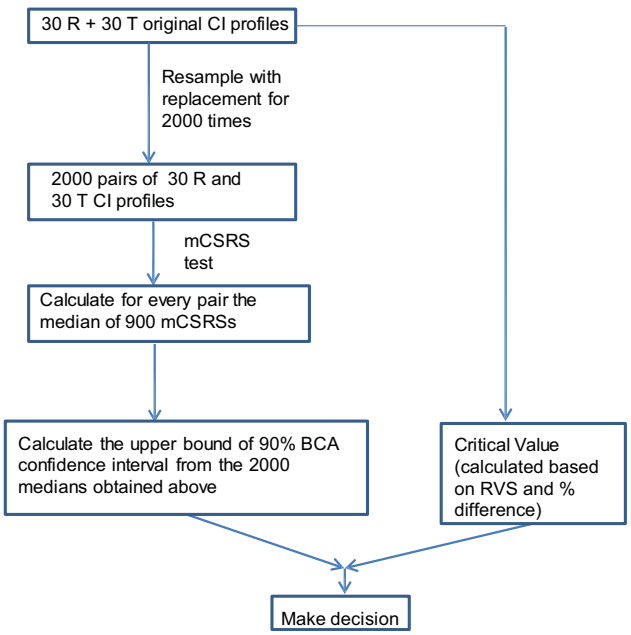

Outline of modified chi-square ratio statistic test

given mean difference and critical value level. The decrease in PE was much more pronounced for higher deposition sites than for lower deposition sites for a given increase in mean difference. At zero mean difference and R/T variance ratio of 1:1, PE decreased when sample size decreased and vice-versa. Larger sample size was required for conferring equivalence at higher levels of mean difference and product variability. With increase in bootstrap number, the variability of the upper bound of the 90% confidence interval of median of mCSRS decreased with an optimal value at 2000 bootstraps.

Conclusion: The study suggested that mCSRS is a robust and sensitive test for comparing CI profiles of T and R inhaled drug products.

Reference

1. Weber B et al, AAPS J. 2015 Mar;17(2):370-9.

W-03

Integrated Network Modeling for Novel Target Searches and Better Predictive Models

Adil Mardinoglu PhD[1], and Jim Bosley, PhD[2]

[1]KTH-Royal institute of Technology and Chalmers Institute of Technology; [2]Clermont Bosley LLC

Objective: Introduce the concept of using GEnome scale Metabolic (GEM) modeling and Integrated Network (IN) modeling to support improved searches for novel drugs and markers. Specifically to show how such modeling approaches leverage a broad array of omics data to give insight and decision support. Specifically, to introduce the point that IN models may allow systems pharmacology models that have higher predictive validity.

Methods: GEM models are used alone and with Protein-Protein INteraction (PPIN) Network and Transcriptional Regulatory Network (TRN) models to allow evaluation of the full set of known pathways and metabolites in searching for novel targets and markers, and also to ensure that systems models contain a complete set of the most relevant pathways.

Results: Results are given for several cases in Non-Alcoholic Fatty Liver Disease (NAFLD) and Non-Alcoholic SteatoHepatitis (NASH) (Mardinoglu et al., 2014), as well as for Hepatocarcinoma (Agren et al., 2014). We will review published results and up-to-date (unpublished) results of a number of clinical and other studies in which IN models have been calibrated and validated(Lee et al., 2016).

Conclusions: GEM and IN modeling represent an advance in integrating a wide variety of heterogenous omics and other data to yield insights not available via traditional approaches. These techniques also highlight the key pathway differences in healthy and diseased tissues (for example, between normal germ-line and cancerous cells). This provides a good check on model completeness for traditional mass-balance models based upon differential equations. The approach highlights relevant pathways that might otherwise not be included. Predictive validity is critical for decision support with high impact (Scannell and Bosley, 2016). The analysis provides models with better predictive validity.

Reference

1. Agren, R., Mardinoglu, A., Asplund, A., Kampf, C., Uhlen, M., and Nielsen, J. (2014). Identification of anticancer drugs for hepatocellular carcinoma through personalized genome-scale metabolic modeling. Mol. Syst. Biol. *10*.
2. Lee, S., et al., Elias Bjornson, Murat Kilicarslan, Brian Donald Piening, Elias Bjornson, Björn M Hallström, A. K. Groen, Ele Ferrannini, Markku Laakso, et al. (2016). Integrated network analysis reveals an association between plasma mannose levels and insulin resistance. Cell Metab.
3. Mardinoglu, A., Agren, R., Kampf, C., Asplund, A., Uhlen, M., and Nielsen, J. (2014). Genome-scale metabolic modelling of hepatocytes reveals serine deficiency in patients with non-alcoholic fatty liver disease. Nat. Commun. *5*, 3083.
4. Scannell, J.W., and Bosley, J.R. (2016). When Quality Beats Quantity: Decision Theory, Drug Discovery, and the Reproducibility Crisis. PLOS One.

W-04

Model-optimized safe and efficacious anaemia treatment in Non-Small Cell Lung Carcinoma

Agustin Rodriguez-Gonzalez[1,2,3,*], Max Schelker[4,5,*], Andreas Raue[4,9,*], Bernhard Steiert[4,*], Florian Salopiata[1,3], Lorenz Adlung[1], Martin E. Böhm[1], Markus Stepath[1], Sofia Depner[1,2,3], Marie-Christine Wagner[1], Ruth Merkle[1,3], Bernhard A. Kramer[1], Susen Lattermann[1], Marvin Wäsch[1,3], Andreas Franke[6], Edda Klipp[5], Patrick Wuchter[7], Anthony D. Ho[7], Wolf D. Lehmann[1], Michael Jarsch[6], Marcel Schilling[1,$], Jens Timmer[4,8,$] and Ursula Klingmüller[1,2,3,$]

[1]Systems Biology of Signal Transduction, German Cancer Research Center (DKFZ), Germany; [2]Bioquant, Heidelberg University, Germany; [3]Translational Lung Research Center (TLRC), Member of the German Center for Lung Research (DZL), Heidelberg, Germany; [4]Institute of Physics, University of Freiburg, Germany; [5]Theoretical Biophysics, Institute of Biology, Humboldt-Universität zu Berlin, Germany; [6]Pharma Research and Early Development (pRED), Roche Diagnostics GmbH, Roche Innovation Center Munich, Germany; [7]Department of Medicine V, Heidelberg University, Germany; [8]Centre for Biological Signalling Studies (BIOSS), University of Freiburg, Germany; [9]Discovery Division, Merrimack, Cambridge, MA, USA; *: Contributed equally; $: Shared senior authorship

Anaemia is a frequent complication in cancer patients, and particularly exacerbated at late stages of lung carcinoma. Erythropoiesis-Stimulating Agents (ESAs) are widely used to correct chemotherapy-associated anaemia. However, it was reported that 30-50% of patients do not respond. An increased risk of mortality, thromboembolic events and tumour progression was associated with ESA treatments in the context of cancer and low levels of erythropoietin receptor (EpoR) expression was observed in cancer cells, raising safety concerns on the use of ESAs in cancer. Here we establish by mathematical modelling an innovative approach to optimize a personalized ESA treatment for anaemia in Non-Small Cell Lung Carcinoma (NSCLC) patients. Based on in-vitro experiments we calibrate a mechanistic dynamic pathway model that enables the estimation of ESA binding sites and the determination of the binding properties of ESAs. We show that ESAs with low affinity towards the EpoR activate signal transduction more efficiently in cells exhibiting high levels of ESA binding sites, such as primary erythroid progenitor cells, and that in a defined range of concentrations the risk of ESA-induced activation of the EpoR in the context of NSCLC cells is reduced. By combining mechanistic dynamic pathway modelling with pharmacokinetic and pharmacodynamic data of ESAs in human subjects, we identify the number of ESA binding sites per patient and the haemoglobin degradation rate as key patient-specific parameters. The integrative model enables a personalized prediction of the minimum efficacious ESA dose, and the stratification of patients into groups of low and

high risk of fatal outcome. In sum, our integrative mechanistic model quantitatively describes the dynamic interaction of ESAs at molecular, cellular and systemic level in the human body and provides a quantitative tool to optimize the dosing regimens in clinical trials, and to personalize ESA treatment in cancer.

W-05

A model-based pharmacokinetic/pharmacodynamic analysis of hydrocortisone, 17-hydroxyprogesterone (17OHP), and androstenedione (D4A) in children with congenital adrenal hyperplasia (CAH)

Ahmed MA[1], Sarafoglou K[2], Al-Kofahi M[1*], Gonzalez-Bolanos MT[3], Brundage RC[1]

[1]Experimental and Clinical Pharmacology, Minneapolis; [2]Department of Pediatrics, Minneapolis

Objectives: CAH due to 21α-hydroxylase deficiency is a rare form of adrenal insufficiency characterized by impaired cortisol synthesis and excessive adrenal androgen production. Oral replacement with 10-15 mg/m^2/day hydrocortisone is recommended in children with CAH. Although efficacy is monitored by 17OHP and/or D4A concentrations every 3-6 months, assessment is complicated by diurnal variations, changes occurring with puberty, and high between-individual sensitivity in pharmacodynamic response. PK/PD relationships of hydrocortisone and adrenal steroids have not been well characterized in this group limiting clinician ability to compare concentrations at different times. In this study, quantitative models were developed to describe the relationships of cortisol, 17OHP and D4A.
Methods: A nonlinear mixed-effect modeling approach (NONMEM) was used to analyze 12 hydrocortisone, 17OHP and D4A serum samples obtained over six hours from 41 children (21 male; age: 1.5-18 years; weight: 10.8-80.6 kg; 34 pre-pubertal) with CAH (36 classic/5 nonclassic CAH) following their usual morning hydrocortisone maintenance dose (1.25-12.5 mg). A sequential PKPD modeling approach was used. Turnover models included a dual-cosine function based on literature information to capture 24-hour circadian rhythms of endogenous production rates; a cortisol-based saturable inhibition of production rates; and a 1-compartment first-order PK model for exogenous hydrocortisone dosing. The resulting models were used to simulate 24-hour concentration-time profiles.
Results: PK/PD results are in the table. 17OHP and D4A concentrations respond quickly to rapidly changing cortisol concentrations, indicating all have fast half-lives. No difference in bioavailability was detected between hydrocortisone tablets and an extemporaneously compounded suspension.
Conclusions: Current dosage regimens of hydrocortisone in children with CAH do not capture physiologic circadian rhythms resulting in prolonged periods of hypo- and hypercortisolemia and inadequate control of adrenal steroids. Current doses may be excessive in some children with nonclassic CAH resulting in oversuppression of androgens. The current CAH guidelines that recommend against using hydrocortisone suspension should be re-evaluated as it often requires splitting tablets into 2-4 dosage units.

Table 1 PKPD parameter estimates

PARAMETER	ESTIMATE	RSE%	SHRINKAGE
CORTISOL			
Rin,baseline (mg/h)	THETA * (WT/70)**0.75		
Classic salt waster	0.109	17	
Classic simple virilizer	0.244	27	
Nonclassic	2.1	32	
CL/F (L/h) THETA * (WT/70)**0.75	24.0	4	
V/F (L) THETA * (WT/70)	14.5	3	
KATR (h^{-1}) 4 transit compartments	9.88	6	
Effect of cortisol on endogenous production			
IC50 (ug/dL)	1.29	10	
gamma sigmoidicity	3 (fixed)		
Random Effects			
Rin,baseline (%CV)	93.9	13	6
CL/F (%CV)	28.2	11	0.7
V/F (%CV)	16.2	15	12
KATR (%CV)	40.5	12	4
RUV (%CV)	15.5	4	15
17OHP			
Rin,baseline (ng/dL/h)			
Classic salt waster	4880	12	
Classic simple virilizer	3880	18	
Nonclassic	743	38	
Kout (h^{-1})	1.02	3	
Effect of cortisol on endogenous production			
IC50 (ug/dL)	2.03	10	
gamma sigmoidicity	2 (fixed)		
Random Effects			
Rin,baseline (%CV)	213	12	0
Kout (%CV)	17.9	16	17
IC50 (%CV)	90.4	13	4
RUV (%CV)	27.6	4	10
D4A			
Rin,baseline (ng/dL/h)			
Pre-pubertal	60.4	16	
Non-pre-pubertal (fractional)	2.24	50	
Kout (h^{-1})	0.618	7	
Effect of cortisol on endogenous production			
IC50 (ug/dL)	4.17	4	
gamma sigmoidicity	3 (fixed)		
Random Effects			
Rin,baseline (%CV)	125	14	1
Kout (%CV)	20.7	6	20
IC50 (%CV)	32.6	12	4
RUV (%CV)	13.4	4	10

W-06

Estimation of Pediatric Dosages Considering Rapid Development of Physiological Functions after Birth with Approximated Simple Formulae: Implementation and Comparison with Dosages Described in the Labeling

Akihiro Hisaka[1,*], Tomoko Mayuzumi[2], Hiroki Koshimichi[2], Yuko Sekine[1], and Hiroshi Suzuki[2]

[1]Section of Advanced Practical Pharmacology, Graduate School of Pharmaceutical Sciences, Chiba University, Japan; [2]Department of Phamacy, The University of Tokyo Hospital, Japan.

Background and Objectives: Previously, we reported an estimation method for pediatric dosages which is applicable to premature and mature infants considering rapid development of hepatic and renal functions after birth (Fujino et al, World Conference on Pharmacometrics 2012). In this study, simple linear formulae were derivatized by approximating the previous nonlinear function, and they were applied to 45 oral and 28 intravenous drugs of which pediatric dosages have been described in Japanese labeling for comparison.
Methods: In the previous study, the pediatric hepatic clearance was estimated considering changes of CYP expression and development of the hepatic weight. Similarly, the renal clearance was estimated from development of GFR. In this study, changes of the hepatic and the renal clearances were approximated with segmented linear equations. The pediatric dosage for an arbitrary age can be calculated using Excel as a ratio versus adult from the urinary excretion ratio (Xu) in adults. The equations were applied to drugs of which pediatric dosages have been described in Japanese labeling for comparison between the theory and the current situation.
Results and Discussion: Segmented linear equations successfully approximated the previous model within 20% error. We compared the calculated dosages with those in the Japanese product labeling for ages from 0.25 to 6 years old. For 45 oral drugs, the median of the ratio (estimated versus described) was 1.15 and the interquartile range was 0.93-1.36. For 28 intravenous drugs, the median was 0.93, and the interquartile range was 0.64-1.48. Overall, the estimated dosages were agreed excellently with those described in the product labeling. On the other hand, for drugs whose discrepancies between the estimated and described dosages are significant, it seems necessary to check their efficacy, safety and pharmacokinetics in pediatric population in the future. The results in this abstract have been previously presented in part at 19th North American ISSX Meeting and 29th JSSX Annual Meeting (San Francisco, USA) and published in the conference proceedings.

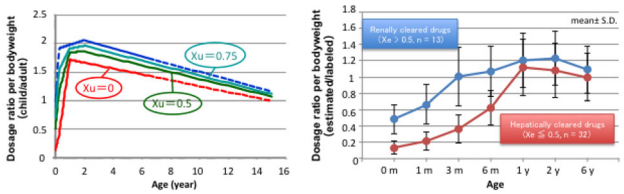

Figure 1 Linearized PB-PK based pediatric dosage calculation formulae (A) and ratio of estimated dosage versus described dosage in Japanese labeling for 45 oral and 28 intravenous drugs (B) (Color figure online)

W-07

A simple PK/PD-based model for maintained self-administration of dopamine agonists in rats

Alexander C. Ross, Andrew B. Norman

Department of Pharmacology, University of Cincinnati College of Medicine

Objectives: Rats trained to self-administer dopamine agonists do so with a regularity capable of being predicted by $T = \ln(1 + D_U/D_{ST})/k$, where T is the interval between self-administration events, D_U is the agonist unit dose, k is the agonist elimination rate constant, and D_{ST} is the minimum level of agonist maintained in the body. D_{ST}, dubbed the satiety threshold, is presumed to correspond to an amount of agonist-receptor complexes in the brain. Herein is detailed a simple PK/PD-based model of dopamine agonist self-administration with self-administration events occurring based on the amount of agonist-receptor complexes as a function of time.
Methods: A one-compartment PK/PD model was made in MATLAB Simbiology. The agonist (A) binds to the receptor (R) according to the law of mass action. The response of the system—further agonist self-administration events—is dictated by $AR(t)$. If $AR(t)$ is below an amount qualifying as satiety, $AR_{satiety}$, agonist self-administration events occur at set intervals until $AR(t)$ is greater than $AR_{satiety}$. As the agonist is eliminated from the system via a first-order elimination process, $AR(t)$ decreases back to $AR_{satiety}$, at which point another self-administration event occurs. R is synthesized and degraded with the assumption of steady state conditions.

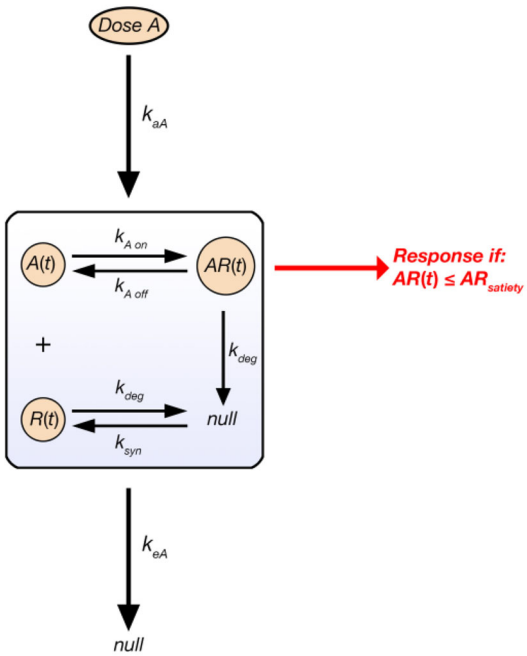

Figure 1 PK/PD-Based Model for Dopamine Agonist Self-Administration in Rats (Color figure online)

Results: Simulations of the model were consistent with what has been observed in rats self-administering apomorphine, a direct dopamine receptor agonist. As the simulated D_U was increased, the simulated T proportionally (and non-linearly) increased with simulated D_{ST} not changing. This simulation output is in line with rat apomorphine self-administration data.
Conclusions: A one-compartment PK/PD model with self-administration events programmed around the amount of agonist-receptor complexes appears sufficient in explaining apomorphine self-administration behavior in rats.

References

1. Tsibulsky, V. L. & Norman, A. B. *Brain research* **839**, 85-93 (1999).
2. Norman, A. B., Tabet, M. R., Norman, M. K. & Tsibulsky, V. L. *Journal of neuroscience methods* **194**, 252-258, (2011).

W-08

The pharmacodynamics of Sertraline as Anti-fungal

Ali Alhadab[1], Joshua Rhein[1,2], Kathy Huppler Hullsiek[1], David Meya[2], David Boulware[1], Richard Brundage[1]

[1]University of Minnesota, Minneapolis, MN; [2]Infectious Disease Institute, Kampala, Uganda

Objective: To determine a sertraline dose associated with the fastest rate of fungal clearance from cerebrospinal fluid (CSF) and to quantify the clinical benefits of sertraline when added to amphotericin B and fluconazole for the treatment of HIV-associated cryptococcal meningitis.
Methods: A Poisson regression was used to model log-transformed fungal counts in CSF obtained from ASTRO-CM pilot study and COAT trial for the calculation of CSF fungal clearance rate ($\log_{10}$ CFU/mL/day). Correlations of counts within a patient was accounted for using a three-state Markov model to represents an increase, decrease or no change in $\log_{10}$ CFU/mL from a previous day. A mono-exponential decline with a random effect was also added as a time-effect. Estimated fungal clearance rates were compared among sertraline doses ranging from 100-400 mg daily for the selection of optimal dose. To determine the clinical benefit sertraline, overall fungal clearance from ASTRO-CM was compared to that of COAT trial which served as a control. A previously developed PK model of sertraline in HIV patients was used with the measured minimum inhibitory concentrations (MICs) of sertraline against Cryptococcus isolates to simulate, calculate and explore the relationships of various PK/PD indices with the daily change in $\log_{10}$ CFU/mL. Time-to-death analysis was performed to calculate the survival probability over time as a clinical outcome
Results: Rate of CSF fungal clearance was similar among 100, 200, 300, and 400 mg of sertraline. The addition of sertraline increased fungal clearance by 38% relative to standard therapy alone. Cumulative AUC/MIC of 50 mcg/mL was associated with 2.5 log reduction in $\log_{10}$ CFU/mL/day. Female and 400 mg of sertraline daily had lower 2-week survival rate.
Conclusion: Sertraline increased the rate of CSF fungal clearance independent of dose and whether a patient was on anti-retroviral therapy or not. Yet, no survival benefit was observed likely to due to lack of power. A well-powered, randomized clinical trial is required to evaluate the potential survival benefit of sertraline.

W-09

Population Pharmacokinetics of Sertraline: A Model-based Meta-Analysis

Ali Alhadab[1], Richard Brundage[1]

[1]University of Minnesota, Minneapolis, MN

Objective: To develop a population pharmacokinetics of sertraline in healthy subjects using mean-level data from the literature and model-based meta-analysis (MBMA), and to use estimated clearance and absorption later as inputs for a PBPK model to predict sertraline concentrations at various target tissues.
Methods: PubMed literature search was performed to identify pharmacokinetics studies of sertraline that include at least one arm of healthy subjects who are 18-year or older and have the mean concentration-time profile data tabulated or plotted. Data were extracted using the software "WebPlotDigilizer" then modeled with NONMEM 7.30. Three-level nested random effects were included exponentially for study (ISV) and study arm (IAV), and proportionally for residual error (RUV). IAV and RUV were weighed by the inverse square root of total number of subjects in an arm. Time-dependent absorption was used with a fixed KA50 of 3 hr informed by sensitivity analysis. After visual screening, steady-state status (Y/N) and dose were added and found significant on inter-compartmental clearance (Q) and oral bioavailability (F), respectively. Final model was selected based on OFV, diagnostic plots, plausibility of parameter estimates, and relative standard of errors and assessed by visual predictive check. Bootstrap was not performed due to the long computation times.
Results: A total of 712 observed concentrations of 57 mean concentration-time profiles from 26 studies with doses ranging from 5 to 400 mg daily were included in the MBMA. Data were best fitted by 2-compartment model with dose-dependent bioavailability, time-dependent absorption, and 1st-oreder elimination. Estimated maximum F was 62% and 15 mg daily was the dose at which F was half maximum (D50). Maximum absorption rate constant (KAMAX) was 0.52/hr with a shape factor of 1.47 (GAM). Body clearance was similar for single and multiple dosing at 55 L/h while Q for steady state was 60% lower than that of a single dose.
Conclusion: This meta-analysis suggests that nonlinear changes in exposure are due to changes in bioavailability with dose, rather than being mediated through an effect on clearance.

W-10

Abstract withdrawn.

W-11

Characterizing effects of carbimazole on free thyroxine levels in pediatric patients with Graves' disease

Catherine Ollagnier Morel[1], Gilbert Koch[1], Gabor Szinnai[2], Marc Pfister[1]

[1]Pediatric Pharmacology and Pharmacometrics, University Children's Hospital Basel, University Basel, Basel, Switzerland; [2]Department of Endocrinology/Diabetology, University Children's Hospital Basel, University Basel, Basel, Switzerland

Objectives: Graves' disease (GD) is a serious autoimmune thyroid disease and the most common cause for hyperthyroidism. A majority of pediatric GD patients are treated with an anti-thyroid medication. The aim of this study was to characterize effects of carbimazole on free thyroxine (FT4) level in blood by pharmacometric modeling.
Methods: Data from 58 pediatric GD patients (median age of 12 years) treated with carbimazole between 1990 and 2012 and followed for up to 115 days were available. Dose of carbimazole was linked to individual pharmacokinetic profiles and effects of carbimazole on FT4 level were modeled with various structural models. Non-linear mixed effect modeling was applied and key covariates such as age, sex and weight were investigated [1].
Results: Developed indirect response model described individual dynamics of FT4 levels and effects of carbimazole on FT4 levels well.
Conclusions: We report the first pharmacometric model that characterizes effects of carbimazole on FT4 levels in pediatric GD patients. As next steps, FT4 will be related to heart rate (HR), as elevated HR is a clinically important endpoint of GD with the ultimate goal to personalize and optimize dose adjustments based on individual FT4 and or HR dynamics.

Reference

1. Kaguelidou F et al. (2008) Predictors of autoimmune hyperthyroidism relapse in children after discontinuation of antithyroid drug treatment. J Clin Endocrinol Metab, 93:3817-3826.

W-12

Utility of Physiologically-Based Pharmacokinetic Model (PBPK) for Prediction of Effects of Renal Impairment: A Learn-Confirm Paradigm

Christine Xu, Vanaja Kanamaluru

Sanofi Bridgewater, NJ

Objectives: Renal impairment (RI) not only affects drug elimination in the kidney, but may also the non-renal routes clearance. The objective of this PBPK modeling was to predict the effects of RI on the exposure in subjects with RI relative to healthy volunteers (HV).
Methods: A PBPK model of an investigational agent for treatment cancer patients was developed and verified in SimCYP integrating in vitro, in silico, and in vivo PK data in healthy subjects. The virtual population with moderate and severe RI incorporated changes in CYP abundance, protein binding, renal function, tissue composition and blood flows in subjects with varying degrees of RI from the literatures. PK profiles of a single dose were simulated using a virtual population (10 trials of 8 individuals each) with normal, moderate and severe RI and used to optimize clinical trial design of a Phase 1 special population study in RI subjects. The results of the Phase 1 study and later a population PK modeling using pooled Phase 1 to 3 data allowed to verify the PBPK modeling and simulation results.
Results: Simulated concentration-time profiles of in HV were consistent with observed data in the Phase 1 study. However, PBPK model over-predicted exposures ($\geq$ 2 fold) in subjects with moderate and severe RI. After modifying CYP abundance in default virtual population with RI, concentration time profiles of subjects with normal renal function, moderate and severe RI were reasonable captured. PBPK model successfully predicted the RI effects (1.4 fold predicted vs 1.3 fold observed in moderate RI, 1.8 fold predicted vs 1.6 fold observed in severe RI). PBPK model predicted the effect was also confirmed using a population PK modeling. The PBPK model was utilized to further investigate of the RI effects at different dose and dose regimens (repeated doses vs single dose).
Conclusions: PBPK model predicted of effects of RI on PK exposure and was utilized to clinical development and supported potential dose modification for renal impairment population.

W-13

A PKPD Model-Based Meta-Analysis of Subcutaneously Administered Insulins in Clinical Glucose Clamp Studies

Craig Fancourt[2], Jos Lommerse[1], Bhargava Kandala[2], Thomas Kerbusch[1], Sandra A.G. Visser[2]

[1]Certara Strategic Consulting, Oss, The Netherlands; [2]Merck & Co. Inc., Kenilworth, NJ, USA

Objectives: A model-based meta-analysis (MBMA) of subcutaneously (SC) administered insulins in clinical glucose clamp studies was conducted to develop pharmacokinetic (PK) and glucose metabolism (PD) models to support systems pharmacology model development and clamp trial design.
Methods: Insulin concentration and glucose infusion rate time-action profiles were digitized for 3 to 15 published trial arms per Standard of Care insulin (lispro, RHI, glargine, and degludec) and patient population (Type 1/2 diabetics (T1DM/T2DM), and non-diabetics (ND)). A one-compartment PK model (Figure) with two sequential absorption compartments and constant endogenous infusion was applied to estimate apparent absorption rate, elimination rate, and volume. A second parameterization used clearance and volume from IV clamp studies [1,2], allowing estimation of SC bioavailability (ex-degludec). Both non-linear mixed effects models implemented variability as inter-trial baseline, and inter-arm absorption rate and bioavailability. The PD model (Figure) utilized an insulin effect compartment (for time-delay), which acts on a Hill function predicting GIR [1].
Results: Both PK models adequately described the database. Across patient populations, absorption half-life was 1.4–2.5 hr (lispro), 2.7–4.0 hr (RHI), 10.7–14.7 hr (glargine), and 21.5–25.4 hr (degludec). The half-life for insulin effect delay was 33 min, and for elimination was 5 min (ex-degludec). The PD model EC50 in ND/T1DM/T2DM was 210, 270, 480 pM (ex-degludec), and 9.0, 14.7, 38.8 nM (degludec), respectively, using GIRmax 900 mg/min (ND) and 750 mg/min (T1/2DM) from IV clamp studies [1].
Conclusions: A curated database of SC insulins in clinical glucose clamp studies was modeled, affirming that lispro, RHI, and glargine time-action profiles can be explained by the same structural PKPD model with differences in bioavailability and absorption. The models are useful both as comparators and hypothetical backbones for novel insulins.

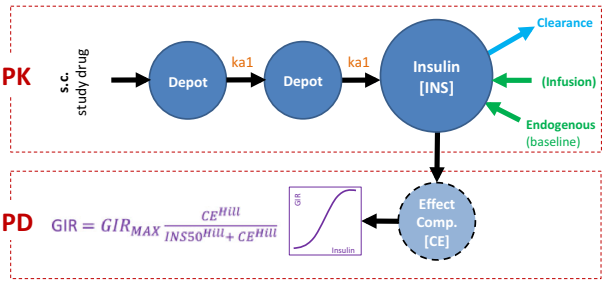

Figure 1 PKPD structure for SC Insulin Glucose Clamp MBMA (Color figure online)

References

1. Burroughs et al., ACOP 2015.
2. Kandala et al., ACOP 2015.

W-14

Physiologically Based Pharmacokinetic Modeling of Imatinib Using Simcyp

Deshun Lu[1], Kundan Kunapareddy[2], Edward Simpson[3,4], Nimita Dave[1], Sara Quinney[4,5,6]

[1]Division of Clinical Pharmacology, [2]School of Informatics and Computing; [3]Department of Bioinformatics; [4]Center for Computational Biology and Bioinformatics; [5]Department of OB/GYN; [6]ICTSI Disease and Therapeutic Response Modeling Program, Indiana University School of Medicine, Indianapolis, Indiana

Objectives: We utilized PBPK modeling and mouse tissue distribution data to predict human brain and liver concentrations of imatinib, and used this model to predict the effect of CYP3A inhibition.
Methods: A mouse full-body PBPK model for imatinib was developed using Simcyp v15 Animal (Certara®). Partition coefficients (Kp) were derived from published plasma, liver, and brain concentrations[1]. A full-body PBPK model for imatinib was developed using Simcyp V15. Liver and brain Kp's were adapted from the mouse model; default values were used for other distribution parameters. Clearance was calculated based upon published *in vitro* intrinsic clearance[2]. The effect of ketoconazole, a CYP3A inhibitor, on imatinib disposition was predicted using the default ketoconazole inhibitor profile[3].
Results: We estimated Kp values of 2.8 and 0.1 for liver and brain based upon mouse data. Using these values, the predicted:observed plasma AUC ratio following a 200 mg oral dose of imatinib mesylate in humans was 1.16 (Table 1), with AUC in liver and brain estimated as 2.9x and 0.1x plasma AUC, respectively. Ketoconazole was predicted to increase imatinib exposure 30% in plasma and 33% in liver and brain.
Conclusions: The imatinib PBPK model predicted plasma concentration in good agreement with experimental data. Uptake to liver and brain were predicted based on mouse data. The model was able to adequately predict the effect of ketoconazole on imatinib plasma disposition. Continued development of the model, including incorporation active transport, will improve the prediction of brain tumor oncentrations of imatinib.

Table 1 Predicted and observed changes in imatinib (200 mg PO) plasma AUC and Cmax when coadministered with ketoconazole (400 mg PO)

	Predicted			Observed		
	− KTZ	+ KTZ	Ratio	− KTZ	+ KTZ	Ratio
AUC (mg/L*h)	16.5	22.0	1.3	14.2	19.7	1.4
Cmax (mg/L)	0.91	1.0	1.1	0.94	1.2	1.3

References

1. Gardner et al. J Clin Exp Cancer Res 28:99 (2009)
2. Filppula et al. Drug Metab Dispos 41:50 (2013)
3. Dutreix et al. Cancer Chemother Pharmacol 54: 290 (2004)

W-15

GGvisualizer – a visualization toolkit to facilitate ggplot2 adoption in pharmacometrics

Devin Pastoor[1], Neha Mehta[1], Vijay Ivaturi[1]

[1]Center for Translational Medicine, School of Pharmacy, University of Maryland

Objectives: The purpose of this project is to create an interactive cookbook of Pharmacometric plots created with the popular R visualization library ggplot2[1] to increase efficiency and empower users to leverage the powerful customizations offered by ggplot2. Though the ggplot2 package is powerful and versatile, coding each plot can become tedious and remembering customizations can be difficult.
Methods: A selection of plots relevant to pharmacometrics such as concentration-time, visual-predictive check (VPC), distribution of demographics were designed layer by layer using ggplot2 idioms to publication quality standards. Changes for each step were noted, along with the code for each step. An R package, diffr, was created to ingest each plot and produce a visualization for each step, along with highlighted code changes compared to the previous step. Each plot was collected into a gallery of for easy visual perusal, along with a tagging system to filter plots by type.
Results: The ggvisualizer presents the user a grid of publication quality plots, further organized by various tags, such as "concentration time". Users can select a single plot to see the how the plot is created element-by-element (Figure 1), thereby allowing quick and easy lookup of relevant customizations for their particular use case. New plots can be created and added by other users using the Rmarkdown templating engine and the diffr package created for this project.
Conclusions: GGvisualizer empowers users by offering code snippets relevant for many pharmacometric scenarios. The step-by-step differences provide insight into the specifics of how each snippet of code impacts the final plot, offering the ability to extend the examples to user-specific scenarios. The creation of the diffr package further extends this concept to users interested in creating their own examples, and addresses one of the biggest pain points of ggplot2 – finding and understanding the various customizations offered.

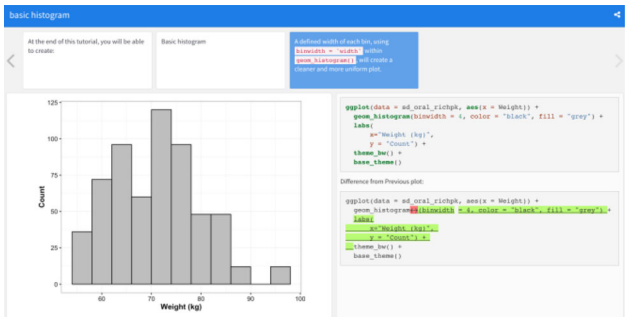

Figure 1 An example step from a previous version of a histogram to the next iteration showing the code and differences from the previous version (Color figure online)

Reference

1. H. Wickham. ggplot2: Elegant Graphics for Data Analysis. Springer-Verlag New York, 2009.

W-16

Simulation Patterns – Techniques for Optimizing Clinical Trial Simulations using R

Devin Pastoor[1], Vijay Ivaturi[1]

[1]Center for Translational Medicine, School of Pharmacy, University of Maryland

Objectives: Clinical Trial Simulations (CTS) have become a staple of the decision process across all phases of drug development. Historically, bespoke tools such as Trial Simulator have been used. Over the past couple years, the R statistical programming language has become a mainstay of data analysis tasks. As the ecosystem has evolved to introduce more powerful tooling and users have become more experienced, clinical trial simulation in R has become more and more common. This poster serves as a reference for users interested in adapting their workflows to maximize the R's potential by demonstrating pitfalls to avoid, techniques to parallelize code to take advantage of multiple cores, covering ways to monitor long-running processes, and providing code snippets utilizing new packages such as dplyr, purrr, PKPDmisc, and mrgsolve to provide a complete CTS pipeline.
Methods: The CTS pipeline was broken into three common tasks – dataset creation and resampling, scenario mapping (eg different parameter combinations), and the simulation + analysis step.
Results: Dataset creation and resampling were performed using PKPDmisc, dplyr, and tidyr idioms to both create novel datasets quickly, and resample from existing 'databases' created externally. Exploration of difference scenario combinations was handled using the functional constructs such as *by_row* in purrr. Mrgsolve was used for in-memory simulations, and ran 10-1000x faster than the same scenarios using NONMEM. Parallel simulations and processing via multidplyr and parallel packages demostrated a linear decrease in processing time per core, illustrating the increased throughput potential.
Conclusions: It was shown that R is a highly flexible and powerful tool for clinical trial simulations. By avoiding explicit looping structures, and leveraging new tooling, especially dplyr and purrr, a pharmacometrician can create flexible, modular CTS pipelines that run order of magnitude(s) faster than naïve implementations with minimal additional effort. In addition, such modular designs are ideally positioned to be wrapped in graphical user interfaces such as R Shiny to allow non-technical users to engage in further scenario exploration.

W-17

Data Science & Big Data: An Opportunity or A Threat for Pharmacometrics?

Edward Gash, Richard Pugh

Mango Solutions

Objectives: In recent years, the analytic world has become awash with buzz phrases such as "data science" and "big data", with organisations across a variety of sectors investing heavily to become more "data-driven". There are close parallels between the worlds of data science and pharmacometrics with opportunities and potential threats to both from this shift to proactive analytics.
Methods: Experience gained within the wider "data science" community provides a unique perspective on the rapid growth and demand for proactive analytics and how this can relate to the aims, constraints and behaviours found in the world of Pharmacometrics. The increasing "data science" demands in terms of core skills, techniques and approaches are evaluated to determine their alignment with the pharmacometrics world.
Results: Pharmacometricians are, by definition, early "data science" adopters in respect of the skills being sought by world-leading organisations. The identification of gaps in the pharmacometricians' typical skillsets can help identify opportunities for further training. Analysis of how the analytics function is structured within other organisations provides a key to how analytics could be further exploited in the world of PKPD. At first glance, the world of "big data" would seem to have nothing to offering to the world of pharmacometrics, since it is aimed at harnessing data sizes that are not present in life sciences. However, if we ignore the "big data" label, there are opportunities that can be harnessed (such as data streaming and distributed computing). Not only are there opportunities, but many of the required skills to exploit these opportunities already exist in the pharmacometricians' day-to-day lives (for example, an understanding of cluster computing).
Conclusions: Pharmacometricians are certainly "data scientists" based on their skillsets and remit. However, there are further opportunities in this evolving "data science" field that could be harnessed to great effect.

References

1. Justin J. Wilkins, E. Niclas Jonsson. Reproducible Research. PAGE Meeting, Glasgow (2013).
2. S Locke (2015, November 20). Launching the Data Science Radar [blog]. Retrieved from http://www.mango-solutions.com/wp/2015/11/launching-the-data-science-radar/
3. R Pugh (2015, June 25). The Single Most Important Skill for a Data Scientist [blog]. Retrieved from http://www.mango-solutions.com/wp/2015/06/the-single-most-important-skill-for-a-data-scientist/

PAGE, Lisbon, Portugal, 9th of June 2016 PAGE 25 (2016) Abstr 5800 [www.page-meeting.org/?abstract=5800]

W-18

Model-Based Sotalol Pediatric Dosing Recommendations

Elyes Dahmane[1], Jogarao V.S. Gobburu[1], Vijay Ivaturi[1]

[1]Center for Translational Medicine, School of Pharmacy, University of Maryland

Objectives: Sotalol is approved in pediatrics to treat atrial and ventricular arrhythmia. The label dosing recommendations based on body surface area (BSA) and age-dependent renal maturation are prone to error calculations due to their complexity. Patients under sotalol need to be monitored for QTc prolongation for at least 3 days until steady-state exposure is reached. Our objectives are, first, to provide a dosing chart based on body weight (BW) and age, secondly, to develop an IV/Oral switch regimen to reduce length of hospital stay.
Methods: Parameters from a sotalol population pharmacokinetic model[1] was used to develop an easy to use BW based dosing chart as opposed to BSA. Three different BW-only based formulae (Livingston and Lee, Boyd and Costeff) were evaluated as an alternative to Mosteller formula to estimate BSA. Model-based simulations were performed to determine an optimal IV loading dose before switching to an oral maintenance regimen.
Results: Costeff formula provided the closest estimation to the BSA-based doses with a median bias (95% CI) of 0% (-3.6% to 2.8%) and 0.6% (-3.1% to 5.7%) for the 0-2 years and 2-20 years old age groups, respectively. The resulting dosing charts for treatment initiation are

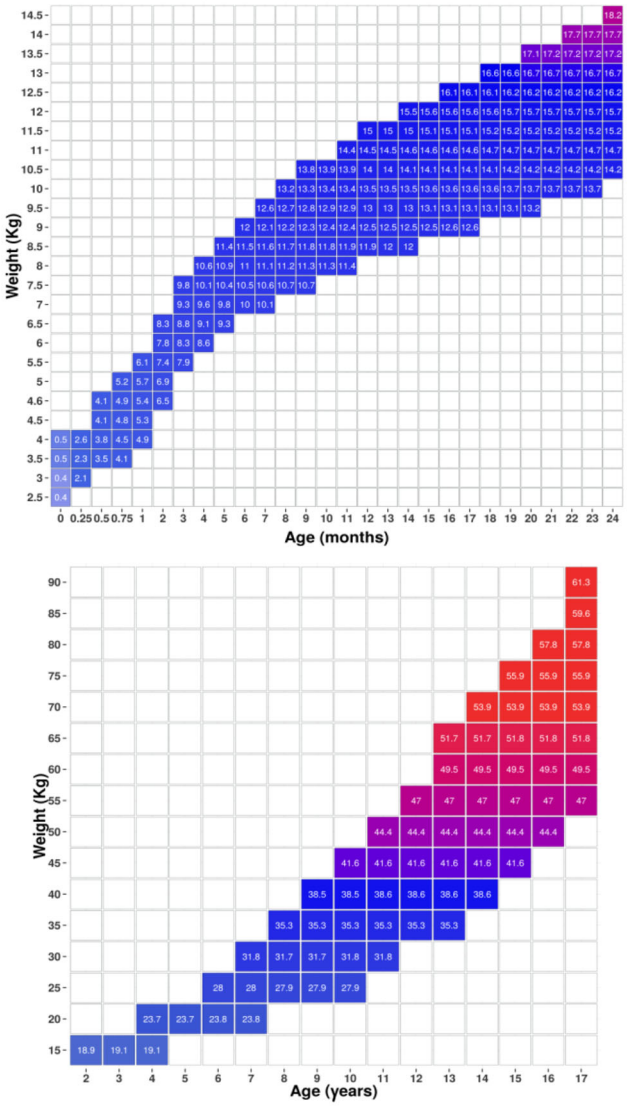

Figure 1 Sotalol dosing nomogram, equivalent to the approved 30 mg/m^2 t.i.d, in patients with normal renal function: (*upper panel*) neonates and infants from 0 to 2 years old and (*Lower panel*) children and adolescent from 2 to 17 years old (Color figure online)

illustrated in in Figure 1. An IV loading dose of 1.5 mg/kg over a 2-hour infusion followed by the recommended t.i.d oral sotalol initiation dose is the optimal dosing regimen that would allow the achievement of target exposures in neonates. For patients older than 1 month, an IV loading dose corresponding to half of the recommended oral dose infused over 1 hour, followed by the regular oral dosing regimen allowed to achieve the target exposure on day 1.

Conclusions: The proposed dosing chart based on age and BW, provides clinicians with a useful tool for dose selection, consistent to the label-approved doses. We also provide a safe alternative to use IV sotalol formulation in clinics to optimize sotalol therapy and to facilitate early attainment of target exposures.

Reference

1. Betapace Pharmacology Review. http://www.accessdata.fda.gov/drugsatfda_docs/nda/2001/19-865S010_Betapace_pharmr.pdf.

W-19

Best Practices for Preparation of Submission Quality Data Sets for Pharmacometric Analysis

Erin Dombrowsky, Prema Gopalakrishnan, Amit Roy, Jyothi Bandaru, Neelima Thanneer

Clinical Pharmacology and Pharmacometrics, Bristol Myers Squibb, NJ

Objectives: Accurate and transparent preparation and reporting of pharmacometric (Pm) analysis datasets is critical for ensuring the quality and reproducibility of Pm analyses, and facilitating regulatory review. We describe Best Practices that have enabled the preparation of submission quality datasets that are consistent with the FDA eCTD electronic submission requirements, and are transparent with respect to variable imputations and exclusion of data.

Methods: General recommendations to ensure traceability and transparency of Pm analysis data sets are given below:

- Include key header variables to enable merging of data from other data sets
- The analysis data set variables should include all of the observations in the source data, irrespective of whether all values are included in the analysis
- Retain transparency for imputed values
- The SAS transport file submitted to the regulatory should be the model input file. A supporting document can be submitted explaining how to plug in the SAS transport file into the model to enable reproducibility of the analysis

In the data definition file (define.pdf) labels of quantitative variables should include units, and codes for numeric versions of categorical variables should be provided.

The analysis population, should clearly be described in the data set specification, and the Pm report should include a table summarizing the derivation of the analysis population from the overall study population.

Overall and study level summaries of the analysis data set should be provided, including a summary of the missing values of each variable included in the analysis

Results: Inclusion of header variables ensures traceability and facilitates incorporation of additional variables from source data, as needed. Transparency is attained by inclusion of all relevant source data in the analysis data set and visibility of imputations in data set specification. Data set records excluded from the analysis are identified with a flag variable together with the reason for exclusion

Conclusion: Best practices have resulted in more streamlined e-submissions, and avoided data-related questions from regulatory authorities.

W-20

A Browser-based NONMEM Data Specification Order Form

Robert Fox[1], Huan Liu[1], Nidal Al-Huniti[1]

[1]Quantitative Clinical Pharmacology, AstraZeneca, Waltham, MA

Objectives: The objective was to develop a browser-based NONMEM data specification order form to improve the process for creating POP PK NONMEM data specifications. The order form needed to have end-user and administrator functionality and with the potential for PKPD and multi-study or project level expansion.

For end-users, the tool needed to be easy to understand, easy to use and to be immediately effective. It needed to provide clear, consistent

instructions, and produce consistent layout. It needed to easily enforce standards (variable names, labels, instructions, code lists, and formulae) in a natural way and to control versions. For the administrators, the tool needed to be sufficiently flexible to allow additions and updates of variable names and definitions; yet, sufficiently secure to prevent unauthorized changes. It needed to allow updates to on-the-fly instructions (pop-ups) and to manage and modify code lists, formulae, drop-down selections and variable groupings.

Methods: JAVA was used to program the browser-based order form with separate end-user and administrative capabilities. Oracle was used as the backend for storing, initializing and maintaining standards, formulae, code list, groupings, etc and for archiving and maintaining NONMEM specification versions.

Results: The tool is being used for all new studies as AstraZeneca. Legacy studies are considered on a case-by-case basis. Feedback from pharmacometricians has been positive. Suggestions for "nice-to-have" enhancements denote positive uptake.

Conclusions: The browser-based order form eases the burden in developing the NONMEM programming specifications. It produces fast and reliable data instructions with consistent variable definitions that can be efficiently applied across studies and drugs with minimal modification. Its natural enforcement of standards enables programmers to develop generic SAS code for data set generation and for diagnostic data summaries and diagnostic plots.

W-21

Quality Award Winner (Non-Trainee Category)

Mechanistic approach to describe multiple effects of regulatory molecules on cell dynamics process in immune response

Oleg Demin[1], Evgeny Metelkin[1], Galina Lebedeva[1], Sergey Smirnov[1]

[1]Institute for Systems Biology Moscow

Objectives: To develop mechanistic approach enabling to describe multiple effects of cytokines, chemokines and other regulatory molecules on immune cell proliferation, differentiation, migration, apoptosis and cytokine production; to derive formula describing multiple effects of activators, inhibitors and (de-)sensitizers and to explore the ways of integration of the formula in systems pharmacology models of immune response and identification of its parameters against *in vitro* data.

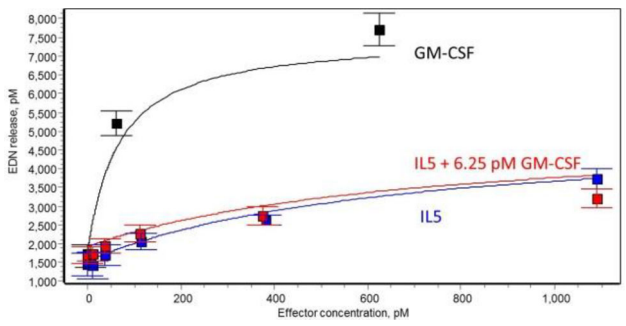

Figure 1 Effect of GM-CSF (*black*), IL5 alone (*blue*) or in combination with 6.25 pM of Gm-CSF (*red*) on release of eosinophil-derived neurotoxin. Data taken from [3] (Color figure online)

Methods: General principles of receptor theory are applied to develop an approach for description of multiple effects of regulatory molecules on cell dynamics. The formula describing the combined effect of activators, inhibitors and (de-)sensitizers is derived within the framework of quasi-equilibrium approach and represents an upgrade of the multiple effect description implemented in Immune Response Template database [1] constructed by Institute for Systems Biology Moscow. Parameters of the formula are fitted against *in vitro* data from multiple sources using the Hook-Jeeves method as implemented in the DBSolve Optimum package [2].

Results: The formula derived within the framework ofthe mechanistic approach enables successfull description of the multiple effects of regulatory molecules on cell dynamics of immune cells. The ways to integrate the formula within systems pharmacology models describing immune response and to identify its parameters against *in vitro* data are proposed. The approach is applied to describe cell dynamics of lymphocytes and eosinophils (Fig 1).

Conclusions: The approach allows to successfully describe effect of multiple activators, inhibitors and (de)sensitizers on cell dynamics of immune cells.

References

1. Nikitich A, Demin O Jr, Demin O. 2016. ASCPT. San Diego, CA.
2. Gizzatkulov N, et al. BMC Systems Biology, 2010, 4 (109): 1-11
3. Horie S, et al. J Allergy Clin Immunol 1996;98:371-81

W-22

Immune Response Template for Quantitative Systems Pharmacology Modeling of Immunotherapy in Oncology

Oleg Demin Jr[1], Antonina Nikitich[1]

[1]Institute for Systems Biology Moscow

Objectives: The main aim of this study is to develop a tool (Immune Response Template (IRT)) describing interaction of different types of immune cells, cytokines and facilitating the development new immunotherapies and their combinations.

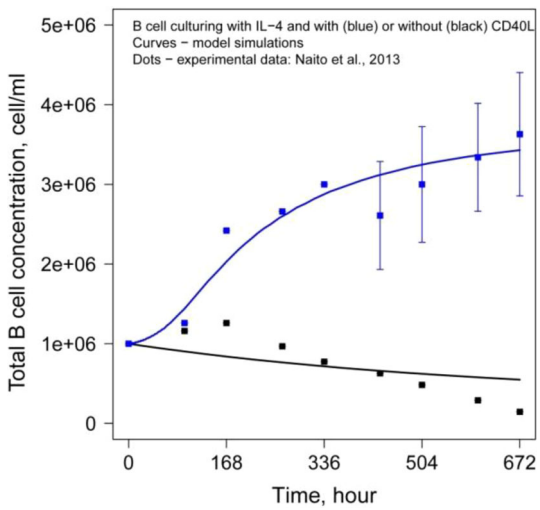

Figure 1 Effect of CD40 ligand on B cells (Color figure online)

Methods: IRT represents a family of ODE- based models including both models of individual immune cells and integrated simulation platform describing interactions of multiple immune cell types, cancer cells, soluble mediators, cell-cell contact effects (via surface molecules PD-1:PD-L1, CD40:CD40L, CD3:MHC-II) etc.
Results: The models was partially calibrated against publicly available in vitro and in vivo data including activation of T helper cells, CD40-ligand effect on dendritic and B cells (see Figure 1), production of cytokines by immune and cancer cells, half-lives immune cells, effect of cytokines on different processes etc.
Conclusions: IRT recapitulates essential immune response pathways, effect of immune response on tumor and vice versa. IRT could be used as a tool for data analysis and interpretation, understanding of mechanisms of action of different immunotherapies and their effects, optimization of treatments related to immune response and evaluation of new target in immune system for cancer treatment.

W-23

Pharmacometrics in mHealth: the Driving Force for Patient Centered Care

Fahima Nekka PhD[1], Chantal Csajka PhD[2], Mélanie Wilbaux PhD[3], Sachin Sanduja MD[4], Jun Li PhD[5], Marc Pfister MD[6]

[1]Montreal, Canada; [2]Lausanne, Switzerland; [3]Basel, Switzerland; [4]North Brunswick, USA; [5]Montreal, Canada; [6]Basel, Switzerland

Objectives: Computerized tools are becoming increasingly important in the field of research and development of new pharmaceuticals as well as in the daily management of every individual patient's health and disease. These computerization processes promote high efficiency, low cost and less burden on the health system.
Methods: A multiple steps operating model was proposed and adopted for a successful pharmacometrics-based mHealth development. It consists of validated scientific knowledge, up-to-date technical options, regulatory concerns, and commercialization avenues.
Results: Three mHealth tools in different therapeutic areas and purposes were developed following this process. This consists of a mobile App for psychiatrists to personalize treatment of attention deficit hyperactivity disorder for children, a user-friendly Bayesian software tool for dosage individualization to optimize therapeutic drug monitoring and personalize dosing, and a web-based interface to forecast and manage individual weight changes in term neonates.
Conclusions: Pharmacometrics will be pivotal in the transition of health care towards mHealth. This will bring a large benefit to specific patient groups or individuals.

W-24

Modelling the Emergence of Resistance to Chemotherapeutics with Virtual Tumour

Frances Brightman, Eric Fernandez, David Orrell, Christophe Chassagnole

Physiomics plc, Oxford, UK

Objectives: Drug resistance is a major cause of treatment failure in cancer [1] that arises from mutations in the genome of cancer cells and/or epigenetic changes [2]. This issue is compounded by considerable tumour genetic heterogeneity, and it is therefore becoming increasingly clear that cancer should be managed through personalized medicine [3, 4]. Recent studies have shown that the emergence of drug resistance can at least be delayed using novel dosing regimens [5,6].
Methods: Physiomics has developed a 'Virtual Tumour' (VT) technology that can predict how a tumour will respond to drug exposure. The VT technology integrates pharmacokinetic and pharmacodynamic effects, and models the way individual cells behave within a tumour population. These agent-based methods are particularly suitable for modelling multiple cell populations, and representing the tumour heterogeneity. As a first step toward developing personalized medicine solutions, we have incorporated chemotherapeutic resistance into our VT platform.
Results: The VT has been extended with a resistance module, which has been developed, calibrated and qualified using literature data [6]. This module captures the fundamental mechanism by which resistance arises. Through this case study, we demonstrate that the extended VT can be applied to model the emergence of resistance in patient-derived xenografts. Furthermore, we show that the VT can be used to identify and optimize therapeutic strategies for delaying the emergence of drug resistance.
Conclusions: Our enhanced VT capability represents the first step towards a tool for developing personalized treatment, which is set to revolutionize cancer therapy in the near future, especially for patients with resistant disease.

References

1. Farrell, A. Nat. Med. 17, 262–265 (2011).
2. Gottesman, M. M. Annu. Rev. Med. 53, 615–627 (2002).
3. Rebucci, M. & Michiels, C. Biochem. Pharmacol. 85, 1219–1226 (2013).
4. Gonzalez de Castro, D. et al. Pharmacol. Ther. 93, 252–259 (2013).
5. Chmielecki, J. et al. Sci. Transl. Med. 3, 90ra59 (2011).
6. Das Thakur, M. et al. Nature 494, 251–255 (2013).

W-25

A Semi-Mechanistic Binding Model for the Population Pharmacokinetics and Pharmacodynamics of BMS-986168, a Tau-directed Monoclonal Antibody

Giridhar S. Tirucherai[1], Jessie Wang[2], and Malaz AbuTarif[1]

[1]Clinical Pharmacology and Pharmacometrics, Bristol-Myers Squibb, Princeton NJ 08540; [2]Global Biostatistics, Bristol-Myers Squibb, Princeton, NJ 08540

Objectives: To develop a PK-PD model that simulatenously characterizes the PK in serum and cerebrospinal fluid (CSF) and the PD (reduction in free extracellular tau, "eTau") in CSF following single IV infusion administration of BMS-986168 to normal healthy volunteers.
Methods: A semi-mechanistic binding model with a quasi-equilibrium (QE) approximation was used to describe the PK of BMS-986168 in serum and CSF, and the corresponding reduction in free eTau levels in CSF. The model was fit to free BMS-986168 concentrations in serum and CSF and free eTau in CSF following administration of single IV infusion doses in a SAD study. Nonlinear mixed effect modeling was performed using Phoenix NLME. The model was assessed using goodness of fit plots and visual prediction checks. A Bayesian Emax exposure-response model was also fit to observed data of percent suppression of etau in CSF and concentration of BMS-986168 in CSF at matching time points.
Results: Serum PK of BMS-986168 after an IV infusion was described by a 2-compartment model. A 3rd compartment was used to

characterize the entry of drug into CSF, and the association and disposition of drug and eTau in CSF. The biology of eTau fragments was characterized using zero-order production (ksyn) and first-order elimination rate constants (kdeg). The binding of BMS-986168 to the eTau fragments was captured by Kd. Concentration dependent increase in Kd was observed and modeled using an Emax relationship. Inter-individual variability in model parameters was estimated using exponential error structure. Residual variability in serum and CSF BMS-986168, and eTau concentrations were modeled as proportional. The robust suppression of eTau levels in CSF (extent and persistence of suppression) was well described using the PK-PD model. There was good agreement between the predicted percent suppression of eTau based on the PK-PD model and the Bayesian Emax model at discrete timepoints.

Conclusion: The semi-mechanistic PK-PD model was able to simultaneously describe the concentration-time profile of both BMS-986168 (in serum and CSF) and free eTau in CSF across the dose range studied. The model developed in normal healthy volunteers has broad applications and can be used with appropriate modifications to predict the PK-PD in various patient populations, as well as to simulate previously untested dosing regimens.

W-26

Evaluation of the Relationship between Changes in PK Parameters and its Corresponding Change on Steady-State Drug Exposure

Haitao Yang[1], Yan Feng[2], Xiaoyu Yan[3], Stephan Schmidt[1], Lawrence Lesko[1], Amit Roy[2], Liping Zhang[3], Honghui Zhou[3], Xu Steven Xu[3*]

[1]University of Florida, FL, [2]Bristol-Myers Squibb, NJ, [3]Janssen Research & Development, NJ

Objectives: Identification of clinically relevant covariates/factors in Population PK analysis (PPK) is often based on the magnitude of their effects on PK parameters. A >20-25% effect on PK parameter is commonly considered clinically relevant. However, the translation of a covariate effect from on PK parameters to on steady-state exposure is not well understood and not always straightforward. The current analysis aims to evaluate the PK-to-exposure translation for a covariate effect.

Methods: The values of PK parameters of 74 drugs with 1-comparmtent and 51 drugs with 2-comparment kinetics were obtained from literatures and were used to predict the change in steady-state exposures, ie, trough (C_{minss}) and peak (C_{maxss}) concentrations, assuming a 20% change in PK parameters. All drugs were orally administered (either QD or BID). The relationship between changes in exposure and change in PK parameters was assessed.

Results: Exposure was mostly influenced by apparent clearance (CL/F); 20% change of CL/F could lead to a substantial change of C_{minss} (ΔC_{minss}; up to a few folds), particularly for compounds whose half-life ($T_{1/2}$) is shorter than the actual dosing interval. ΔC_{minss} decreased with increasing $T_{1/2}$ and reached plateau when $T_{1/2}$ was large. However, 20% change in Ka, Vp/F and Q/F had only minimal impact on exposure (<20%). Additional subgroup analysis showed similar pattern of PK-to-exposure translation across all four Biopharmaceutics Classification System classes, indicating that this translation may be independent of drug's physicochemical properties.

Conclusions: The PK-to-exposure translation could be more than proportional for some compounds. When assessing clinical relevance of covariates in PPK analysis, their influence on steady-state exposure should be taken into consideration.

W-27

Interactive Web Applications for Clinical Trial Simulation and Reporting: R Shiny with 'adsim' Package for Model-based Simulation in Alzheimer's Disease

Haoyu Wang[1], Dan Polhamus[2], Jim Rogers[2], Klaus Romero[3], Puneet Gaitonde, Brian Corrigan[4] and Kaori Ito[4]

[1]Department of Statistics, North Carolina State University, Raleigh, NC; [2] Metrum Research, Tarrifville CT, Critical Path Institute, Tucson, AZ, [4] Pfizer Inc., Groton, CT

Objectives: An open-source web-based Alzheimer's Disease (AD) trial simulation application was developed using the R packages "shiny" and "adsim". The app allows for simulation, visualization and reporting of simulation results of common AD trial designs utilizing ADAS-cog, a common measure of cognition used as a primary endpoint in AD clinical trials. The tool is designed for all users in a clinical development team, including individuals and does not require knowledge in R.

Methods: Individual and Summary level data from AD patients was used to develop a longitudinal disease progression model, which was then developed as an R package (adsim) for trial simulation in mild and moderate AD. Using the adsim package shiny, an open-source R based application suitable for use by members of a drug development team was developed. The code is maintained in an open source repository to allow for ongoing use/upgrade by any interested party.

Results: The app is available at https://isop.shinyapps.io/Alzheimer/. The source code is available at https://github.com/why94nb/shiny-app-for-adsim . The app consists of six tabs that allow the user to set up, run and view results from the simulation. Spaghetti plots and figures about baseline information (gender, age, ApoE and MMSE) are available to download. A test statistics summary is shown in the "Simulation Summary" tab. In addition, patient tables are downloadable for further analysis and the user can also download a report summarizing parameter settings and all the outputs generated during the simulation.

Conclusions: We have developed an open-source R shiny app to allow development team members to perform Alzheimer's Disease clinical trial simulation, utilizing an open and reproducible way to visualize simulation results and to share the results within the clinical team(clinical pharmacology, statistics and clinicians) .

Figure 1 Snapshots of the user interface of the app (Color figure online)

W-28

Development of a translational systems physiology model of renal function in normal and diabetic mice, rats, and humans

Hari Shankar Mahato[1,*], Christine Ahlstrom[2], Rasmus Jansson Löfmark[2], Melissa Hallow[1]

[1]College of Engineering, University of Georgia; [2]CVMD iMed DMPK Astrazeneca R&D, Gothenburg, Sweden

Objectives: Interspecies differences in renal function may contribute to challenges in predicting clinical responses from preclinical models of kidney disease. Mathematical models may provide a means to interpret these interspecies differences, and thus we aimed to parameterize a systems model of renal physiology for humans, rats, and mice, to facilitate translational prediction of responses to therapies from common animal models to humans.
Methods: The basic physiological processes of renal function (filtration/reabsorption) are consistent across species. Some structural and functional characteristics are also preserved (e.g. glomerular ultrafiltration coefficient, pressures, single nephron flow rates), while others differ markedly (e.g. vascular resistances, nephrons number, tubular lengths, etc). Using an existing systems model of renal hemodynamics, we utilized literature studies in mice, rats, and humans to parameterize the model for each species. We also collected literature data on the phenotypic behavior of each species (e.g., glomerular filtration rate [GFR], cardiac output, blood pressure, etc.). We then simulated the phenotypic behavior using species-specific model parameters. After modeling the normal animal, we repeated this for the db/db mouse model, characterizing differences in input parameters (e.g., glucose levels, sodium and water intake) and phenotypic responses between mouse and human diabetes (e.g., hyperfiltration).
Results: With a small number of parameter changes, the model was able to reproduce phenotypic responses in all three species. The model also implicitly reproduced the magnitude of GFR rise (hyperfiltration) observed in db/db mice.
Conclusions: These results confirm that this mechanistic model provides a valid description of renal function across different species. Going forward, we will also characterize differences in the timecourse of kidney disease progression, and use responses to benchmarking therapies enalapril and eplerenone, for which both preclinical and clinical data is available, to validate the model's translational ability. The healthy and db/db mice models would help to interpret the progression of diabetic nephropathy in humans.

W-29

A New Tumor Dynamics Mathematical Model

Helen Moore

Bristol-Myers Squibb, Princeton, NJ

Objective: To propose a new mathematical model to capture tumor dynamics in clinical treatment data.
Methods: During analysis of clinical data from cancer patients receiving various treatments, the need for a different tumor dynamics model arose—in particular, one that allows a nonzero horizontal asymptote and does not have unbounded long-term growth. The model proposed here satisfies these requirements and was able to fit clinical data from a variety of oncology therapy studies. The model was compared with certain historical models, including some from [1], [2], and [3], using the FOCE-ELS algorithm in Phoenix NLME version 6.4.0.768 (Certara USA, Inc.). Several data sets were used in order to include multiple indications and therapies. The new model allows for tumor sizes that first increase then decrease, first decrease then increase, or change only monotonically. The figure below shows example model curves that exhibit each of these behaviors.

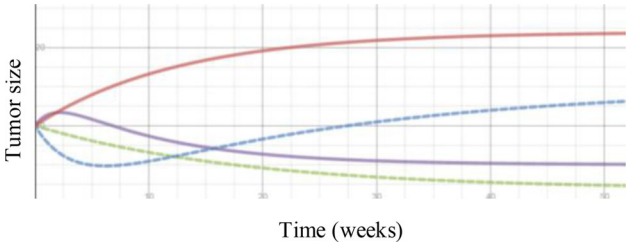

Results: In a number of goodness-of-fit measures, including diagnostic plots and the Bayesian information criterion, the new model (without covariates) performed better than several historical models considered (also without covariates). These results held across indications and therapies.
Conclusions: The new model proposed here fit certain clinical data sets better than several historical models and may provide advantages in future modeling and simulation of tumor dynamics.

References

1. Ribba B, Holford NH, Magni P, et al. A review of mixed-effects models of tumor growth and effects of anticancer drug treatment used in population analysis. *CPT Pharmacometrics Syst Pharmacol*. 2014;3:e113.
2. Stein WD, Gulley JL, Schlom J, et al. Tumor regression and growth rates determined in five intramural NCI prostate cancer trials: the growth rate constant as an indicator of therapeutic efficacy. *Clin Cancer Res*. 2011;17:907-917.
3. Wang Y, Sung C, Dartois C, et al. Elucidation of relationship between tumor size and survival in non-small-cell lung cancer patients can aid early decision making in clinical drug development. *Clin Pharmacol Ther*. 2009;86:167-174.

W-30

PK – PD of Crohn's Disease Activity Index after treatment with risankizumab, an IL-23 inhibitor

Hugo Maas[1], Matthias Diebold[1], Wulf Boecher[3] Bojan Lalovic[2]

Translational Medicine Clinical Pharmacology[1,2] and Medicine[3] Boehringer Ingelheim Pharma GmbH & Co. KG, Germany and Boehringer Ingelheim Pharmaceuticals Inc., Ridgefield, CT, USA

Objectives: To develop a longitudinal PK-PD model of Crohn's disease activity index (CDAI) after at least 12 weeks of induction treatment with two doses of risankizumab vs. placebo in an ongoing Proof of Concept trial.
Methods: Moderate-to-severely active CD Patients (N=121) were treated with 200 or 600 mg risankizumab or placebo every 4 weeks (q4w) intravenously (IV) for 12 weeks, followed by 600 mg IV q4w from week 14 until week 26 in patients who were not in deep remission (CDAI <150 and CDEIS $\leq$4 [$\leq$2 for isolated ileal disease]) at week 12. Patients achieving clinical remission at week 26 continued with 180 mg SC q8w through week 52 in a maintenance period. Risankizumab pharmacokinetics (humanized IgG) were described using a two compartment model, based on phase I and II studies in

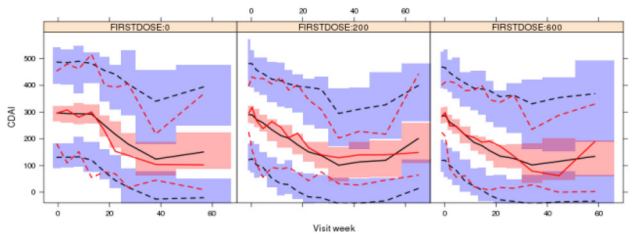

Figure 1 Visual predictive check for the CDAI model stratified by starting treatment ("FIRSTDOSE"). Observation times were binned using planned visit times. The *solid black line* denotes the predicted median CDAI, the solid red line denotes the observed median CDAI. The *dashed lines* represent predicted (*black*) and observed (*red*) 2.5th and 97.5th percentiles. The *blue* and *red* areas represent 95% confidence intervals around the predicted percentiles (Color figure online)

psoriasis and CD. An indirect response PK-PD model accounted for patients' dosing history, demographics, individual-level PK and available CDAI data.

Results: Current model adequately described available CDAI time-course data, reflecting the characteristics of this combined re-/induction and maintenance study. At week 12, typical 600 mg IV q4w treatment was estimated to achieve CDAI remission of 29% (CDAI < 150 points) vs. 21% for 200 mg IV q4w and was predicted to increase with time. Body weight was noted to be inversely related to risankizumab exposure and baseline CDAI scores. Compared to patients who proceeded into maintenance, patients who had their last observation between week 12 and 26 were less likely to improve, expressed in terms of a higher IC_{50} parameter.

Conclusions: The model represents the initial characterization of risankizumab exposure vs. CDAI time course. Beyond week 26, lower, SC dosing may suffice for maintenance of clinical efficacy. This may be partially due to protocol-specified enrichment of patients exhibiting lower IC_{50} estimates and a low baseline CDAI, since only patients with clinical remission continued beyond week 26.

W-31

Predicting morphine drug exposure in elderly using an age-informed physiologically based pharmacokinetic approach

Jan-Frederik Schlender[1,2], Michaela Meyer[2], Kirstin Thelen[2], Markus Krauss[2], Michael Block[2], Stefan Willmann[2], Thomas Eissing[2], Ulrich Jaehde[1]

[1]Institute of Pharmacy, Clinical Pharmacy, University of Bonn, 53121 Bonn, Germany; [2]Bayer Technology Services GmbH, Computational Systems Biology, 51368 Leverkusen, Germany

Objectives: Elderly patients are often underrepresented in clinical trials, yet receive the majority of the prescribed drugs. The resulting knowledge gap regarding the pharmacokinetic (PK) drug exposure of elderly subjects may jeopardize their pharmacotherapy. The goal of this study was to apply a recently developed age-informed physiologically based pharmacokinetic (PBPK) approach to encompass the full course of healthy aging supporting dose selection of the test compound morphine. The results in this abstract have been published in part [DOI: 10.1007/s40262-016-0422-3].

Methods: The capability of the age-informed PBPK database to predict PK of drugs was verified using the software PK-Sim®, using intravenously administered Morphine as test compound. Morphine is mainly cleared by phase II metabolism. Literature information about plasma concentration time profiles and major PK parameters for morphine was compared to those predicted by PBPK simulations, for both younger and older adults.

Results: Based on the age-informed physiology, the predicted PK parameters described age-associated trends well. Using the age-informed physiology, the root mean squared prediction error was reduced by 49% for the simulations of plasma concentrations in elderly subjects. Individual V_{ss} and $t_{1/2}$ values were mostly within the two-fold range for the elderly population simulations.

Conclusions: The results of this study support the feasibility of using a knowledge-driven PBPK model to predict PK alterations throughout the entire course of aging, and thus to optimize drug therapy also in elderly individuals. These results indicate that pharmacotherapy and safety-related control of geriatric drug therapy regimens may be greatly facilitated by the information gained from PBPK predictions.

W-32

Value of Model-Based Characterization of Time-Profile of Tumor Lesion Data to Assess Treatment Effect in Patients With Non-Small Cell Lung Cancer (NSCLC)

Jingshan Zhang, Satyendra Suryawanshi, and Amit Roy

Bristol-Myers Squibb, Princeton, NJ

Objective: Conventionally, response to treatment of patients with solid tumors is assessed by RECIST criteria, whereby the sum of the longest diameters of index tumor lesions is employed as a measure of the aggregate tumor burden. This measure of response is agnostic to the number of index lesions used to compute the aggregate tumor burden. This analysis investigated the value of describing patients' tumor lesion level response to treatment, relative to describing the aggregate index tumor burden response.

Methods: Longitudinal tumor lesion data from 426 patients with NSCLC treated with docetaxel were fit to 3 versions of the tumor growth dynamics model of Wang et al [1], describing alternative measures of tumor response: aggregate tumor burden (Model 1), average of the longest diameters of index lesions (Model 2), or longest diameter of each index lesion (Model 3). All 3 models were parameterized in terms of baseline tumor burden/lesion size, shrinkage rate constant (TS), and growth rate (TG). Models 1 and 2 incorporated between patient variability in these model parameters, whereas Model 3 incorporated both between and within patient variability of these parameters.

Results: Table 1 presents the parameter estimates of the 3 alternative models of tumor response. The between patient variability of TS and TG were comparable across the 3 models. However, the within patient variability of TS and TG parameters in Model 3 was higher than the between patient variability.

Conclusions: Between lesion variability in response may inflate the extent of between patient variability in response. Tumor growth dynamic models describing the time-profile of individual lesions may

Table 1. Parameter estimates of models describing alternative measures of tumor response.

Parameter	Model 1	Model 2	Model 3
Fixed Effects, estimate (5-95%CI)			
TS (1/week)	0.0234 (0.0188-0.0280)	0.0202 (0.0159-0.0245)	0.0127 (0.0102-0.0152)
TG (cm/week)	0.116 (0.0980-0.134)	0.0494 (0.0415-0.0571)	0.0266 (0.0229-0.0303)
BASE(cm)	6.68 (6.23-7.13)	3.16 (3.01-3.31)	2.65 (2.55-2.75)
Random Effects, Variance (5-95%CI)			
TSpatient	0.792 (0.537-1.05)	0.833 (0.557-1.11)	1.17 (0.884-1.46)
TSlesion			2.71 (2.11-3.31)
TGpatient	1.01 (0.751-1.27)	0.790 (0.588-0.992)	0.514 (0.443-0.585)
TGlesion			1.18 (0.957-1.40)
BASE	0.385 (0.323-0.447)	0.210 (0.176-0.244)	0.324 (0.289-0.359)

be more sensitive to detecting the effect of treatment than models of aggregate tumor burden

Reference

1. Wang Y, et al. *Clin Pharmacol Ther*. 2009;86:167-174.

W-33

Simulations of Dulaglutide Phase 3 Studies Using a Quantitative Systems Pharmacology Model of Diabetes

Jeanne Geiser[1], Lai San Tham[2], Zvonko Milicevic[1]

[1]Eli Lilly and company, Indianapolis, IN; [2]Lilly-NUS Centre for Clinical Pharmacology, Singapore

Objectives: Evaluate quantitative systems pharmacology (QSP) metabolism model predictions for 2 trials of once-weekly glucagon-like peptide-1 receptor agonist (GLP-1 RA) dulaglutide conducted in type 2 diabetes (T2D) patients with different baseline disease states.
Methods: A QSP metabolism model of diabetes was developed that describes glucose and insulin fluxes following adminstration of GLP-1 RA or insulin glargine titrated base on target glucose. Two Phase 3 dulaglutide (DU) studies were simulated using virtual T2D patients (VP) with wide range of insulin secretion and sensitivity which were generated with baseline characteristics matched to the protocol criteria. Study A compared weekly DU to individually titrated daily GL in a 52 week trial [AWARD 2] [1]. Study B compared 1.5 mg QW DU to placebo as add-on to individually-titrated glargine. The predictive performance of the model was evaluated using the observed results from the completed trials.
Results: Study A (250 VPs, 8.1% mean baseline HbA1c) predicted a greater change of HbA1c for 1.5mg DU over GL, agreeing with the observed LS mean difference of −0.45%, 95% CI [−0.60%, −0.29%]. Study B (150 VPs, 8.4% mean baseline HbA1c) predicted a greater change in HbA1c with DU over placebo, agreeing with the observed LS mean difference of −0.77%, 95% CI [−0.97%, −0.56%)]. The model predicted well for change in body weight and self-monitored blood glucose (SMBG). However, hypoglycemic event counts were overpredicted compared to the observed, although the difference between treatments was consistent with the observed. This may be attributed to differences between the continuous recording of glucose in simulations versus frequency of reporting in clinical settings.
Conclusions: This QSP model adequately predicted HbA1c, body weight, and SMBG in 2 DU Phase 3 trials in T2D patients for DU and GL. These results give greater confidence in using the model to evaluate alternative pharmacological agents, study designs and patient populations.

Reference

1. Giorgino F, et al. Diabetes Care 38.12: 2241-2249, 2015.

W-34

Model-Based Study Design Revealing the PKPD Relationship of Pembrolizumab in the KEYNOTE-001 Melanoma Trial

Jeroen Elassaiss-Schaap[1], Stefaan Rossenu[2], Andreas Lindauer[3], S. Peter Kang, Rik de Greef[4], Jeffrey R. Sachs, Dinesh P. de Alwis

PPDM-QP2, Merck & Co., Inc., currently [1]PD-Value, [2]Janssen Pharmaceuticals, [3]SGS Exprimo NV, [4]Quantitative Solutions

Objectives: Evaluation of PKPD properties played an important role in the early clinical development of pembrolizumab. Analysis of data from a traditional 3+3 dose-escalation design in KEYNOTE-001 revealed several critical uncertainties in PKPD properties. A trial design able to clarify these properties needed to be quickly developed, executed, and analyzed to provide an early assessment of potential pembrolizumab dose regimens to be tested for clinical efficacy.
Methods: A model-based approach was implemented to design and evaluate a robust follow-up study. Intensive multidisciplinary consultation rounds led to the establishment of a paradigm (template) of fast, within-patient dose escalation to minimize patients' exposure to potentially ineffective concentrations.
14,000 virtual trials (leveraging this within-patient dose escalation) were stochastically generated (Figure) using that clinically acceptable design template, wide dose-ranges, and wide PKPD-parameter-ranges that included estimates from previous data. Designs were evaluated (using simulated data) for ability to correctly identify parameters.
Results: Design optimizations led to a clinical study with three dose levels per subject, extending the dose range by 200-fold. Modeling of the data resulting from execution of that design demonstrated that pembrolizumab pharmacokinetics are nonlinear at <0.3 mg/kg every 3 weeks (Q3W), but linear in the clinical dose range. Saturation of *ex vivo* target engagement in blood began at ≥1 mg/kg Q3W, and a steady-state dose of 2 mg/kg Q3W was needed to reach 95% target engagement, supporting examination of 2 mg/kg Q3W in ongoing trials in melanoma and other advanced cancers.
Conclusions: Multidisciplinary collaboration and modeling and simulation enabled rapid design of an efficient clinical study with desired properties. Model-based analysis of that study's data successfully contributed to choosing the pembrolizumab dose to test for clinical efficacy: 2 mg/kg Q3W.

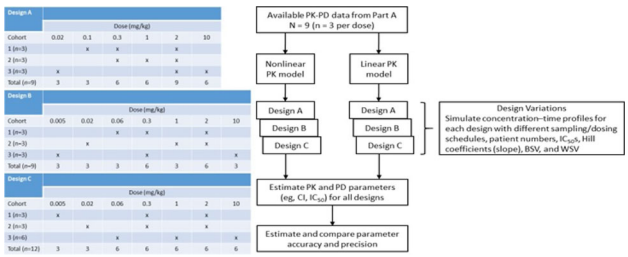

Figure 1 Designs and simulations (Color figure online)

Reference

1. J. Elassiass-Schaap, et al., Using model-based "Learn and Confirm" to reveal the PKPD relationship of pembrolizumab in KEYNOTE-001 melanoma trial, CPT-PSP, accepted.

W-35

Systems Modeling of the Contribution of SGLT to Sodium Handling in the Diabetic Kidney

Jessica Boss, K. Melissa Hallow, Ph.D.

University of Georgia

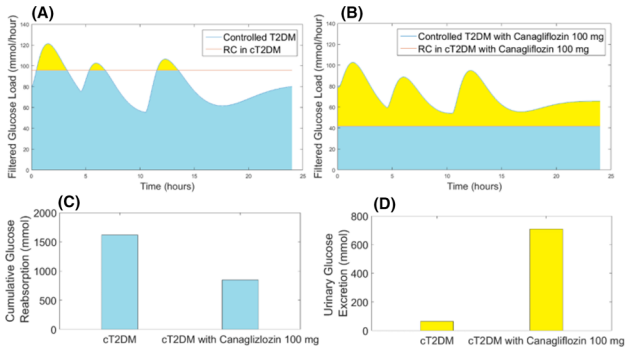

Figure 1 By reducing RC, SGLT2 inhibition with canagliflozin reduces glucose (and thus Na) reabsorption by half. *Blue* – reabsorbed glucose; *Yellow* – excreted glucose (Color figure online)

Objectives: Sodium-glucose cotransporter 2 inhibitors (SGLT2i) may improve renal function through changes in tubular sodium (Na) reabsorption. We aimed to determine the quantitative contribution of SGLT2 to Na reabsorption in healthy and type 2 diabetes mellitus (T2DM) subjects, and the impact of SGLT2i on Na reabsorption.
Methods: A published model of glucose dynamics (1,2) was extended to include prediction of urinary glucose excretion (UGE). System parameters describing the normal and diabetic states (including the renal capacity for glucose reabsorption [RC]) were estimated by fitting published plasma glucose and UGE data (3,4). We then simulated glucose and Na filtration, reabsorption, and excretion in healthy and T2DM subjects, and in T2DM subjects treated with SGLT2i canagliflozin 100 mg (modeled by changing only RC).
Results and Discussion: 24 hour glucose reabsorption was estimated to be 811 and 1618 mmol for healthy and T2DM subjects respectively. SGLT2 reabsorbs Na and glucose at a 1:1 molar ratio, and these amounts correspond to 4.6% and 9.1% of total PT Na reabsorption. Thus, PT Na reabsorption through SGLT2 is more than doubled in diabetes, an increase that is likely sufficient to drive pathologic changes in renal hemodynamics (5). Treatment with SGLT2i canagliflozin returned total PT Na reabsorption to the healthy range (851 mmol, or 4.8% of total PT Na reabsorption) (Figure 1).
Conclusions: This study provides critical quantitative information for understanding the role of SGLT2 in renal Na handling and hemodynamics, the potential mechanisms of renoprotection through SGLT2 inhibition, and the impact of SGLT2i on PT Na reabsorption.

References

1. Silber, H. E., Journal of Clinical Pharma, 2007, 47: 1159–1171.
2. Jauslin, P. M, Journal of Clinical Pharma, 2012, 52: 1861–1871.
3. Devineni, D., Journal of Clinical Pharma, 2013, 53(6): 601-610.
4. Sha, S., Diabetes, Obesity and Metabolism, 2011, 13: 669-672.
5. Hallow, KM., Experimental Biology 2016, B195 740.6.

W-36

Mechanistic models of the combination of sonidegib and ribociclib to treat sonic hedgehog medulloblastoma

Jessica K. Roberts[1], Zack W. Jones[1], Martine F. Roussel[2], Clinton F. Stewart[1], John C. Panetta[1]

[1]Department of Pharmaceutical Science, St. Jude Children's Research Hospital, Memphis, TN, USA; [2]Department of Tumor Cell Biology, St. Jude Children's Research Hospital, Memphis, TN, USA

Objective: A mechanistic model of the sonic hedgehog (SHH) and CDK4/6 pathway was developed to evaluate the combination of sonidegib (smoothened inhibitor) and ribociclib (CDK4/6 inhibitor) for the treatment of SHH medulloblastoma. The uncertainty and sensitivity of the model parameters were evaluated to interpret the effects of amplification or deletion of nodes in the pathway, evaluate potential targetable nodes, and identify sensitive parameters which need robust quantification.
Methods: Mathematical models of the cell-cycle including the upstream CDK/Cyclin D/Rb pathway along with the effects of sonidegib and ribociclib on this pathway and the cell-cycle were implemented in MATLAB®. Models were parameterized using serially measured cell counts, cell-cycle distribution, and biomarkers (e.g. pRb, Cyclin D) from *in-vitro* studies in SHH medulloblastoma cell-lines. For the sensitivity and uncertainty analysis Latin Hypercube Sampling was used to generate 1000 parameter sets and partial rank correlations were used to quantify significant nodes.
Results: The largest parameter uncertainty occurred in the percentage of cells in G0/G1 phase followed by the percentage of cells in S phase. Sensitivity analysis showed that perturbations in CDK4/6 (e.g. ribociclib) and Cyclin D (e.g. sonidegib) nodes from the CDK/Cyclin D/Rb pathway had the largest effect on both the doubling time and percentage of cells in G0/G1 phase. Inclusion of these two nodes allows the evaluation of the effects of sonidegib and ribociclib independent of each other on the cell-cycle.
Conclusions: Mechanistic models of the cell-cycle incorporating pathways related to inhibitors of interest are a potent way to better understand the dynamics of combination therapy through evaluating efficacy and drug resistance. This model of the CDK/Cyclin D/Rb pathway can be used to evaluate the effects of sonidegib and ribociclib individually or in combination on the cell-cycle and help guide the most effective use of these agents in the clinic.

W-37

Population PK Analysis of C1 Esterase Inhibitor in Adult and Pediatric Patients for the Prevention and Treatment of Hereditary Angioedema Attacks

JF Marier[1], Grygoriy Vasilinin[1], Jennifer Schranz[2], Patrick Martin[2], and Yi Wang[2]

[1]Certara Strategic Consulting, Canada, [2]Shire, Lexington, MA

Objectives: CINRYZE® (C1 esterase inhibitor [human]; C1INH) is a normal constituent of human blood and primarily regulates activation of the coagulation, contact, and complement pathways. Intravenous administration of 1000 units (U) of CINRYZE every 3–4 days is currently approved in the US and EU for routine prophylaxis of hereditary angioedema (HAE) and in the EU for treatment of HAE in adolescents and adults. A population PK analysis of C1INH was performed to support dosing recommendations in younger pediatric patients for the prevention and treatment of HAE.
Methods: Concentration-time data of functional C1INH from 8 clinical (prevention or treatment of HAE attacks) were included in the population PK analysis. Of the 278 patients included in the analysis, a total of 3, 32, and 26 subjects were in the 2-5, 6-11 and 12-17 years of age cohorts, respectively. Sources of variability (age, sex, race, baseline C1INH, indication, HAE attacks, and dose) were explored and formally tested using a full model approach (NONMEM Version VII).
Results: A one-compartment model with baseline C1INH resulted in adequate goodness-of-fit of functional C1INH. Typical clearance and volume of distribution (V) were 0.105 L/h and 3.13 L, respectively. Pediatric patients between 2-5 and 6-11 years of age are expected to

have V values 1.38- and 1.22-fold higher than adults, respectively. Mean area under the curve up to 4 h (AUC_{0-4}) and maximum concentrations (C_{max}) following dosing of 500 U every 3-4 days in patients 2–5 years of age were within 5% of adults treated with 1000 U. Mean AUC_{0-4} and C_{max} following dosing of 500 U in patients 6-11 years of age were within 20% of adults treated with 1000 U.
Conclusions: The exposure to C1INH following CINRYZE 500 U in patients 2–5 and 6-11 years of age every 3-4 days are expected to closely match those observed in adults treated with 1000 U.

W-38

Exploratory Analysis of Age on Longitudinal CD4+ T-Cell Reconstitution in HIV-Infected Patients Using a Semi-mechanistic Model

Jingxian Chen, Julie Dumond

UNC Eshelman School of Pharmacy, Chapel Hill, NC, USA

Objectives: To interrogate the effect of chronological age on CD4+ T-cell (CD4+) recovery in HIV-suppressed subjects under antiretroviral therapy, considering thymus output, naïve T-cell death and immune activation.
Methods: Model parameters were obtained from the literature. CD4+ data from two published studies were digitized for parameter optimization and model validation: 978 subjects (median age: 36 years) followed for 144 weeks[1] and 95 subjects (median age: 41 years) followed for up to 15 years[2]. Model development was conducted in Berkeley Madonna and Phoenix WinNonlin 6.4, with simulation and data visualization in R. The effects of age were explored on three CD4+ dynamic parameters, and CD4+ count plateaus from 20 to 80 years for each scenario were calculated.
Results: Total CD4+ were split into two compartments, naïve CD4+ and memory CD4+ cells. Generation of naïve CD4+ was zero-order. The conversion between and death rate of both cell populations were first-order, and proliferation was capacity-limited. Rate constant of naïve CD4+ conversion and memory cells death were optimized using reference 1, with other parameters fixed to literature values (converted into years). Simulations from the final model well correlated with observed data (R^2 = 0.9517). Age effects were described using exponential models for thymus output and naïve CD4+ death rate, and linear for immune activation. Decreased thymus output with age drove the change of CD4+ plateau. Increased activation and extended naïve CD4+ with age were shown to play minimal roles.
Conclusions: A semi-mechanistic model to describe longitudinal CD4+ reconstitution in mid-aged HIV-suppressed subjects was established. Based on simulation, age on thymus output has the largest effect on plateau CD4+ counts, revealing the decreased thymus output with aging is the major factor of impaired CD4+ reconstitution. This study supports the negative effect of aging on CD4+ T-cell recovery in HIV-suppressed patients.

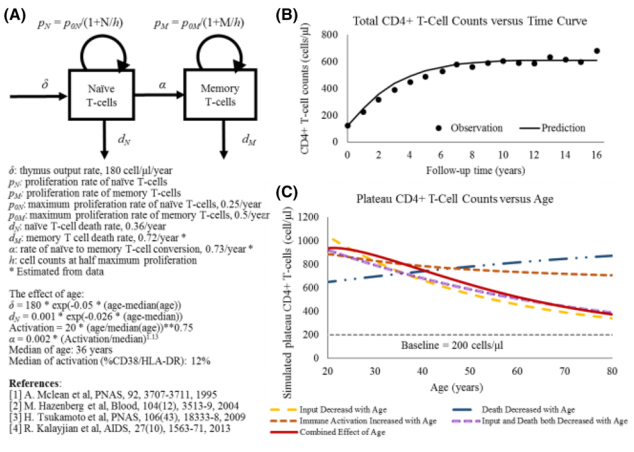

Figure 1 (A) Model structure and parameterization of age, (B) Representative of goodness of fit plots and (C) Plateau CD4+ T-cell counts change with age on different CD4+ T-cell recovery dynamic parameters (Color figure online)

References

1. G. Robbins et al, Clinical Infectious Disease, 48(3), 350-361, 2009
2. X. Zhang et al, HIV Clinical Trials, 14(2) 61-7, 2013

W-39

Interspecies Scaling in Pre-clinical Population Pharmacokinetics of CF-301

Joannellyn Chiu[1], Tatiana Khariton[1], Parviz Ghahramani[1], Paula Lapinskas[2], Cara Cassino[2], Teresa Carabeo[2]

[1]Inncelerex, Jersey City, NJ; [2]ContraFect Corporation, Yonkers, NY

Introduction: CF-301, the first bacteriophage-derived lysin to enter US clinical trials, completed the first Phase 1 trial recently (separate asbstract). CF-301 exhibits rapid *S. aureus*-specific bacteriolysis, antibiofilm activity, low propensity for resistance and pronounced synergy with antibiotics.
Objectives: Develop a pre-clinical population PK model to predict human target exposures. Data was pooled from 9 PK and toxicology studies in rats and dogs with various infusion regimens. Also, to predict exposures of CF-301 in rats following a single dose of 2.5 mg/kg 2-h infusion (the clinically relevant dose in toxicology studies).
Methods: 2- and 3-compartmental models with zero-order infusion were evaluated to characterize the concentration-time profiles of CF-301 in rats and dogs. Allometric scaling based on body weight was included *a priori* on all PK parameters. Covariates of interest (Sex, Age, Formulation) were evaluated for significance. Final model was evaluated using pcVPC. Primary species of interest in CF-301 toxicology studies were rats. Therefore, PK parameters for the 270 rats were used to predict exposures (Cmax, AUC) in rats following 2.5 mg/kg 2-h infusions.
Results: 1,969 concentrations from 270 rats and 78 dogs were included in the analysis. The pcVPC suggested that the final model (3-compartmental) adequately predicted CF-301 concentrations in both rats and dogs (Figure 1). Simulation of rat concentration profiles following 2.5 mg/kg 2-h infusions predicted a mean AUC=3,600 ng.h/mL and mean Cmax=1,750 ng/mL. Concentration-time profiles for typical male and female rats showed comparable AUC, C_{max} and T_{max}. There were no significant effect of age or formulation.
Conclusions: The population PK model for CF-301 described the plasma concentrations in rats and dogs parsimoniously, and was deemed appropriate for simulations. No relevant effect of covariates were found on the exposures. Simulations predicted a mean AUC of 3600 ng.h/mL and Cmax of 1750 ng/mL following 2.5 mg/kg 2-h infusion in rats.

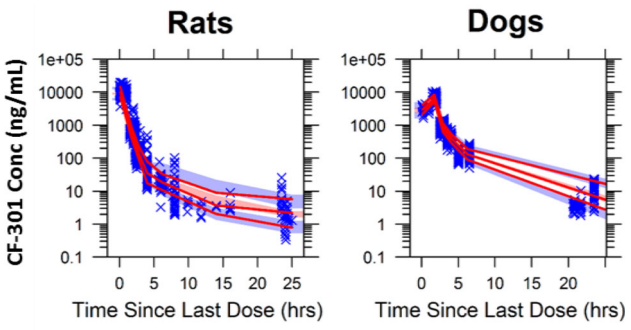

Figure 1 pcVPC Stratified by Species (Color figure online)

W-40

Bridging from the Intravenous to Subcutaneous Formulation of Tocilizumab for Polyarticular Juvenile Idiopathic Arthritis and Systemic Juvenile Idiopathic Arthritis by Leveraging Prior Pharmacometrics Knowledge

Joy C. Hsu[1], Leonid Gibiansky[2], Kamal Bharucha[3], Alysha Kadva[3], Mohamed Kamal[1], Navita Mallalieu[1], Nicolas Frey[4]

[1]Roche Pharma Research and Early Development, Roche Innovation Center, New York, USA; [2]QuantPharm LLC, North Potomac, Maryland; [3]Genentech, South San Francisco, USA; [4]Roche Innovation Center, Basel, Switzerland

Objectives: To recommend and confirm the subcutaneous (SC) dose regimen of tocilizumab (TCZ) proposed for Polyarticular Juvenile Idiopathic Arthritis (pJIA) and Systemic Juvenile Idiopathic Arthritis (sJIA) using modeling and simulation.
Methods: TCZ is a monoclonal antibody directed against the interleukin-6 (IL-6) receptor. The intravenous (IV) formulation for TCZ was approved for sJIA in 2011 and for pJIA in 2013. The mechanism of action for TCZ is well understood, and the efficacy has shown to be well correlated with the target saturation of IL-6 receptors. The exposure-response relationships between TCZ steady-state C_{trough} ($C_{trough,ss}$) and PD/efficacy parameters were well established for the IV formulation for both pJIA and sJIA. Hence, bridging from IV to SC formulation for TCZ was based on exposure achieved at $C_{trough,ss}$.
Utilizing the population PK models developed for the IV formulation for pJIA and sJIA in combination with prior knowledge on the SC formulation from the adult rheumatoid arthritis population, SC dose regimens that were able to achieve similar ranges of $C_{trough,ss}$ as the IV dose regimen were recommended for pJIA and sJIA. Interim analyses (IA) were then conducted for the SC studies using the population approach to assess and confirm that $C_{trough,ss}$ achieved by the SC formulation was indeed similar to that achieved by the IV formulation for pJIA and sJIA.
Results/Conclusions: The application of pharmacometrics was critical for the bridge from IV to SC formulation for both pJIA and sJIA. Importantly, IA guided the recommendation of the appropriate SC dose regimens for both indications. The SC studies are on-going, and the appropriateness of the dose regimens will be confirmed again when the studies are completed. Biomarker data and efficacy/safety responses will also be used to further support the bridging strategy.

W-41

Population Pharmacokinetics and Exposure-Efficacy and Safety Analyses of Alectinib in Crizotinib-Progressed or Intolerant Population

Joy C. Hsu[1], Ronan Carnac[2], Katrijn Bogman[2], Meret Martin-Facklam[2], Elena Guerini[2], Bogdana Balas[2], Ali Zeaiter[2], Alex Phipps[3], Peter N. Morcos[1], Nicolas Frey[2]

[1]Roche Pharma Research and Early Development, Roche Innovation Center, New York, USA; [2]Roche Innovation Center, Basel, Switzerland; [3]Roche Innovation Center, Welwyn, UK

Objectives: To characterize the pharmacokinetics (PK) and exposure-efficacy/safety relationships of alectinib (a potent and selective CNS-active ALK inhibitor which has received FDA accelerated approval) and its main active metabolite M4 in patients with ALK+ NSCLC who have progressed on, or are intolerant to, crizotinib.
Methods: A population PK analysis was conducted to characterize the PK of alectinib and M4 in the target patient population using data from two Phase 2 studies (NONMEM 7.2). The potential influence of covariates (weight, race, disease status, etc.) that contribute significantly to the between-patient variability in PK parameters were explored and quantified. Graphical analyses were conducted to investigate the exposure-efficacy/safety relationship for alectinib and M4 and to determine whether variability in efficacy and occurrence of safety events could be attributed to variability in exposure. In addition, relationship between alectinib and M4 exposure and progression free survival (PFS) was characterized using a Cox proportional-hazards regression model.
Results: The concentration-time course for alectinib and M4 were best described by a one-compartment open model with first-order elimination and with a sequential zero and first-order absorption/formation. Weight was the only covariate found to statistically influence the clearance and volume for both alectinib and M4. No other covariate had a statistically significant effect. There was a clear exposure-efficacy relationship across 300-900 mg BID, with lower exposure associated with less decrease in tumor size. This relationship appeared to plateau at exposures achieved with the 600 mg BID regimen. Based on results from the Cox proportional-hazards analysis, there was no statistically significant relationship between exposure and PFS following 600 mg BID. There was also no significant relationship between exposure and any AEs analyzed.
Conclusions: Results of these analyses demonstrated that the 600 mg BID dose is appropriate in a crizotinib-progressed or intolerant population.

W-42

Evaluation of Open Source PKPD Simulators in R

Justin Penzenstadler, Devin Pastoor, Vijay Ivaturi

University of Maryland School of Pharmacy, Center for Translational Medicine

Objectives: A key component of the pharmacometrician's toolkit are PKPD simulators for decision making. However, most PKPD simulation packages require to be purchased (e.g. Berkley Madonna, NONMEM, Phoenix NLME) or are difficult to use. Simulators built within R could allow users to seamlessly transition from simulation data to R's powerful statistics and plotting tools. This study was designed to demonstrate the utility of open source alternatives in the R programming language.

Methods: Four packages, PKPDsim, RxODE, mrgsolve and mlxr were subjected to a standardized test scenario. The test scenario was developed to reflect both clinician driven (complicated regimens, individual level covariates) and drug-development (population pharmacokinetics) applications. Dependencies, inputs, outputs, user experience, and unique attributes were noted.
Results: User experience was similar among the four packages, and each package was all able to sufficiently perform the test scenario. mrgsolve has a NONMEM like syntax for writing the ODE part of the model, whereas PKPDsim, RxODE and mlxR are more R based. All packages provide a better and seamless simulation workflow as opposed to commercial software which require pre and post processing in different software such as R.
Conclusions: This study indicates that open source PK/PD simulation packages are reasonable alternatives to paid software. Tests involving simulator speed, precision, and overall functionality are in progress for various simulation frameworks.

References

1. Kyle T. Baron, Alan C. Hindmarsh, Linda R. Petzold, Bill Gillespie, Charles Margossian and Metrum Research Group LLC (). mrgsolve: Simulation from ODE-Based Population PK/PD and Systems Pharmacology Models. R package version 0.5.11.9005. http://metrumrg.com/opensourcetools.html
2. Ron Keizer (2015). PKPDsim: Simulate ODE models. R package version 0.2.
3. Wang W, Hallow KM, James DA. A Tutorial on RxODE: Simulating Differential Equation Pharmacometric Models in R. CPT Pharmacometrics Syst Pharmacol. 2016;5(1):3-10.
4. Marc Lavielle (2016). mlxR: Simulation of Longitudinal Data. R package version 3.0.0. http://CRAN.R-project.org/package=mlxR

W-43

Modeling tumor progression in patients with hematologic malignancies, following Idelalisib monotherapy

K. Bhasi, S. Sharma, A. Mathias

Gilead Sciences Inc. CA

Background: Idelalisib (Zydelig®) is currently approved at 150 mg BID for the treatment of hematological malignancies (CLL, FL and SLL). A model was developed to characterize the relationship between idelalisib exposure and change in lymph node size (measured as sum of the product of the perpendicular diameters of index lesions; SPD) over time in cancer patients.
Methods: A longitudinal tumor growth inhibition (TGI) model describing the drug dependent change in SPD was fitted to the observed data (N=161), following idelalisib at a dose range of 50 to 350 mg; QD and BID. The model equations are as provided below:

$$\frac{dy(t)}{dt} = K_L \cdot y(t) - K_D(t) \cdot Exposure(t) \cdot y(t)$$
$$K_D(t) = K_{D,0} \cdot e^{-\lambda t}$$
$$y(0) = y_0$$

where, y(t) represents the SPD at time t; K_L represents the rate of increase in SPD; $K_D(t)$ represents the rate of reduction in SPD; λ represents the rate constant describing the exponential decrease in K_D; and y(0) represents the baseline SPD. Idelalisib pharmacokinetics was well described by a 2-compartment model with a first-order absorption rate constant and absorption lag time. Covariates such as, dose, dosing frequency, disease type (CLL, DLBCL, MCL, and iNHL), and baseline SPD value were evaluated on each PD (pharmacodynamic) parameter.
Results: Time course of changes in tumor size was well characterized by the model. The final model consisted of an exponential error model for IIV, estimated on all parameters, and a combined error model to describe the residual error. The model captured dose and time dependent inhibition of SPD with higher doses demonstrating a greater magnitude of tumor size reduction and a quicker onset of action. Mean (CV%) of PD parameters were: K_L 0.21 y^{-1} (27.2%), K_D 1.1 mL/ng/y (16.6%), and λ 11.6 y^{-1} (8.8%).
Conclusion: The current work represents a first step in using a TGI model as an early quantitative assessment of the effect of Idelalisib in hematological malignancies. Future models linking tumor dynamics (TGI) to survival will allow prediction of important clinical endpoints (PFS or OS).

W-44

Assessment of Combination Therapy Effects on Tumor Growth Using PBPK/PD Modeling

Kristin Dickschen[1], Thomas Gaub[1], Lars Küpfer[1], Sabine Pilari[1], Michael Block[1]

[1]Bayer Technology Services GmbH, Computational Systems Biology, Leverkusen, Germany

Objectives: Current treatment regimens for cancer patients tackle tumor growth using combination therapies to increase efficacy and reduce adverse effects [1]. A major challenge remains the decision for the most efficacious dosing regimen of a combination therapy taking into account tumor properties, PK properties, and mode of action. This applies for combination therapies of small molecules and biologics [2]. The objective of this approach is to assess the usability of PBPK/PD combination models for these questions.
Methods: PBPK/PD models of bevacizumab and imatinib were established using PK-Sim® and MoBi®. The generic PBPK model was extended by a physiological representation of the tumor. Relevant biological processes integrated comprise target expression, binding, and dynamics. A PD model was integrated to represent tumor growth of the physiological tumor as well as the effect of the combination therapy. Impact of dosing schedule for combinations of bevacizumab and imatinib was investigated on a population scale.
Results: The established PBPK/PD model structure is able to describe the impact of a combination therapy of bevacizumab and imatinib on tumor growth on a population scale. The combined PBPK/PD model of bevacizumab and imatinib predicts a median stable disease according to the RECIST criteria in a patient population which is well in line with published data [3].
Conclusions: PBPK/PD models of combination therapies can improve decision making in the clinic. The integration of relevant biological processes driving PK and PD of small molecules and biologics in one model structure allows for assessment of a combination therapy in the example. Further assessments of combination therapies by such models are required to further evaluate the potential to improve decision making in the clinic.

References

1. Hanahan, Weinberg. Cell. 2011. 144 (5): 646-674
2. Garg, Balthasar. J Pharmacokinet Pharmacodyn. 2007. 34 (5): 687-709
3. Hoehler et al. British J of Cancer. 2013. 109: 1408-1413

W-45

Viral Dynamics Modeling and Simulation to Support Development of Grazoprevir (GZR) and Elbasvir (EBR) for Treatment of Hepatitis C (HCV) Infection

Larissa Wenning[1], Kyle Baron[2], Matthew Riggs[2], Marc Gastonguay[2], Luzelena Caro[1], Ed Feng[1], Bob Nachbar[1], Julie Stone[1]

[1]Merck and Co., Inc., [2]Metrum

Objectives: To characterize the dose-response relationships for EBR/GZR in the treatment of genotype (GT) 1 and 4 Hepatitis C (HCV) infection and to simulate expected outcomes of regimens with reduced EBR/GZR doses.
Methods: A 2-species viral dynamics model was developed and qualified using viral load and sustained virologic response (SVR12) data from studies in which GZR and EBR were administered as monotherapy at a range of doses; a study in which GZR (25, 50, or 100 mg) was administered for 12 weeks in combination with Pegylated Interferon/Ribavirin (PR); and studies in which 100 mg GZR + 20 or 50 mg EBR ±RBV were administered for 8 or 12 weeks. The effect of EBR/GZR in inhibiting production of HCV from infected cells was related to GZR and EBR doses using a sigmoid Emax relationship. The death rate of infected cells was assumed to increase for doses or regimens that lead to greater antiviral activity. Efficacy and resistance parameters were scaled based on in vitro relative potency data to predict efficacy in genotypes other than GT1.
Results: The final model accurately describes both the time-course of decline in HCV viral load for short-term monotherapy treatments and SVR12 for longer-term treatment across the range of doses, treatment durations, and regimens studied. Simulations were conducted to explore the effect of reducing the exposure of one or both compounds. Reducing the dose of either EBR or GZR by half compared to the recommended doses of 50 mg EBR/100 mg GZR still results in high projected SVR12 rates.
Conclusions: Dose response relationships for GZR and EBR were characterized using monotherapy data and data from clinical studies that evaluated varying EBR and GZR doses and varying regimens. The model allowed simulation of the likely outcome of reduced doses/exposures of EBR/GZR in a combination regimen, and supported assessment of acceptable reductions in exposure for both compounds.

W-46

Population Pharmacokinetics and Pharmacodynamics of the Effect of Sarilumab on DAS28-CRP in Patients With Rheumatoid Arthritis

Lei Ma[1], Christine Xu[1], Yaming Su[1], Anne Paccaly[2], Vanaja Kanamaluru[1]

[1]Sanofi Genzyme, Bridgewater, NJ; [2]Regeneron Pharmaceuticals, Inc, Tarrytown, NY

Objectives: Sarilumab is a human mAb blocking the IL-6Rα in development for rheumatoid arthritis (RA). Study objectives were to develop and qualify a population pharmacokinetic and pharmacodynamic (PopPK/PD) model describing the time course of DAS28-CRP in RA patients with inadequate response to DMARDs or TNF-α antagonists and to identify covariates influencing PK/PD relationships using pooled phase 2/3 data.
Methods: A sequential approach was used: a PopPK model was developed first, followed by PopPK/PD model development. Model-predicted individual concentration time course was used to develop a PopPK/PD model for DAS28-CRP over time after subcutaneous administrations of sarilumab 100 to 200 mg every week (qw) or every 2 weeks (q2w) (N=2082). Full model with backward elimination was used to identify the final covariate model. The final PopPK/PD model was evaluated by visual predictive check and bootstrap.
Results: DAS28-CRP time course was described by an indirect-response model linking sarilumab concentrations with DAS28-CRP via inhibition of DAS28-CRP input rate. Population parameter estimates in the final model translated into a population mean decrease of DAS28-CRP from baseline of 6.06 to 2.67, with IC_{50} of 2.32 mg/L. Effect on DAS28-CRP reduction from baseline was less for 150 vs 200 mg q2w (46.5% vs 50.3%, respectively, at week 24). Effect of covariates included the final PopPK/PD model (baseline CRP, physician's global assessment of disease activity, Health Assessment Questionnaire–Disability Index, body weight, and prior corticosteroid treatment) on PD parameters was small, with no clinically meaningful influences on DAS28-CRP time course.
Conclusions: DAS28-CRP time course after subcutaneous sarilumab administration was described by a semi-mechanistic, indirect-response model, with no clinically meaningful covariates, including body weight and baseline disease activity. Consistent with observed results in clinical studies, the PopPK/PD model showed less reduction in DAS28-CRP after 150 vs 200 mg q2w, thus supporting a starting dose of 200 mg q2w with a decrease to 150 mg q2w in the event of laboratory abnormalities.

W-47

Population Pharmacokinetics and Pharmacodynamics of the Effect of Sarilumab on Absolute Neutrophil Counts in Patients With Rheumatoid Arthritis

Lei Ma[1], Christine Xu[1], Yaming Su[1], Anne Paccaly[2], Vanaja Kanamaluru[1]

[1]Sanofi Genzyme, Bridgewater, NJ; [2]Regeneron Pharmaceuticals, Inc, Tarrytown, NY

Objectives: Sarilumab is a human mAb blocking the IL-6Rα currently in development for rheumatoid arthritis (RA). Objectives of this analysis were to develop and qualify a population pharmacokinetic and pharmacodynamic (PopPK/PD) model describing the time course of absolute neutrophil count (ANC) in RA patients and to identify covariates influencing PK/PD relationships using combined data from phase 1 through 3 studies. In sarilumab clinical studies, no relationship between decreases in ANC and infection was identified.
Methods: A sequential approach was used: a population pharmacokinetic model was developed first, followed by PopPK/PD model development. Model-predicted individual concentration time course was used to develop a PopPK/PD model for ANC over time after subcutaneous administrations of sarilumab 50 to 200 mg every week or every 2 weeks (q2w) in 1672 patients. Covariates were evaluated using a stepwise approach. The final PopPK/PD model was evaluated by visual predictive check and bootstrap.
Results: ANC time course after sarilumab administration was described by an indirect-response model, linking sarilumab concentrations with ANC via stimulation of ANC elimination rate. Population parameter estimates in the final model translated into a population mean 60% maximal decrease of ANC from baseline, and the population-lowest-possible ANC level was 2.15×10^9/L with EC_{50} of 10.3 mg/L. Effect on ANC reduction was less (31% reduction from baseline) and fluctuations within each dosing interval were higher for 150 mg q2w than for 200 mg q2w (39% reduction from baseline). The final PopPK/PD model included covariates of smoking status, prior corticosteroids, and body weight on PD parameters.

Effect of the above covariates was small, with no clinically meaningful influences on ANC time course.
Conclusions: Consistent with observed dose-related ANC reduction in clinical studies, ANC described by an indirect-response model decreased rapidly within 1 to 2 weeks and stabilized 4 weeks after subcutaneous sarilumab administration in RA patients. There was no clinically meaningful influence of the covariates investigated.

W-48

A Physiological-based Pharmacokinetic (PBPK) Modeling Approach to Quantifying Drug-Drug Interactions: Applications to the Development of Fenfluramine (ZX008) for Treatment of Seizures in Dravet Syndrome (DS)

Li Zhang[1], Brooks Boyd[2], Michael Trang[1], Mohamed Ismail[1], Gail Farfel[2], Christopher Rubino[1]

[1]ICPD, Schenectady, NY; [2]Zogenix, Inc. Emeryville, CA

Objectives: DS is a severe form of childhood epilepsy in which seizures are often refractory to traditional antiepileptic drugs (AEDs). Low dose fenfluramine (ZX008; Zogenix, Inc.) has shown promise in DS patients and is currently under development worldwide. Treatment of DS patients often requires a regimen of several AEDs that are metabolized via CYP450. The objective of this analysis was to construct a PBPK model system to quantify potential drug-drug interactions and facilitate dose justification for clinical trials of ZX008.
Methods: The PBPK model for fenfluramine was comprised of ten perfusion-limited tissues with tissue-to-plasma partition coefficients calculated by integrating physiochemical and *in vitro* properties based upon tissue composition-based equations. Fenfluramine was eliminated by renal excretion and hepatic metabolism; 76% of hepatic intrinsic clearance (CL_{int}) went to norfenfluramine. The PBPK model was employed to predict the joint disposition of fenfluramine and norfenfluramine in Berkeley Madonna. The joint PBPK model was qualified using plasma PK profiles of d-fenfluramine and d-norfenfluramine from healthy adults. The remainder of the PBPK model system is comprised of models for concomitant AEDs (stiripentol, clobazam, valproic acid) constructed from literature sources.
Results: Model simulations adequately replicated the mean plasma PK profiles of d-fenfluramine and d-norfenfluramine in adults (Figure 1). Predicted mean $AUC_{0\text{-}24,SS}$ and $C_{max,ss}$ were within 1.25- fold of observed fenfluramine and norfenfluramine data in adults, supporting model robustness. Sensitivity analyses demonstrated that fenfluramine $AUC_{0\text{-}24,SS}$ is highly sensitive to changes in liver partition coefficient and CL_{int}, where 30% decrease in CL_{int} resulted in 1.5-fold increase of fenfluramine $AUC_{0\text{-}24,SS}$ in healthy adults. PBPK models for other AEDs showed similar robustness when evaluated using published data.
Conclusions: The developed joint fenfluramine PBPK model well characterized d-fenfluramine and d-norfenfluramine PK profiles in healthy adults. Data from an ongoing adult drug–drug interaction study will be used to qualify the PBPK model system for use in pediatric studies.

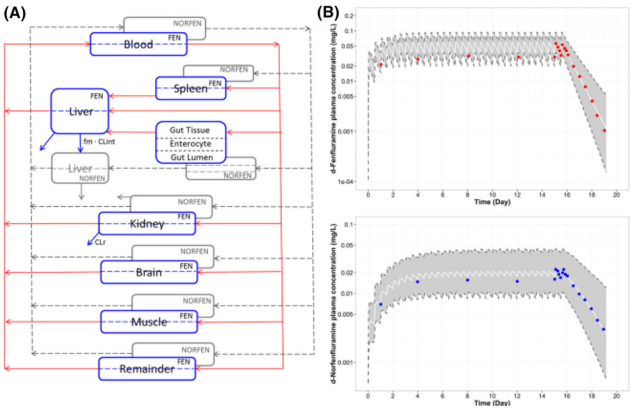

Figure 1 (A) Scheme of joint PBPK model for fenfluramine and norfenfluramine after fenfluramine oral dosing in healthy adults; (B) Model simulated versus observed PK plasma profiles of d-fenfluramine and d-norfenfluramine after administration of d-fenfluramine 15 mg twice daily orally for 15 days in healthy adults. Note: *Solid line/grey shaded area* represented median/ 90% confidence interval of model simulations for 1,000 virtual healthy adults; *solid dots* represented observed d-fenfluramine or d-norfenfluramine mean plasma PK data from healthy adults (Caccia, et al. Eur J Clin Pharmcol. 1985; 29: 221-4) (Color figure online)

W-49

Dosing Regimen Selection under the Animal Rule for Pegfilgrastim to Treat Patients with Hematopoietic Syndrome of Acute Radiation Syndrome (HS-ARS)

Lian Ma[1], Luning Zhuang[1], Gene Williams[1], Andrew Chow[2], John Harrold[2], Murad Melhem[2], Bing-Bing Yang[2], Dhananjay Marathe[1], Yaning Wang[1], Kimberly Bergman[1], Yanli Ouyang[1], William Dickerson[1], Lan Huang[1], Frank Lutterodt[1], Adebayo Laniyonu[1], Jyoti Zalkikar[1], Alex Gorovets[1], Libero Marzella[1], Nitin Mehrotra[1]

[1]Food and Drug Administration, Silver Spring, MD, [2]Amgen, Inc., Thousand Oaks, CA

Objectives: To determine an effective human dosing regimen for pegfilgrastim for the treatment of patients acutely exposed to myelosuppressive doses of radiation.
Methods: The applicant developed a population PK/PD model relating radiation injury and pegfilgrastim treatment to absolute neutrophil count (ANC) time course in patients. This model was based on both data from the pivotal animal efficacy study of pegfilgrastim in the HS-ARS setting and human data from cancer patients with chemotherapy-induced neutropenia. Simulations were conducted to select a dosing regimen in patients $\geq$ 45 kg by optimizing the following relevant pharmacodynamic endpoints: time to ANC recovery and duration of grade 3 and4 neutropenia. Dosing in pediatric patients $<$ 45 kg was selected based on PK matching to the dose selectedfor adults.
Results: As compared to placebo, adult patients given two 6-mg doses of pegfilgrastim on day 1 and 8 following irradiation were predicted to have a reduced duration of grade 3 and 4 neutropenia and a quicker recovery to baseline. This dosing regimen was also supported by the totality of the safety data. In addition, a weight-tiered

Body Weight (kg)	Pegfilgrastim Dose
<10	100 μg/kg
10–20	1.5 mg
21–30	2.5 mg
31–44	4 mg
>45	6 mg

dosing was selected in children that produces exposures similar to that in adults receving the regimen of two 6 mg doses one-week apart.
Conclusions: Based on population modeling and simulation results and benefit/risk considerations, the regimen of 6-mg pegfilgrastim given on days 1 and 8 following irradiation was approved for patients with body weight ≥45 kg, and a weight-tiered dosing was approved for pediatric patients <45 kg.

W-50

Dose sensitivity of pharmacokinetic difference between similar biologics with target-mediated drug disposition

Liang Li, Ping Ji*, Shamir Kalaria, Lei He, Jianmeng Chen, Anshu Marathe, Suresh Doddapaneni, Yaning Wang, Chandrahas Sahajwalla

Division of Clinical Pharmacology II, Food and Drug Administration, Silver Spring, MD, USA

Objectives: Target-mediated drug disposition (TMDD) indicates the high affinity binding of a therapeutic biologic to its pharmacological target site to such an extent that this affects its pharmacokinetic (PK) characteristics. The nonlinarity PK caused by TMDD has signifiant impact on clinical study design especially dose selection. The present work evaluated the sensitivity of dose in detecting PK difference between two similar biologics with nonlinear PK caused by TMDD.
Methods: Two similar therapeutic monoclonal antibodies exhibiting TMDD were compared in a randomized two-period crossover trial of 100 patients. Difference between the two biologics on binding affinity to the intended target and the binding affinity of the fragment crystallizable region (Fc) to the neonatal Fc receptor (FcRn) was assumed to lead to up to 10-fold difference in PK parameters such as linear clearance and TMDD. Inter-individual variability was assumed at 30% for these parameters. Random residual variability was applied using a proportional error model with a coefficient variation of 20%. Over a 100-fold dose range was tested in the simulation. Each scenario was simulated 1000 times using R software. The 90% confidence interval of geometric mean ratio C_{max} and AUC between products were calculated for power analysis.
Results: Higher dose is more sensitive with higher power to detect the difference due to FcRn binding. Lower dose is more sensitive with higher power to detect the difference in affinity binding involving TMDD. The doses in the middle are not as sensitive to detect the differences.
Conclusions: More than one dose, preferable high and low doses, appears necessary to evaluate the difference in receptor binding affinity in various regions of the protein structure between biologics exhibiting nonlinear PK caused by TMDD when conducting the PK comparability trials.
Disclaimer: The views expressed in this abstract are those of the authors and do not necessarily reflect the official views of the FDA.

W-51

Interactive Code for Guiding Dose Selection

Luann Phillips[1,*] and Eyas Raddad[2]

[1]Cognigen Corporation a Simulations Plus Company, Williamsville, NY, USA; [2]Chorus, Eli Lilly Company, Indianapolis, IN, USA

Objectives: Assuming a linear one compartment model for the pharmacokinetics (PK) with and without dose-dependent saturable bioavailability, and a direct inhibitory Emax model for bio-marker effect (PD), develop an interactive PK/PD response simulation tool to guide dose selection for a first in human study of an orally administered medication. The tool will simulate various scenarios of target plasma concentration and PD time profiles with and without consideration of discrete dose strength constraints.
Methods: Predicted human PK parameters allometrically scaled from an animal study and concentration required to achieve 50% suppression (IC50) from an in vitro experiment of the bio-marker were provided. Berkeley Madonna® was selected to implement the coding to allow use of interactive sliders for parameter values (PK, absorption type, and IC50) and 'batch run' mode to cycle through suppression values of IC10 to IC90. Equations were derived to calculate the exact dose needed to achieve steady-state trough, maximum, and average concentrations equivalent to ICx (x=10 to 90% suppression). For each exact dose the following information was calculated: discrete dose to be administered, concentration/effect-time profiles, area under the curve (AUC) for concentration/effect-time, average effect, drug holiday (time effect is < 20% suppressed), and doses expected to achieve drug holidays of specific length.
Results: The interactive simulation tool allowed the drug development team to explore numerous scenarios allowing for uncertainty in predicted potency and PK, as well as various scenarios of target PK/PD profiles and dose-strength constraints, in a matter of minutes. The tool also allowed the team to quickly explore new scenarios that were not predefined.
Conclusions: Solving for dose instead of simulating to find the dose needed to acheive specific PD goals and front-loading other design choices into a simple interactive tool, significantly increased the speed and confidence in dose selection for first-in-man studies.
The authors would like to acknowledge PRCL Research Inc. for their support of this project.

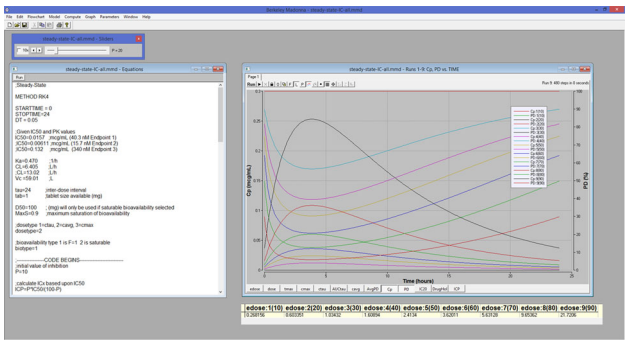

W-52

Multiple-model, AUC-guided vs. standard trough-guided vancomycin dosing in patients

Michael Neely*†, Lauren Kato†, Gilmer Youn†, Emi Minejima†, Walter Yamada*, Mike van Guilder*, David Bayard*

*Laboratory of Applied Pharmacokinetics and Bioinformatics, Children's Hospital Los Angeles, †University of Southern California

Objectives: Guidelines[1] suggest vancomycin 40-60 mg/kg day and troughs of 10-20 mg/L. We hypothesized that pharmacometric dosing with an AUC target would permit lower doses and troughs.
Methods: This was a single-center, prospective study of hospitalized adults receiving IV vancomycin with ≥1 trough prior to enrollment. Cohorts were as follows. Year 1: Predict vancomycin levels using a non-parametric population model and the BestDose software (www.lapk.org), with no dose control. Year 2: BestDose Multiple-

Model (MM) dosing control targeting AUC:MIC ≥400 (max AUC 800), with unknown MIC set to 1 mg/L. All prior troughs iteratively generated each subject's Bayesian posterior model for each dose calculation. Year 3: Schedule individually, optimally timed single samples using BestDose's novel MMopt algorithm prior to each MM dose optimization.

Results: See the table for results. In years 1, 2 and 3 there were 83, 90 and 76 evaluable subjects, with 119, 107 and 78 blood samples, respectively. The median (range) age was 51 (18-93) years, with 63% males. Weight was 76 (15-194) kg. Age (P=0.06), sex (P=0.49) and weight (P=0.56) were similar across years. Planned MMopt sample times in year 3 were 11 peaks, 31 troughs, and 36 others. Median vancomycin concentrations in those with/without nephrotoxicity were 18.1 vs. 11 mg/L (P<0.001).

Conclusions: This is the first prospective evaluation for MMopt individualized sampling and the second for BestDose.[2] Our institution underdoses vancomycin with 70% troughs sub-therapeutic (year 1) relative to guidelines. However BestDose Bayesian control nevertheless justified this lower dosing based on AUC. Pharmacometric dosing significantly reduced the number of required blood samples, percentage of troughs >20 mg/L, and prevalence of vancomycin-associated nephrotoxicity. Hospitals with more aggressive standard vancomycin dosing would see even greater benefits with individualized dosing and sampling.

Table 1 Results by cohort

	Cohort Year			
	1: Pred Only	2:MM Pred+Control	3:MMopt Pred+Control	P-value
Prediction %bias, median (IQR)[a]	−9% (−26 to 12)		-4% (−18 to 9)	0.34
Daily dose mg/kg, median (IQR)	23.3	(17.0–28.9)	21.8 (17.7–26.6)	21.2
(15.6–27.3)	0.96			
Blood samples, mean (range)	2.9 (1–10)	2.2 (18)	1.7 (1–5)	0.005
%Trough therapeutic (N)[b]	30% (119)	24% (107)	15% (31)	0.18
%AUC therapeutic (N)[c]	80% (119)	74% (107)	80% (78)	0.43
%Trough >20 mg/L (N)	21% (119)	8% (107)	11% (31)	0.02
%Nephrotoxicity (N)[d]	6% (83)	0% (90)	1% (76)	0.008
%Treatment Failure (N)[e]	1% (83)	0% (90)	0% (76)	0.61

[a] %bias = (pred-obs)/obs for each level by excluding it (i.e. using all prior levels in a subject) when generating the Bayesian posterior, IQR=interquartile range

[b] By guidelines[1]

[c] AUC:MIC ≥ 400 or ≥300 and responding and AUC < 800

[d] Creatinine rise >0.5 mg/dL or >50% from baseline

[e] Relapse in resolved symptoms ≤72 hours after stopping vancomycin

References

1. Rybak M, et al. Am J Health Syst Pharm **2009**; 66:82–98.
2. Størset E, et al. Transplantation **2015**; 99:2158–2166.

W-53

A User-friendly Computational Tool to Simulate Energy Balance Components in Pharmacological Interventions

MN Trame[1], Hartmann S[1], C Bouchard[2], V Antonetti[3], CK Martin[2], DM Thomas[4]

[1]Center for Pharmacometrics and Systems Pharmacology, University of Florida, Orlando, FL; [2]Pennington Biomedical Research Center, Baton Rouge, LA; [3]Manhattan College, Riverdale, NY; [4]Center for Quantitative Obesity Research, Montclair State University, NJ

Objectives: Components of energy balance such as energy intake represent critical measurements for evaluating pharmaceutical interventions. Unfortunately, current practice relies on self-reported energy intake (EI) measures which are deemed invalid for scientifically based conclusions. Mathematical models have been proposed as a scalable and feasible alternative. To date, no accurate model has been derived that simultaneously calculates EI for multiple subjects with measured body weights (BW) at non-uniform time points. The aim was to develop an algorithm which allows for accurate calculations of free-living EI, energy expenditure (EE), energy deficit (ED) and resting metabolic rate (RMR) between measured longitudinal BW during pharmaceutical interventions.

Methods: A two part algorithm was developed to estimate EI between measured BW. The first part of the algorithm is based on a newly developed thermodynamic energy balance model that predicts weight change from change in EI. The model was derived with minimal parameter inputs relying on Kleiber's scaling law and known energy density constants (7700 kcal/kg) for BW. The model was evaluated on data from energy surplus and deficit studies. This model yields a closed form solution which was used to calculate EI between time points of measured BW as the solution of a nonlinear algebraic equation.

Results: The energy balance model accurately predicted change in BW in a 168 days energy deficit study (R^2=0.98, y=0.96x+3.77) and a 100 day energy surplus study (R^2=0.92, y=0.98x+0.54). The algorithm outputs individual subject level EI, EE, ED, and RMR which were algebraically extracted from the validated energy balance model. The algorithm was programmed into a user-friendly R-based Shiny application for immediate widespread pharmaceutical and clinical use.

Conclusions: The newly developed algorithm and Shiny application offers a novel scalable tool that generates real-time calculations of energy balance components during pharmaceutical interventions.

W-54

Target-Mediated Drug Disposition (TMDD) Population Pharmacokinetics (PopPK) Model Using the Quasi-Steady-State (QSS) Approximation of Alirocumab in Healthy Volunteers or Patients: Pooled Analysis of Randomized Phase I/II/III Studies

Nassim Djebli, Jean-Marie Martinez, Laura Lohan, Sonia Khier, Aurélie Brunet, Fabrice Hurbin, David Fabre

Sanofi, Montpellier, France

Objectives: Proprotein convertase subtilisin kexin type 9 (PCSK9) inhibition with monoclonal antibodies such as alirocumab significantly reduces low-density lipoprotein cholesterol levels both with and without other lipid-lowering therapies. We aimed to develop and qualify a PopPK model for alirocumab in healthy volunteers or patients, taking into account the mechanistic TMDD process.

Methods: This TMDD model was developed using a subset of the alirocumab clinical trial database, including 9 Phase I/II/III studies (N=527): NCT01026597; NCT01074372; NCT01161082; NCT01448317; NCT01723735; NCT01288443; NCT01288469; NCT01266876; NCT01644474. Subsequently, the model was expanded to a larger data set of 13 studies (N=2870), including 4 additional studies: NCT01812707; NCT01623115; NCT01644188; NCT01507831. Potential model parameters and covariates relationships were explored, and predictive ability was validated using Visual Predictive Check (VPC).
Results: The TMDD model was built using the QSS approximation, occurring in the central compartment of a two-compartment model. The final TMDD-QSS model included only 1 significant parameter-covariate relationship between the disease state and the distribution volume of the central compartment (V_c): 3.16 L for healthy subjects versus 4.93 L for patients (i.e. 1.56-fold higher V_c in patients). Separately, application of the model to the expanded data set revealed a significant relationship between statin co-administration and linear clearance (CLL): 0.176 L/day without statin versus 0.224 L/day with statin (i.e. 1.27-fold higher CLL with statin). The good predictive performance of the TMDD model was assessed based on graphical and numerical quality criteria, together with the VPC and comparison of the predictions to those from a PopPK model with parallel linear and Michaelis-Menten clearances (i.e. simplification of the TMDD PopPK model).
Conclusions: This mechanistic TMDD PopPK model integrates the interaction of alirocumab with PCSK9 and accurately predicts alirocumab and total PCSK9 concentrations in healthy subjects and patients. This is the first published TMDD model developed on such a large population.

W-55

Model-based meta-analysis (MBMA) for relapsed/refractory multiple myeloma (RRMM): Application of a quantitative drug-independent framework for efficient decisions in oncology drug development

Neeraj Gupta, Zhaoyang Teng, Richard Labotka, Guohui Liu, Zoe Hua, Vivek Samnotra, Karthik Venkatakrishnan

Millennium Pharmaceuticals, Inc., Cambridge, MA, USA, a wholly owned subsidiary of Takeda Pharmaceutical Company Limited.

Objectives: The failure rate for phase 3 trials in oncology is high, and quantitative predictive approaches are needed. We developed an MBMA framework to predict progression-free survival (PFS) from overall response rates (ORR) in RRMM.
Methods: A linear relationship was developed between ORR and PFS using data from four Phase 3 RRMM trials (PANORAMA, N=768[1]; ENDEAVOR, N=929[2]; ELOQUENT-2, N=646[3]; ASPIRE, N=792[4]) to predict PFS based on ORR. A Bayesian analysis was used to predict the probability of technical success (PTS) for achieving desired phase 3 PFS targets from phase 2 reports of ORR. An external validation of this MBMA framework was done by comparing predicted to observed PFS for ixazomib plus lenalidomide-dexamethasone (IRd) in RRMM patients from the phase 3 TOURMALINE-MM1 study.
Results: Based on the strongly correlated (R^2=0.90) linear relationship between ORR and PFS (Figure), MBMA predicted a PFS of 20 months based on an observed ORR of 78% with IRd in TOURMALINE-MM1. This is consistent with the reported PFS of 20.6 months[5]. As a representative application of the framework, MBMA predicted that an ORR of approximately 70% would be needed in a phase 2 study to achieve a target PFS of 15.8 months. Estimation of PTS for achieving PFS targets based on ORR using a Bayesian analysis will be illustrated.
Conclusions: A quantitative drug-independent framework for RRMM has been developed to predict PFS based on an earlier endpoint (ORR). This model can be used to enhance proof-of-concept assessment and estimate PTS to enable objective decision-making.

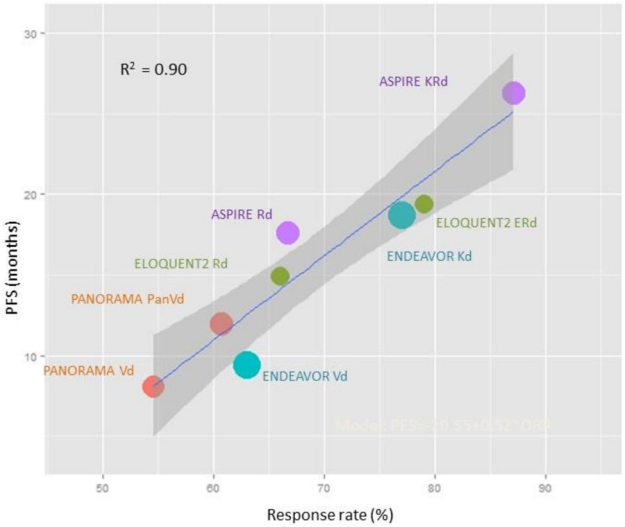

Figure 1 Relationship between response rates and PFS using data from 4 phase 3 studies. Linear regression (*blue line*) and 95% confidence interval (*grey band*) are shown. ERd, elotuzumab + lenalidomide-demethasone; Kd, carfilzomib + dexamethasone; KRd, carfilzomib + lenalidomide-demethasone; panVd, panobinostat + bortezomib-dexamethasone; Rd, lenalidomide-demethasone; Vd, bortezomib-dexamethasone (Color figure online)

References

1. San-Miguel JF, et al. Lancet Oncol. 2014;15:1195–206.
2. Dimopoulos MA, et al. Lancet Oncol. 2016;17:27–38.
3. Lonial S, et al. N Engl J Med. 2015;373:621–31.
4. Stewart AK, et al. N Engl J Med. 2015;372:142–52.
5. Moreau P, et al. N Engl J Med. 2016;374:1621–34.

W-56

Global population pharmacokinetic (PK) analysis of ixazomib, an oral proteasome inhibitor, including data from the phase 3 TOURMALINE-MM1 study: an application of model based analysis to influence posology decisions in oncology drug development

Neeraj Gupta,[1] Paul M Diderichsen,[2] Michael J Hanley,[1] Deborah Berg,[1] R. Donald Harvey,[3] Karthik Venkatakrishnan[1]

[1]Millennium Pharmaceuticals, Inc., Cambridge, MA, USA, a wholly owned subsidiary of Takeda Pharmaceutical Company Limited; [2]Quantitative Solutions, a Certara Company, The Netherlands; [3]Winship Cancer Institute of Emory University, Atlanta, GA, USA

Objectives: To develop a population PK model for ixazomib to identify clinically relevant covariates that may impact posology. Ixazomib is approved in the USA combined with lenalidomide and dexamethasone for patients with multiple myeloma who have received at least one prior therapy.

Table: Parameter estimates based on the final population PK model

Fixed effect parameters	Estimate	rse		Untransformed parameter
Absorption rate constant (log Ka)	-1.09	8%		0.34 /hr ~ $t_{1/2}$=124 minutes
Systemic clearance (log CL)	0.62	7%		1.86 L/hr
Central volume of distribution (log V2)	2.62	4%		13.7 L
Absolute bioavailability (log F)	-0.55	9%		58%
First inter-compartmental clearance (log Q3)	1.65	7%		5.18 L/hr
Volume of the first peripheral compartment (log V3)	5.73	1%		309 L
Second inter-compartmental clearance (log Q4)	3.26	2%		26.1 L/hr
Volume of the second peripheral compartment (log V4)	5.32	1%		205 L
Absorption lag time (log T_{LAG})	-1.52	0%		13 minutes
Impact of BSA on V4 (V4(BSA))	2.06	18%		-37% and +46% at the 5th and 95th percentile (1.5 m^2 and 2.25 m^2) on V_4 relative to median BSA (1.87 m^2)
Random effect parameters	**Estimate**	**rse***	**η shrinkage**	
Inter-individual variability on log CL	44%	11%	21%	
Inter-individual variability on log F	73%	8%	13%	
Correlation between log CL and log F	82%	11%		
Inter-individual variability on log V4	79%	12%	37%	
Initial SD of the residual error (SD_1)	1.90	11%		
Steady state SD of the residual error (SD_0)	0.46	3%		
Time constant of residual error SD (K_{SD})	0.84	22%		$t_{1/2}$=50 minutes

rse, relative standard error
Inter-individual variability shown as % coefficient of variation. *rse inter-individual variability is derived as 100%·$se_{\omega 2}/\omega^2$

Methods: Plasma concentration data were collected from 755 patients who received oral or intravenous ixazomib, in once- or twice-weekly schedules, in ten trials, including the phase 3 TOURMALINE-MM1 study. Data were analyzed using nonlinear mixed-effects modeling (NONMEM version 7.2).
Results: Ixazomib plasma concentration-time data were described by a three-compartment model with linear distribution and elimination, including first-order linear absorption with a lag time describing the oral dose PK. The developed model included log-normally distributed patient-level random effects on systemic clearance (CL), absolute bioavailability (F), and volume of the second peripheral compartment (V_4). Body surface area (BSA) on V_4 was the only patient covariate included in the final model. Residual unexplained variability of the log-transformed concentrations was described by an additive error model with time-varying variance described by an exponential decline in standard deviation (SD) from a starting level (SD_1) towards a steady state (SD_0). The geometric mean terminal half-life and steady-state volume of distribution were 9.5 days and 543 L, respectively. F was estimated to be 58% (Table).
Conclusions: None of the patient covariates tested, including BSA (1.2–2.7 m^2), sex, age (23–91 years), race, mild or moderate renal impairment, mild hepatic impairment, smoking status, and strong CYP1A2 inhibitors, were found to meaningfully explain variability in CL, suggesting that no dose adjustment is required based on these covariates. These results were included in the US prescribing information.

W-57

Population Pharmacokinetics and Total T-cell Dynamics of a Bispecific Antibody in Cynomolgus Monkeys

Olivia Campagne[1,2,3], Audrey Delmas[1], Marylore Chenel[1], Gurunadh R. Chichili[4], Hua Li[4], Ralph Alderson[4], Jean-Michel Scherrmann[2], Donald E. Mager[3]

[1]Clinical Pharmacokinetics and Pharmacometrics, Institut de Recherches Internationales Servier, Suresnes, France; [2]INSERM UMR-S-1144, Universités Paris Descartes-Paris Diderot, Paris, France; [3]Department of Pharmaceutical Sciences, University at Buffalo, SUNY, Buffalo, NY; [4]MacroGenics, Inc., Rockville, MD

Objectives: MGD006 (S80880) is a Dual Affinity Re-Targeting molecule that recognizes both CD3 and CD123 membrane proteins, redirecting T-cells to kill CD123-expressing cells [1]. This work aimed to develop a model describing MGD006 pharmacokinetics (PK), its immunogenicity, and the total T-cell dynamics in cynomolgus monkeys.
Methods: 32 animals received multiple escalating doses (100-300-600-1000 ng/kg/day) *via* intravenous infusion continuously 4-days a week. Total plasma MGD006 concentrations, anti-drug antibodies (ADA), and total T-cell counts were simultaneously analyzed using MONOLIX and Berkeley-Madonna. ADA development (yes/no) was categorized into three groups (low, medium, and high effect) and was included as a time-varying covariate on total clearance. Data below the limit of quantification was censored using the Beal M3 method [2]. 8 monkeys receiving 7-day continuous infusions were used to externally evaluate the model.
Results: A two-compartment model with linear elimination described the PK profiles well (mean clearance 635 mL/hr). The binding of MGD006 to CD3-cells led to dose-dependent T-cell trafficking, which was captured by an indirect response model with an adaptive feedback loop [3] (IC_{50} 1.99 ng/mL). Suppression of T-cell redistribution in the presence of ADA was well-characterized. T-cell counts showed a 2-fold increase in steady-state after treatment, described with a logistic synthesis rate function. Simulations of 7-day infusion treatments were consistent with observations in the model evaluation group.
Conclusions: A model was successfully developed to simultaneously describe the PK, immunogenicity, and T-cell trafficking induced by MGD006 in monkeys across investigated dosing schedules. The increase in T-cell baseline may reflect immune activation and is the subject of further investigation and modeling.

References

1. Chichili et al. Sci Transl Med. 7:289ra82 (2015).
2. Beal. J Pharmacokinet Pharmacodyn. 28:481–504 (2001).
3. Karlsson et al. Basic Clin Pharmacol Toxicol. 96:206-11 (2005).

W-58

Model Evaluations in Antimicrobial Drug Development-Common Misconceptions and Best Practices

Parviz Ghahramani, Tatiana Khariton, Joannellyn Chiu, Nicolas Simon.

Inncelerex, Jersey City, NJ

Introduction: In antimicrobial drug development, coefficient of determination (R^2) is often used for evaluation of target attainment and determination of PK indices driving the antimicrobial efficacy. This abstract presents current extent of R^2 application and suboptimal selection of PK index driving the efficacy that may occur by this approach.
Objectives: To evaluate the current common practice of using R^2 as a model-selection criterion in the development of antimicrobial agents, and to provide recommendations on selection of PK drivers of antibacterial efficacy.
Methods: A literature search was performed using variety of terms related to R^2 and PK indices in articles published since January 2006 in the journal of Antimicrobial Agents and Chemotherapy and The Journal of Antimicrobial Chemotherapy. Each publication was scrutinized for methodology used to evaluate the relationship between PK parameters and the antimicrobial effect of the drug under investigation to determine best PK driver of antimicrobial effect.
Results: There were a total of 15,313 published articles (2006-present) in the two journals. Out of these, 63 met the search criteria.

While 26 publications were not relevant, the remaining 37 publications all used R^2 as the criterion to compare non-linear models and to select a PK parameter best correlated with the efficacy of the antimicrobial agent. In addition, none attempted to look at combination effect of one or more PK parameters (e.g., AUC/MIC+Cmax/MIC).

Conclusions: The results confirm a widespread use of R^2 for selecting PK parameters driving efficacy of antimicrobial agents without considering the nature of the relationship. Vast majority of the articles identified in this search were comparing non-linear models using R^2 in nature. It is well established that R^2 has major inadequacies for comparing non-linear models and may result in erroneous conclusions. In addition, it appears that current practice rely mainly on the assumption that only one PK index influences the efficacy and no attempt is made to examine the combined predictive value of parameters. An example of application of appropriate alternative methodology using Residual Standard Error is presented.

W-59

Pharmacokinetic Indices Driving Antibacterial Efficacy of CF-301- a Novel First-In-Class Lysin

Parviz Ghahramani[1], Tatiana Khariton[1], Ray Schuch[2], Jimmy A Rotolo[2], Ricardo A. Ramerez[2], Michael Wittekind[2].

[1]Inncelerex, Jersey City, NJ; [2]ContraFect Corporation, Yonkers, NY

Introduction: CF-301 is being developed for treatment of *S. aureus* bacteremia, exhibits rapid *S. aureus*-specific bacteriolysis, anti-biofilm activity, has low propensity for resistance and pronounced synergy with other antibiotics.

Objectives: To determine the PK indices driving the antibacterial effect of CF-301.

Methods: Mice infected with 10^6 CFU (colony forming units) *S. aureus* were administered CF-301 divided into 1, 2, 3, or 4 doses over 24-h. Change in $\log_{10}$CFU at 24-h post infection was used as the dependent variable in a regression analysis to examine the predictive value of PKPD indices (AUC/MIC, Cmax/MIC, percent time concentration stays above MIC over a 24-h period (%T>MIC), or a combination of these indices), in more than 20 different models ranging from linear to nonlinear. The model fits were assessed by comparing the Residual Standard Errors. Also, efficacy of CF-301 (1 to 60 mg/kg in 4 divided doses), alone or in the presence of subtherapeutic doses of daptomycin (0.5-5 mg/kg), was evaluated in a separate experiment against 10 clinical *S. aureus* isolates (MIC range: 4-64 μg/mL), and various models were fit to the data.

Results: While all indices and index combinations displayed a degree of relationship with CF-301 efficacy, the AUC/MIC alone had the best predictive value and followed a sigmoidal Emax model. %T>MIC was numerically as strong a predictor of efficacy, but AUC/MIC had a larger shape parameter (Hill power 4 vs. 2) with a smaller EC_{50} (Figure), which indicates antibacterial effect of CF-301 is more sensitive to changes in AUC/MIC compared to %T>MIC.

Conclusions: AUC/MIC is the PKPD index most predictive of CF-301 efficacy against *S. aureus.* Based on estimated AUCs from a Phase 1 study in humans (separate abstract), AUC/MIC targets of approximately 1.5 and 0.5 are expected to be achieved in humans at CF-301 doses in the ranges of 0.1-0.2 mg/kg (as a single agent) and 0.03-0.1 mg/kg (in combination with daptomycin).

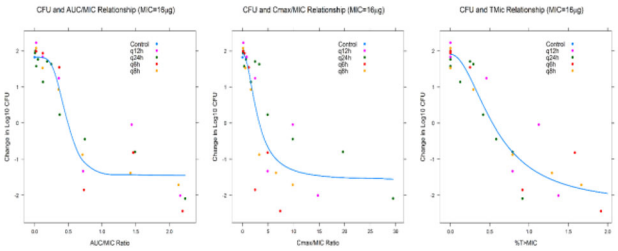

W-60

Population Pharmacokinetic/Pharmacodynamic Analysis of Intravenous Zanamivir in Healthy and Hospitalized Subjects with Influenza

Peiying Zuo[1], Jon Collins[1], Denise Shortino[1], Helen Watson[2], Grace Roberts[3], Amanda Peppercorn[3], Mohammad Hossain[3]

[1]PAREXEL International, USA; GlaxoSmithKline, [2] UK [3] USA

Objectives: Build a population pharmacokinetic model for IV zanamivir using healthy subjects and hospitalized influenza patients to explore dosing regimens and exposure-response relationship.

Methods: Serum concentrations of zanamivir from 8 studies were pooled, including two studies of patients hospitalized with severe influenza. Population pharmacokinetic/pharmacodynamic analysis was performed using a nonlinear mixed-effects modelling approach in NONMEM VII (FOCE-I). Posthoc estimates (Cmax, AUC(0-τ) and Cτ) were generated for use in Cox-Proportional hazard model to assess impact of exposure on clinical and virological endpoints. Additional Monte Carlo simulations were performed for 300 and 600mg (QD & BID) dosing to determine percentage of infected subjects with steady-state concentrations above the *in vitro* IC_{50} for zanamivir.

Results: A two-compartment model adequately described zanamivir PK in healthy (n=125, 19-77years) and influenza-infected (n=533, 0.6-101years) subjects. The estimated clearance was 5.16 L/hr in influenza patients, which decreased linearly with a reduction in creatinine clearance. The steady-state volume of distribution was 18.8 L for adult subjects and along with inter-compartmental clearance was positively correlated with body weight. The posthoc PK exposure estimates suggested current BID dosing regimen based on age, weight and creatinine clearance will achieve target exposure in adult and pediatric patients. Simulations indicated that 300 and 600mg BID dosing resulted in a saturated dose-response relationship with individual trough exposures substantially above the *in vitro* IC_{50} values over the entire dosing interval. These results were confirmed by PK/PD analysis; the exposure achieved with 300 and 600mg doses did not show difference for the clinical or virologic endpoints in patients with severe influenza. Simulated QD dosing, however, appeared to be less effective at maintaining steady-state trough exposure above IC_{50} levels.

Conclusions: The population PK/PD model supports a BID dosing regimen for IV zanamivir and suggests 300 and 600mg BID are superior to QD with both doses at the saturation range of the dose-response relationship.

W-61

Clinical Trial Design Based on Disease Progression and Pharmacological Effects in the Irbesartan Diabetic Nephropathy Trial (IDNT)

Phyllis Chan, Chunlin Chen, David Clawson, Holly Soares, Lara Pupim, Frank LaCreta, Malaz AbuTarif

Bristol-Myers Squibb, Princeton, NJ

Objectives: To characterize the type of drug action of amlodipine and irbesartan in diabetic nephropathy (DN) patients using a previously developed disease progression model[1], and to utilize the model with the added treatment effects to conduct clinical trial simulations, to investigate study design options, and to perform a power analysis.
Methods: Immediate and delayed types of symptomatic and disease-modifying forms of drug actions were investigated to account for the time component of the drug effect in the two active treatment arms (amlodipine or irbesartan) of the IDNT. The updated model, that accounted for correlations between patient-specific characteristics in the trial, and incorporating previously identified statistically significant covariates for disease progression, was used for clinical trial simulation. Sample size power analysis for a hypothetical trial design was determined using Monte-Carlo mapped power method[2], and the results were compared to a power calculation using a t-test.
Results: The model estimated an irbesartan effect of 17.4% less decline in glomerular filtration rate (eGFR) compared to placebo, whereas the effect of amplodipine was not statistically significant. Despite fitting repeated eGFR measurements for up to 48 months, statistical significance could not be differentiated between symptomatic and disease-modifying drug actions, and the final irbesartan model was determined to be immediate disease-modifying based on literature information[3]. Clinical trial sample size from the power analysis was greatly reduced (from 1800 to 1100 at 80% power) using the disease progression model-based method.
Conclusions: Longitudinal eGFR profiles in DN patients undergoing irbesartan treatment were best described by an immediate disease-modifying model. The results of this disease progression modeling can be utlized as part of a model-based tool to assist with designing trials in progressive chronic kidney diseases.

References

1. Chan P et al, poster session presented at American Conference on Pharmacometrics; 2015 Oct 4-7; Crystal City, VA.
2. Vong C et al, AAPS J. 2012; 14(2): 176-86.
3. Evans M et al., Nephrol Dial Transplant. 2012; 27(6): 2255-63.

W-62

An open-source platform for Sensitivity Analysis of QSP models

Prakash Packirisamy[1], Rukmini Kumar[1]

[1]Vantage Research, Chennai, India

Objective: Quantitative Systems Pharmacology (QSP) models tend to have a number of unknown parameters, which can introduce uncertainty in system behaviour. Sensitivity Analysis (SA), therefore, becomes an essential aspect of the model qualification process. However, modelers often lack tools for easy analysis and visualization for SA. We have created a tool that allows users to explore the parameter space, analyze options and easily create visualizations. A QSP PKPD model of "5-Lipoxygenase Inhibitors" by Denim et al [1] is used as an example to showcase this tool.

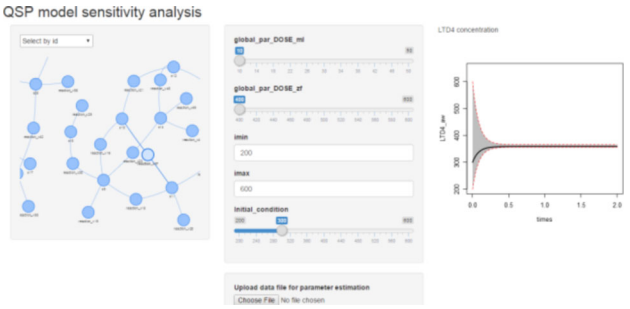

Figure 1 A snapshot showing a physiological map, dose regime, parameter sweep and the corresponding result (Color figure online)

Methods: For a QSP model, the following components are important: a physiological map, corresponding equations, estimated parameters and sensitivity of the parameters. This tool enables model visualization, global SA and parameter estimation using R Shiny [2].
We considered a model of Zileuton, a 5-lipoxygenase (5LO) inhibitor, which inherits complex pharmaokinetic-pharmacodynamic (PK/PD) characteristics. The authors hypothesize that the effectiveness of treatment is better after 1–2 weeks. Model analysis with this tool evaluates this hypothesis. This model was uploaded (as an R program) and the tool provides a GUI for the user to explore desired range of parameters. Further a parameter estimation algorithm is available to determine the appropriate range for a given data-set.
Results: Figure 1 shows model map, dosage regimen parameters as sliders and the corresponding plot of LeukotrieneD4 concentration, a key read-out in the model.
Conclusion: In general, given a model in SBML format, this tool provides the following capabilities: (i) physiological map, (ii) parameter slider and visualization of dynamic trajectories and (iii) parameter estimation given a single time trajectory. Future improvements, such as additional optimization algorithms, identification of sensitive parameters, generation of multiple parameter combination that match available data, could be added which can further increase the utility of such a tool.

References

1. Demin O, Karelina T, Svetlichniy D, et al. Systems Pharmacology Models Can Be Used to Understand Complex Pharmacokinetic-Pharmacodynamic Behavior: An Example Using 5-Lipoxygenase Inhibitors. CPT: Pharmacometrics & Systems Pharmacology. 2013;2(9).
2. RStudio Inc. shiny: Web Application Framework for R.

W-63

Prediction of Cardiac Contractility and Hemodynamics in Conscious Dogs using Mechanism Based Platform

Raja Venkatasubramanian[1], Teresa A. Collins[2], Lawrence J. Lesko[1], Jay T. Mettetal[3], Mirjam N. Trame[1]

[1]Center for Pharmacometrics and Systems Pharmacology, University of Florida, Orlando, FL; [2]Drug Safety and Metabolism, AstraZeneca, Cambridge, UK; [3]Drug Safety and Metabolism, AstraZeneca, Waltham, MA.

Objectives: Cardiovascular safety is one of the most frequent causes of safety related attrition both pre-clinically and clinically. The objective was to develop a mechanism based platform to assess drug

induced changes in contractility along with hemodynamic end-points routinely measured in dog telemetry studies.
Methods: Data from contractility ($dPdT_{max}$), heart rate (HR) and blood pressure (MAP) were available from dog telemetry studies for atenolol (n=27), albuterol (n=5), L-NG-Nitroarginine methyl ester (L-NAME; n=4), and milrinone (n=4). The model developed by Snelder et al. [1,2] was used as a starting point and was adapted to include $dPdT_{max}$. Separate drug effects for all drugs included in this analysis were evaluated using linear and (sigmoid) E_{max} relations on $dPdT_{max}$, HR and/or TPR. Nonparametric bootstrap (n=500) was performed to assess model robustness. Model was further evaluated using Sobol Sensitivity analysis to identify the most influential parameters.
Results: Population PK models for dogs were developed for atenolol and milrinone using available and literature data, while for albuterol and LNAME, literature PK models were utilized. Drug effects of atenolol, albuterol, LNAME and milrinone were included on either $dPdT_{max}$, HR and/or TPR capturing the drug effects adequately well for all studies. Bootstrap analysis demonstrated adequate model robustness with comparable mean values of parameter estimates to the final model. Preliminary results from sensitivity analysis suggest that baseline, diurnal rhythm and feedback related parameters were more important than first order rate constants (k_{out}).
Conclusions: The developed mechanism based platform can be used to simultaneously capture drug induced changes in $dPdT_{max}$ along with other hemodynamic end-points, HR and MAP, for multiple drugs in order to assess the hemodynamic safety profiles.

References

1. Snelder et al., British Journal of Pharmacology (2014)
2. Snelder et al., British Journal of Pharmacology (2013)

W-64

Population Pharmacokinetics of Dolutegravir in HIV-Infected Pediatric Subjects

Rajendra P Singh[1], Alena Yin Edwards[2], Theodore Ruel[3], Andrew Wiznia[4], Edward Acosta[5], Rohan Hazra[6], Ann M Buchanan[7]

[1]CPMS, GlaxoSmithKline, PA; [2]ICON plc Ireland; [3]University of California at San Francisco, CA; [4]Albert Einstein College of Medicine, Bronx, NY; [5]University of Alabama at Birmingham, AL; [6]NICHD/NIH Bethesda, MD; [7]ViiV Healthcare RTP, NC

Objective: Dolutegravir (DTG) is a once-daily integrase inhibitor, currently approved for use in treatment-naïve and treatment-experienced adults as well as adolescents and children weighing at least 30 kg. The main objectives of the analysis were to develop a population pharmacokinetic (Pop PK) model of DTG following oral administration, to evaluate subject covariates, and to obtain DTG exposure metrics via simulation to evaluate the appropriateness of the current pediatric weight based dosing regimens.
Methods: Data (n=41) from study P1093, an ongoing Phase I/II multicenter study in HIV-infected children and adolescents was used for the model development. On enrollment, DTG (dosed by weight bands) was started as monotherapy (if not on antiretrovirals) or added to a stable-failing regimen. Intensive PK evaluations were completed between days 5-10, after which background therapies were optimized. The Pop PK model was developed with NONMEM VII software (ICON, Ellicott City, MD) using the first-order conditional estimation with interaction method. The structural model was refined to incorporate separate absorption and bioavailability parameters for DTG tablet and granule formulations. Final model selection was based on evaluation of goodness-of-fit plots, biological plausibility and precision of parameter estimates. Further simulations were performed to evaluate appropriateness of weight-based dosing.
Results: DTG PK in HIV-1 infected treatment-experienced pediatric subjects was adequately described by a one-compartment model with first-order absorption, absorption lag time and first-order elimination. The estimated mean (95% CI) parameter values were clearance (CL/F)=1.02 (0.853, 1.19) L/hr and volume of distribution (V/F)=18.1 (15.7, 20.5) L. For the range of weights in the analysis (17.0-91.0 kg), CL/F ranged from 0.353-1.24 L/hr and V/F ranged from 4.40-23.5 L. Inter-individual variability (IIV) for CL/F was moderate at 32.4% whilst inter-occasion variability (IOV) for CL/F was slightly higher at 47.4%. Large IIV (CV=204%) and IOV (CV=257%) for tablet Ka was observed. Simulation showed that the exposures from DTG tablets were comparable to the adult 50 mg dose across all weight bands.
Conclusion: Dosing of DTG tablets on a weight-band basis (20, 25, 35, 50 mg) in children provides comparable exposures to that observed in adults (50 mg) whilst higher PK variability in pediatric patients was observed.

W-65

Effect of Altered *In Vitro* Dissolution on Lamivudine, Tenofovir, and Emtricitabine Pharmacokinetic Parameters: A PBPK Model Based Simulation Study

Rajendra P. Singh[1], Jafar Sadik B. Shaik[1, 2] Chris Spancake[3], Bela Patel[1]

[1]CPMS, GlaxoSmithKline, King of Prussia PA; [2]Department of Pharmaceutical Sciences, University of Florida, Gainesville, FL; [3]PTS, GlaxoSmithKline, RTP NC

Objective: The primary objective of this analysis is to assess the effects of delayed *in-vitro* dissolution due to over-encapsulation (OE) on exposure parameters of Lamivudine (3TC), Emtricitabine (FTC), and Tenofovir (TFV). Additionally, effect of food and repeated dose administration on exposure parameters between marketed and OE formulations were evaluated.
Methods: A full PBPK model was developed for 3TC, FTC, and TFV in Simcyp® v15 and validated by comparing the observed data to the simulated plasma concentration time profiles [N=2500; 50 trials and 50 sub/trial] after single dose administration. Simulations were repeated with *in vitro* dissolution data of OE formulation using advanced dissolution, absorption, and metabolism (ADAM) model in Simcyp. Additional simulations were run under fed conditions and at steady-state for OE formulation. Simulated exposure parameters and concentration-time profiles were compared between marketed and OE formulations.
Results: Simulated PK parameters (C_{max}, T_{max}, $AUC_{0-\tau}$, CL/F), based on dissolution profiles of 3TC, FTC, and TFV were comparable to the parameters from observed data. Simulated Cmax values of 3TC, FTC, and TFV in marketed formulation and OE formulation were: 3TC: 2.14 & 2.10 μg/mL; FTC: 1.75 & 1.74 μg/mL; TFV: 0.39 & 0.39 μg/mL respectively. Similarly, simulated $AUC_{0-\tau}$ values of 3TC, FTC, TFV were: 11.98 & 11.75 μg*h/mL; FTC: 1.75 & 1.74 μg*h/mL; TFV: 2.92 & 2.90 μg*h/mL. Simulated concentration-time profiles for both marketed and OE formulations were nearly identical under fasted and fed conditions. Simulated PK parameters for three compounds in marketed and OE formulations were similar after single or multiple dose administration. A sensitivity analysis with lowest dissolution of OE formulation showed less than 5% variation in PK parameters of FTC and TFV as compared to marketed formulation.
Conclusions: The PBPK model based simulations showed no significant effect of delayed dissolution on exposure parameters of 3TC,

FTC, and TFV. These simulations can support the waiver of BE study for OE formulation.

W-66

nlmixr: an open-source package for pharmacometric modelling in R

Rik Schoemaker[1], Yuan Xiong[2], Justin Wilkins[1], Christian Laveille[3], Wenping Wang[2]

[1]Occams, Netherlands; [2]Novartis Pharmaceuticals, USA; [3]SGS Exprimo, Belgium

Objectives: *nlmixr* is an open-source R package under development for nonlinear mixed-effects model parameter estimation, built on *RxODE*[1] and *nlme*[2]. *nlmixr* expands *nlme* by providing an efficient, versatile way to specify pharmacometric models and dosing scenarios, incorporating rapid execution via C++. NONMEM[3] (first-order conditional estimation with interaction) was used as a comparator during testing.
Methods: Richly-sampled profiles were simulated for 4 different dose levels using 30 subjects each, as single doses, multiple doses, single and multiple doses combined, and steady state dosing, for a range of test models: 1- and 2-compartment, with and without 1st order absorption, with either linear or Michaelis-Menten (MM) clearance. In total, 42 test cases were explored. All interindividual variabilities (IIVs) were set at 30%, residual errors at 20% and overlapping PK parameters were the same for all models. Parameter estimates, standard errors and run times were compared. A similar set of models was previously used to compare NONMEM and Monolix[4].
Results: Parameter estimates were comparable. Figure 1 provides results for central volume of distribution (Vc) as illustration (although all are available). *nlmixr* was faster than NONMEM for ODEs and comparable for closed form models.
Conclusions: *nlmixr* has the potential to become a useful tool for fitting nonlinear mixed-effects models in R.
The results in this abstract have been previously presented in part at WCoP (Brisbane, 2016) and published in the conference proceedings as abstract 45.

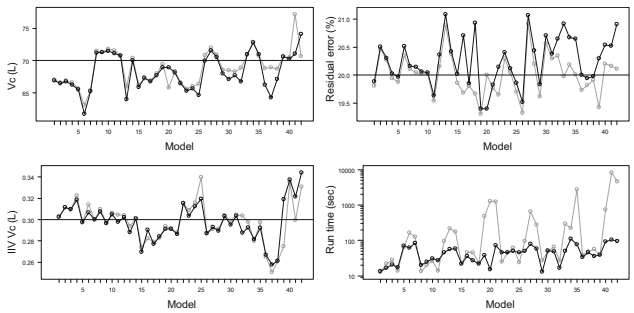

Figure 1 Fixed effects (*top left*) and IIV (*bottom left*) estimates for Vc, residual error (*top right*) and run times (*bottom right*) comparing NONMEM (*grey lines*) and *nlmixr* (*black lines*). *Horizontal black line*: true value

References

1. Wang W *et al*. CPT:PSP (2016) 5, 3–10.
2. Pinheiro J *et al.* (2016). nlme: Linear and Nonlinear Mixed Effects Models. R package version 3.1-126,
3. Beal SL *et al*. 1989-2011. NONMEM Users Guides. Icon Development Solutions, Ellicott City, Maryland, USA.
4. Laveille C *et al* PAGE 17 (2008) Abstr 1356 [www.page-meeting.org/?abstract=1356]

W-67

Empowering Non-Modelers to Query and Use Your Models

Samer Mouksassi

Certara Strategic Consulting

Objectives: Pharmacometrics is a knowledge integration platform that must be accessible and well understood by Clinicians, Regulatory Affairs and other stakeholders. When a current best model is reached it is but a start to communicate[1] the model and make others apply it in practice. Our goal is to show how nonmodelers can become model users and part of the process rather than being a back seat viewer.
Methods: We developed interactive tools using R Shiny in partnership with the clinicians to enable them to query the model with their own questions of interest. Example 1 is a population pharmacokinetics model with several covariates. Example 2 is a cox proportional model with three way interactions.
Results: Example 1 showing a static forest plot with the relative fold change of min-max of the covariate with respect to the median was incomplete since it did not enable the clinicians to answer their own questions like: For a specific patient how likely that he/she will reach the therapeutic range? The Interactive app allowed to input any combination of covariates and to hide/show relevant information by enabling some checkboxes. Example 2 it was hard for the clinicians to compute the hazard ratios (HR) with three way interactions let along computing the confidence interval using the delta method. The Interactive app allowed the clinicians to compare any two patients HR and associated confidence intervals.
Conclusions: Allowing nontechnical audience to use/apply models using interactive tools that they helped in shaping and designing open the doors to a more collaborative environment where models are no longer seen as luxury black boxes.

Reference

1. Be a Model Communicator: And Sell Your Models to Anyone Peter Bonate. 2014

W-68

Systems pharmacology analysis of oncology drug combinations to evaluate adverse events due to drug-drug interactions

Sarah Kim[1], Gezim Lahu[2], Lawrence J. Lesko[1], Mirjam N. Trame[1,*]

[1]Center for Pharmacometrics and Systems Pharmacology, University of Florida, Orlando, FL; [2]Takeda Pharmaceuticals International GmbH, Zurich, Switzerland

Objectives: Targeted therapy drug (TTD) side effects are frequently unexpected and long-term toxicities detract from otherwise impressive tolerability and exceptional efficacy of new TTDs. Efficacy of TTDs is compromised by an additional host factor, i.e. serious drug-drug interactions (DDI). Using a systems pharmacology approach and trastuzumab-drug pairs, the objectives were i) to investigate the underlying molecular mechanisms triggering cardiotoxicity, one of its most severe adverse drug reaction (ADR) of trastuzumab and ii) to

compare findings from trastuzumab (#1) alone and in combination with doxorubicin (#2), tamoxifen (#3), paroxetine (#4) and/or lapatinib (#5).

Methods: The data analytical platform "Molecular Analysis of Side Effect" (MASE^{TM}) was used to analyze data from the FDA Adverse Event Reporting System and link those findings to chemical and biological databases for molecular pathway and target evaluation. MASE^{TM} uses the proportional reporting ratio to assess the statistical relevance of the ADR occurrence and the molecular mechanisms causing a specific ADR. The established hypotheses of molecular causation of cardiotoxicity were evaluated through literature findings and compared to our findings.

Results: We found the combination therapy of #1 and #2 induced a synergistic effect of mitochondrial dysfunction in cardiomyocytes through different molecular pathways such as BCL-X and PGC-1α proteins, leading to a synergistic effect of cardiotoxicity. We found, on the other hand, #1-induced cardiotoxicity was diminished by concomitant uses of #3, #4 and/or #5 during treatment with #1. Each of both #3 and #4 caused less cardiotoxicity through an increase in the antioxidant activities such as glutathione conjugation. #5 decreased the apoptotic effects in cardiomyocytes by altering the effects of #1 on BCL-X proteins.

Conclusions: This systems-based approach provides an exemplar for a detailed investigation of an ADR, i.e. cardiotoxicity, due to a DDI at the pathway and target level and provides a process to better understand drug pair adverse events.

W-69

An R Shiny-based, Interactive Visualization Tool to Exploit Clinical Trial and Real World Data: Application to Acid Sphingomyelinase Deficiency and Olipudase Alfa ERT

Shayne Watson[1,3], Chanchala Kaddi[1], Jason Williams[2], Edouard Ribes[1], Jeffrey S. Barrett[1], Karim Azer[1]

[1]Translational Informatics, TMED, Sanofi, Bridgewater, NJ; [2]TMCP, Sanofi, Bridgewater, NJ; [3]Drexel University, Philadelphia, PA

Objective: Acid Sphingomyelinase Deficiency (ASMD: Niemann-Pick disease types A and B), is a rare lysosomal storage disease resulting in sphingomyelin accumulation. Olipudase alfa, an ERT for ASMD, is currently under development. Natural history registries and clinical studies evaluating olipudase alfa encompass heterogeneous data types, including pharmacokinetic, pulmonary, and lab measurements. We have developed a tool to facilitate integrative data analysis, QSP model-based data assessment, and interdisciplinary communication.

Methods: The visualization tool was developed using R Shiny, a web-based program, which allows the tool to be hosted and distributed using an HPC environment. The R Shiny platform is ideal because of powerful R visualization packages and the ease of designing custom GUI layouts. A QSP simulator was also developed based on R Shiny, allowing for concurrent evaluation of model simulations and clinical data. Design criteria were selected through input from the clinical and modeling teams at Sanofi working on late-stage olipudase alfa development.

Results: The tool enables real-time interactive visualization of data across four clinical studies and two natural history registries. Key features include allowing the user to select studies, data types, and features of interest (Figure 1A), and visualization options, such as comparing data within or between studies (Figure 1B).

Conclusion: The tool enables interactive and flexible visualization, including cross-comparisons of PK, PD, clinical response, and model simulations, thereby facilitating data interpretation and communication between clinical and modeling teams. Future development will focus on integrating the tool into an evolving data analysis, visualization, and simulation platform for lysosomal storage diseases.

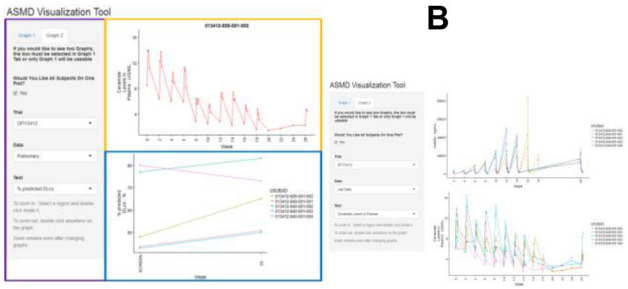

Figure 1 (A) The tool features customizable visualizations such as simultaneously viewing different data types, and examining subject-specific (*orange*) or collective (*blue*) data. (B) The tool enables rapid assessment of a large number of potential PD markers to determine those most likely to correlate with olipudase alfa concentrations (Color figure online)

W-70

Combination Strategies for Psychostimulant Drugs Used in ADHD

Sara Soufsaf[1], Guillaume Bonnefois[1], Philippe Robaey[2], Fahima Nekka[1], Jun Li[1]

[1]Université de Montréal, Montréal, Québec, Canada; [2]University of Ottawa, Ottawa, Ontario, Canada

Objectives: Attention Deficit Hyperactivity Disorder (ADHD) is a neurodevelopmental disorder with an up to 12% prevalence in children worldwide [1]. The most presribed drugs are psychostimulants, with methlyphenidate (MPH) recommended as the front-line prescription. Though extended release (ER) formulations of MPH of different generic forms are widely used, immediate release (IR) are still prescribed in combination to reach therapeutic results while respecting a child's daily activities. The present study aims to provide a quantitative way to compare the performance of MPH combinations in order to determine the most approriate drug regimen fitting a patient's specific needs.

Methods: Using population pharmacokinetic models of different MPH formulations, we generalized a previous computational strategy of dose adaptation to IR MPH [2] to the case of IR and ER combination . Based on the criteria of regimen performance, an in silico comparaison was proposed.

Results: Our identified combined regimen outperforms the most widely used clinical regimens. It also allows a better flexibility in terms of a child's activities.

Conclusions : The developed combination strategy will be included into the existing mobile application that we previously developed.

References

1. Polanczyk G, de Lima M, Horta B, et al. The worldwide prevalence of ADHD: a systematic review and metaregression analysis. Am J Psychiatry. 2007;164(6):942
2. Bonnefois, G., Robaey, P., Barrière, O., Li & J Nekka, F.. An evaluation approcha for the performance of dosing regimen in ADHD treatment. Submitted to *Journal of Child and Adolescent Psychopharmacology*.

W-71

Pharmacokinetic-pharmacodynamic modeling and simulation to predict efficacy outcomes with eslicarbazepine acetate 800 mg once-daily as monotherapy for partial-onset seizures

Soujanya Sunkaraneni,[1] Julie Passarell,[2] Elizabeth Ludwig,[2] Janet Pitner,[1] Todd Grinnell,[1] David Blum[1]

[1]Sunovion Pharmaceuticals Inc., Marlborough, MA, USA; [2]Cognigen Corporation – a subsidiary of Simulations Plus, Buffalo, NY, USA

Objectives: Eslicarbazepine acetate (ESL) is a once-daily (QD) oral anti-epileptic drug (AED) indicated for partial-onset seizures (POS) treatment. Conversion to ESL monotherapy (1200 mg and 1600 mg QD) was studied in patients taking one or two AEDs. Modeling and simulation using plasma eslicarbazepine (primary active metabolite of ESL) concentrations and time to monotherapy study exit data were performed to predict the efficacy of conversion to ESL monotherapy at 800 mg QD.
Methods: A population PK model for eslicarbazepine during ESL monotherapy (1-compartment, first-order absorption/linear elimination) provided minimum concentration [Cmin]) prediction in 1500 virtual patients taking [one (n=500) or two (n=1000)] AEDs at baseline, treated with ESL 400 mg QD for one week, then 800 mg QD for 16 weeks (similar to ESL monotherapy trials). Data for 500 simulated clinical trials were generated. Model-predicted C_{min} and number of baseline AEDs were used to determine the weekly probability of each patient meeting pre-defined study exit criteria indicating worsening seizure control, calculated using a PK-PD model relating eslicarbazepine exposure and time to exit in ESL monotherapy trials. The 90% prediction interval for study exit was determined for patients taking one or two AEDs at baseline.
Results: For virtual patients receiving ESL monotherapy (800 mg QD), the 90% upper prediction limits for exit rates at 112 days were below the 65.3% threshold calculated from historical control trials for patients taking either one or two AEDs at baseline (15.2% and 34.7% respectively; Figure 1).
Conclusions: The model-based assessment supports conversion to ESL 800 mg QD monotherapy for partial-onset seizures in adults previously taking one or two AEDs. For patients taking two AEDs, however, prescribers should consider maintenance doses of 1200 mg or 1600 mg QD to reduce the likelihood of seizure worsening, if conversion to ESL monotherapy is contemplated.

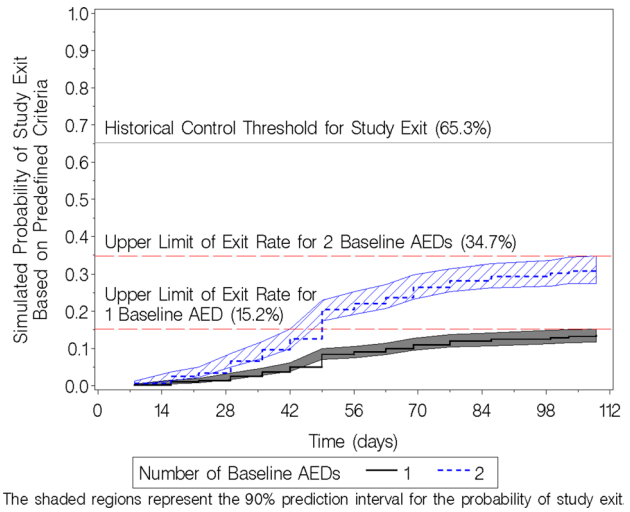

Figure 1 Simulated probability of study exit versus time, for ESL 800 mg QD, by number of AEDs taken during baseline (Color figure online)

The results in this abstract have been previously presented in part at the American Academy of Neurology, Vancouver, BC, Canada, April 17, 2106, and published in the conference proceedings as abstract [P2.025].

Reference

1. French JA, et al.. Historical control monotherapy design in the treatment of epilepsy. Epilepsia 2010;51:1936-1943.

W-72

Development of a longitudinal Parkinson's Disease Progression Model using Item-Response-Theory

Souvik Bhattacharya[1], Timothy Nicholas[2], Lawrence J. Lesko[1], Mirjam N. Trame[1]

[1]Center for Pharmacometrics and Systems Pharmacology, University of Florida, Orlando, FL; [2]Global Clinical Pharmacology, Pfizer Inc, Groton, CT

Objectives: To evaluate and understand the natural history of early and long-term disease progression in Parkinson's Disease (PD) by applying Item-Response-Theory (IRT) to analyze the longitudinal change of item-level data from the Unified Parkinson Disease Rating Scale (UPDRS).
Methods: Item-level UPDRS data from 317 patients followed over 15 months from a non-interventional NINDS trial (DATATOP) was used to develop a longitudinal IRT model. The model was developed in R 3.2.3 to predict patient-specific latent traits of individual subscores of the UPDRS at each study visit and estimate the change of each subscore for each individual over time in a Bayesian framework with normal prior distribution. A linear time-varying function was implemented, based on results from an initial Bootstrap clustering, in order to obtain a hierarchical structure of all UPDRS subscores and to determine the pattern of linkage between the UPDRS subscores over time. The Bayesian analyses were carried out using Markov Chain Monte Carlo simulations in the "brms" package in R which uses STAN. Estimation of inter-individual variability was allowed at each time point to describe the variability within the latent traits between the study population.
Results: The model was able to identify "Rigidity" and "Hand Movements" as the subscores being most influencial for predicting the subscores higher in hierarchy, identified by the Bootstrap clustering analysis (e.g. "Handwriting" and "Preparing for Bed"). The simulated results using the developed model were utilized to simulate patient characteristics at specific time points from an external dataset. For each subject in the dataset, data from their respective visits were compared to the longitudinal simulations from the developed longitudinal IRT model, and were found to be in good agreement.
Conclusion: This approach is a promising tool being able to predict the overall disease progression in PD based on early disease progression information. The developed IRT model is embedded in a Shiny application.

W-73

Short-term Risks Involved in Transitioning Between Two HIV Treatments: Predictions Through a Quantitative Systems Pharmacology Approach

Steven Sanche[1], Jun Li[1], Nancy Sheehan[1,2], Thibault Mesplède[3], Mark Wainberg[3], Fahima Nekka[1]

[1]Université de Montréal; [2]McGill University Health Centre; [3]Jewish General Hospital - Montreal, Quebec, Canada.

Objectives: Clinicians frequently decide on new treatments for HIV-infected patients. During this transition period, the resurgence of viral loads, often associated with decreased immunity and emerging new resistance mutations, has to be avoided. Thus, assessment of the short-term risks is crucial for treatment transition. In this study, predictions from switching from efavirenz to dolutegravir, both in combination with two nucleoside reverse transcriptase inhibitors, were obtained.
Methods: A Quantitative Systems Pharmacology (QSP) model that we previously developed was used. This model was calibrated using available information on drug-drug interaction (DDI). Using an *in silico* approach, viral load curves resulting from the treatment transition were obtained taking into account the variability in population. These curves were then used to assess the risks of high viral loads in the patient population.
Results: The model adequately reproduced the viral rebounds observed in a population of patients interrupting treatment. The variability in drug disposition, immunity, and quasi-species along with the presence of resistance mutations prior to treatment change, were identified responsible for a high variability in short-term response to the new treatment.
Conclusions: To lower the risks of viral loads resurgence during treatment switch, the parameters significantly varying between individuals should be paid special attention. The study results highlight the importance of patient focused data collection.

Reference

1. Sanche S, Sheehan N, Mesplède T, Wainberg M, Nekka F, Li J, *A Mathematical Model to Predict HIV Virological Failure and Elucidate the Role of Physiological Structures,* article in progress.

W-74

Population PK in humans and Target Attainment Simulations for CF-301 -a First-In-Class Antibacterial Lysin

Tatiana Khariton[1], Joannellyn Chiu[1], Cara Cassino[2], Parviz Ghahramani[1]

[1]Inncelerex, Jersey City, NJ; [2]ContraFect Corporation, Yonkers, NY

Introduction: CF-301, first bacteriophage-derived lysin to complete the first Phase 1 trial in the US, is being developed for treatment of *S. aureus* bacteremia, exhibits rapid *S. aureus*-specific bacteriolysis, anti-biofilm activity, has low propensity for resistance and pronounced synergy with antibiotics.
Objectives: To develop a population PK model for CF-301 in humans and perform target attainment simulations to determine optimal doses for Phase 2 study in patients.
Methods: Data from 13 healthy subjects (received single doses of CF-301, 0.04-0.4 mg/kg 2-hr infusion) were used to develop the model. The clinical relevance of statistically significant covariates were assessed based on the magnitude of effect on $AUC_{0\text{-}24}$ and C_{max}. The final model was used to perform target attainment simulations for various IV dosing regiments to select dose for the first patient study.
Results: 200 plasma concentrations were included in the analysis. Two-compartment model with proportional residual error described the data best. PK parameters were well estimated, CL=7 L (RSE=5.4%) and Vc=6.5 L/hr (RSE=6.5%). Sex and weight were determined to be statistically significant covariates for CL. Females are expected to have ≤15% lower $AUC_{0\text{-}24}$ or C_{max} than males; impact of weight on $AUC_{0\text{-}24}$ and C_{max} was ≤25%. Dose was a statistically significant covariate on CL and Vc while the relationship between dose and AUC or C_{max} was linear with a slope of approximately 0.75. Target attainment simulations determined that doses ≤0.4 mg/kg (2-hr infusions) maintain $AUC_{0\text{-}24}$ and C_{max} clinically relevant exposure in in rat toxicology studies.

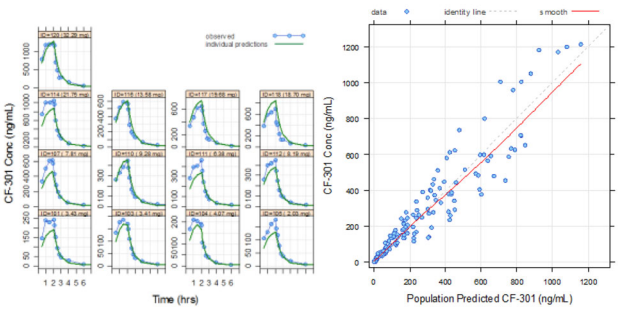

Conclusions: The population model described the PK of CF-301 adequately (Figure). Weight and sex, although statistically significant covariates, were not clinically relevant (≤25% effect). PK of CF-301 was linear and a 2-fold increase in dose results in a 1.75-fold increase in C_{max} and AUC. Target attainment simulations predicted doses 0.12-0.4 mg/kg (2-hr infusion) to be efficacious with almost all patients expected to achieve targets (AUC/MIC≥0.5), while maintaining $AUC_{0\text{-}24}$ and C_{max} below the NOEL (Color figure online).

W-75

Joint longitudinal ordered categorical model for drug-induced diarrhea and colitis: a case example in oncology

Tong Lu[1], Laurent Claret[2], René Bruno [2], Joe Ware[1], Jin Jin[1]

[1]Genentech Research and Early Development, South San Francisco, CA; [2]Pharsight Consulting Services, Marseille, France, current affiliation: Genentech/Roche-France, Marseille, France

Objectives: Serious diarrhea and colitis adverse events (AEs) are commonly encountered toxicities impacting cancer chemotherapy, molecular targeted agents, and/or cancer immunotherapy. The objective of this work is to illustrate the application of a joint longitudinal ordered categorical model to quantitatively assess the occurrence of diarrhea and colitis and the exposure-safety relationship to support early clinical development in oncology.
Methods: A joint longitudinal ordered categorical model with first order Markov chain was developed based on diarrhea and colitis grade data from 357 patients received an oncology compound in phase I/II trials. Exposure-response was investigated using kinetic-pharmacodynamic (KPD) model. A two-compartment catenary model was used to explain the delay between the occurrences of two AEs.
Results: Both AEs showed positive exposure-response relationship based on exploratory graphical analysis, with lesser extent for colitis. Because of limited occurrences, grade 1 (32%), >=2 (27%) for diarrhea and grade >=2 (7%) for colitis were modeled. The joint model successfully captured the data for both AEs, and was qualified by posterior predictive check for the proportion of AE grade over time. The KPD model described the gradual accumulation of exposure (dose) driving the diarrhea events, with half-life ~60 days. An extra compartment (with same half-life) was needed for colitis given the further delayed occurrence. A correlation coefficient of 0.6 between patient-level random effects for the two events was

estimated. Anti-diarrhea co-medication (steroid) was also significant in the model.

Conclusions: The longitudinal ordered categorical modeling has been increasingly used for safety endpoints to inform dose/regimen selection. This work exemplifies its application for diarrhea and colitis, which are common toxicities for many anti-cancer agents. The joint model can be a good approach to explore the dependence of such mechanistically correlated AEs. Medical interventions must also be considered in the analysis as it impacts AE grade and duration.

Reference

1. Zingmark et al. JPKPD 2005;32(2)261-81.

W-76

MAPS, an R Shiny Application, to Assist with Biosimilar Clinical Study Design

Vadryn Pierre[1], Seth Berry[2]

[1]Division of Pharmacotherapy and Experimental Therapeutics, UNC Eshelman School of Pharmacy, Chapel Hill, North Carolina; [2]Quintiles

Objectives: The design of comparative pharmacokinetic/pharmacodynamic (PK/PD) studies for biosimilar programs involves several challenges due to the high within- and between-subject variability with these compounds. Factors such as batch inconsistency, disease state or severity, neutralizing antibodies, and target-mediated clearance can cause high variability in the disposition of biologics.[1] An approximation of variability for concentrations and/or non-compartmental analysis (NCA) PK parameters, comparable over the desired sampling time frame, in the disposition of these compounds is useful for sample size estimation.[2] The goal of this project was to develop an R shiny application to address some of the aforementioned challenges using established population pharmacokinetic models.

Methods: MAPS (Monoclonal Antibody PK Simulator) was developed to assist with components of biosimilar clinical trial designs. The application incorporated published population pharmacokinetic models of several monoclonal antibodies in biosimilar development to simulate virtual subjects' demographics data, concentration-time profiles along with estimates of NCA parameters using the R ncappc package.[3] For verification, NCA parameter estimates were compared to literature values at various dose levels. The concentration-time and NCA data are easily downloadable within MAPS as time-stamped CSV files for further processing (e.g., bootstrap of parameters for sample size estimation, phase 1 study design sampling schemes).

Results: The NCA estimates from the simulation results for four monoclonal antibodies are shown in Table 1. These estimates were within the range of reported literature values (Table 1). On average, it took 2 minutes to simulate and estimate the PK parameters of 1000 virtual profiles for a typical multiple dose simulation (6-10 cycles). This application can be further expanded to include pharmacodynamics and exposure-response analyses to assist with the design of later phase studies.

Conclusion: MAPS uses published population pharmacokinetic models to provide an approximation of biosimilar PK variability estimates to facilitate bootstrap of PK parameters for sample size estimation.

Table 1 Simulation Results Compared to Literature Values

Bevacizumab (IV, 7.5 mg/kg q3w)			
Parameter	Geometric Mean (95LCI, 95UCI)	Literature Values	Reference Model
$C_{max,ss}$ (μg/mL)	215 (217–236)	216 - 242[1]	2-cmt linear clearance[5]
$AUC_{ss,(0-\tau)}$ (day*μg/mL)	2391 (2444–2686)	1759–2457[1]	
$C_{min,ss}$ (μg/mL)	70 (74–84)	60–80[1]	
Trastuzumab (IV, 8, 6mg/kg q3w)			
$C_{max,ss}$ (μg/mL)	157 (158–171)	182	(132–240)[2]
2-cmt parallel linear, non-linear clearance[6]	$AUC_{ss,(0-\tau)}$ (day*μg/mL) 1994 (1324–2764)[2]	1516	(1570–1751)
$C_{min,ss}$ (μg/mL)	39 (43–50)	56 (27–83)[2]	
Adalimumab (SC, 160, 80, 40mg q2w)			
$C_{min,ss}$ (μg/mL)	5 (5–6)	7 (5–10)[3]	1-cmt linear clearance 1st order absorption rate[7]
Infliximab (IV, 5mg/kg, 0, 2, 6, q8w)			
$C_{min,ss}$ (μg/mL)	2 (0 - 3)	3 (0–25)[4]	2-cmt linear clearance[8]

1. Zhi, *C.C.P.* 68:1199-1206,
2. Quartino, *C.C.P.* 77:77-88,
3. Humira Package Insert,
4. Remicade Package Insert,
5. Han, K. *AAPS* 16:1056-1063,
6. Cosson, V.F. *C.C.P.* 73:737-747,
7. Ternant *B.J.C.P.* 79:286-287, 8. Dotan, I. *I.B.D.* 20:2247–2259

References

1. FDA Biosimilarity Guidance April 2015
2. Plock. N. *ITJCP*. **51**:495-508
3. C. Acharya. *CMPD*. **127**:83-93

W-77

The NCA Consortium: Standardizing Qualification of Noncompartmental Analysis

William S. Denney[1,*], Jan Huisman[2], Klaas Prins[2], Seth Berry[3], Peter Schaefer[4], Frank Hoke[5], Kevin Dykstra[2]

[1]Human Predictions LLC, Somerville, MA; [2]qPharmetra, Netherlands or Boston, MA; [3]Quintiles, Kansas City, MO; [4]Validated Cloud Applications, Inc., Raleigh, NC; [5]Parexel International Corp., Raleigh-Durham, NC

Objectives: Methods for noncompartmental analysis (NCA) have long been described in many journal articles, textbooks, and regulations, and a nearly-standardized feature set has been identified. As a result, a multitude of software solutions are used for calculating NCA parameters: home-grown, open-sourced, and proprietary. However, every organization must generate its own requirements and validation specifications for NCA software. The objective of the NCA Consortium is to generate a standard, modular set of requirements documents to enable software developers and users to validate with a single standard ensuring interoperability and standardization of NCA calculations.
Methods: Using guidance documents, data standards, literature, and individual expertise and experience, a set of requirements, algorithms, and test cases for NCA parameter calculations were enumerated. The scope for the specifications include:
Calculations

- Single- and multiple-dose administration
  - For multiple-dose administration, prior to or at steady-state
- Intravascular and extravascular administration
  - For intravascular, including bolus, short-duration infusion, and continuous infusion
- Plasma and excretion-related (e.g. urine and feces) measurements

Data cleaning

- With or without unscheduled samples included
- With multiple options for below limit of quantification (BLQ) rules
- With interpolation, extrapolation, and corrections for time deviations from nominal times and concentration deviations

The scope of NCA parameters attempts to match commonly-used parameters from the SDTM PK Parameters controlled vocabulary.[1]
Results: A public draft specification will be available prior to ACoP 2016 incorporating each of the items defined in the Methods section.
Conclusions: By standardizing the methods of calculation, algorithmic choices, and validation tests across software and organizations, research will be more reproducible, teams in disparate organizations and working environments can work more closely together, and create more consistent NCA results.

Reference

1. CDISC SDTM Controlled Terminology, 2016-03-25 http://evs.nci.nih.gov/ftp1/CDISC/SDTM/SDTM%20Terminology.pdf (accessed 15-June-2016)

W-78

Closed-form solutions and some pharmacokinetic properties of a compartment model where endogenous input is taken into account

Xiaotian Wu[1,2], Fahima Nekka[2,3] and Jun Li[2,3]

[1]Department of Mathematics, Shanghai Maritime University, Shanghai, China; [2]Faculté de Pharmacie, Université de Montréal, Québec, Canada; [3]Centre de recherches mathématiques, Université de Montréal, Québec, Canada;

Objectives: Hematopoietic growth factors are often used in cancer chemotherapy to promote blood cell growth and bone marrow proliferation. While these substances are exogenously administered, they are also endogenously produced. Moreover, with a complex elimination, generally linear and nonlinear saturate types combined together, it is challenging to elucidate their pharmacokinetics (PK).
Methods: Working on a one-compartment PK model, with constant endogenous production and exogenous intravenous bolus administration as well as a parallel linear and Michaelis-Menten (M-M) elimination, we propose a closed form mathematical expression for its drug plasma concentration time curve. As fallout, some key PK parameters, such as the area under the curve (AUC) and elimination half-life ($t_{1/2}$), will be derived and analyzed.
Results: Closed-form solutions are well established, for each case of single- or steady-state multiple- intravenous bolus dose administrations, using a previously introduced X function.[1] For the single dose, our analysis showed that, depending on the ratio between the endogenous production rate (r_{prod}) and the maximum change rate of M-M kinetics, $t_{1/2}$ can either increase or decrease for different starting drug concentrations, while $AUC_{0\text{-}\infty}$ presents a sigmoid behavior with respect to r_{prod}, with the upper bound value corresponding to that of the model without the M-M elimination. For multiple doses, steady-state $AUC^{ss}_{0-\tau}$ can be notably larger than single dose $AUC_{0\text{-}\infty}$ because of the endogenous production.
Conclusions: For drugs manifesting the above properties, their PK properties are clearly in contrast with those explained using linear compartment models. The closed-form solutions provide a theoretical base for their investigation and elucidation.

Reference

1. X. Wu, J. Li and F. Nekka. 2015. *J Pharmacokinet Pharmacodyn* 42:151-161.

W-79

Development of a mechanism-based pharmacokinetic/target occupancy/pharmacodynamic model to characterize the effect on neutrophil count by JNJ-61610588, an anti-VISTA monoclonal antibody, in cynomolgus monkeys

Xiling Jiang[1], Jin Niu[1,2], Jocelyn Leu[1], Indrajeet Singh[1], Linda A. Snyder[1], Yu-Nien Sun[1], Weirong Wang[1]

[1]Janssen Research & Development, LLC; [2]Department of Pharmaceutical Sciences, State University of New York at Buffalo

Objectives: The V-domain immunoglobulin suppressor of T-cell activation (VISTA) is a recently discovered co-inhibitory molecule that shares limited sequence homology with the IgV domain of immune regulators of the B7 family. JNJ-61610588, a first-in-class monoclonal antibody (mAb) that targets VISTA is currently in development for evaluation in patients with non-small cell lung cancer and other types of cancer. The objective of this project was to use mechanistic modeling to characterize the dose dependent JNJ-61610588 induced depletion of neutrophils in peripheral blood in cynomolgus monkeys.
Methods: A mechanism-based pharmacokinetic/ pharmacodynamic (PK/PD) model was developed, which integrated PK, target occupancy (TO) and the depletion of neutrophils by JNJ-61610588 by incorporating key physiological processes. A two-compartment pharmacokinetic model with target mediated disposition (TMDD) was used to characterize the nonlinear clearance of JNJ-61610588. The impact of anti-drug antibody on JNJ-61610588 PK was also modeled. The turnover and depletion of neutrophils was characterized with a modified myelosuppression model, where the turnover of neutrophils was characterized with a proliferation compartment, three transit compartments that represented maturation, and a compartment

of circulating neutrophils where binding of JNJ-61610588 to VISTA on the cell surface led to neutrophil depletion. Neutrophil depletion induced feedback mechanism on neutrophil generation was also considered. A stress compartment was also included to characterize the transient neutrophil release subsequent to animal handling and dosing.

Results: The developed model simultaneously captured the observed JNJ-61610588 PK, TO and PD data in cynomolgus monkeys following JNJ-61610588 treatment at different dose levels and with different dosing intervals. The developed model was ready to be applied to predict JNJ-61610588 mediated neutrophil depletion in humans.

Conclusions: This work presents the potential of how mechanistic modeling and simulation can support first-in-human dose selection and dosing regimen optimization for immunomodulatory mAbs for anticancer immunotherapy.

W-80

Network Analysis of Proteomics of Combined Gemcitabine and Birinapant in Pancreatic Cancer Cells

Xu Zhu[1], Xiaomeng Shen[2], Jun Qu[1,2], Robert M. Straubinger[1], William J. Jusko[1]

[1]Department of Pharmaceutical Sciences, University at Buffalo, The State University of New York; [2]Department of Biochemistry, University at Buffalo, The State University of New York

Objectives: Combinations of gemcitabine and birinapant showed synergistic effects in inhibiting the growth of pancreatic cancer PanC-1 cells [1]. In this study, we seek to understand the key pathways related to cell proliferation and apoptosis in PanC-1 cells, and to explain the mechanisms of action and interactions for combined gemcitabine and birinapant examining changes of proteins. Such data were incorporated with cell distributions and cell numbers to develop a multi-scale network model. The network model was applied in target selection, prediction of gemcitabine efficacy with different genetics, and efficacy of gemcitabine-based combinations.

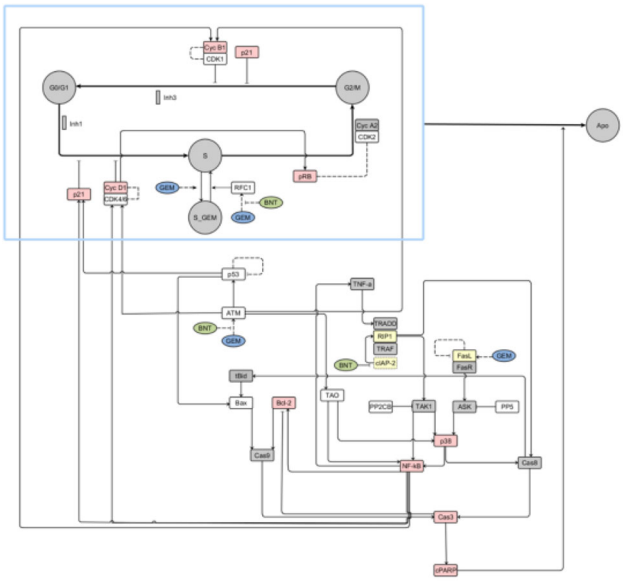

Figure 1 Structure of the multi-scale network model quantitatively linking changes of selected proteins, cell distributions and cell numbers. *White box* represents protein profiles from proteomics analysis; *red box* represents protein profiles from western blot analysis; *yellow box* represents protein profiles from literature digitization (Color figure online)

Methods: PanC-1 cells were incubated with control, gemcitabine (20 nM), birinapant (100 nM) or combinations of the two. Total proteins were extracted, and mass spectrometry (MS)–based proteomics was applied for a universal identification and quantification of proteins changed after treatments. A total of 1481 significantly changed proteins were clustered by KEGG functional pathways, and relevant pathways were selected for further investigation. A total of 20 proteins were selected to represent the key pathways. Western blot analysis provided additional information of functional change of proteins. Dynamic changes of proteins were linked to cell distributions and cell numbers, the quantitative relations were built in ADAPT V software, and a multi-scale network model was developed (Figure 1).

Results: Gemcitabine activated DNA damage response (DDR) and induced DNA repair proteins, which were blocked by birinapant. Thus the cell cycle arrest effect was enhanced in the combination group. NF-κB pathways were activated by both gemcitabine and birinapant, and enhanced in combination. Both intrinsic and extrinsic apoptotic pathways were activated in combination.

The network model was tested in the presence of external TNF-α for model validation [2]. Clinical applications of the model were also explored: 1) Sobol Sensitivity analysis was applied to identify potential drug targets to increase the efficacy of gemcitabine; 2) The role of mutated p53 was assessed; 3) Model prediction indicated no beneficial interactions when combining gemcitabine and curcumin, consistent with our observations.

Conclusion: Comprehensive network model includes information for both drug actions and biological systems. It may be applied for novel drug target selection and efficacy prediction.

References

1. Zhu X, et al. J Pharmacokinet Pharmacodyn. 2015 Oct;42(5):477-96. doi: 10.1007/s10928-015-9429-x.
2. Benetatos CA, et al. Mol Cancer Ther. 2014 Apr;13(4):867-79. doi: 10.1158/1535-7163.MCT-13-0798.

W-81

Systems pharmacology model describing the kinetics of insulin-like growth factors

Zinnia P Parra-Guillen[1], Alvaro Janda[2], Ulrike Schmid[3], Iñaki F Troconiz[1]

[1]Pharmacometrics & Systems Pharmacology Group, School of Pharmacy and Nutricion, University of Navarra, Spain; [2]School of Engineering, University of Edinburgh, United Kingdom; [3]Translational Medicine, Boehringer Ingelheim Pharma, Germany

Objectives: Insulin-like growth factors (IGF-I and IGF-II) signalling is involved in growth and survival of different human cancer cells [1]. Therefore, neutralising their activity has been suggested as a potential target in oncology [1]. This work aimed at developing a systems pharmacology model describing the kinetics of both factors together with their main binding protein (IGFBP-3), tightly regulating their fate.

Methods: Total and free IGF-I and/or IGFBP-3 plasma time profiles after administration of recombinant IGF-I to healthy subjects were extracted from [2-4]. Total IGF-II and IGFBP-3 levels at baseline were partly assumed as reported in literature (total IGF-II was set to

three times total IGF-I and total IGFBP-3 to the sum of total IGF-I and IGF-II [5]). Ordinary differential equations describing protein synthesis, degradation and binding kinetics were implemented in Matlab. Parameter estimates from literature were explored as initials followed by a fine tuning process.

Results: Initially, protein profiles could be characterised assuming equal binding properties to IGFBP-3 and different synthesis rate constans, but also assuming different dissociation constant (K_D) and same synthesis rate (to fullfill the 3:1 ratio above mentioned). After fine tuning, a lower K_D and an increase IGFBP-3 baseline level (accounting for binding other than IGFBP-3) were needed to describe all scenarios in both cases.

Conclusions: A system pharmacology model characterizing the disposition of IGF-I, IGF-II and IGFBP-3 has been developed using literature data. Additional data are needed to discreminate between both parameterisation. The model provides a quantitative framework to explore the impact of drugs binding to IGFs, that could assist drug development and guide dose optimisation.

References

1. Pollak, Nature Rev, 2012
2. Laron et al. Acta Endocrinologica, 1990
3. Boroujerdi et al. Am J Physiol Endocrinol Metab1997
4. Mizuno et al. Pharm Res, 2001
5. Rajaram et al, Endocr Rev, 1997
6. Vorwerk et al., Endocrinology, 2002